PNL-4800 Suppl. 1
UC-70

C1

In Situ Vitrification of Transuranic Waste: An Updated Systems Evaluation and Applications Assessment

J. L. Buelt
C. L. Timmerman
K. H. Oma
V. F. FitzPatrick
J. G. Carter

March 1987

Prepared for the U.S. Department of Energy
under Contract DE-AC06-76RLO 1830

Pacific Northwest Laboratory
Operated for the U.S. Department of Energy
by Battelle Memorial Institute

Battelle

PNL-4800 Suppl. 1

DISCLAIMER

PACIFIC NORTHWEST LABORATORY
operated by
BATTELLE
for the
UNITED STATES DEPARTMENT OF ENERGY
under Contract DE-AC06-76RLO 1830

Printed in the United States of America
Available from
National Technical Information Service
United States Department of Commerce
5285 Port Royal Road
Springfield, Virginia 22161

NTIS Price Codes
Microfiche A01

Printed Copy

Pages	Price Codes
001-025	A02
026-050	A03
051-075	A04
076-100	A05
101-125	A06
126-150	A07
151-175	A08
176-200	A09
201-225	A010
226-250	A011
251-275	A012
276-300	A013

PNL-4800 Suppl. 1
UC-70

IN SITU VITRIFICATION OF TRANSURANIC WASTES: AN UPDATED SYSTEMS EVALUATION AND APPLICATIONS ASSESSMENT

J. L. Buelt
C. L. Timmerman
K. H. Oma
V. F. FitzPatrick
J. G. Carter

March 1987

Prepared for
the U.S. Department of Energy
under Contract DE-AC06-76RLO 1830

Pacific Northwest Laboratory
Richland, Washington 99352

ABSTRACT

In situ vitrification (ISV) is a process whereby joule heating immobilizes contaminated soil in place into a durable glass and crystalline waste form. Numerous technological advances made during the past three years in the design, fabrication, and testing of the ISV process are discussed. Performance analysis of ISV focuses on process equipment, element retention (in the vitrified soil during processing), melt geometry, depth monitors, and electrodes. The types of soil and waste processed by ISV are evaluated as process parameters. Economic data provide the production costs of the large-scale unit for radioactive and hazardous chemical wastes (wet and dry). The processing of transuranic-contaminated soils are discussed with respect to occupational and public safety. Alternative applications and operating sequences for various waste sites are identified. The technological data base warrants conducting a large-scale radioactive test at a contaminated soil site at Hanford to provide a representative waste form that can be evaluated to determine its suitability for in-place stabilization of transuranic-contaminated soils.

EXECUTIVE SUMMARY

EXECUTIVE SUMMARY

In situ vitrification (ISV) is an emerging technology that converts contaminated soils into a durable glass and crystalline waste form in place. In situ vitrification is based on the joule-heating principle used by electric melter technology developed at Pacific Northwest Laboratory (PNL) for the immobilization of high-level nuclear waste (Buelt et al. 1979). In situ vitrification was initially tested by researchers at PNL in August 1980. Since then ISV has grown from a concept to an emerging technology through a series of 4 bench-scale tests, 24 engineering-scale tests, 14 pilot-scale tests, and 4 large-scale tests. The process has been broadly patented (U.S. Patent 4,376,598--Brouns, Buelt, and Bonner 1983) domestically and abroad, and Battelle Memorial Institute, who operates PNL, has been granted exclusive worldwide rights to all ISV technology except for ISV of radioactive wastes. The program has been sponsored by the U.S. Department of Energy (DOE) for potential application to contaminated soil sites.

The ISV development program is using four development vitrification systems. The distinguishing characteristics of each system are power level, electrode spacing, and mass of block produced, as shown below:

System	Power	Electrode Spacing	Block Mass
Bench Scale	10 kW	11 cm	1 to 10 kg
Engineering Scale	30 kW	30 cm	50 to 1000 kg
Pilot Scale	500 kW	1.2 m	10 to 40 t
Large Scale	3750 kW	5 m	400 to 800 t

One of the more prominent pilot-scale tests, completed in June 1983, vitrified a makeup site in which 25 kg of soil containing 600 nCi/g of transuranic (TRU) waste simulated a highly radioactive area (or "hot spot"). The made-up source also contained mixed fission products with a total activity of 30,000 nCi/g and exhibited a surface exposure rate of 100 R/h before it was emplaced at the test site. No radionuclides were released to the environment during the vitrification process. Subsequent to this test, one of the major accomplishments of this task was the design, fabrication, and successful

testing of the large-scale unit (shown in Figure 1 with the pilot-scale unit). Four nonradioactive tests have been conducted, and the system and technology are ready to be tested in a large-scale radioactive test (LSRT) at an actual contaminated soil site.

Major advantages of ISV as a means of stabilizing radioactive waste are:

- long-term durability of the waste form
- cost effectiveness
- safety in terms of minimizing worker and public exposure
- applicability to different kinds of soils and buried wastes.

This document describes the ISV technology and its process capabilities and limitations as another viable tool for in-place stabilization of waste sites. The following sections correspond to the chapters in the body of this document:

- description of the ISV development units
- analysis of the performance of the ISV tests conducted
- process parameters of ISV
- economic analysis
- analysis of occupational and public exposure
- assessment of waste site applications.

PROCESS DESCRIPTION

To initiate the ISV process, electrodes are inserted vertically in the contaminated soil in a square array as shown in Figure 2. A mixture of graphite and glass frit is placed in 5-cm x 5-cm trenches on the surface of the soil between the electrodes to form a conductive path. An electrical current is passed between the electrodes, creating temperatures high enough to melt the soil. The graphite is consumed by oxidation as the molten zone grows downward, incorporating the soil contaminants and producing a vitreous mass. Convective currents within the melt distribute the wastes evenly. During the process, off gases emitted from the molten mass carry a small percentage of radionuclides (typically 0.01% of the inventory being vitrified). The gases are collected by a hood over the area and routed to a treatment system. When power to the

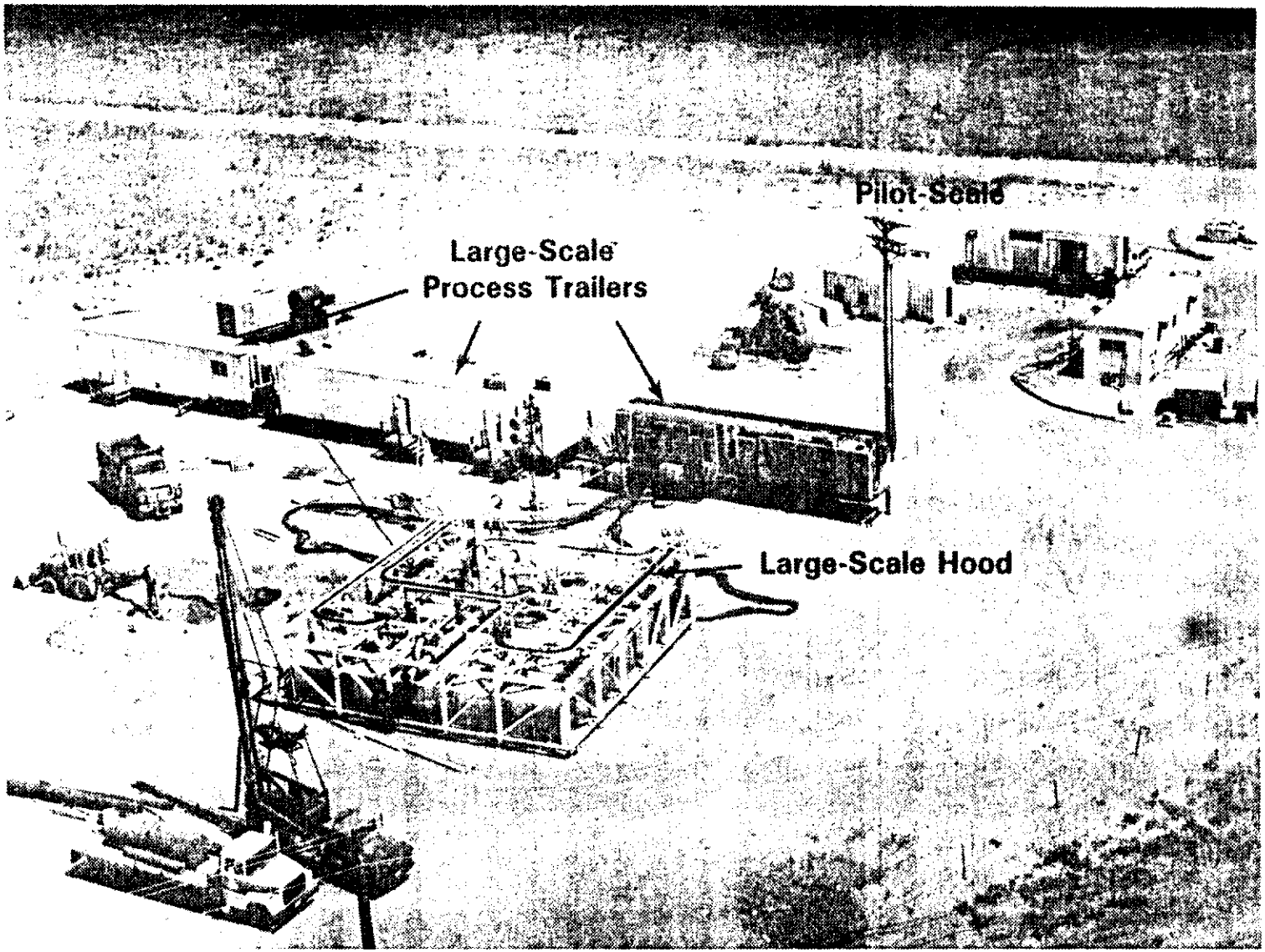

FIGURE 1. In Situ Vitrification--Large Scale and Pilot Scale Units

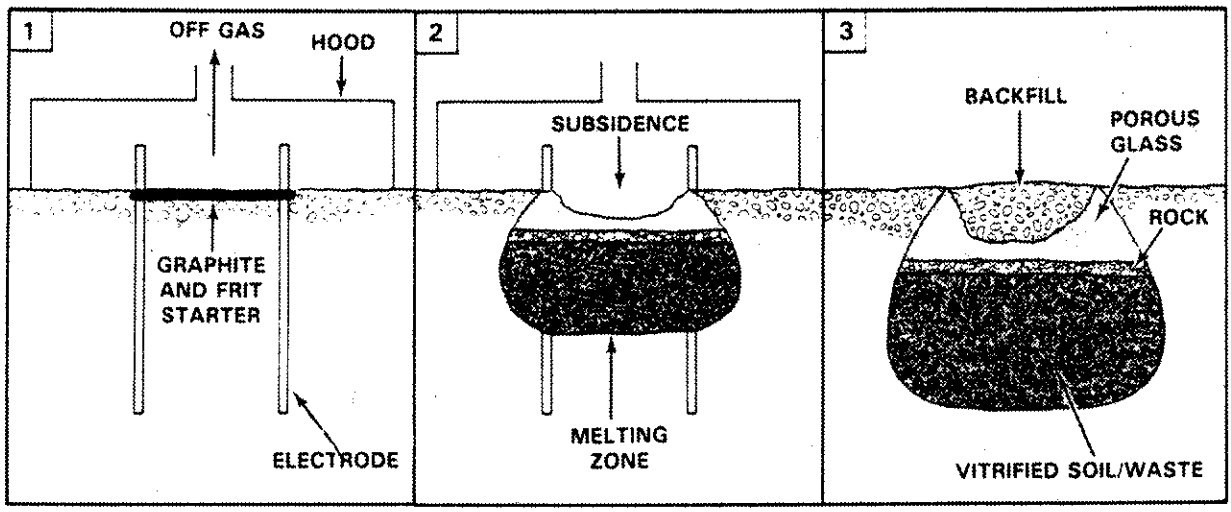

FIGURE 2. Sequence of the ISV Process

system is turned off, the molten volume begins to cool, producing a block of glass and crystalline material that resembles natural obsidian or basalt. The subsidence that occurs can be covered with uncontaminated backfill to the original grade level.

The principle of ISV operation is based on joule heating, which occurs when an electrical current passes through the molten mass. As the molten mass grows, resistance decreases, so to maintain the power level high enough to continue melting the soil, the current must be increased. This is accomplished by a transformer equipped with multiple voltage taps and a saturable reactor power controller. The multiple taps allow for more efficient use of the power system by maintaining the power factor (the relationship between current and voltage) near maximum. The process continues until the appropriate depth is reached. Melt depth is limited as the heat losses from the melt approach the energy level that is deliverable to the molten soil by the electrodes.

A more detailed system description outlining the power system and the off-gas treatment system follows.

Power System Design

The power system consists of a transformer connection that converts three-phase alternating-current electrical power to two single-phase loads. Each

electrical phase is connected to one diagonally opposed pair of electrodes in a square pattern, creating a balanced electrical load on the secondary. The even distribution of current within the molten soil produces a vitrified product that is almost square in shape to minimize overlap among adjacent settings. Multiple voltage taps and a balanced load allow for a near-constant power operation, which shortens run time and thus minimizes cost.

Off-Gas Treatment System

In both the large-scale and the pilot-scale systems, the off-gas containment and electrode support hood collects the off gas, provides a chamber for the combustion of pyrolyzed organics, and supports the four electrodes embedded in the soil. Much of the heat generated during the ISV process is released to the off-gas stream. The heat is removed in the off-gas treatment system so that the temperature of the gas that exits after treatment is close to ambient.

There are three major kinds of treatment for the off-gas system (see Figure 3). First, the gases are scrubbed in two stages, with a quencher and tandem nozzle scrubber. These scrubbers remove particles down through the submicron range. Second, the water aerosols in the saturated gas stream are removed by a vane separator followed by a condenser and a second vane separator. The gases are then reheated, to ensure that there is an unsaturated gas stream at a temperature well above the dewpoint. In the third treatment phase, the off gas is filtered with two stages of high-efficiency particulate air (HEPA) filters. Both large- and pilot-scale systems are trailer mounted and therefore mobile.

The off gases from the engineering- and bench-scale systems are treated by the air handling system of the facility in which they are located.

PERFORMANCE ANALYSIS

The ability of the waste form to retain the incorporated radionuclides (some with very long half-lives) and the destruction/immobilization of hazardous chemical wastes that may be associated with TRU-contaminated soil sites are of prime importance in establishing the usefulness of the ISV process.

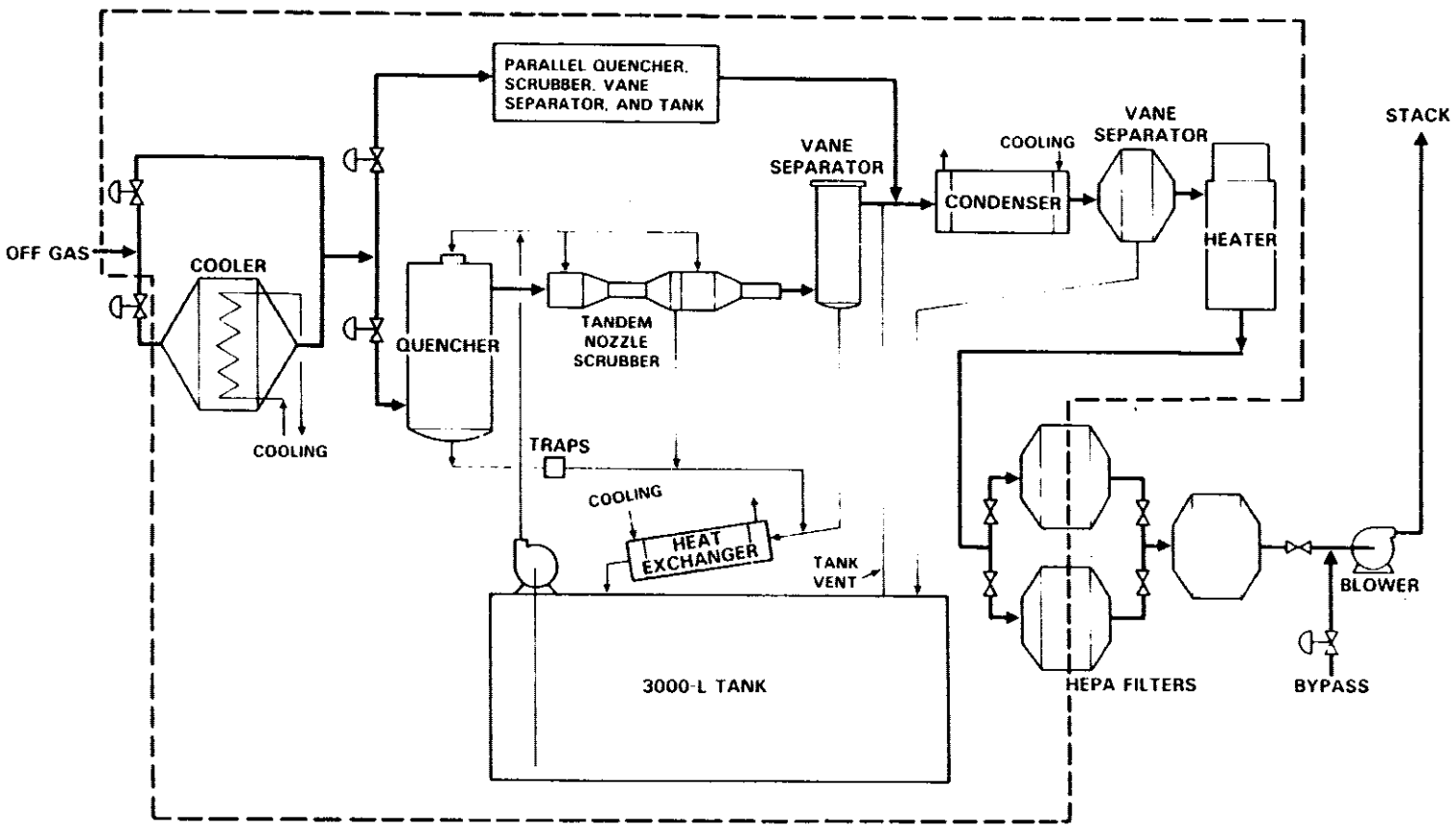

FIGURE 3. Schematic for the Large-Scale Off-Gas System

Vitrified soil blocks were analyzed to determine their chemical durability with a series of tests including 24-h soxhlet leach tests, Materials Characterization Center tests (MCC-1) (MCC 1981), and hydration. The soxhlet leach rate for all radionuclides was less than 1×10^{-5} g/cm^2/day, which is an acceptable value. A 28-day MCC-1 test was also conducted on a contaminated soil sample that was vitrified in the laboratory at 1600°C. The overall leach rate of the vitrified soil was comparable to specially developed high-level waste (HLW) glasses and other TRU waste forms. However, the normalized release rate of Pu from the vitrified soil (2×10^{-7} g/cm^2/day) was higher than the rates for the borosilicate and aluminosilicate glasses. Longer vitrification times at temperatures like those experienced in the field are expected to lower the observed Pu leach rate making it more comparable to HLW glasses. As an example of the excellent leach characteristics of field samples, TRU leach rates from the vitrified block produced during the pilot-scale radioactive test (PSRT) were too low to be detectable.

Another indication of the durability of the ISV waste form is found in a study of the weathering of obsidian, a glasslike material that is physically and chemically similar to the ISV waste form (Ewing and Hoaker 1979). In the natural environment, obsidian weathers at a rate of 1 to 20 μm^2/1000 yr (Laursen and Lanford 1978). The release of various soluble species, whose release is a measure of the depth of hydration, has been determined to be 2 μm^2/yr at 90°C. The activation energy of obsidian of 20 kcal/mole (Friedman and Long 1976) is used to determine the hydration rate of 1 μm^2/1000 yr @10°C (e.g., buried in the soil). A conservative value of 10 μm^2/1000 yr yields an estimate of 1 mm of weathered ISV waste form for a 10,000-yr time span. This suggests extremely long lifetimes for ISV waste forms, in excess of one million years.

Another important factor to consider in the waste form evaluation is the migration of the radionuclides once they are a part of the molten waste form. In the PSRT the radionuclides did not migrate beyond the vitrified block. Furthermore, analysis of the block from the test revealed that the radionuclides did not concentrate in the block, but instead were uniformly distributed. This substantiates the results from several nonradioactive tests.

Also studied was the release of radionuclides to the off gas. Retention of elements within the vitrification zone has been high during the pilot-scale and large-scale tests. Retention during large-scale ISV operations has matched or exceeded (up to a factor of 35 tons) the pilot-scale performance and large-scale predictions based on pilot-scale data because the waste elements are normally buried deeper. During large-scale ISV, soil-to-off-gas decontamination factors (DFs)[a] for less volatile elements such as Pu, Sr, and U are expected to be greater than 1×10^4. More volatile elements such as Cs have been measured with DFs greater than 1×10^2. Retention of fluorides in the vitrified product has been measured at 98.8% (DF = 83), and ISV has been shown to be an excellent destructor of nitrates, with a minimum destruction efficiency of 99.6% (DF = 250). These values vary depending on waste burial depth, the presence of a cold cap, and the presence of gas generators within the melt zone. Element retention increases with burial depth and the presence of a subsided cold cap, and it decreases with the presence of gas generators.

The high retention/destruction of radionuclides and hazardous chemicals results in only small percentages released to the off-gas system. The off-gas system for ISV has proven to be extremely effective in providing additional decontamination to meet environmental release criteria. For the large-scale system, the off-gas system DFs for Sr and Cs are 4.4×10^5 and 2.6×10^4, respectively. The performance of TRUs is expected to be similar to Sr. The mass distribution of particle sizes exiting the scrubber confirms the efficiency of the wet scrubber system below 0.5 μm. The small percentage of particulates getting through the scrubber system is generally between 0.2 and 0.8 μm, which can be easily removed by one bank of HEPA filters by a factor of 99.97% ($DF > 10^3$). The high removal efficiency of the off-gas system results in overall process DFs, when combined with the retention in the molten soil, of 1.2×10^{10} for Sr and 3.4×10^6 for Cs.

A significant development evolved from large-scale and pilot-scale testing. To enhance the subsidence of the rising cold cap experienced with 5-cm-dia Mo electrodes, a Mo/graphite combination electrode was developed.

(a) The decontamination factor is defined as the output or final mass of an element divided by the input or initial mass of the element.

This electrode design, with surface insulation, allows for the subsidence of the cold cap below the original grade without oxidation damage to the electrode. The use of 30-cm-dia graphite collars around a 5-cm-dia Mo core coated with oxidation inhibitors is expected to exceed the short-term performance criteria of 150 hours and approach the longer term performance criteria of 400 hours. This electrode design is planned to be tested during the LSRT.

Large-scale tests also proved the effectiveness of a fiber optic depth transmitter system for monitoring vitrification depth during processing. The fiber optic depth sensor technique was developed because monitoring vitrification depth by temperature probes is impractical. Laboratory tests identified the appropriate fiber optic materials and sensitivity adjustments--two important factors that ensure reliability. The fiber optic design was then verified during the most recent large-scale test.

PROCESS PARAMETERS

Parameters that affect the ISV process have been evaluated, including soil properties, site geometry, and waste type. The highlights of these evaluations are discussed below.

Soil samples from nine waste sites were analyzed and found to have little variation. Soils were tested from Barnwell, South Carolina; Hanford, Washington; Idaho National Engineering Laboratory (INEL), Idaho; Los Alamos National Laboratory (LANL), New Mexico; Maxey Flats, Kentucky; Nevada Test Site (NTS), Nevada; Oak Ridge National Laboratory (ORNL), Tennessee; Sheffield, Illinois; and West Valley Nuclear Services Co., Inc. (WVNS), New York. The fused soil properties that are most important to the operation of the ISV process are fusion temperature, specific heat, thermal conductivity, and electrical conductivity. These properties were similar to those of Hanford soils, which have been successfully vitrified during multiple engineering-, pilot-, and large-scale tests. For the soils tested, no ISV limitations due to fused soil property variations have been identified.

A mathematical model was developed as a tool to predict ISV process performance for different soil conditions and geometries. The model predicts that melt depths of 10 to 20 m are possible with a 3750-kW large-scale process,

depending on the magnitude of assumed surface heat losses. These depths are possible at a closer electrode separation of 3.5 m. As electrode separation is increased, the attainable melt depth becomes limited by the increased surface heat-loss area. At a wider separation of 6.5 m, the attainable depth ranges from 4 to 10 m, again being dependent on the heat losses.

The model predicts that an increase in the moisture content of unsaturated soil above the water table will not reduce the attainable melt depth; however, the energy and time required to vitrify the soil will increase. If the vitrification zone is below the water table, the soil must have a relatively high permeability, allowing for water recharge before the ISV depth limit is reduced significantly. Model predictions were made for ORNL soil, assuming that the water table is at ground level. The predictions show that soil moisture levels will not limit the ISV depth at ORNL, provided that areas of high permeability are not below or adjacent to the vitrification zone. Techniques are available for lowering the water table in permeable aquifers by pumping and the installation of barriers so that the attainable depth can be increased.

The performance of ISV with a variety of different types of waste has been analyzed. Waste types evaluated include metals, cements, ceramics, combustibles, sludges, hazardous organics, sealed containers, explosives, and fissile material.

Both mathematical modeling and engineering-scale testing predict that the effects of metal inclusions will be insignificant unless a full electrical short circuit between electrodes is approached. During testing, the metal limit was not reached. A metal inclusion that accounted for 5% of the final block weight and occupied 70% of the distance between electrodes was successfully vitrified. The electrode voltage was reduced 21% compared to the case when no metal was present; however, this is within the capabilities of the power supply. The large-scale ISV power system has 14 usable (16 available) voltage taps, which give the system the ability to adapt to voltage changes caused by metal inclusions of up to 90%. This makes the process applicable to metal drum and distribution pipe inclusions.

When subjected to the ISV process, soils that contain concrete or pure cement somewhat decrease the electrical conductivity of the melt zone and add

water vapor to the off-gas system. The flexibility designed into the large-scale power system compensates for any conductivity change resulting from vitrification of concrete or cement. With a design capacity of 104 std m^3/min, the large-scale off-gas system will handle water vapor and air inleakage generated during vitrification of pure cement.

Ceramic materials may not completely melt or dissolve during ISV. Nevertheless, they are effectively encapsulated by the molten glass and do not pose any process limitations.

Combustible wastes pyrolyze, move to the melt surface, and burn during the ISV process. This increases both gas volume and heat load to the off-gas system. The capacity of the large-scale off-gas system will allow for the vitrification of a variety of waste configurations. Calculations based on the off-gas release rate and attenuation experiments show that multiple combustible packages including sealed containers, each as large as 0.9 m^3, and multiple void volumes up to 4.3 m^3 each can be processed without loss of hood vacuum. Multiple combustible package and void volumes are allowed in each setting because the off-gas release associated with each inclusion is limited to the short duration of the total processing time. If combustibles are distributed relatively evenly throughout the soil, the off-gas system is capable of handling gases from soil that contains 3200 kg of combustibles per meter of depth.

A zirconia/lime sludge was successfully vitrified during both bench-scale and pilot-scale testing, thereby demonstrating the applicability of ISV to a nonsoil waste (Buelt and Freim 1986). The pilot-scale ISV system melted the sludge to a depth of 3 m, significantly reducing its volume and driving the 55- to 70-wt% moisture from the sludge. Analysis of the off-gas data shows that the retention of fluorides, chlorides, and sulfates and the destruction of organics and nitrates were extremely high, thus minimizing the requirements of an off-gas treatment system. Also, the waste form produced from Ra-bearing sludges reduces the Rn emanation rate by more than three orders of magnitude.

The engineering-scale ISV system was tested to illustrate the capabilities of the ISV process on soils contaminated with hazardous polychlorinated biphenyls (PCBs) (Timmerman 1986). The ISV process exhibited a destruction

removal efficiency (DRE) for PCBs of greater than 99.9%, exclusive of the off-gas treatment. The overall DRE can be expected to exceed 99.9999%. Only 0.05% of the organic was detected in the off-gas system. The soil surrounding the vitrified block contained 0.0 to 0.7 ppm of PCBs, much less than the 500-ppm concentration that was originally added. The highest concentration (0.7 ppm) was adjacent to the vitrified block, as expected, indicating that migration away from the block is neglibile. As a result of this test it is apparent that ISV holds promise for application at selected hazardous waste sites.

In situ vitrification changes the geometry and moderation characteristics of a burial site. When fissionable materials are present in the site, it is important to determine the effects of ISV on criticality potential ($k_{effective}$). The study of the effects of ISV on the criticality potential of various TRU waste sites indicates the following:

- No credible concentration mechanism for ^{239}Pu or any other fissionable nuclei has been identified.
- As long as a waste site to be vitrified has an areal concentration of <1.0 kg Pu/m^2, it should be able to be safely stabilized by ISV. For safety reasons, these limits are set at 33% of the minimum critical values.

ECONOMIC ANALYSIS

The cost of using ISV as an in-place stabilization technique was estimated and is presented in this report. The estimate uses an extensive base of experience for reliable cost numbers and represents updated estimates from those provided in previous reports (Oma et al. 1983; Buelt, FitzPatrick, and Timmerman 1986).

The components that contribute to the cost of ISV are site preparation activities, annual equipment charges, operational costs such as labor, and consumable supplies such as electricity and electrodes. The costs of vitrifying three different types of waste (TRU-contaminated soil, soil contaminated with

hazardous chemicals, and wet industrial sludge) are presented as functions of electrical rates. The costs of vitrifying contaminated soils at varying moisture contents are also presented.

Transuranic-contaminated soil sites can be vitrified for a total cost that ranges from $\$227/m^3$ to $\$286/m^3$ ($\$173$ to $\$219/yd^3$) of soil vitrified. The costs are reduced to a range of $\$183/m^3$ to $\$247/m^3$ ($\$140/yd^3$ to $\$189/yd^3$) for hazardous chemical waste due to reduced off-gas system and labor constraints. Wet industrial sludges with 70% moisture content can be volume-reduced by ISV for a cost of \$70 to $\$120/m^3$ ($\$53$ to $\$92/yd^3$). The costs of additional electrical energy and increased processing time to vitrify wet soils are the principal factors that govern the range of costs for each waste type. However, the effect on the maximum attainable geometric limits of ISV is small. Soil moisture is an economic consideration, not a process impediment. In the case of swelling, wet industrial sludges, the extremely high-moisture-content sludges (e.g., 70 wt% water) can be vitrified at a significantly reduced cost since these types of sludges generally possess a lower bulk density and a high volume reduction characteristic when treated, processing costs on a volumetric basis are greatly reduced.

ANALYSIS OF OCCUPATIONAL AND PUBLIC SAFETY

To analyze the occupational and public safety of routine and nonroutine ISV operations for both the short and the long term, a representative waste site was selected as a reference (Oma et al. 1983). Radionuclide release rates from the soil during vitrification were estimated. Ten times the waste inventory for the tile field reported by Owens (1981) was the basis for the radionuclide source term to account for concentrated TRUs around the distribution pipe(s).

Tables 1 and 2 give the radiation doses from routine operations in the short term for the ISV worker and the public, respectively. For all routine exposures, radiation doses are estimated to be well below the federal guidelines set by the DOE. Of all activities associated with ISV operations, the maximum occupational dose is expected to occur while the worker is placing electrodes in the soil. The low exposure levels can be seen in Table 1, where

TABLE 1. Whole Body Radiation Doses from Routine Operations

Occupational Dose (Electrode Emplacement)
- All workers: 0.09 man-rem
- Maximum-exposed worker: 0.01 rem

Natural Background
- Exposure rate: 7 μR/h
- Total (1880 h): 0.01 rem

TABLE 2. Public Dose Commitments from Routine Operations (critical organ)(a)

	Max. Exposed Indiv., rem	Population, man-rem
1st-yr dose (lungs)	3×10^{-8}	9×10^{-3}
50-yr dose (bone)	1×10^{-5}	5×10^{-1}

(a) The critical organ is the organ that receives the highest dose.

the occupational dose for this activity is compared to the dose that would be received during the same time period from natural background. The maximum-exposed worker would receive a dose that is roughly the same as background radiation. The doses calculated for ISV operation at this reference site are substantially below the DOE regulations on exposure for routine operations to both workers and the general public [DOE Order 5480.1A, Chapter 11 (U.S. DOE 1981a)].

Abnormal exposures for both the ISV worker and the public from the vitrification process were calculated using postulated accident scenarios. The most serious abnormal condition is a break in the off-gas line. For the specific exposures calculated see Tables 3 and 4. For the break in the off-gas line scenario the maximum individual dose to a member of the public was estimated to be 0.3 rem or about 3 times the average annual dose from natural background radiation from which no adverse effects would be expected.

TABLE 3. Occupational Doses from Accidental Releases (120-h run, 15 settings, concentrated inventory)

Accident	Number of Personnel	Length of Exposure	1st-Year Dose Commitment to Each Worker, rem		
			Total Body	Bone	Lung
Uncontrolled venting	1	1 min	1×10^{-3}	2×10^{-2}	2×10^{0}
Break in off-gas line	1	5 min	6×10^{-3}	1×10^{-1}	1×10^{1}
Excess overburden removal	2	10 min	3×10^{-3}	4×10^{-2}	5×10^{0}

TABLE 4. Public Dose Commitments from Postulated Abnormal Occurrences

	Maximum Exposed Individual, rem	Population, man-rem
Uncontrolled Venting		
1st-yr dose (lungs)	5×10^{-5}	2×10^{-1}
50-yr dose (bone)	5×10^{-4}	2×10^{0}
Off-Gas Line Break		
1st-yr dose (lungs)	3×10^{-2}	1×10^{2}
50-yr dose (bone)	3×10^{-1}	1×10^{3}
Excessive Overburden Removal		
1st-yr dose (lungs)	1×10^{-2}	3×10^{1}
50-yr dose (bone)	9×10^{-2}	3×10^{2}

ASSESSMENT OF WASTE SITE APPLICATIONS

Testing the ISV process with simulated radioactive and hazardous chemical components indicates that the technology is also highly applicable to mixed radioactive and hazardous chemical wastes. While immobilizing the radionuclide portion of mixed wastes, the process also fixes fluorides and heavy metals and destroys organic and nitrate chemicals at high efficiencies. Mixed waste applications are applicable not only to contaminated soil sites, but to residual heels of underground tanks, classified waste in containers, and process sludges as well.

Many of the process limitations identified for TRU and mixed wastes are extended to hazardous chemical waste applications. However, the applicability of ISV has three important additional benefits: 1) handling operations of the waste before treatment are simplified allowing for more cost-effective operational alternatives for the ISV process, 2) ISV potentially converts hazardous materials to a nonhazardous classification by altering the chemical compound which results in delisting the waste, and 3) extended liability to the hazardous waste generator is reduced.

The overall conclusion derived from this study is that the technology has been developed sufficiently to conduct the LSRT at a TRU-contaminated soil site. The radioactive test is necessary to confirm process behavior under actual conditions, and so that a long-term performance assessment of the waste form can be performed.

ACKNOWLEDGMENTS

The authors acknowledge the Department of Energy for providing the opportunity for Pacific Northwest Laboratory to develop in situ vitrification (ISV) technology. Many fellow scientists and technicians contributed to the research effort. The list below includes individual contributors and their areas of expertise:

Dr. Will Barry[a] - Nitrate Analysis
J. Beale[b] - Large-Scale Fabrication
R. A. Brouns - ISV Tests
D. R. Brown - Economic Analysis
R. K. Farnsworth - ISV Tests
F. T. Hara - Analytical Chemistry
K. A. Hawley - Safety Analysis
T. D. Hinkle - ISV Tests
C. R. Hymas - ISV Tests
J. T. Jeffs - ISV Tests
N. Karagianes[c] - Programmatic Review and Support
Y. B. Katayama - Product Durability
R. A. Libby - Criticality Analysis
S. C. Liikalla - ISV Tests
M. L. Longaker - ISV Tests
C. L. Matsuzaki - Analytical Chemistry
P. J. Mellinger - Safety Analysis
B. A. Napier - Safety Analysis
R. N. Rogers[d] - Explosive Inclusion Analysis
J. L. Ryan - Chemistry of Plutonium in Glass
D. J. Silviera - Safety Analysis
J. K. Soldat - Safety Analysis
S. L. Stein - Safety Analysis

(a) From Gonzaga University, Spokane, Washington.
(b) From A. J. Zinda Co., Portland, Oregon.
(c) From U.S. Department of Energy, Richland, Washington.
(d) From Los Alamos National Laboratory, Los Alamos, New Mexico.

L. A. Stout - Safety Analysis

E. C. Watson - Safety Analysis

C. C. Wentz and his staff - Maintenance Services

Substantial effort has been expended in editing, typing, and coordinating the production of this report. We appreciate the contributions of the following people:

S. K. Ennor, Editor

B. D. Gottsch, Word Processing Coordinator

P. Goodenough, Word Processor

D. A. Perez, Word Processor

J. A. Richelieu, Word Processor

J. M. Zama, Word Processor

CONTENTS

FIGURES

TABLES

INTRODUCTION

INTRODUCTION

Pacific Northwest Laboratory (PNL) is developing a remedial action process for contaminated soils that could be potentially significant in enhancing in-place stabilization of these wastes. The process is in situ vitrification (ISV). It is being developed for the U.S. Department of Energy (DOE) with emphasis on TRU-contaminated soils. It is expected that with some additional development and/or feasability testing the process could also be applied to a wide variety of chemical waste sites.

In situ vitrification is a thermal treatment process that converts contaminated soil to a chemically inert and stable glass and crystalline product. Figure 4 illustrates how the process operates. A square array of four Mo electrodes is inserted into the ground to the desired treatment depth. Because soil is not electrically conductive when its moisture has been driven off, a conductive mixture of flaked graphite and glass frit is placed among the electrodes to act as a starter path. An electrical potential is applied to the electrodes to establish an electrical current in the starter path. The

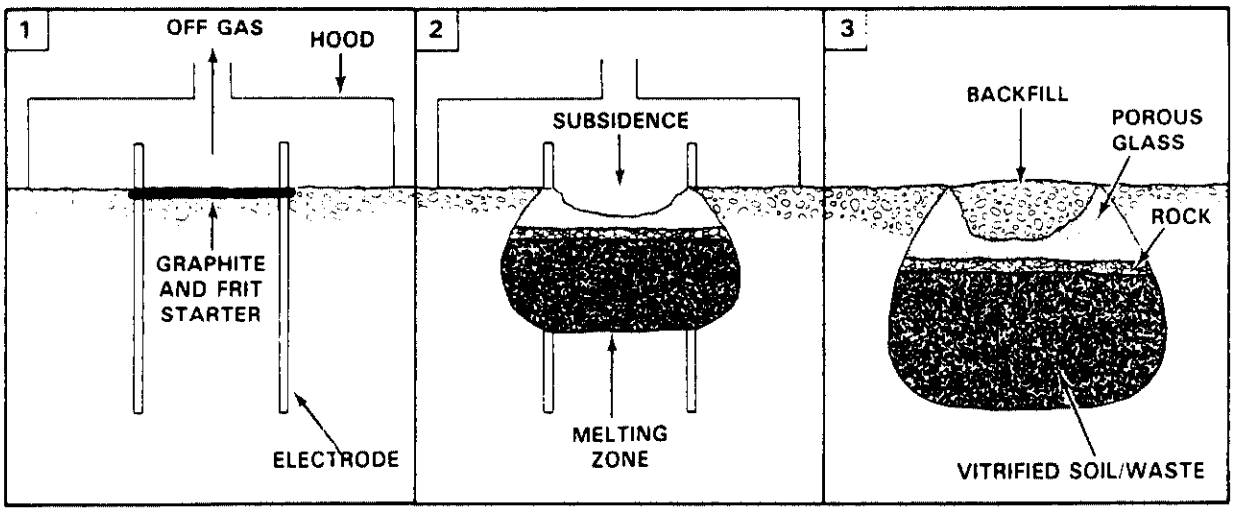

FIGURE 4. The Process of In Situ Vitrification

resultant power heats the starter path and surrounding soil initially to 2000°C, well above soil-melting temperatures of 1100 to 1400°C. The graphite starter path is eventually consumed by oxidation, and the current is transferred to the molten soil, operating between 1450 and 1600°C. As the molten or vitrified zone grows, it incorporates any radionuclides and nonvolatile hazardous elements, such as heavy metals, that may be present. The high temperature of the process destroys organic components by pyrolysis. The pyrolyzed byproducts migrate to the surface of the vitrified zone, where they combust in the presence of air. A hood placed over the area being vitrified directs the gaseous effluents to an off-gas treatment system, if necessary.

Pacific Northwest Laboratory began developing ISV technology in 1980 under contract to the DOE. Since that time, numerous experimental tests under a variety of conditions and with a variety of waste types have been conducted (Oma et al. 1983, Timmerman and Oma 1984, Timmerman et al. 1983, Buelt and Carter 1986a). Table 5 describes the different scales of testing units that PNL uses in developing and adapting ISV technology. The successful results of 38 engineering- and pilot-scale tests have proven the feasibility of the process. Also, economic studies have indicated that tremendous economies of scale are attainable with the ISV process (Oma et al. 1983). Successful radioactive testing of the large-scale ISV process will provide the developmental information necessary to demonstrate process applicability to TRU-contaminated soils on a production scale.

TABLE 5. Testing Units for Developing ISV Technology

Equipment Size	Electrode Separation	Block Size	Tests Completed
Bench Scale	0.11 m	1 to 10 kg	4
Engineering Scale	0.23 to 0.36 m	0.05 to 1.0 t	24
Pilot Scale	1.2 m	10 to 50 t	14
Large Scale	3.5 to 5.5 m	400 to 800 t	4

The decision to proceed with the design, fabrication, and testing of the large-scale unit was made on the basis of the extensive data base collected from engineering- and pilot-scale tests. The pilot-scale unit was used to demonstrate the process with radioactively spiked soils in direct support of the decision to proceed with the large-scale system design and fabrication. Tests have been conducted subsequently with the bench-, engineering-, and pilot-scale units to determine processing behavior under various waste conditions and to develop improved operational techniques. Table 6 summarizes all of the major developmental tests conducted during the six-year life of ISV technology.

The large-scale process equipment has been fabricated and installed, and the large-scale operational acceptance tests (LSOATs) and a large-scale verification test (LSVT) have been completed. The objective of the LSOATs was to verify conformance of the process characteristics to the established functional design criteria relevant to the large-scale radioactive test (LSRT). The LSVT was performed to verify the effectiveness of process modifications identified during the LSOATs in readying the process for radioactive testing.

This report is intended to serve as the updated base technology document for ISV. It updates the previous technology base document authored by Oma et al. (1983). Consequently, the relevant information presented in that document is repeated here. However, many technological advances have been made during the last three years, not the least of which is the design, fabrication, and testing of the large-scale system. The Process Description section of this report describes the large-scale process and other developmental units. The Performance Analysis section presents a comprehensive analysis of the performance of the process equipment, retention of elements in the vitrified soil during processing, melt geometry, depth monitors, and electrodes. The Process Parameters section provides an evaluation of the types of soils and wastes that can be processed by ISV. The Economic Analysis section provides the estimated production costs of the large-scale unit for radioactive and hazardous chemical

TABLE 6. Summary of Results of Developmental ISV Units

Bench-Scale

Test	Objectives	Results
BST-1[a]	Determine feasibility of ISV on 10-cm electrode separation	Successful, Hanford soil vitrified
BST-2	Determine volume and mass reduction potential of ISV on wet industrial sludge	Successful, lime sludge vitrified
BST-3	Determine feasibility of immobilizing nickle-contaminated soils	Successful test
BST-4	Determine feasibility of immobilizing cyanide-contaminated soils	Successful test

Engineering-Scale

Test	Objectives	Results
ESLT-1[b]	Verify concept feasibility	Successful vitrification of 130 kg of soil
ESLT-2	Vitrify simulated waste box	Incomplete test: electrode extension failed
ESLT-3	Vitrify simulated waste box	Successful test
ESLT-4	Evaluate test startup techniques	Surface startup successful in reducing CO generation
	Evaluate soil moisture effects	Performance not limited by increased moisture
ESLT-5	Obtain heat transfer data	Data confirms predictions
	Evaluate void formation	Voids caused by subsidence of molten soil from cold cap
ESLT-6	Test graphite electrodes	Incomplete test: electrical connection failure
ESLT-7	Test graphite electrodes with improved electrical connection	Successful test
ESLT-8	Test Na additions to increase soil conductivity	Sodium in soil too conductive; melt zone would not grow

TABLE 6. (contd)

Test	Objectives	Results
ESLT-9	Test graphite electrodes and vitrify simulated contaminated soil	Successful test
ESLT-10	Vitrify metal container (35% of full electrical short)	Successful test
ESLT-11	Vitrify simulated waste can of combustibles	Successful test
ESLT-12	Vitrify metal containers (70% of full electrical short)	Successful test; no limit imposed by 5 wt% metal occupying 70% of full electrical short
ESLT-13	Vitrify metal canister using increased power	Successful test
ESLT-14	Vitrify concrete canister	Successful test
ESLT-15	Vitrify concrete and cement monoliths	Successful test; no limits identified
ESLT-16	Test Scott-Tee (Lazar 1977) power system	Successful test
ESLT-17	Test saturable reactor power control	Successful test
ESLT-18	Test controller multi-tapped Scott-Tee power system	Successful test
ESLT-19	Test ISV performance at large depth to electrode separation ratios for model calibration	Successful test
ESLT-20	Test SiC, TiC, and Ta graphite electrode coatings	Coatings effective unless first exposed to molten soil
ESLT-21	Test SiC graphite electrode coatings applied by different techniques	Coatings effective unless first exposed to molten soil
ESLT-22	Determine feasibility of vitrifying soils contaminated with heavy metals and organics	Successful, product passes proposed EPA[c] product quality standards
ESLT-23	Determine feasibility of vitrifying PCB-contaminated soil	Successful, overall DRE[d] of greater than 99.9999% attained
ESLT-24	Determine feasibility of vitrifying a simulated waste trench with dolomite backfill	Successful test

TABLE 6. (contd)

Pilot-Scale

Test	Objectives	Results
PSFT-1[e]	Verify process scale-up	Successful vitrification of 5670 kg of soil
PSFT-2	Evaluate migration and volatilization of simulated hazardous species	No migration outside of vitrified zone and very low element volatilizations
PSFT-3	Vitrify 208-L (55-gal) waste drum containing soil and simulated combustible wastes	Successful vitrification of drum and contents. Temporary system shutdown due to high off-gas particulate loading. Successful restart on one pair of electrodes.
PSFT-4	Test two side-by-side vitrification operations (PSFT-4A and PSFT-4B)	Successful vitrification of 25,400 kg of soil
	Vitrify various combustible and noncombustible waste packages	Successful test
PSCT-1[f]	Vitrify simulated waste package	Successful vitrification of waste package. Off-gas system maintained total containment of volatile elements.
	Perform operator training and equipment checkout	Identification of items requiring upgrade.
PSCT-2	Vitrify simulated waste package	Successful test of system upgrade
	Verify correct operation of system upgrade	
PSRT[g]	Vitrify a makeup site containing known quantities of radionuclides	Successful vitrification with no release of radioactivity
PSCT-3	Determine long-term (5-day) performance of Mo electrodes	Electrodes performed extremely well but produced rising cold cap
PSCT-4	Verify performance of graphite collars around Mo electrodes with insulated surface as cold cap subsidence technique	Cold cap subsidence was effectively attained; however, significant oxidation to Mo electrode was noted
PSCT-5	Verify performance of $ZrB_2/MoSi_2$ sintered powder as Mo oxidation barrier in graphite/Mo combination electrode	Successful in regions greater than 2 ft below original soil surface

TABLE 6. (contd)

Test	Objectives	Results
CCT-1[h]	Duplicate rising cold cap phenomenon on parametric scale (0.16-m electrode separation) with pilot-scale equipment using Mo electrodes	Successful, rising cold cap formed
CCT-2	Determine effectiveness of graphite collars on cold cap subsidence on parametric scale	Cold cap subsidence attained
CCT-3	Determine effectiveness of graphite collar and surface insulation on cold cap subsidence	Cold cap subsidence attained
PSLW-1[i]	Determine volume reduction potential of ISV on wet industrial sludge using pilot-scale equipment	High volume reduction achieved with lime sludge

Large-Scale

Test	Objectives	Results
LSOAT-1[j]	Verify operational performance of large-scale unit using Mo electrodes	Rising cold cap experienced. Off-gas system equipment performed satisfactorily with minor modifications.
LSOAT-2	Verify operational performance of large-scale unit using Mo electrodes and surface insulation	Low scrubber system efficiency attained. Cold cap subsidence moderately improved.
LSOAT-3	Verify operational performance incorporating scrubber modifications and Mo/graphite combination electrode	Retention of simulated radionuclides improved to above acceptable standards. Cold cap subsidence obtained, but electrode failures experienced. Electrode recovery technique demonstrated.
LSVT-1[k]	Simulate large-scale verification test and verify performance	Cold cap subsidence obtained and off-gas system performed as expected, but electrode failures experienced

(a) BST - Bench-Scale Test
(b) ESLT - Engineering-Scale Test
(c) EPA - Environmental Protection Agency
(d) DRE - destruction removal efficiency
(e) PSFT - Pilot-Scale Field Test
(f) PSCT - Pilot-Scale Cold Test
(g) PSRT - Pilot-Scale Radioactive Test
(h) CCT - Cold-Cap Test (Pilot Scale)
(i) PSLW - Pilot-Scale Lime Test
(j) LSOAT - Large-Scale Operational Acceptance Test
(k) LSVT - Large-Scale Verification Test

wastes, both wet and dry. The testing of ISV on a TRU-contaminated soil is discussed with respect to dose consequences in the Analysis of Occupational and Public Safety section. The report concludes with a Waste Site Applications Assessment that identifies alternative applications and operating sequences for various waste sites.

CONCLUSIONS

CONCLUSIONS

The technology base developed during the six years of development of the ISV process is extensive. A wide variety of scales of equipment, site parameters, and waste inclusions has been tested to initiate technology transfer and commercialization of the process. The ISV process has been broadly patented within the United States, Canada, Great Britain, and France. Battelle, who operates PNL for the DOE, holds a partially exclusive license to those patents: Battelle has exclusive worldwide rights to all ISV technology except for radioactive waste applications of ISV. The technical data presented in this report provide the basis for establishing the performance of the system and waste form, economics and safety, and waste site applications for radioactive wastes, hazardous chemical wastes, barriers, and soil stabilization.

SYSTEM AND WASTE FORM PERFORMANCE

- The minimum estimated depth limit of the large-scale ISV system is 10 m, independent of moisture content. Model predictions show that melt depths in excess of 20 m are attainable. The electrode separation, which determines maximum melt depth, can be adjusted from 3.5 to slightly over 6 m, although the existing large-scale system is designed for a maximum electrode separation of 5.5 m; the 3.5-m separation is required to obtain maximum depth. The demonstrated peak flow capacity of the off-gas treatment system is 116 std m^3/min; 104 std m^3/min is more than adequate to contain gaseous releases from buried combustibles and sealed containers.
- Radionuclides and heavy metals are retained within the melts and nitrates and organics are destroyed during processing sufficiently to meet emission standards for the off-gas treatment system. Areas of high concentration of radionuclides are diluted and distributed in the melt by convection currents. When gas venting occurs when the molten glass encounters contaminated combustibles, only small quantities of contaminants associated with the combustibles are available for release to the off-gas system. Those releases are

acceptably low. Large-scale process tests have achieved higher retention/destruction efficiencies in the molten soil because of greater buried depths that are typical of most waste sites.

- An off-gas treatment system is included in the process to remove the small percentage of contaminants from the gaseous effluents that escape from the vitreous mass during processing. The pilot- and large-scale systems perform admirably in the removal of radionuclide and heavy-metal particulates and semivolatiles, SO_x gas, and fluoride particulates. For example, the off-gas system removal efficiency enhances the natural ability of the vitreous block to retain/destroy contaminants, thereby coming well within the environmental criteria for principal radionuclides at a TRU burial site (Buelt and Carter 1986b). With the combination of the off-gas system and retention characteristics in the soils the combined DF results in maximum stack concentrations for a highly contaminated TRU site that are below the maximum permissible limits published in Attachment XI-1, DOE Order 5480.1A (1981a) (see Table 7).

- A depth transmitter system has been developed to be used for economical and reliable monitoring of the vitrification zone depth. It can be installed with one of the electrodes. The system consists of a series of sensors attached along the length of an electrode and connected to a transmitter device at the bottom of the electrode. During the ISV operation, sensors detect the molten glass and transmit the information to an above-ground receiver, thus giving an operator the melt depth information. The system has been

TABLE 7. Maximum Stack Concentrations of ^{239}Pu, ^{240}Pu, and ^{241}Am and Their Maximum Permissible Concentrations

Transuranic	Maximum Stack Concentration, μCi/mL	Maximum Permissible Concentration, μCi/mL
^{239}Pu	1.8×10^{-14}	1×10^{-12}
^{240}Pu	4.6×10^{-15}	1×10^{-12}
^{241}Am	7.5×10^{-14}	4×10^{-12}

successfully tested, but only specific types of fiber optics are compatible with the ISV process. In addition, sensitivity adjustments of the sensor electronics must be set within the 25- to 40-μA range to ensure reliable performance.

- A reference electrode design, shown in Figure 5, has been established for future ISV applications. This design employs a Mo/graphite combination to promote subsidence of the surface of the melt below the original soil grade. In the event of complete oxidation of the graphite collar, which is not expected for a 30-cm-dia collar, two additional barriers are included to prevent oxidation of the Mo electrode. The first is an electrically conductive powder in the annulus that sinters, leaving a protective surface coating on the Mo electrode (primary candidates are 88% ZrB_2/12% $MoSi_2$ and $MoSi_2$), and the second is a fused or controlled-atmosphere plasma spray coating of the same powdered materials. This electrode design is expected to last beyond the 150-h short-term criteria and 400-h long-term performance requirements for the ISV process. Studies are recommended, however, to develop a less costly electrode material, since the cost of electrodes composes up to 40% of the total operational costs.

- Experimental evidence shows that the large-scale system is representative of the more efficient version of the mathematical model used for large-scale predictions--the low-heat-loss model. However, the actual vitrified block is generally less deep, but wider, than predicted. This is not expected to limit the 13-m criteria established for the large-scale system. In fact, conformance to the low-heat-loss model indicates that vitrification depths in excess of 20 m are attainable. The LSRT will help determine whether shallower melt shape is caused by conducting tests in partially disturbed soil or by failed electrodes that were not extended to the entire vitrification depth. Fluid dynamic modeling will also be considered to assess these effects.

- Metal inclusions do not significantly affect ISV unless a full electrical short circuit is approached. In situ vitrification tests have

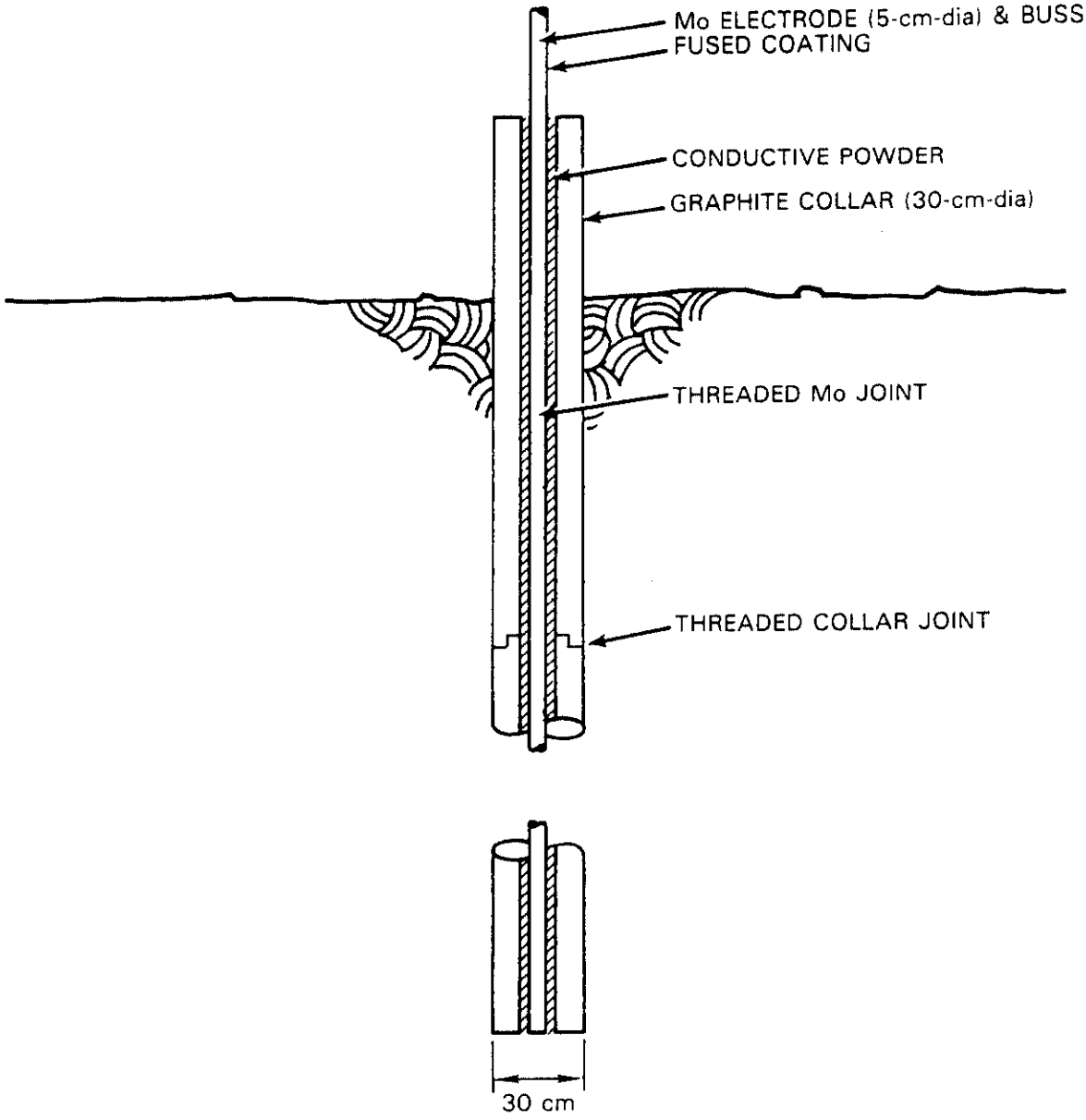

FIGURE 5. Reference Electrode Design

demonstrated that metal occupying more than 70% of the electrode spacing and 5% of the final block weight can be successfully vitrified. Although the upper limit has not been identified, the correlation of the data indicates that up to 90% of the electrode

separation may be occupied by metal. The process is therefore adaptable to large amounts of metal inclusions such as pipes, well casings, and 208-L (55-gal) drums.

- Cement inclusions are completely dissolved within the glass waste form. Cement and concrete inclusions within a waste site fracture as they are heated during ISV. Strong convective currents within the melt promote distribution and dissolution of the fragmented pieces.
- In situ vitrification is capable of processing various soil types throughout the United States. Soils from nine different U.S. locations were found to be similar in the properties that could affect the ISV process. Minor soil modifications may be necessary for high-viscosity soils by using small amounts of chemicals that produce Na_2O or CaO.
- Transuranic waste sites with areal concentrations of <1.0 kg Pu/m^2 can be vitrified safely without a criticality. Sites that contain hydrogenated organics in waste containers are limited to an areal concentration of <0.8 kg Pu/m^2.
- No credible concentration mechanism for ^{239}Pu or other TRU fissionable isotopes has been identified. The ISV melt zone has strong convective currents that promote dilution and thorough mixing of waste species.
- Leachability of vitrified soil from Hanford is estimated to be $<1 \times 10^{-5}$ g leached/g solid/yr, based on MCC-1, 28-day leach data and a nominal fractured size of 15 cm on a side. Weathering of obsidian, the natural analog of vitrified soil, is limited to 20 to 10 μm^2/1,000 yr. Experimental data from the ISV waste confirms these rates. At these rates, the ISV waste form could be expected to exceed a one-million-year lifetime.

ECONOMICS AND SAFETY

- Operational and consumable costs such as those for electrodes, labor, and electrical energy are dominant, accounting for >80% of the total processing cost. Other cost elements are site preparation activities and annual equipment charges.
- Soil sites contaminated with TRUs can be vitrified for a total cost ranging from $\$227/m^3$ to $\$286/m^3$ ($\$173$ to $219/yd^3$) of soil vitrified. The costs are reduced to a range of $\$183/m^3$ to $\$247/m^3$ ($\$140/yd^3$ to $\$189/yd^3$) for hazardous chemical wastes due to reduced off-gas system and labor constraints. Wet industrial sludges with 70% moisture content can be volume-reduced by ISV for a cost of $70 to $\$120/m^3$ ($\$53$ to $\$92/yd^3$). The costs of electrical power and increased processing time to vitrify wet soils are the principal factors governing the range of costs for each waste type.
- Soil moisture increases the time and power required to vitrify a waste site; however, the effect on the maximum attainable geometric limits of ISV is small. Soil moisture is an economic penalty, not a process impediment. In the case of swelling, wet industrial sludges, extremely high-moisture-content sludges (e.g., 70 wt% water) can be vitrified at the same energy consumption as dry soils.
- Public and occupational exposures for routine operations are acceptably low. The 1st-year dose commitment for the maximum-exposed individual is 3×10^{-8} rem, and the 50-year dose commitment is 1×10^{-5} rem. The maximum occupational dose is 0.01 rem.
- Occupational doses for postulated abnormal occurrences range from 2 to 10 rem. Public dose commitments for these same scenarios range from 5×10^{-5} to 3×10^{-2} rem for the first-year dose to the maximum-exposed individual.

APPLICATION OF IN SITU VITRIFICATION

- In situ vitrification is an emerging technology that, when selectively applied, can be an economical and highly effective in-place waste disposal option.
- The process is ready for deployment to soil sites that are contaminated with heavy metals and nonradioactive inorganics. Feasibility testing is required, however, for each potential application to determine the performance requirements of the off-gas treatment system and to determine the type and quantity of secondary waste generated.
- Experience with uncontained, low-boiling-point organics is limited, and extensive feasibility testing is recommended to determine the extent of destruction and migration away from the site and to develop methods, if necessary, to improve destruction and decrease migration.
- Experience with PCBs, process sludges, and soils contaminated with plating wastes indicates that only limited feasibility testing is required prior to adaptation of ISV technology.
- The process is highly applicable to industrial process sludges that have high moisture content (up to 70 wt%) as a volume reduction method. Use of alternative operational sequences by transporting sludge to within the confines of the electrodes applies the process more cost-effectively than standard operation when high volume reduction potential exists.
- With the ISV process being tested in field (large-scale) conditions, the risks of scale-up, which is the major risk area of developing and deploying a new technology, have been eliminated. The applicability of the ISV process to a particular waste using existing ISV equipment can be determined with a significantly reduced level of effort than required for development of the technology. Thus, feasibility testing is relatively inexpensive.

- Application of ISV to hazardous chemical wastes converts the waste to a potentially delistable waste form. This would reduce long-term liability of the generator.
- In situ vitrification holds potential application for groundwater and intrusion barriers. Barriers offer an alternative to complete vitrification of a site by forming a solid wall to divert groundwater flow or to act as a containment device against migration of hazardous components out of a site. Barrier formations offer a long-term solution that is competitive with slurry walls.
- In situ vitrification may also be used for selected soil stabilization options (erosion barriers, slope stabilization, simulated building materials, etc.), especially in remote or cold weather regions where aggregate, cement, and conventional building materials are very costly.
- It is anticipated that the ISV process can be used for a broader application of waste management problems. It is also recognized that no single treatment process is applicable to all waste management needs. Within this context, ISV is a new and powerful tool that should be considered and evaluated for radioactive, mixed hazardous, and hazardous chemical applications that fall within the treatment capabilities of the process.

In conclusion, the technological data base is sufficiently developed to warrant conducting a LSRT at a contaminated soil site as planned. The test will provide a representative waste form that can be evaluated to determine its suitability for in-place stabilization of TRU-contaminated soils.

PROCESS DESCRIPTION

PROCESS DESCRIPTION

Development and deployment of the large-scale ISV system is the ultimate goal of the ISV program, because it is less costly to operate, and it is more adaptable to numerous types of waste sites than the pilot-scale system. The cost of vitrifying a given waste volume with the large-scale system is one-seventh that of the pilot-scale system. The large-scale system is more adaptable because its high-capacity off-gas system, which can process off gas at a rate of 104 std m^3/min, is better equipped to contain sudden gaseous releases from combustible and other gas-generating wastes. Nevertheless, the pilot-, engineering-, and bench-scale systems provide important data that are used to determine the performance of the large-scale system at a significantly reduced development cost. All four development units are described in this section.

LARGE-SCALE SYSTEM

The large-scale system described in this section is designed to vitrify contaminated soils with an electrode separation of up to 5.5 m on a side. The specific process description is for a system that could be applied to highly contaminated portions of TRU-contaminated soil sites, caissons, and solid waste burial sites. The ISV large-scale process equipment is shown in Figure 6.

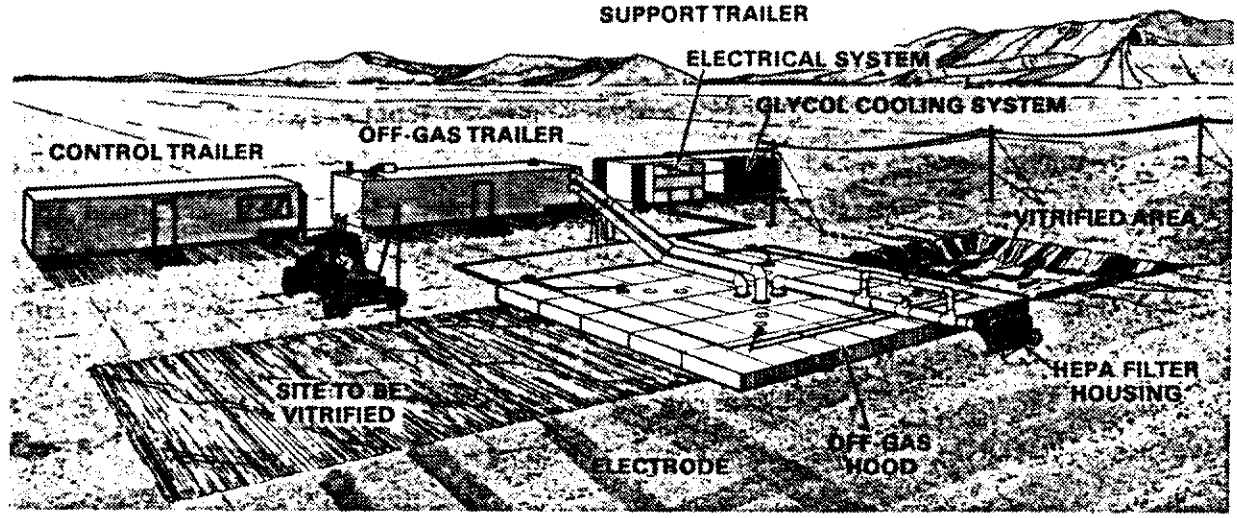

FIGURE 6. Large-Scale Process Equipment for In Situ Vitrification

Controlled electrical power is distributed to the electrodes, and special equipment contains and treats the gaseous effluents. The process equipment required to perform these functions can be described most easily by dividing it into six major components:

- electrical power supply
- off-gas hood
- off-gas treatment system
- glycol cooling system
- process control station
- off-gas support equipment.

Except for the off-gas hood, all of the components are contained in three transportable trailers, as shown in Figure 7. They consist of an off-gas trailer, a process control trailer, and a support trailer. All three trailers are mounted on wheels to accommodate a move to any site over a compacted ground surface. The off-gas hood and off-gas line, which are installed on the site to collect gaseous effluents, are dismantled and placed on a flat-bed trailer for transport. The effluents exhausted from the hood are cooled and treated in the off-gas treatment system. The entire process is monitored and controlled from the process control station. Buelt and Carter (1986b) provide a detailed description and design basis for the process, but a brief summary is also provided here.

Power System

The power system for the ISV process uses a Scott-Tee transformer connection to convert three-phase electrical power to two single-phase loads (Lazar 1977). Each single-phase load is connected to two electrodes, arranged in a square pattern, as shown in Figure 8. The Scott-Tee transformer was selected on the basis of its even distribution of current within the molten soil, which produces a vitrified product almost square in shape to minimize the overlap between adjacent settings. The connection has been employed during pilot- and engineering-scale tests and is commonly used in the glass industry.

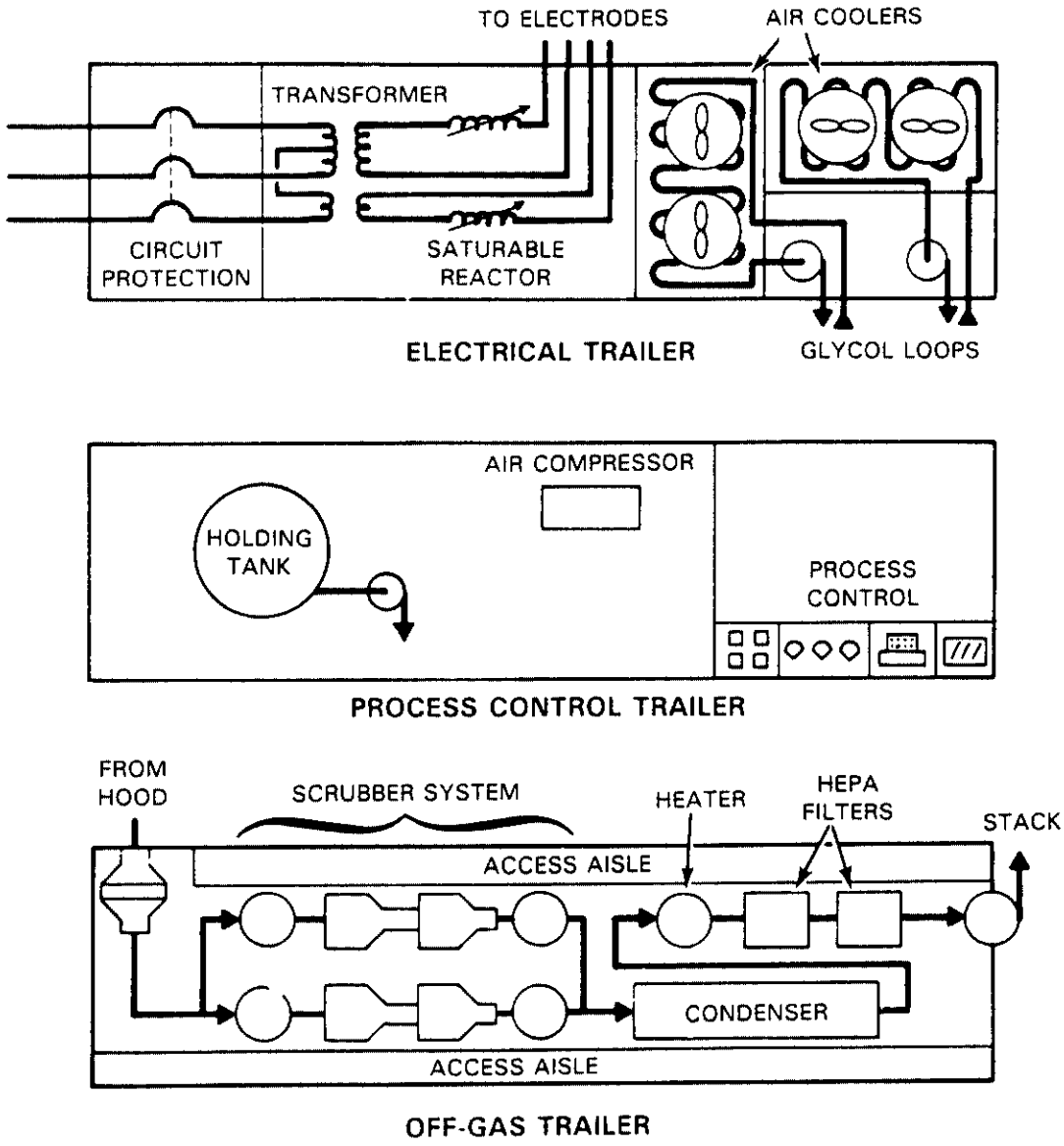

FIGURE 7. Process Trailers for Large-Scale In Situ Vitrification

The vitrification zone continually grows as the ISV process is supplied with power. This creates a constantly changing voltage/current relationship, which requires multiple voltage taps on the Scott-Tee transformer. The multiple taps allow for more efficient use of the power system by maintaining the power factor (the phase relationship between current and voltage) near maximum, which is 3750 kW for the large-scale system. Figure 9 shows the increase in the achievable average power input when using 16 voltage taps rather than 4.

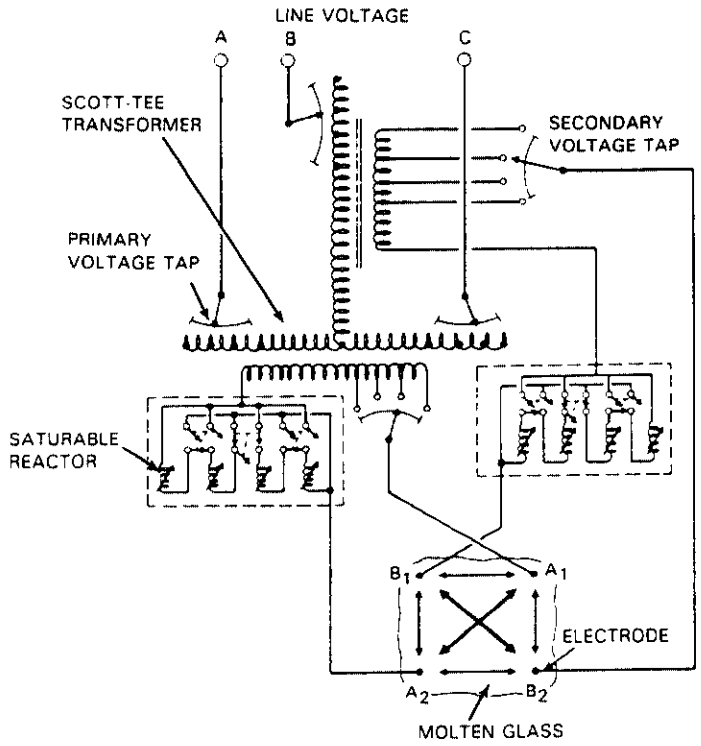

FIGURE 8. Scott-Tee Transformer Design for the Large-Scale System

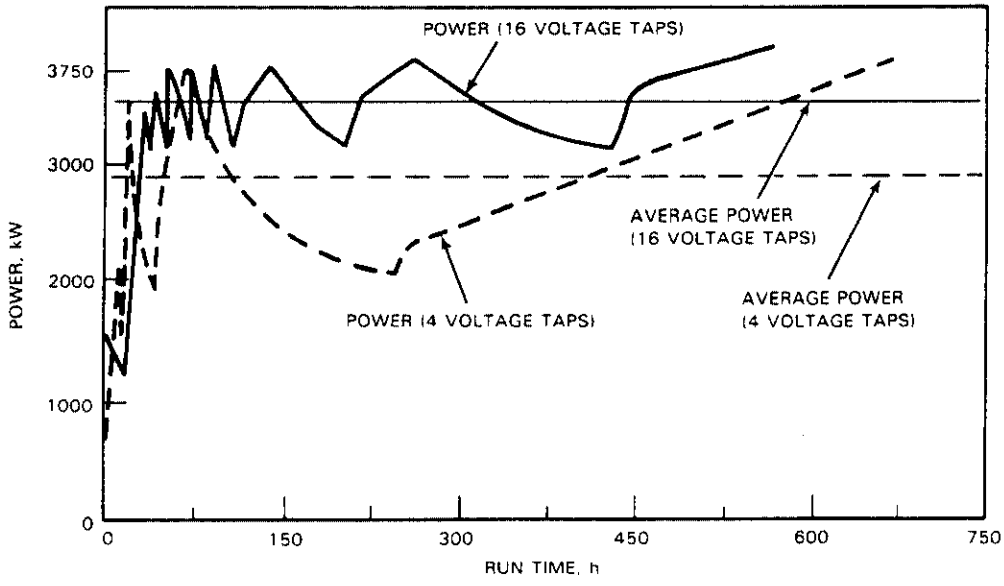

FIGURE 9. Effect of Increased Number of Voltage Taps on Average Power Output

Average power is 2900 kW when four voltage taps are used. With 16 voltage taps the average power has been increased to 3500 kW, which is much more efficient use of the maximum capabilities of the system.

To control the current and/or voltage being introduced into the electrodes, saturable reactors with their respective control windings are used for the large-scale system. Saturable reactors have been used extensively for power control systems in various applications. Their principle of operation is similar to a variable inductor in series with the load, as shown in Figure 8 (Platt 1958). By changing the control winding current to the saturable reactor, the level of saturation of the saturable reactor's core is varied. This changes the inductance in series with the load of the system. By decreasing the level of saturation, a higher voltage drop is attained across the saturable reactor, leaving less voltage and current available to the load, thus controlling the power to the load.

Saturable reactors were selected rather than solid-state components for large-scale operation because solid-state components are not available above 600 V, unless operated in series. Saturable reactors also introduce fewer harmonic frequencies into the grid system. However, the saturable reactors have a detrimental effect on the power factor. The power factor is the cosine of the phase angle between the current and voltage waveforms distributed to the power system (Del Toro 1972). A power factor that is much less than one generally results in cost penalties to the user, and is discouraged by both the power generation and transmission people. This problem can be overcome by using up to 16 multiple voltage taps on the Scott-Tee transformer, which keeps the average predicted power factor for the large-scale system high (near 0.9--well within the acceptable range).

The control scheme is to use two saturable reactors on the secondary side of the Scott-Tee transformer. This has the advantage of independently controlling the power to each of the single-phase loads. However, the saturable reactors had to be designed to accommodate the full voltage and current ranges caused by the variable resistance of the melt in this batch operation process. This requires multiple reactors for each phase connected in series and/or parallel to be compatible with the range of voltage and current ratings.

The power supply system was specified to meet functional criteria determined by a mathematical model, described further in the Process Parameters section of this report. From the mathematical simulations, a 3750-kW power supply was selected for the large-scale system. The modeling predictions also stipulate that to meet the functional criteria, a load voltage of between 4160 to 400 V must be supplied with a corresponding current capacity on each of the two secondary phases of between 450 and 4000 A, respectively.

Off-Gas Containment and Electrode Support Hood

A stainless steel off-gas hood is placed over the vitrification zone to contain any gaseous and radioactive effluents from the process and to direct them to the portable off-gas treatment system. The hood (shown in Figure 10) is kept under a slightly negative pressure (0.25 to 2.5 cm water).

The hood is constructed of 2.4- x 1.2-m panels that can be dismantled and stored in type A[(a)] transportation containers. Because of the high heat load from burning combustible wastes at the vitrification surface, the off-gas hood is constructed of materials that are capable of withstanding 900°C. A non-welded (bolted) hood design was favored for the large-scale system because thermal expansion from ambient temperature to 900°C creates >2.5-cm expansion in any direction. The panels are assembled in a manner to relieve stresses that might result from thermal expansion. The existing hood is designed for a skin temperature of 550°C; higher combustible loadings in the soil, for which the off-gas treatment system is designed, would require a high-temperature hood design.

The hood is sealed to the surface of the soil surrounding the zone to be vitrified by a flexible skirt of tightly woven, high-temperature resistant fiber covered with a few centimeters of dirt. The skirt maintains a seal during processing, which normally tends to dry out the dirt around the hood, thereby increasing air inleakage.

(a) Hanford radioactive shipment classification.

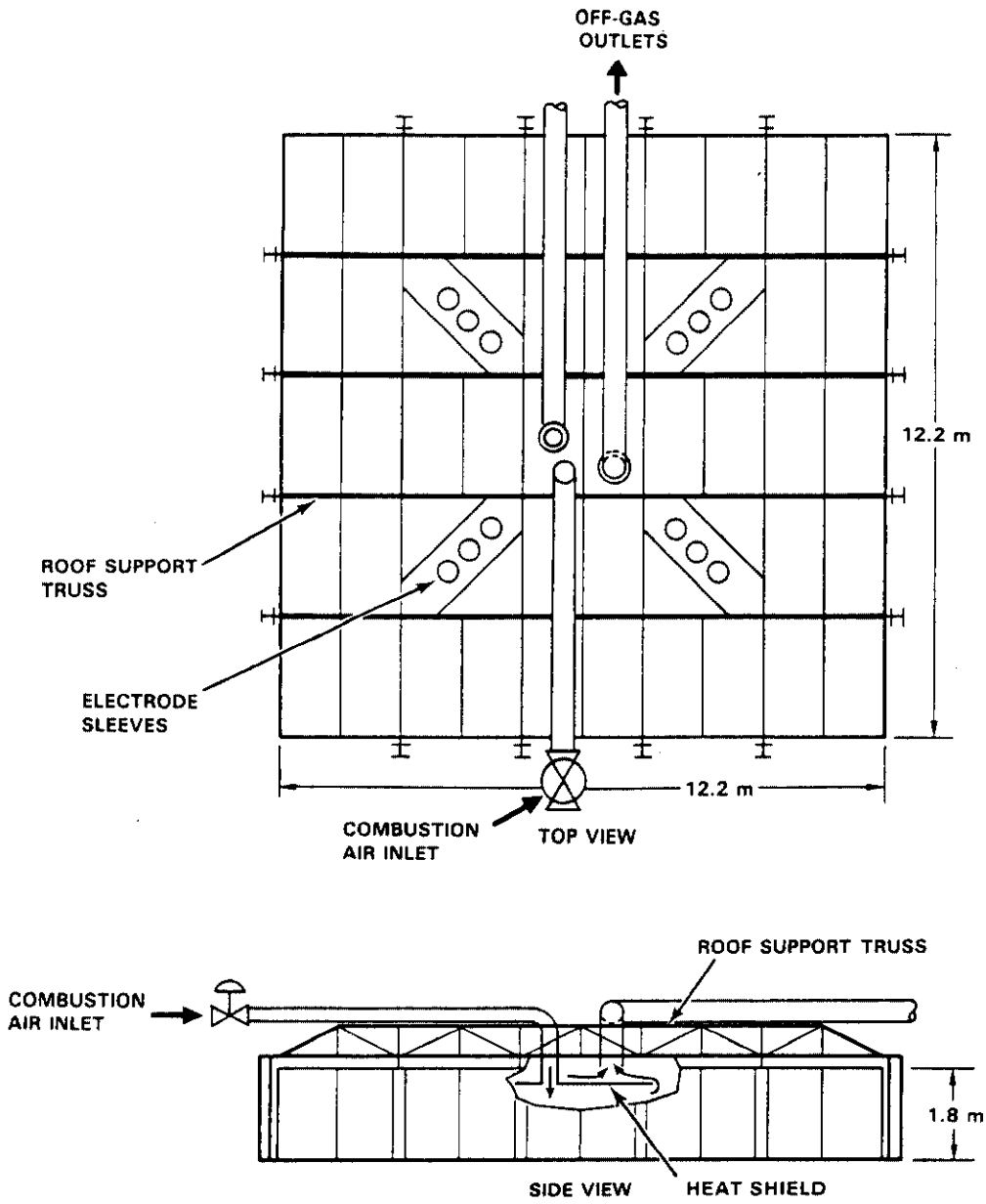

FIGURE 10. Off-Gas Containment Hood for the Large-Scale System

The four Mo electrodes protrude through the hood at variable separations of 3.5 m to 5.5 m on a side. They are surrounded by electrically insulated sleeves that allow for the adjustment of the electrode position. The electrodes are supported by insulators above the sleeve. The insulators are

designed to withstand any movement of the molten mass against the electrodes caused by convective currents and the gravitational or buoyant forces exerted on the electrodes.

Off-Gas Treatment System

The off-gas treatment system (see Figure 11) cools, scrubs, and filters the gaseous effluents exhausted from the hood. Its primary components include: a gas cooler, two wet scrubber systems (tandem nozzle scrubbers and quenchers), two heat exchangers, two process scrub tanks, two scrub solution pumps, a condenser, three mist eliminators (vane separators), a heater, a high-efficiency particulate air (HEPA) filter assembly, and a blower system.

Due to the additional heat load from high concentrations of buried solid and liquid organic combustibles, off gases entering the off-gas trailer can be expected to reach a maximum temperature of 750°C. To keep the size of the heat exchange equipment manageable for a transportable facility, a gas cooler is

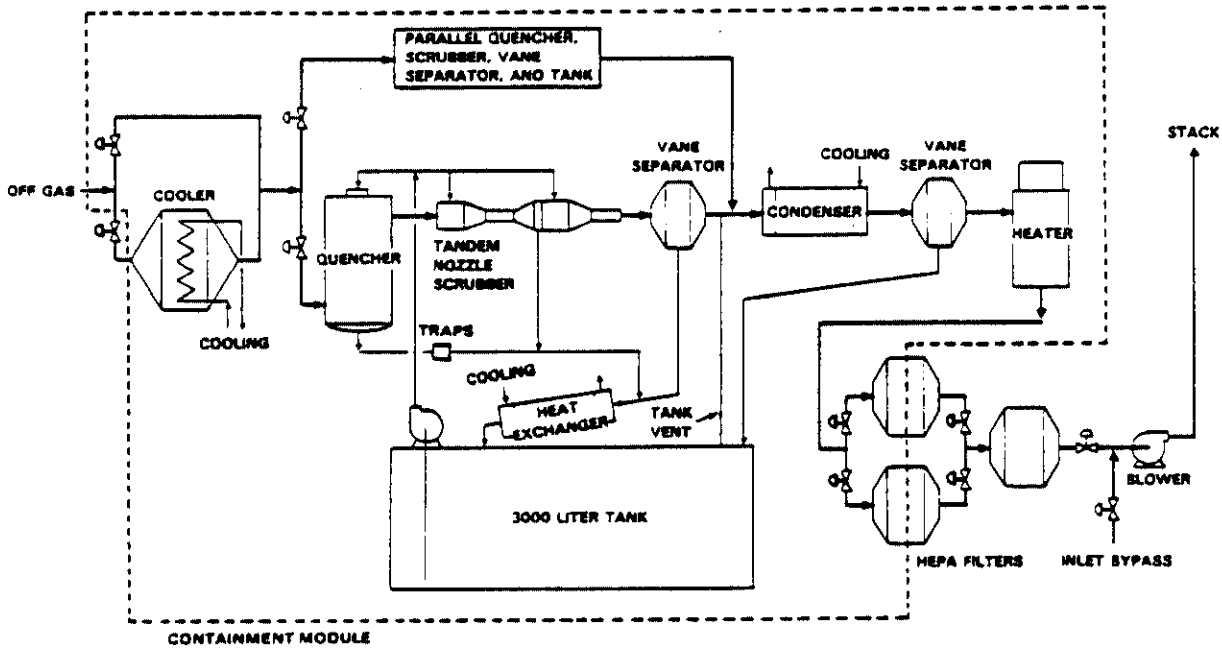

FIGURE 11. Off-Gas System for Large-Scale In Situ Vitrification

provided to remove a major portion of the heat load from the off gases before quenching. The gas cooler is a finned air-to-glycol heat exchanger. It is capable of transferring 1100 kW from the off gas to a glycol loop, cooling the gases to 300°C. The gas cooler can be bypassed by operating three 40-cm pneumatic-actuated butterfly valves.

From the gas cooler, the off gas is split and directed into two wet scrubber systems that operate in parallel. Two scrubber systems provide an operating flow range of between 30 and 104 std m^3/min. At flows less than 60 std m^3/min only one system operates. The dual scrubber system also provides redundancy in the event of single-component failure. Each system is composed of a quench tower, a tandem nozzle scrubber, and a vane separator. The quencher reduces the gas temperature from 300 to 66°C, and provides some scrubbing action to remove a portion of the particles and semivolatile radionuclides. The primary functions of the tandem nozzle scrubber are to remove any remaining particles that are >0.5 μm dia, condense the remaining semivolatile components, and provide additional cooling of the off gas. The vane separator that follows each tandem nozzle scrubber is designed to remove all droplets >12 μm.

The scrub solution that is injected into the quenchers and tandem nozzle scrubbers is cooled through two single-stage heat exchangers before being returned to the process scrub tanks. Each heat exchanger can remove 120 kW from the scrub solution and transfer 120 kW of heat to the glycol solution.

Two independent scrub pumps recirculate the scrub solution from the process tanks to the wet scrubbers. Each pump can deliver 510 L/min with a maximum deliverable pressure of 680 kPa. In addition, the scrub pumps can flush out the gas cooler and off-gas piping that are not wetted by the wet scrubbers.

Following the scrubber systems, the off gas is recombined and cooled. A condenser and mist eliminator provide additional decontamination of the off gas by condensing it and removing water droplets. The condenser transfers 320 kW from the off gas into flowing glycol. The mist eliminator, a vane separator, removes droplets >12 μm. Both the condenser and mist eliminator are rated at 104 std m^3/min. Final decontamination of off-gas particulates is achieved in the two-stage HEPA filter assemblies. The first stage is composed of two

parallel housings, each capable of holding four 61-cm-high x 30-cm-deep filters. With this arrangement, one filter set can be changed out without interfering with the continuous operation of the off-gas system.

The gaseous effluents are drawn through the off-gas system components by an induced draft system. The driving force is provided by a 149-kW (200-hp) blower that is capable of achieving 104 std m^3/min at 90°C and -229 cm of water. A back-up blower rated at one-quarter the capacity is available if the primary blower fails. The back-up blower is not intended to provide excess combustion air, but rather to maintain a negative pressure on the off-gas hood to prevent direct release of effluents until the process can be safely shut down. The back-up blower is automatically activated by the process control system when the main blower header vacuum is reduced below a preset limit. After passing through the blower system, the off gases are exhausted to the stack, which is monitored continuously for radionuclides, NO_x, and SO_2. The stack which is removable and extends high enough to prevent interference with the off-gas and control trailer's heating, ventilating, and air conditioning (HVAC) systems.

Glycol Cooling System

Glycol cooling solution is pumped between the support trailer and off-gas trailer to remove the heat from the gaseous effluents. The glycol is recirculated between trailers through flexible jumpers by two pumps in two independent loops. The glycol recirculating through the heat exchangers and condensers is kept separate from the glycol loop for the off-gas coolers. However, both loops are assembled in one glycol cooling assembly, which is located on the support trailer. The assembly consists of two fan-cooled radiator systems, each dedicated to its respective glycol loop. The entire assembly removes 1600 kW at an ambient temperature of 38°C.

Process Control Station

The process control station consists of a distributed microprocessor monitoring and control system and a control console for the power supply. The

process control station monitors and controls important process parameters and automatically activates back-up equipment or reroutes off-gas flow if certain equipment fails.

The distributed microprocessor control system consists of two process control units and two operator interface units. The process control units are connected to critical and informational sensors located throughout the process. These include sensor readings from pressure elements, thermocouples, gas monitors, and flowmeters. In addition to monitoring key parameters, the control system performs the following functions:

- control of the pressure drop across the scrubber systems by a pneumatic flow control valve at the blower inlet
- control of the blower inlet vacuum with a separate pneumatic valve that governs the magnitude of recycle through the main blower
- control of off-gas differential temperature across the heater
- control of negative pressure in the hood by controlling combustion air flow through a pneumatic valve
- automatic batch logic sequencing of specific operations in the event of equipment failure (22 preprogrammed sequences are included).

As examples of the latter function, if power fails, the control system automatically restarts the off-gas system in a preprogrammed sequence on emergency generator power. If the pressure drop across the HEPA filters exceeds predetermined levels, the system automatically activates the parallel HEPA filter assembly. If either hood vacuum or oxygen concentration is reduced below minimum operating criteria, the system engages the standby scrubber system. And if the primary blower fails, the system automatically shuts down power to the electrodes and starts the back-up blower.

Although the control system is connected to sensors and to an automatic shutdown circuit on the electrode power supply system, it does not directly control the power supply. A separate control console fulfills that function. The power supply controller provides the necessary saturation current to the saturable reactors that govern the power to the electrodes. This control

module maximizes the efficiency of the electrode power system and provides a quick reduction in power in the event of off-standard conditions.

Off-Gas Support Equipment

Various support and back-up equipment are necessary to ensure the safe operation of the off-gas system. This equipment provides electrical, water, and air services to the off-gas equipment. The support equipment includes: a 750-kVA transformer; a 750-kVA diesel generator; an air compressor; and a process water supply tank, pump, and agitator.

Other than the need for electrical power, the ISV process is entirely self-contained. No outside water, sewer, or air services are required. Supply and waste waters are transported to the process trailer by tank truck on an as-needed or scheduled basis. The process is equipped with its own air compressor for actuation of the pneumatic valves and its own water supply tank for scrub solution makeup.

Power to the off-gas process equipment is provided through the 750-kVA transformer and distributed by the motor control center (MCC) from a 13.8-kV supply. If power to the transformer is interrupted, a transfer switch in the MCC automatically activates a standby 750-kVA diesel generator that is equipped with its own battery-powered cranking system. This generator provides emergency power to all off-gas system components including the pumps and fans of the glycol cooling assembly, scrub pumps, heater, blower system, air compressor, and monitoring and control instrumentation. The MCC, located in the control trailer, provides power to this equipment and to the power supply control console and the supply pump and agitator for process water. The 112-kVA transformer, which provides 240-V and 120-V power from the 480-V supply, is also in the control trailer. The 120-V power is also tied into the emergency back-up power generator for emergency lighting.

PILOT-SCALE SYSTEM

The pilot-scale system uses four electrodes with a 1.2-m separation and consists of a power control unit, an off-gas containment hood over the waste site, and an off-gas treatment system that is housed in a portable

semi-trailer (see Figure 12). Prior to and after a radioactive test, this same system was used on six nonradioactive tests. A previous pilot-scale system (Oma et al. 1983) preceded the present pilot-scale design to provide scale-up feasibility; however, it was not mobile or designed for radioactive materials.

Power System Design

Like the large-scale unit, the pilot-scale power system uses a Scott-Tee connection to transform a three-phase input to a two-phase secondary load on diagonally opposed electrodes in a square pattern. The 500-kW power supply may be either voltage or current regulated. The alternating current primary is rated at 480 V, 600 A, 3 phase, and 60 Hz. The three-phase input feeds a Scott-Tee connected transformer (see Figure 8) to provide a two-phase secondary. The transformer has four separate voltage tap settings--1000 V, 650 V, 430 V, and 250 V. Each voltage tap has a corresponding amperage rating of 250 A, 385 A, 580 A, and 1000 A and an off-gas treatment system. Like the large-scale unit, the hood is equipped with a heat shield installed under the center top panel to protect the hood from heat that radiates from the partially molten surface during processing.

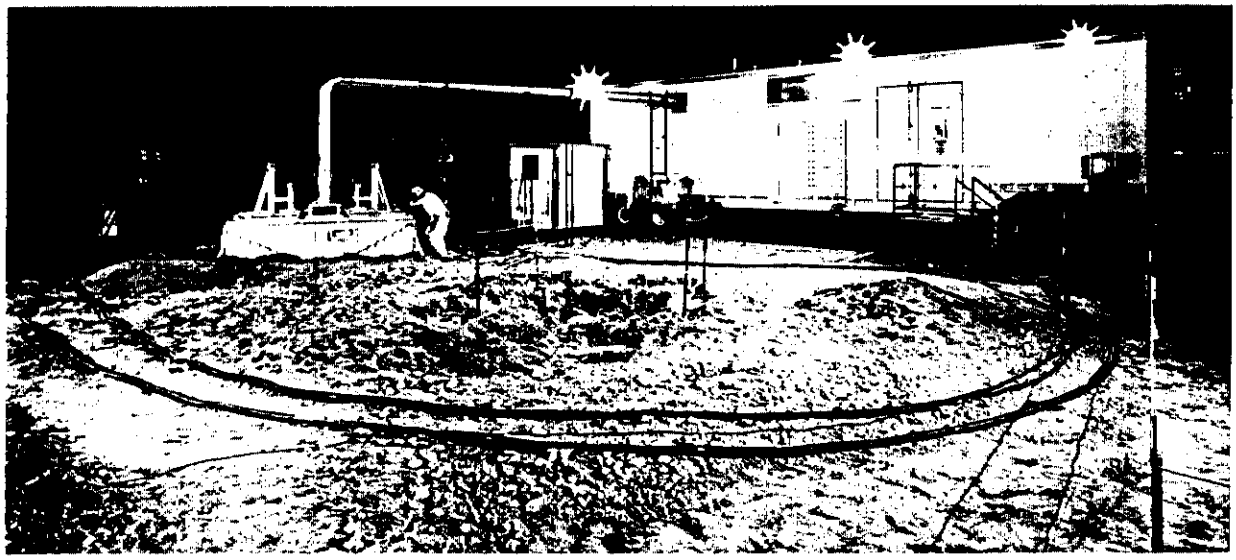

FIGURE 12. Hood and Process Trailer for Pilot-Scale In Situ Vitrification

The hood makes use of the flexible skirt to provide a seal to the surface of the soil surrounding the zone to be vitrified. The skirt extends ~0.6 m away from the hood, allowing for a hood-to-ground seal when covered with a layer of soil.

Electrical bus bars, which are extensions of the Mo electrodes, protrude through the hood and are surrounded by electrically insulated sleeves that allow for the adjustment of the electrode positions. Figure 13 depicts one design of the insulated sleeves that was implemented during the PSRT.

Off-Gas Treatment System

The off-gas system is shown schematically in Figure 14. The off gas passes through a venturi-ejector scrubber and separator, Hydro-Sonic® scrubber, separator, condenser, another separator, heater, two stages of HEPA filtration,

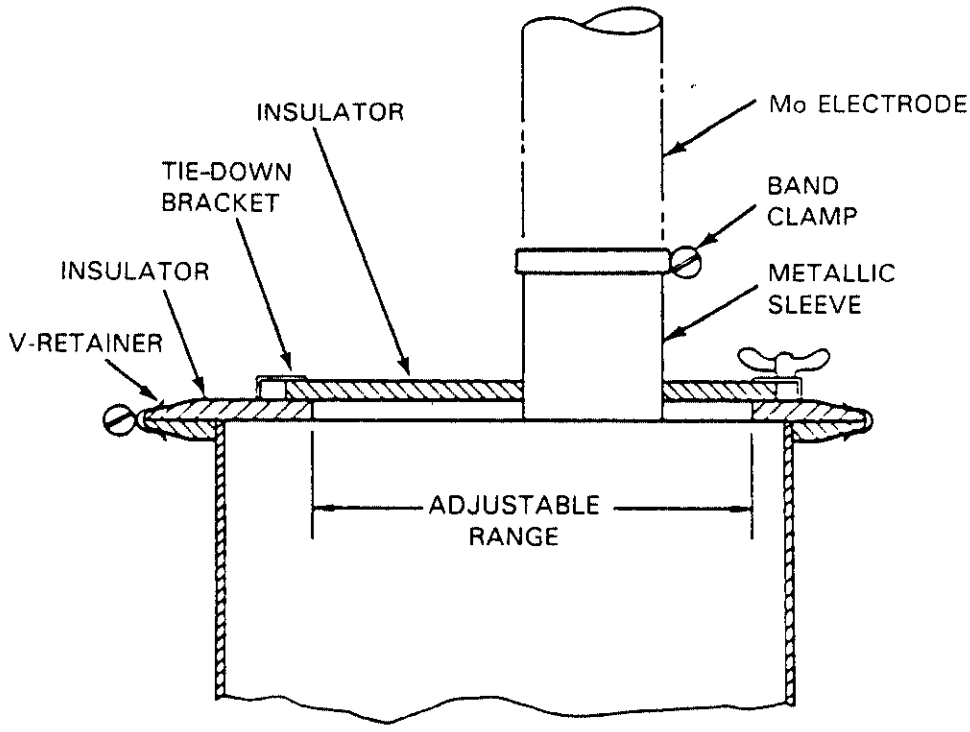

FIGURE 13. Design of Hood Feedthrough for Electrode Bus Bar

® Hydro-Sonic scrubber is a registered trademark of Hydro Sonic Systems, Dallas, Texas.

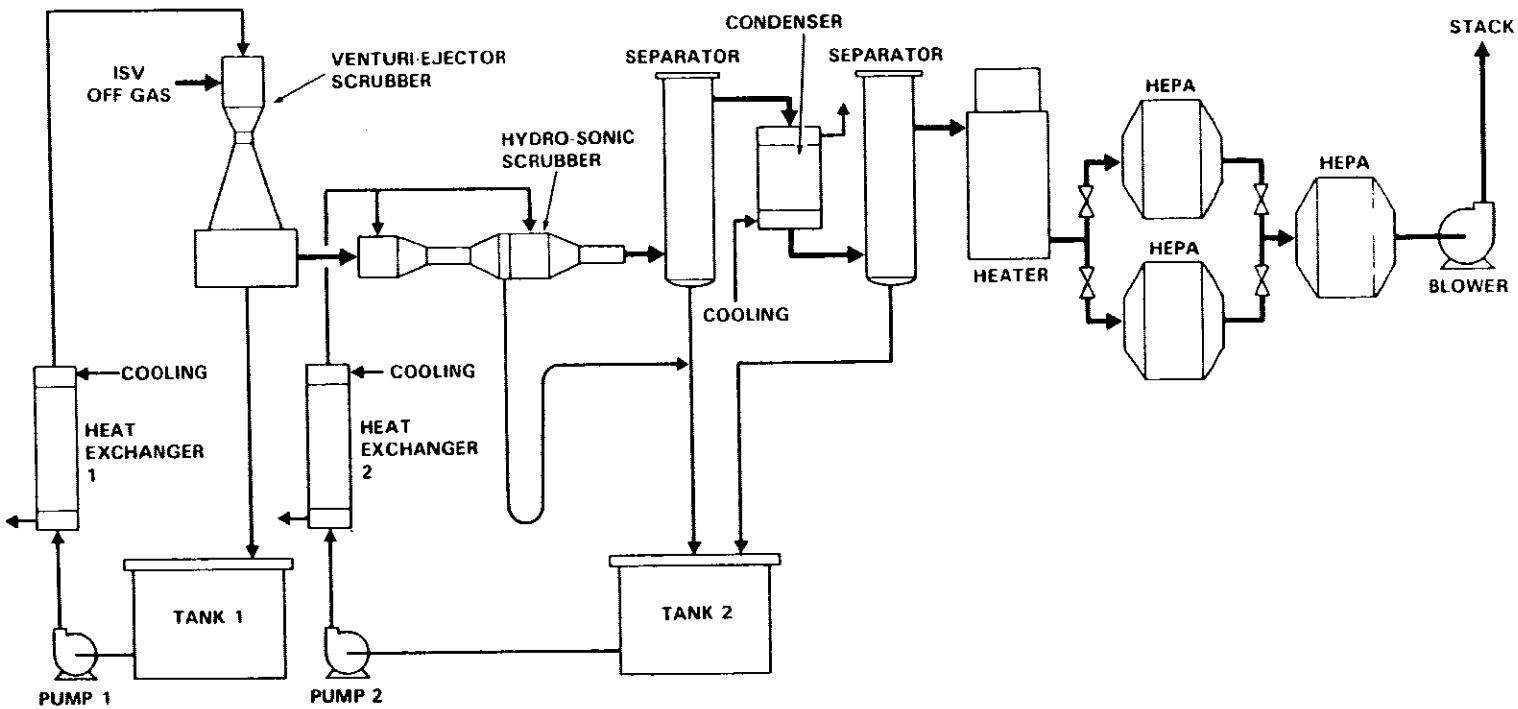

FIGURE 14. Off-Gas System Schematic for the Pilot-Scale ISV Process

and a blower. Liquid to the two wet scrubbers is supplied by two independent scrub recirculation tanks, each equipped with a pump and heat exchanger. The entire off-gas system has been installed in a 13.7-m- (45-ft-) long semi-trailer to facilitate its transportation to a waste site. Equipment layout within the trailer is illustrated in Figure 15. Except for the second-stage HEPA filter and blower, all off-gas components are housed in a removable containment module that has gloved access for remote operations and is maintained under a slight vacuum (see Figure 16).

Heat is removed from the off gas by a closed loop cooling system that consists of an air/liquid heat exchanger, a coolant storage tank, and a pump. A 50% water/ethylene glycol mix is pumped from the storage tank through the shell side of the condenser and the two scrub solution heat exchangers, then through the air/liquid exchanger, where heat is removed from the coolant.

The venturi-ejector scrubber serves both as a quencher and a high energy scrubber. The second scrubber is a two-stage Hydro-Sonic scrubber (tandem nozzle fan drive) as illustrated in Figure 17. The first section condenses vapors, removes larger particles, and initiates growth of the finer particles so that they are more easily captured in the second stage. Particulate is captured when the gas is mixed with fine water droplets produced by spraying water into the exhaust of the subsonic nozzle. Mixing and droplet growth continue down the length of the mixing tube. Large droplets containing the particulate are then removed by a vane separator and drained back into the scrub tank. The unit is designed to remove over 90% of all particulates greater than 0.5-μm dia when operated at a differential pressure of 127 cm of water. Removal efficiency increases with an increase in pressure differential.

Additional water is removed from the off-gas system by a condenser that has a heat exchange area of 8.9 m^2 and a final separator. The gases are then reheated to ~25°C in a 30-kW heater to prevent condensate carryover to the filters.

The first stage of filtration consists of two 61- x 61- x 29-cm (24- x 24- x 11.5-in.) HEPA filters in parallel. During operation, one filter is used and the other remains as a back-up in case the generating filter becomes

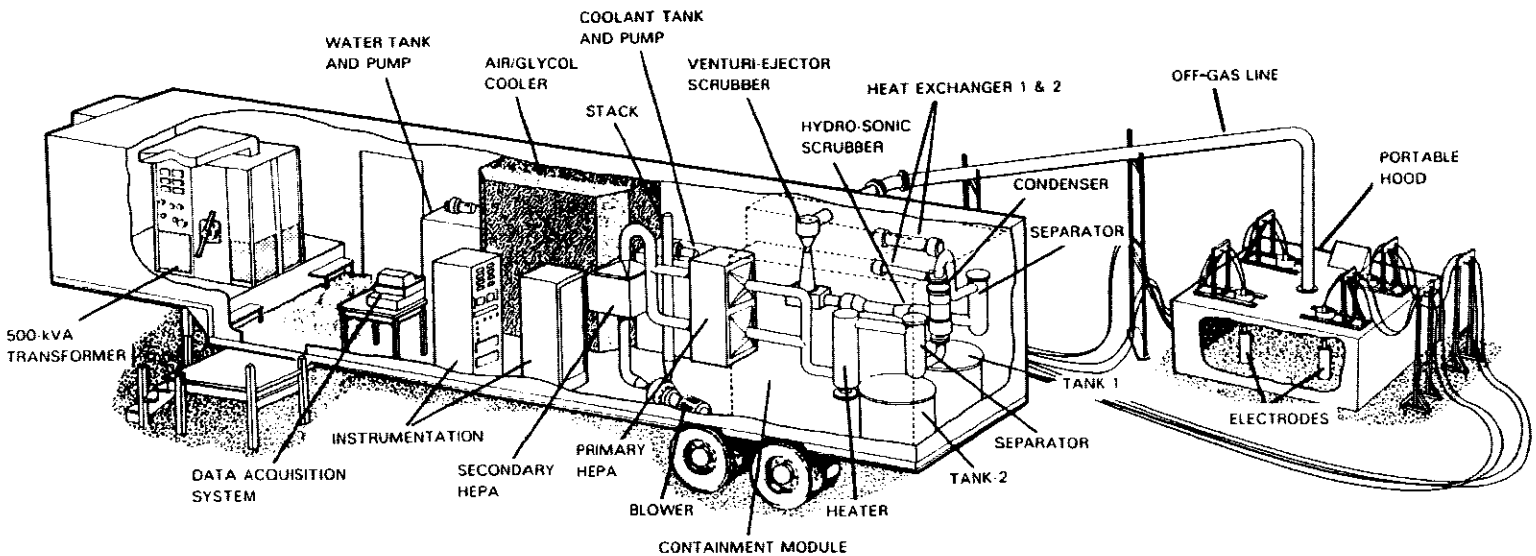

FIGURE 15. Cutaway View of Pilot-Scale ISV Process Trailer and Hood

FIGURE 16. Removable Containment Module for the Off-Gas Treatment System

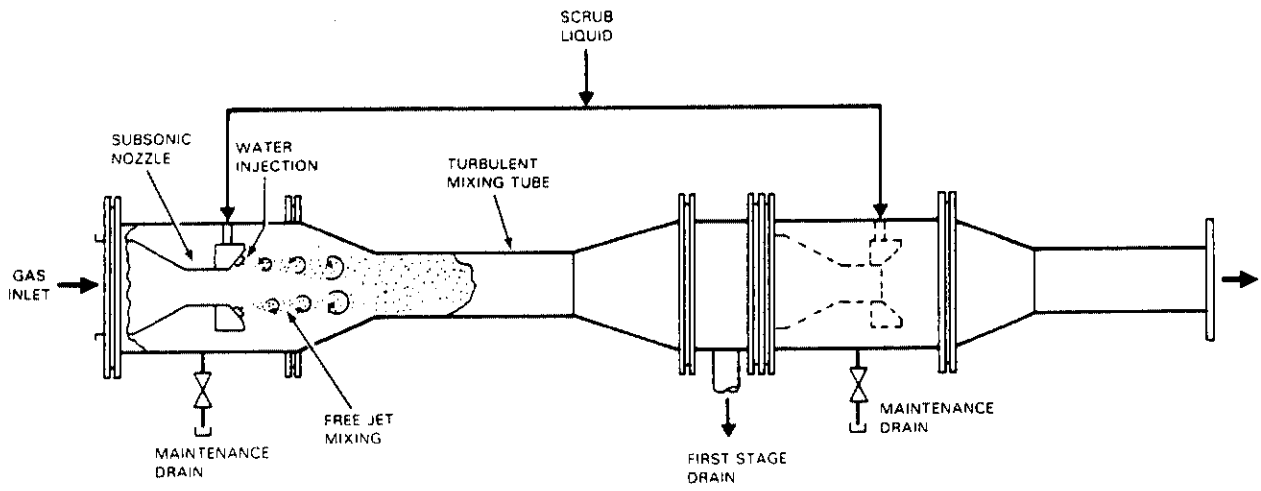

FIGURE 17. Tandem Nozzle Hydro-Sonic Scrubber (Hydro-Sonic Systems, Dallas, Texas)

loaded. The primary filter can be changed out during operation. The second-stage HEPA filter acts as a back-up if a first-stage filter fails.

ENGINEERING-SCALE SYSTEM

One of the primary developmental tools for ISV has been the engineering-scale laboratory test (ESLT), which is operated in the PNL developmental laboratory. The engineering-scale system has many flexible design features for testing new concepts. One of these features is the ability to melt at depth-to-electrode-separation ratios that are much greater than during previous pilot-scale field tests (PSFTs). Computer modeling shows that the ESLT system is capable of melting to a depth of 1.8 m with electrode separations of between 0.2 and 0.35 m. Because of its smaller scale, the engineering-scale system can test new concepts at a reduced cost while maintaining a high level of confidence in its predictive capabilities for larger-scale operations. Also, many of the analyses of ISV process limits described in this report are based on the 24 tests conducted with the engineering-scale unit.

The engineering-scale power system consists of a 30-kW Scott-Tee transformer. The transformer has 16 voltage taps, similar to those described for the large-scale system. It can be wired for either primary or secondary control with saturable reactors or solid-state, silicon-controlled rectifiers

(SCRs) on the primary. The vitrification process is conducted inside a sealed metal container measuring 1.8-m dia x 2.4-m tall (see Figure 18).

Much of the data on process limits were gathered from an earlier version of the engineering-scale unit that was equipped with a single-phase electrode power supply. This unit was installed in a sealed metal container measuring 2-m dia x 0.8-m tall. The hood was maintained under a slight vacuum by a facility off-gas system. Although less flexible than the present unit, it provided much of the data for the process limits analysis on combustible, metal, and ceramic inclusions.

BENCH-SCALE SYSTEM

The bench-scale system is used primarily to verify ISV processability and off-gas characteristics from alternative types of soil and waste inclusions. A portion of the power supply for the existing engineering-scale ISV unit, its soil container, and process off-gas vacuum supply are used to conduct the

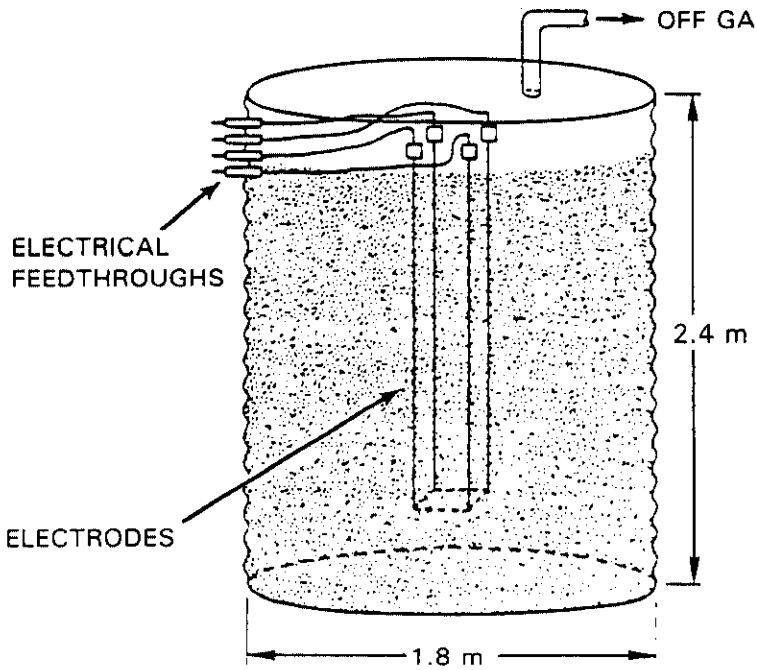

FIGURE 18. Sealed Container for Engineering-Scale System

bench-scale tests. Figure 19 illustrates the 480-V SCR, 40-A breaker, and 10-kVA isolation transformer that are connected in a single-phase arrangement to supply and control electrical power to the bench-scale unit.

Two graphite electrodes, 3.8-cm-dia (1-1/2-in.-dia) half cylinders, are used for bench-scale tests. The electrodes are supported 10 cm apart by unistruts and insulating collars. Type K thermocouples are placed at 5-cm incremental depths at the centerline between the electrodes and 8 cm out from the center on a plane perpendicular to that of the electrodes. The thermocouples provide the ability to monitor the depth and width of the vitrification zone. Each test area is covered with 5 cm of an alumina silica insulating blanket, leaving a 1-cm gap between each electrode and the insulation for venting. The insulation helps promote subsidence of any porous glass produced at the molten surface, and it improves the efficiency of the melting operation.

The bench-scale unit has been used on four occasions for new soil and waste types as a precursor to larger scale testing or onsite demonstrations. It is relatively inexpensive to operate, and it is instrumental in determining the applicability of ISV to various waste types.

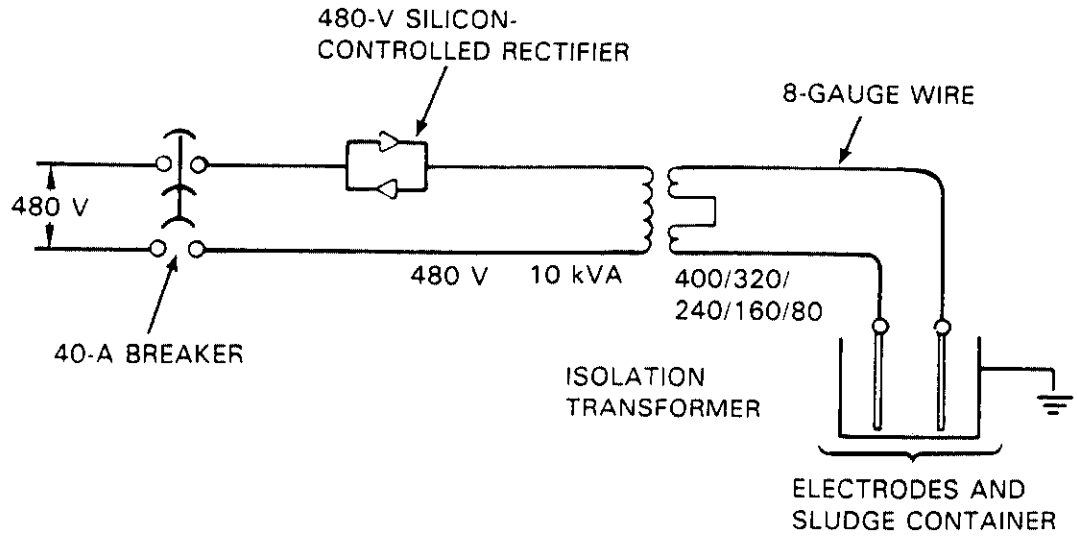

FIGURE 19. Bench-Scale ISV Electrical Diagram

PERFORMANCE ANALYSIS

PERFORMANCE ANALYSIS

The performance of the ISV process has been evaluated using all four developmental units described previously. The performance of the process equipment, processing factors, and the waste form itself is described and evaluated in this section.

EQUIPMENT PERFORMANCE

The power system, off-gas containment hood, and off-gas treatment system were evaluated to determine their effectiveness in immobilizing and/or destroying hazardous and radioactive components. This section summarizes the performance of these equipment components for the pilot- and large-scale systems.

Power System

With only minor exceptions, the power systems for the pilot- and large-scale units have proven to be reliable pieces of equipment. The SCRs for the pilot-scale unit and the saturable reactors for the large-scale unit uniformly control power to the electrodes to achieve maximum process efficiency. The addition of forced air cooling to both systems has kept operating temperatures within operable limits even under 40°C ambient conditions. However, with the Scott-Tee connection, we found that it is important to monitor and alarm the secondary current to the electrodes for maintaining the amperage within the maximum ratings, and monitor the primary current. A slight imbalance in the load can cause more severe imbalances on the primary windings. If the imbalance is severe enough, primary current ratings can be exceeded, thereby overheating the transformer's core or terminations. Revisions to monitoring procedures and alarm specifications eliminate this overheating occurrence.

The graphite/frit startup technique has proven to be reliable when implemented correctly. In all but one pilot-scale test, no further adjustments were necessary once the graphite starter material was put in place. No signs of unstable melting behavior such as arcing, hot spots, or disruptions in continuity were detected during the startup phases. Experience with the large-scale unit has also proven the startup operation to be very stable. However, in the case of frozen or rocky surface soil, nonuniformities in the trench can result

in a loss of the conductive path an hour or two after startup. In this situation, it is advisable to place the starter material in 10 cm of relatively dry sand added to the surface to achieve uniformity in the trench for startup. Also, when vitrifying industrial sludges with extremely high volume reductions (e.g., greater than 80%), it is advisable to cover the surface with 1 m of soil to prevent loss of electrical continuity when sludge begins to reduce in volume during processing (Buelt and Freim 1986).

The power system has been shown to perform much as predicted by a mathematical model that was developed as a design aid (see the Process Parameters section). Figures 20 and 21 give a comparison of predicted and measured values for the voltage and current dissipated between one pair of electrodes. Although the measured values show a higher conductivity (i.e., higher current and lower voltage) than predicted, the measured values are still within the design limits of 4160 to 440 V and 450 to 4000 A.

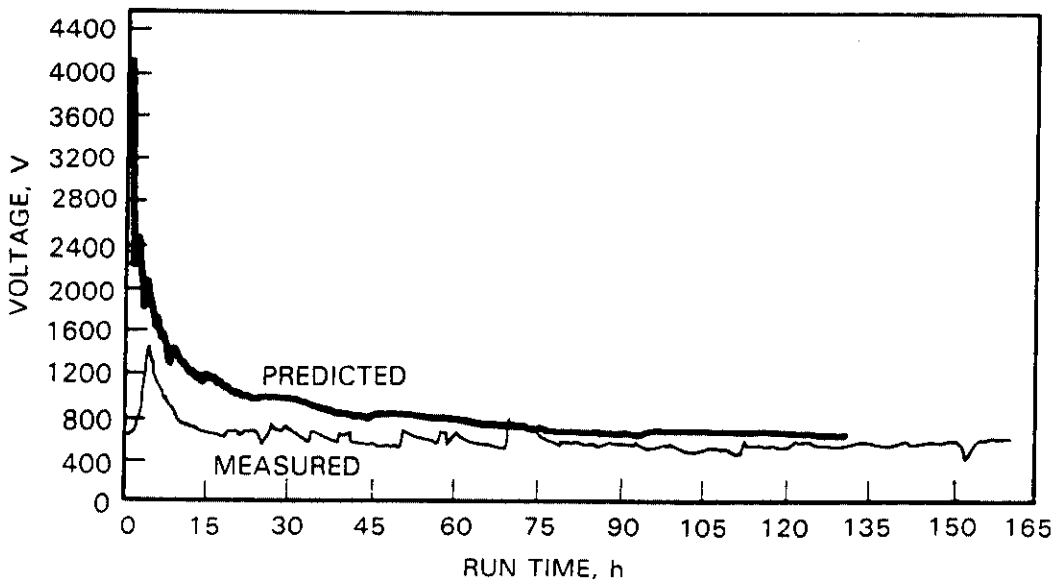

FIGURE 20. Predicted and Measured Electrode Voltage as a Function of Actual Run Time for the Large-Scale Verification Test

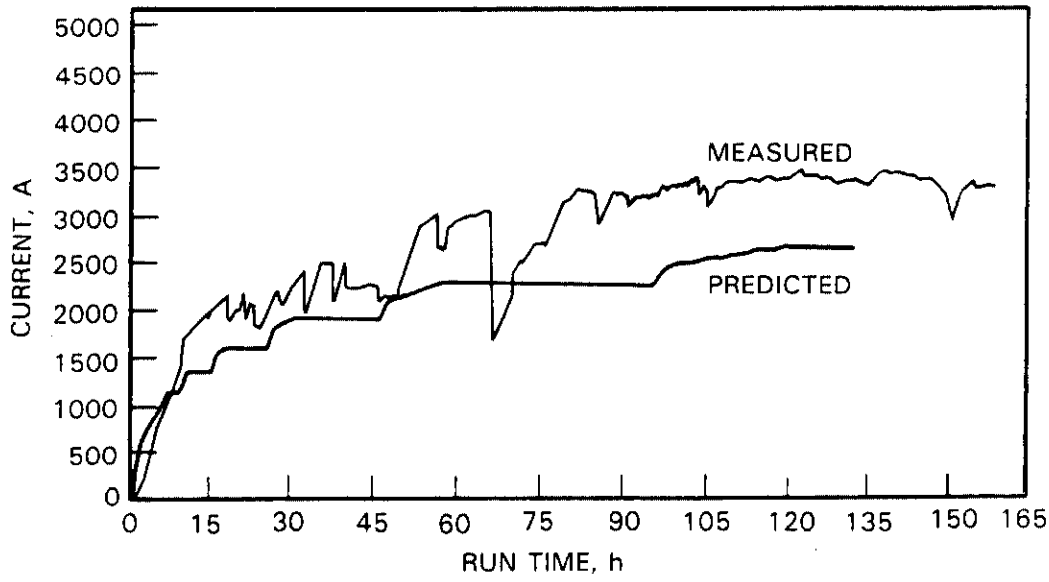

FIGURE 21. Predicted and Measured Current as a Function of Actual Run Time for the Large-Scale Verification Test

As expected, inclusions of metals in the melt do not significantly affect the ability of the power system to vitrify contaminated soil. Numerous pilot-scale tests have been conducted with vitrified metallic drums, containers, and lecture bottles. Vitrification of a 208-L (55-gal) metal drum that occupied 35% of the linear separation between electrodes resulted in only a 10% drop in electrical resistance between the electrodes, which agreed well with predictions. These predictions, based on ESLT results given in the next section, show that greater than 70% of the linear separation between electrodes that is occupied by metal can be vitrified. During vitrification, the metallic drums are completely melted with their contents, contaminated soil and ash from combustible waste, distributed throughout the glass block.

Off-Gas Containment Hood

The principle of containing off gases and incinerating pyrolyzed organics that are generated by the process within a hood has been demonstrated by the nonradioactive and radioactive pilot-scale tests and verified in the four nonradioactive large-scale tests. The hood that covers the vitrification zone effectively maintains a negative pressure over the molten area during

processing. The skirting made of high-temperature fabric effectively eliminates the loss of negative pressure caused by soil drying and potential subsidence at the perimeter of the hood.

Structurally, the principle of constructing the large-scale hood from individual stainless steel panels eliminates warpage by allowing each panel to expand and contract independently. The radiative heat shield installed over the central region of the molten zone substantially reduces temperature to the metal hood, thereby eliminating the potential for small cracks to occur in the hood directly above the melt zone due to heat-related stress. The maximum measured skin temperature on the large-scale hood during testing was 200°C--well below the design limit of 550°C.

To demonstrate reuse of the hood once it has become contaminated by radioactive use, it was necessary to develop materials to immobilize the interior surface contamination. Spray-coating the interior surfaces of the hood and the surface soil with a fixative at the conclusion of each vitrification run has been identified as the appropriate immobilization technique. Studies were conducted to identify a fixative with the following characteristics:

- adherent to vertical surfaces and surfaces already coated with moisture and particulate
- amenable to spray application
- amenable to ready removal of degraded material
- economical, nonflammable, and nontoxic.

Hand-sprayed coatings of seven fixatives including enamels, a welding anti-spatter compound, a strippable coating, and a polyvinyl alcohol coating (clear coat) were evaluated as part of the pilot-scale and large-scale vitrification tests. The high temperatures associated with the vitrification process charred most of the fixatives, making them difficult to remove. The polyvinyl alcohol coating, however, was partially removed by thermal exposure, but was otherwise unaffected. This characteristic, combined with its acceptable performance in the other criteria areas, led to the selection of the clear coat for further evaluation and application studies.

The specific objectives of subsequent clear coat development were to: 1) determine the acceptable temperature conditions for application of the fixative; 2) develop, install, and evaluate a fixative spray system for the hood; and 3) conduct large area tests of the clear coat as part of the LSVT.

The major conclusions derived from the results of this study are that 1) clear coat is a suitable fixative for post-vitrification contamination control inside the containment hood and surface soil, and 2) the fixative can be satisfactorily applied with a properly engineered spray system. Some of the specific findings and conclusions for the individual study areas are listed here:

- The cured coating will not thermally degrade even with relatively long-term exposure to temperatures below 200°C; this indicates that clear coat could be used to precoat the hood prior to exposing it to contamination.
- Even short exposures to temperatures greater than 300°C result in significant degradation or removal of the coating to aid in reapplication for subsequent radioactive use of the hood.
- The fixative should not be applied to hood surfaces until the surface temperature has cooled below 150°C.
- The fixative can be spray applied with good coverage and adherence using either a wide-angle, circular pattern standard spray or a rotating nozzle.
- To avoid thermal degradation, the spray system fittings and components that are located inside the hood should be fabricated of stainless steel or another heat-resistant alloy.
- To prevent plugging by the residual dried fixative, spray components with small or moving internal parts should not be exposed to heat.

Off-Gas Treatment System

The functional design criteria reported by Buelt and Carter (1986b) identify the requirements for the off-gas treatment system. It must have sufficient capacity to contain and treat gaseous releases that result from

vitrifying gas-generating soil inclusions, such as void volumes, combustible packages, liquid organics, sealed containers, and combustibles mixed with soil. The off-gas treatment system is conservatively designed to contain and treat the maximum credible release from vitrifying such an inclusion with a design factor of two. In order to maintain a negative pressure of 0.25 cm of water on the hood under nominal conditions, a flow rate of 50 std m^3/min is required. Only minute quantities of process gases are being generated, so the off-gas system flow rate is balanced by air inleakage through hood panel joints and around the hood's perimeter. Operation of just one scrubber system achieves an off-gas flow rate of 58 std m^3/min and a negative pressure of 0.75 cm of water in the hood, thus exceeding this requirement (Buelt and Carter 1986b). A back-up scrubber system is always in reserve, ready for operation. However, operation of both scrubber systems is necessary to meet the design requirement of 104 std m^3/min. This flow is required to contain the maximum credible gaseous release from vitrifying soil inclusions, while providing adequate combustion air, when necessary, at a design factor of two. The operation of both scrubber systems achieves an off-gas flow of 116 std m^3/min, within 80% of the maximum power rating of the blower. The off-gas system's flow capacity ensures that even the maximum credible release will be contained for treatment with no gaseous releases to the atmosphere.

Retention of Simulated Radionuclides and Chemicals

The efficiency of retaining or destroying hazardous chemicals, TRUs, and associated fission products by an off-gas system component can be expressed as the DF. It is defined as follows:

$$DF = \frac{\dot{m}_i}{\dot{m}_e}$$

where $\dot{m}_i$ is the initial input mass of contaminant in the control volume per unit time, and $\dot{m}_e$ is the exit mass of contaminant from the control volume per unit time. The control volume may be defined as the molten soil, an off-gas system component, or a combination of both.

Even though the retention of TRUs, fission products, and most chemical contaminants in the vitrified soil is high, the gaseous effluents must be decontaminated before they are exhausted to the atmosphere. Analyses of the scrub solution and HEPA filters provide conclusive data on the performance of the off-gas system during processing. The initial large-scale settings established the importance of operating the scrubbers at sufficient differential pressure to be effective, between 102 and 152 cm of water. Analytical results of Sr in the scrub solution from LSOAT-3 and LSVT, demonstrates that Sr accumulates steadily with no propensity to be re-entrained into the off-gas system in water droplets downstream. The higher differential pressure improves the efficiency of the mist eliminators in removing water droplets--a fact that is supported by HEPA filter analyses. Multiple samples from both stages of filters show that the maximum amount of Sr entrained by the wet scrubber system during LSOAT-3 is 7.4 mg, a reduction from previous runs operated under lower differential pressures by a factor of 2500. The overall DF of the wet scrubber system for Sr is 440. Taking credit for the efficiency of one stage of HEPA filters (DF = 10^3) (Flanders Filters, Inc. 1984), the off-gas system's cleanup capability (DF = 4.4×10^5) exceeds the requirement of 10^5 as specified in the functional design criteria (Buelt and Carter 1986). This does not account for the expected additional DF of 10^3 for the second-stage filter. The overall DF of the scrubber system measured for Cs during the LSVT is 26, resulting in an overall off-gas system DF of 2.6×10^4. Likewise this exceeds the 10^4 criteria established for Cs.

The scrubber system DFs for fluorides and sulfates have been measured at 140 and 70, respectively. Accounting for one of two HEPA filter banks, the overall DF of fluorides is 1.4×10^5. The overall DF of SO_x gas, as measured by stack gas samples, ranges from 1000 to 7000 for all four large-scale tests. This is sufficient to maintain stack gas concentrations of SO_2 at 1 ppm under maximum conditions--well below environmental release standards. The additional DF of the off-gas system was obtained from small sulfate deposits on the filters that were probably re-entrained from the off-gas scrubber system.

The successful design of the large-scale off-gas system is based on previously established performance data on the pilot-scale system. The operating

parameters for the off-gas system used during the pilot-scale cold tests (PSCTs) and the PSRT are summarized in Table 8. The removal efficiencies for the PSCT off-gas system were determined from analysis of scrub liquid and HEPA filter samples. The venturi-ejector scrubber effectively removed from 81 to 92% of several of the nonvolatile soil components (Al, Ca, and Fe) during PSCT 1, as shown in Table 9. Semivolatile elements, including Cs, K, and Na, were more uniformly collected by the venturi-ejector and Hydro-Sonic scrubbers. The venturi-ejector scrubber was least efficient at removal of Zn (20%), which was the only heavy metal that appeared in quantity. However, the Hydro-Sonic scrubber and HEPA filters were effective at removing the residual Zn and the other elements entrained in the off gas. Carryover of most elements to the HEPA filter can be attributed to submicron particles, which are not easily removed by the scrubbers and condenser. During normal ISV operations, the mass mean particle diameter ranges from <0.1 to 0.8 μm (Oma, Farnsworth, and Timmerman 1984). When combustible wastes are present, the entrained particle size is larger, averaging 1.4 μm, which can be more easily scrubbed. The HEPA filters have shown ample capacity to handle the loading of off-gas solids that they receive. Nevertheless, improvements to the operation of the pilot-scale system were made prior to the radioactive test. The retention of elements in

TABLE 8. Operating Parameters for the Pilot-Scale Off-Gas System

Parameter	Typical Operating Range Radioactive Field Test Unit[a]
Off-gas flow, std m^3/min	8 to 13
Hood vacuum, cm water	3 to 4.5
Scrub liquid flows, L/min:	
Venturi-ejector scrubber	160
Hydro-Sonic scrubber	60 to 90
Scrubber delta P, cm water:	
Venturi-ejector scrubber	+3
Hydro-Sonic scrubber	-150 to -230

(a) PSCTs and PSRT.

TABLE 9. Element Removal by the Off-Gas System During PSCT-1 and the PSRT

Element	PSCT-1, Total Removed, %			PSRT, Total Removed, %		
	Venturi-Ejector Scrubber	Hydro-Sonic Scrubber	HEPA	Venturi-Ejector Scrubber	Hydro-Sonic Scrubber	HEPA
Simulated and Actual Fission Products						
Co	41	46	13	29	67	4
Cs	31	34	35	19	78	3
Sr	62	33	5	95.2	4.7	0.1
Soil Components						
Al	92	8	0	--	--	--
Ca	83	17	0	--	--	--
Fe	81	16	3	--	--	--
K	47	52	0	--	--	--
Na	40	48	12	--	--	--
Si	53	43	4	--	--	--
Zn	20	52	28	--	--	--

the venturi-ejector and Hydro-Sonic scrubbers was increased by reducing the amount of aerosol carryover to the HEPA filters. Mass distribution histograms of particle size before the PSRT, during startup, and during normal processing (see Figure 22) (Oma and Timmerman 1984) show that the mean mass particle sizes entering the HEPA filters are between 0.2 and 1.0 μm. The HEPA filters are 99.97% efficient at 0.3 μm (Flanders Filters 1984). Timmerman and Oma (1984) have also presented retention data for fission products and TRUs for the PSRT. Some of the results are also shown in Table 9 for comparison.

The secondary cooling loop is very effective at removing heat from the incoming off gas. During the PSCTs the gas inlet temperature averaged 250°C. By the time the off gas exited the condenser, it had been cooled to within 8 to 12°C of the ambient air. Typically 90% of the temperature drop occurs in the venturi-ejector scrubber. Gas exiting the condenser has been cooled to below its original dewpoint, as indicated by a gradual buildup of condensate in the process tanks during operation. The amount of condensate is dependent on

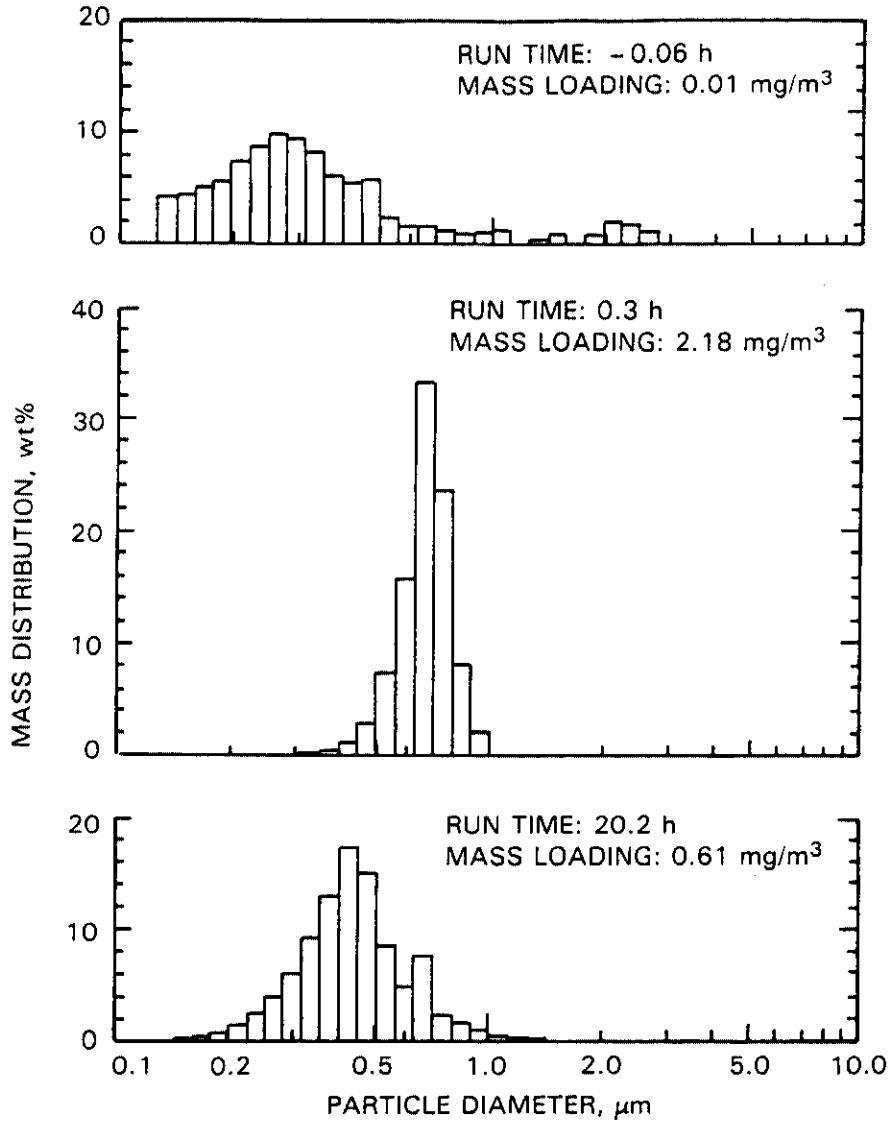

FIGURE 22. Histograms of Particle Mass Distribution

several factors, including soil moisture, relative humidity, temperature of the ambient air, off-gas flow rate, and off-gas temperature.

PROCESSING PERFORMANCE

This section presents data on element retention in the vitrified soil, cold cap subsidence, melt depth monitoring, and electrode performance.

Element Retention

Retention of simulated hazardous species in the vitrified zone is determined by chemical analysis of the soil that is adjacent to the solidified block and element releases to the off-gas system. No migration to the surrounding soil has been found during pilot-scale tests, so releases to the off gas have been the sole source of element losses from the vitrified zone. Releases to the off-gas system were ascertained by chemical analysis of scrub tank solutions, filter solids, and any solids that had accumulated on the hood and walls of the off-gas line. From these data, soil-to-off-gas DFs were calculated, which helped to determine the effects of waste type, operating mode, and burial depth on the retention of selected elements.

Retention of radioactive elements during large-scale operations has been predicted to be very high, based on pilot-scale retention data. Table 10 lists predicted and, where appropriate, measured DFs for the large-scale system assuming that the waste elements are at a burial depth of 1 m. Plutonium,

TABLE 10. Predicted and Measured Soil-to-Off-Gas Decontamination Factors for the Large-Scale System

Element[(a)]	Predicted DF	Measured DF
Co	1×10^2	--
Cs	1×10^2	1.3×10^2
Pu	1×10^3	--
Sb	1×10^2	--
Sr	1×10^4	2.8×10^4
Te	1×10^1	--
U	1×10^3	--
F	--	8.5×10^1
NO_3^-	--	$>2.5 \times 10^2$

(a) Waste elements are assumed to be buried at the 1-m depth.

strontium, and uranium have the highest DFs (10^3 to 10^4). Decontamination factors for the more volatile elements such as Cs and Sb average 1×10^2 or greater. Tellurium is expected to be slightly more volatile, with a DF of 1×10^1.

Large-scale tests have also produced soil-to-off-gas DFs for nitrates fluorides, and sulfates, which were not measured during pilot-scale tests. Nitrates have been added to many of the contaminated soil sites during their active lives. Thermal treatment processes generally decompose the nitrates to NO_x. However, LSOAT data show that the large-scale process is an efficient NO_x destructor. Prior to vitrification, nitrate salts were added to each of the three electrode settings to represent conditions at an actual TRU-contaminated soil site. During vitrification, these nitrates were effectively reduced to diatomic N_2 and O_2, based on nondetectable quantities of nitrates collected by the scrubber system and exhausted by the stack. Less than 0.07 kg of nitrates were collected by the scrubber system, and less than 0.05 ppm NO_x were exhausted out the stack. This results in a minimum NO_x destruction efficiency of 99.6% (DF = 250). This is an important characteristic because many contaminated soil sites may be rich in nitrates.

Numerous technical studies have been performed on the behavior of nitrates in thermal treatment processes to explain the NO_x destruction characteristic of ISV (Buelt and Carter 1986b). There have been a considerable number of basic kinetics studies of NO decomposition at temperatures from 25°C to 5000°C. Above 1300°C the thermal decomposition of NO is homogeneous and occurs by a mechanism involving O_2 atoms. Atomic O is believed to be in thermal equilibrium with molecular O_2 at these high temperatures and is assumed to react with NO by:

$$NO + O \rightarrow O_2 + N$$

which is followed by the much faster reaction:

$$NO + N \rightarrow N_2 + O$$

These two reactions, together with the O_2-O equilibrium reaction:

$$O_2 + M \rightarrow 2O + M$$

where M is a third body, are referred to as the Zeldovich mechanism (Zeldovich 1946). The temperatures of ISV molten soil have been measured between 1400°C and 2000°C, so this is a likely mechanism for destruction of NO_x in the ISV process.

The presence of pyrolysis and combustion products from vitrifying organics in the soil will aid NO_x destruction at lower temperatures. In a study by Mori and Ohtake (1977) the focus of NO decomposition was in the temperature region of 650 to 950°C. Measurements were made to determine the effects of the reducing species, CO and H, in combustion gas. Mori and Ohtake concluded that NO decomposition is obtained by the decomposition reactions of the reducing species as follows:

$$NO + CO \rightarrow 1/2N_2 + CO_2, \text{ and}$$

$$NO + H_2 \rightarrow 1/2N_2 + H_2O$$

This mechanism of NO decomposition may play an important role in ISV above the molten soil where temperatures are lower and reducing components exist. This mechanism for NO_x destruction is supported by analyses of gas bubbles taken in the cold cap region of LSOAT-1. Table 11 gives gas bubble compositions at

TABLE 11. Gas Bubble Composition Above Molten Surface of LSOAT-1

	Composition, %		
Gas	Top	Middle	Bottom
H_2O	0.7	0	0
N_2	55	52 to 88	6
O_2	6	3 to 6	0
CO_2	39	45 to 6	94
SO_2	trace	<0.01	<0.01

three depths within the cold cap. The main constituents, N_2 and CO_2, support the theory that NO_x destruction is accomplished with the aid of reducing agents, as Mori and Ohtake postulated.

The retention of fluorides in the vitrified soil is an important consideration when applying ISV to contaminated soil sites. For example, the 216-Z-12 Crib at Hanford received more than 2.8×10^8 L of 0.05 M fluoride waste during its 25-yr lifetime (Kasper 1982). Much of this sorbed to the underlying soil. High retention of the fluorides in the molten soil will minimize fluoride corrosion of the off-gas system. The fluoride analytical results from LSOAT-3 and LSVT provide consistent, conclusive data that retention of fluoride is 98.7% (DF = 85). In the case of 216-Z-12 Crib, high retention of fluorides keeps the expected accumulation in the off-gas system scrub solution to 0.18 wt%--less than half the functional design criteria limit. This eliminates the need to frequently change out scrub solutions.

Large-scale tests show that sulfates, on the other hand, demonstrate little propensity to be retained by the molten soil. Natural concentrations of sulfates in the soil and those added as waste simulants completely volatilize and are collected by the scrub solution. Normally, vitrification processes retain up to 1 wt% SO_2 in glass. However, the reducing conditions and high temperature that are prominent in ISV and responsible for NO_x destruction reduce solubility of SO_2 in the molten soil. The negligible retention of SO_2 eliminates the concern for creating leachable phases of $NaSO_4$ or FeS in the waste form.

A summary of soil-to-off-gas DFs for the pilot-scale tests is presented in Table 12. These data, support the large-scale data and prediction that most species are retained quite well (i.e., have high DFs) by the molten soil. Decontamination factors for simulated and actual nonvolatile fission products (Co, Mo, and Sr) and simulated and actual TRUs (Ce, La, Nd, Pu, and Am) are very high, ranging from $\sim 1 \times 10^2$ to $>1 \times 10^4$. Retention of semivolatiles, such as Cs, was also quite good, with DFs ranging from 3×10^1 to 2×10^3 depending on burial depth and operating condition. Cadmium, however, consistently exhibited a relatively high loss (DF of 3 to 4) due to its volatile nature at the high temperatures (~1600°C) of the molten soil. Tellurium was retained

TABLE 12. Soil-to-Off-Gas Decontamination Factors for Nonradioactive Pilot-Scale Tests

Trace Element	Decontamination Factors					
	PSFT-2	PSFT-3	PSFT-4A	PSFT-4B	PSCT-1	PSRT
Fission Products						
Nonvolatile						
Co	(a)	(a)	8×10^1	(a)	6.4×10^2	2×10^3
Mo	(a)	(a)	$>1 \times 10^5$	2×10^2	(a)	(a)
Sr	5×10^4	2×10^3	8×10^2	1×10^3	8.1×10^2	3.1×10^3
Semivolatile						
Cs	2×10^3	3×10^1	6×10^1	2×10^2	1.4×10^2	1.3×10^2
Sb	(a)	(a)	8×10^2	3×10^1	(a)	(a)
Te	(a)	(a)	1×10^2	2	(a)	(a)
Ru	(a)	(a)	(a)	(a)	(a)	5.5×10^2
Simulated and Actual Transuranics						
Ce	(a)	7×10^2	9×10^1	(a)	(a)	(a)
La	2×10^2	1×10^3	9×10^1	5×10^3	(a)	(a)
Nd	1×10^2	1×10^3	9×10^2	5×10^3	(a)	(a)
Pu	(a)	(a)	(a)	(a)	(a)	4.5×10^3
Am	(a)	(a)	(a)	(a)	(a)	1.2×10^4
Heavy Metals						
Cd	(a)	3	3	4	(a)	(a)
Pb	(a)	7	3×10^1	2×10^1	(a)	(a)

(a) Element not present during that test.

well when buried at a depth of 1.35 m during PSFT-4A, but exhibited a high loss during PSFT-4B, when it was buried at a relatively shallow depth of 0.4 m. Despite the high releases of these two elements from the soil, they were efficiently removed from the off-gas stream by wet scrubbing and condensing in the off-gas treatment system.

Element releases to the off gas are strongly dependent on burial depth, cold cap condition, and gas generation within the melt zone. The effect of depth on element retention can be seen by reviewing the data for PSFT-3 and -4 presented in Figure 23. At depths of ≥0.5 m, 99% of the nonvolatile species were retained. Simulated semivolatile fission products Cs, Sb, and Te showed the lowest retention; however, their retention in the soil increased to >99% at a 1.35-m burial depth. Over 99.9% of the nonvolatile elements were retained at the greater burial depth. In large-scale operations, it is expected that the vast majority of hazardous species will be buried deeper than 1.35 m. Indeed, large-scale tests verify enhanced retention of elements at greater than the 1-m depth.

Figures 24, 25, and 26 show the accumulation of Sr, Cs, and F in the off-gas scrubber system during LSOAT-3 and LSVT. Note the relative slopes of the accumulation curves at different times during the run. The rate of accumulation is high during the first 25 hours of the tests, but levels off rapidly during the later stages. The measured vitrification depths at 25 hours is 1.5 m. The fact that the maximum accumulation rate is achieved during the first 25 hours when the melt depth is less than 1.5 m supports the correlation

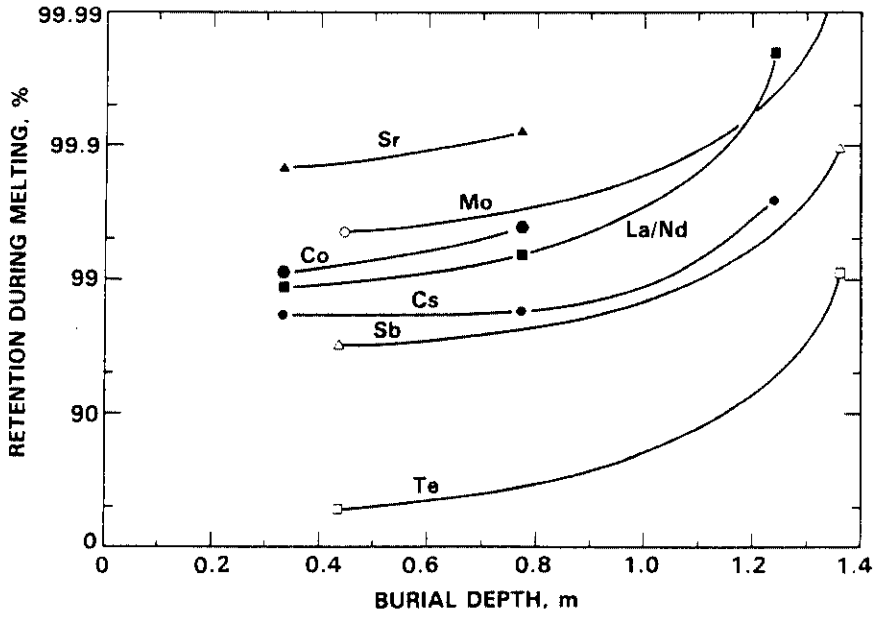

FIGURE 23. Effect of Burial Depth on the Retention of Selected Species Within the Vitrification Zone

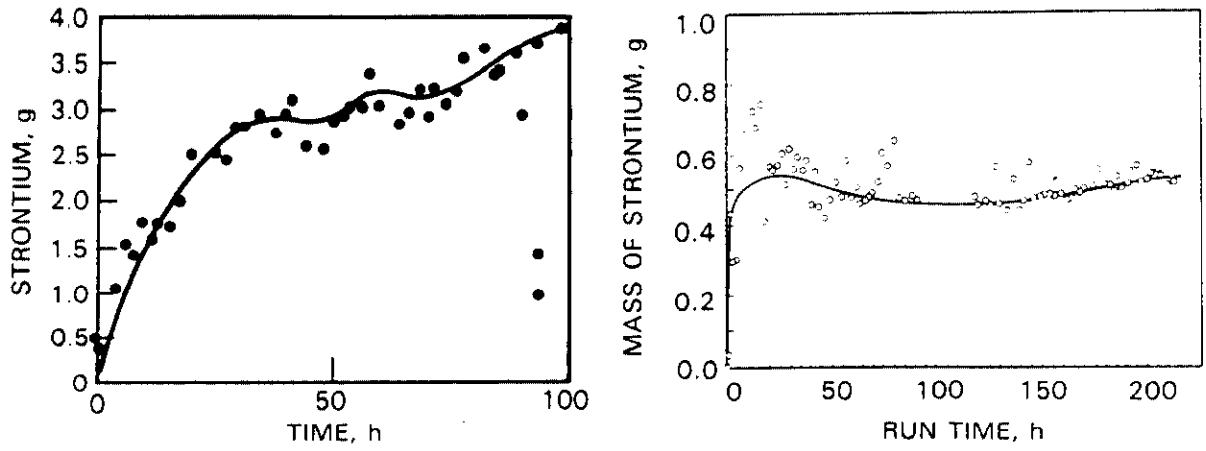

FIGURE 24. Accumulation of Sr in Scrub Solution Tanks for LSOAT-3 and the LSVT

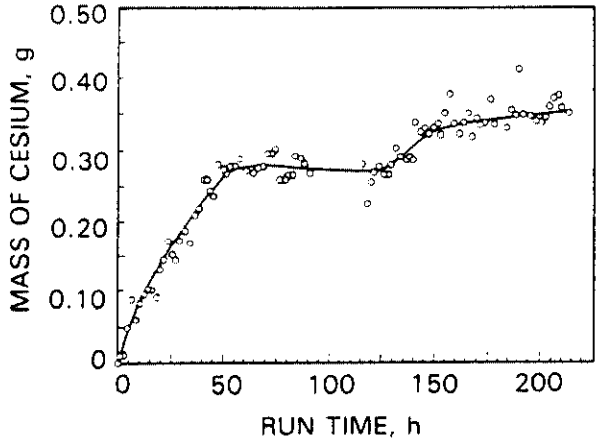

FIGURE 25. Accumulation of Cs in Scrub Solution Tanks for the LSVT

with burial depth. The accumulation curve for sulfates in LSOAT-3 and LSVT (see Figure 27) does not correlate with burial depth; this indicates that the release of sulfates from vitrified soil is a direct function of melting rate and concentration in the soil and is independent of burial depth. However, sulfates are removed efficiently by the scrubber system as described earlier.

The effect of the cold cap on element releases was revealed during PSFT-2, when the cold cap subsided and completely melted, exposing the red-hot molten surface. Figure 28 shows the cumulative releases of Cs and Sr to the off gas as a function of run time during this test. As the cold cap began to subside

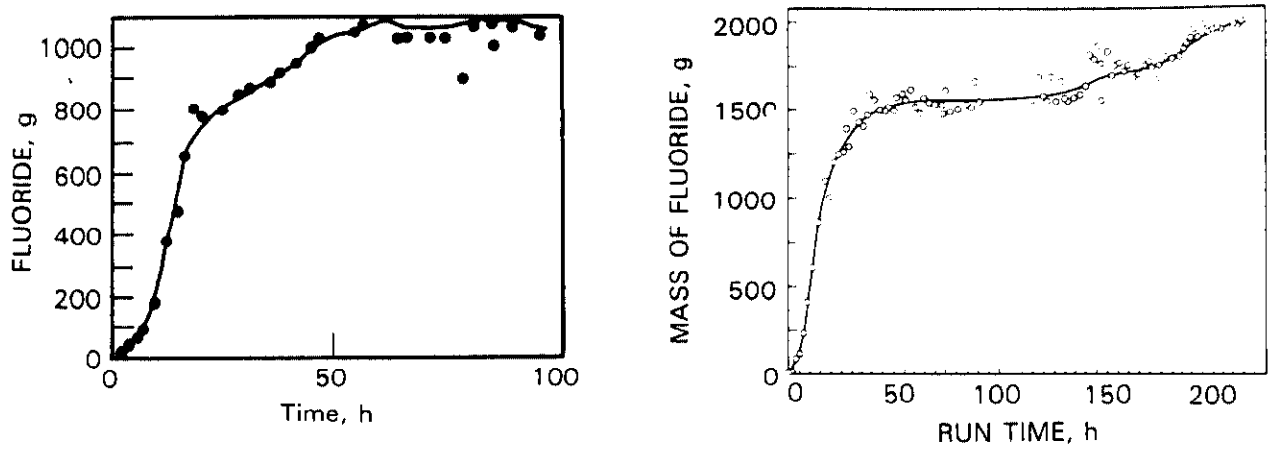

FIGURE 26. Accumulation of Fluoride in Scrub Solution Tanks for LSOAT-3 and the LSVT

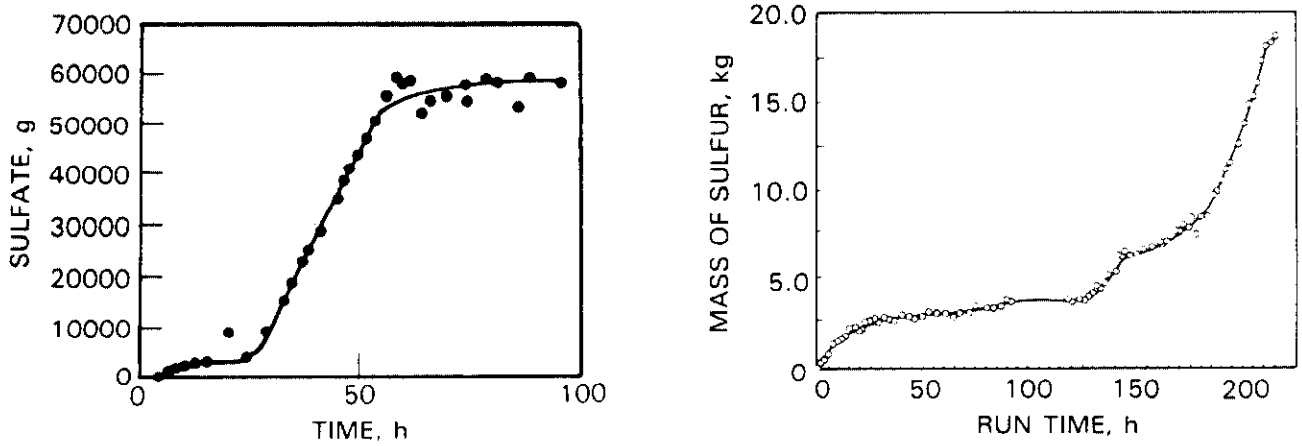

FIGURE 27. Accumulation of Sulfate in Scrub Solution Tanks for LSOAT-3 and the LSVT

(21 hours into the test), the Cs release began to increase steadily to a total loss of 0.047% (DF = 2.1×10^3). Because of its nonvolatile nature, Sr was not released to the same extent. The same type of behavior was observed for simulated TRUs (lanthanide series) in that the effect of the cold cap is much less pronounced for the nonvolatile elements. Releases of these elements are more of a function of rapid gas releases from the molten soil due to the decomposition of combustibles or other gas-generating substances.

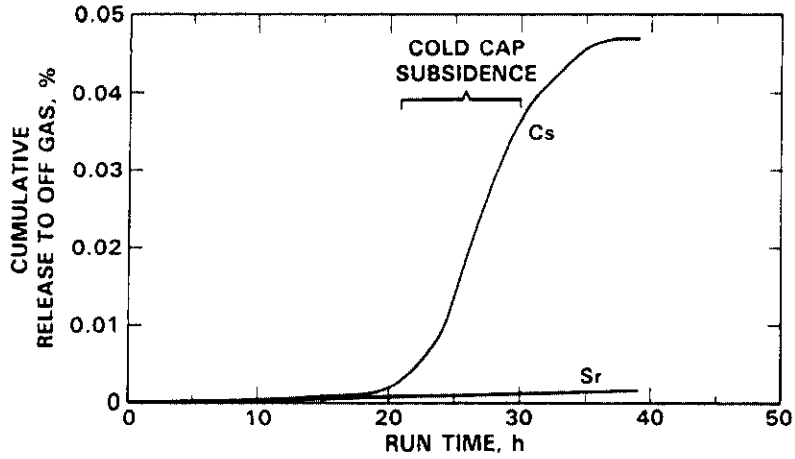

FIGURE 28. Effect of Cold Cap on the Release of Cs and Sr to the Off Gas During PSFT-2

Element releases that depend on rapid gas generation from combustible wastes are best illustrated by PSFT-3. The sequence of events is as follows. As the high-temperature, vitreous zone is achieved, buried combustibles pyrolyze. These pyrolyzed gases move upward through the molten zone and burn on contact with air at the surface. This upward movement of gas increases the entrainment of particles and creates a direct pathway for the release of the more volatile elements. Figure 29 shows the cumulative releases of Cs, Sr, and the lanthanides during PSFT-3, -4A, and -4B. Periods of active gas release are also indicated. Figure 30 shows similar release data for the heavy metals Cd and Pb. For most elements, a notable increase in their release to the off-gas system occurred during the rapid gas release periods.

The chemical form of a hazardous species associated with a gaseous release also affects the quantity released from the vitrification zone to the off gas. This was best illustrated during PSCT-1, in which Cs, Co, and Sr were placed in a simulated waste canister. The element releases to the off gas as a function of run time lapsed are illustrated in Figure 31. Cesium and strontium were primarily released during the initial glass penetration of the waste canister at 10 hours into the run. They were both present as nitrates, which decompose during vitrification. Cobalt, added as an oxide, did not evolve with the gas release to the same extent. Therefore, if the chemical form of an element does

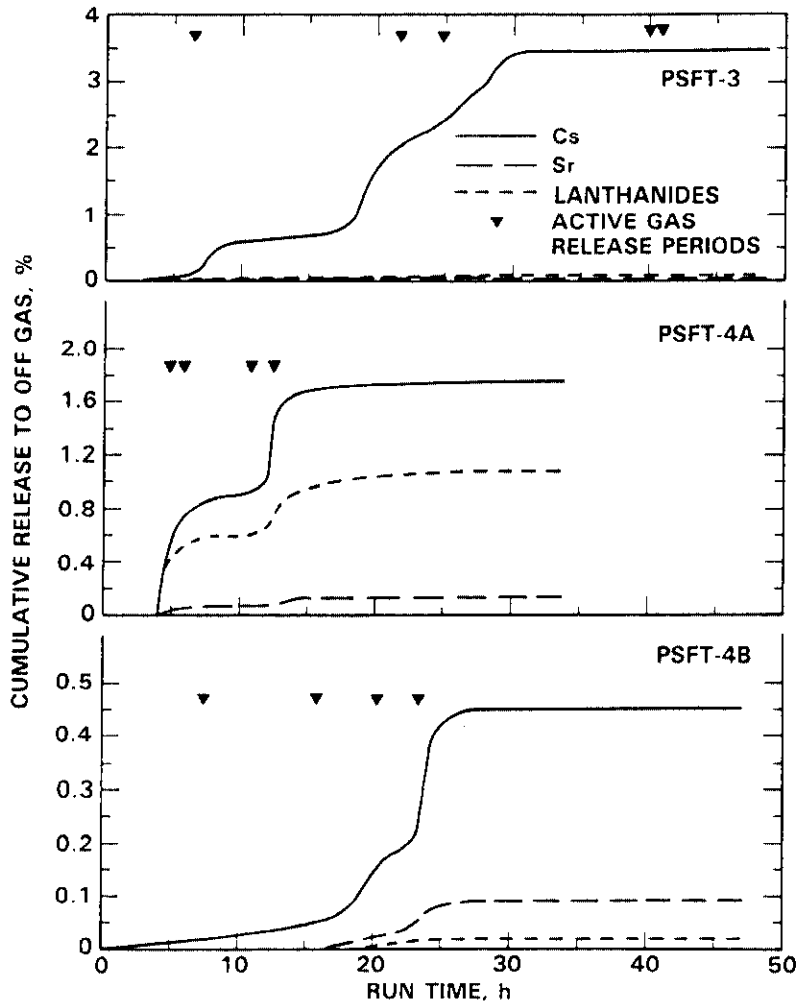

FIGURE 29. Effect of Gas Generation on the Release of Cs, Sr, and Lanthanides to the Off Gas During PSFT-3, -4A, and -4B

not decompose into gaseous byproducts when vitrified, it can be expected to have enhanced retention characteristics.

Cold Cap Subsidence

During the initial test of the large-scale unit (LSOAT-1), a large cold cap of porous molten soil formed on the surface of the melt, eventually rising above the original soil surface. This phenomenon creates a difficult closure problem that requires excessive backfill in the surrounding area and potential future subsidence. A rising cold cap also has the potential of bringing buried TRUs above the soil surface in the porous vitrified soil. Therefore, it was

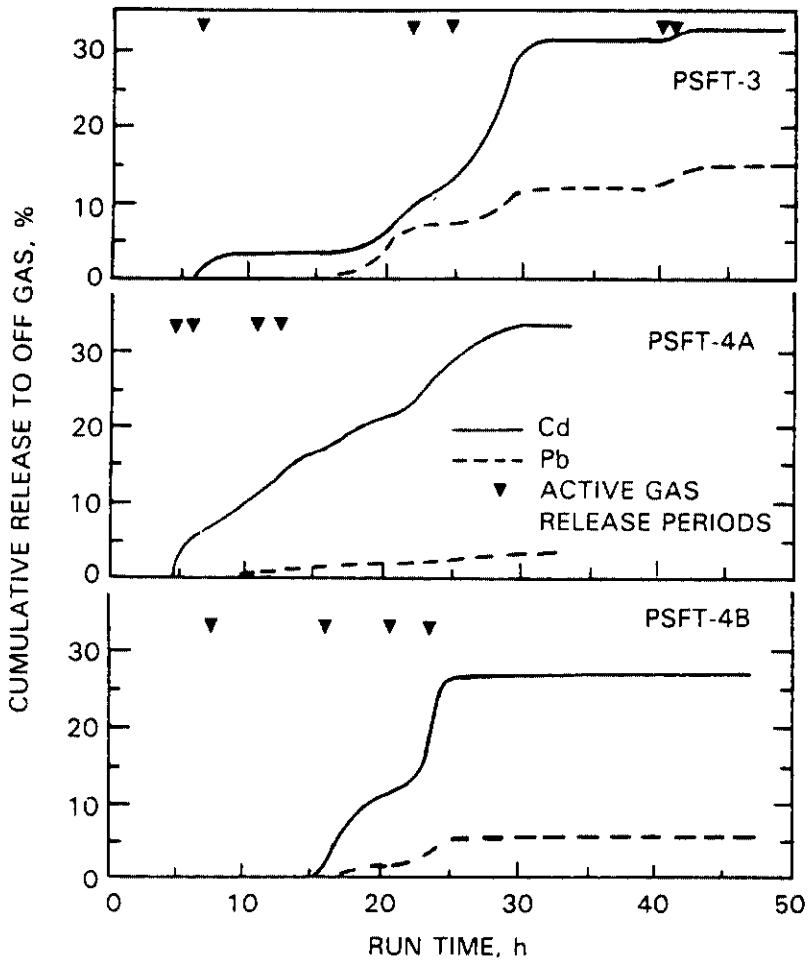

FIGURE 30. Effect of Gas Generation on the Release of Heavy Metals to the Off Gas During PSFT-3, -4A, and -4B

highly desirable to develop ways to eliminate the formation of the rising cold cap and to promote subsidence, without completely melting the cold cap.

A great deal of experience has been amassed on cold cap subsidence with the 14 pilot-scale and 4 large-scale settings, each producing varying degrees of subsidence. A statistical analysis was employed prior to the third large-scale setting to determine the parameters that control cold cap subsidence (Buelt and Carter 1986b). Although many factors are suspected to govern cold cap subsidence, two parameters have the greatest influence: 1) graphite collars around the electrodes and 2) surface insulation. Use of both helps keep

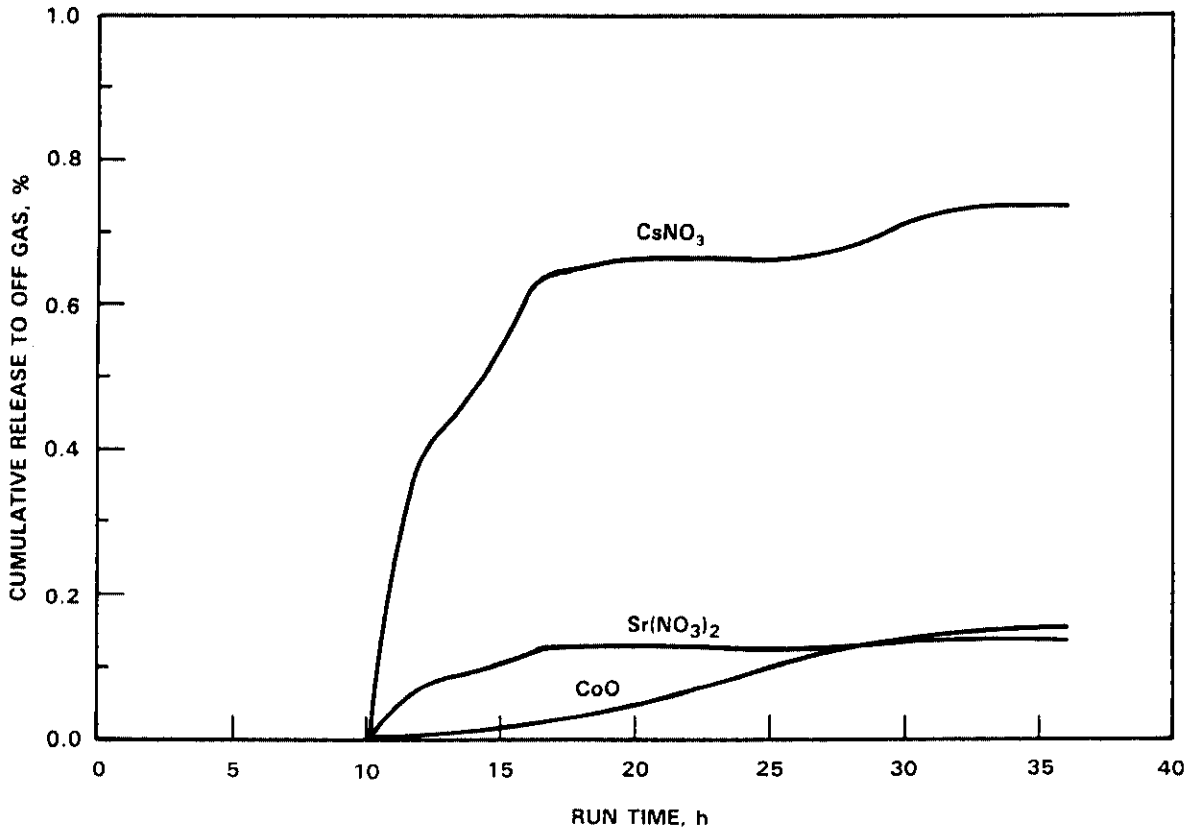

FIGURE 31. Effect of Chemical Form on the Release of Simulated Fission Products to the Off Gas in PSCT-1

the surface partially molten, thereby encouraging gas release during vitrification; the graphite collars enhance the thermal conductivity of the electrode bringing heat to the surface, and the insulative layer reduces heat losses to help keep the vitrified surface partially molten.

Oma et al. (1983) demonstrated the influence that graphite collars have on keeping the porous glass region molten. A thermal analysis was performed to predict the temperature profile of an electrode protruding above the melt zone during ISV. For the analysis the temperature of the plenum gas was 300°C, and the temperature of the electrode at the surface of the cold cap was 1200°C. A plot of the temperature profile for graphite is shown in Figure 32, along with stainless steel, carbon steel, and copper rods of equal diameter for comparison. As shown, graphite is an extremely good conductor of heat, with its

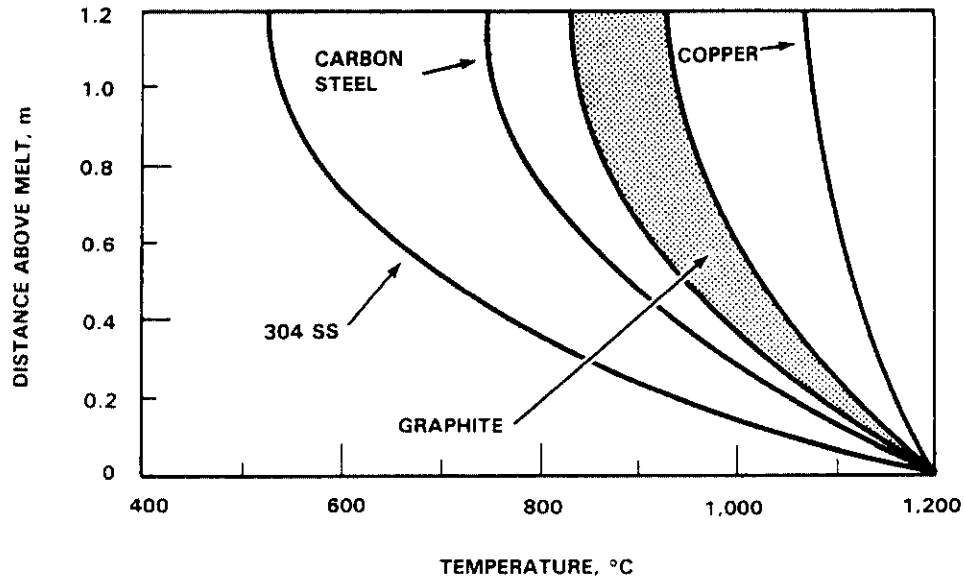

FIGURE 32. Temperature Profiles for Graphite, Stainless Steel, Carbon Steel, and Copper Rods

performance falling between those of carbon steel and copper. The thermal conductivity of graphite is 5 to 10 times higher than that of soil. Although its thermal conductivity is nearly identical to that of Mo, it is impractical to consider 15-cm-dia Mo to achieve high surface temperatures because of cost. Temperatures within 0.4 m of the surface are predicted to be >1000°C for a graphite rod 1.2 m in height. This conduction of heat is thought to be one of the principal causes of cold cap subsidence.

A series of parametric pilot-scale tests was conducted to verify the influence of graphite collars and surface insulation (Buelt and Carter 1986a). A 1 to 10 rating system was developed to quantify the degree of subsidence for each parametric, pilot-, and large-scale test conducted prior to LSOAT-3. The ratings were fit into a matrix shown in Table 13. A three-way, fixed-effects analysis-of-variance technique was used to help predict cold cap subsidence for the third large-scale setting (LSOAT-3). Although the available data were insufficient to base a quantitative prediction on, a qualitative judgment could be made that the graphite collars and surface insulation would be effective in causing the cold cap to subside below the soil surface. The LSOAT-3 results verified the statistical prediction--the cold cap subsided

TABLE 13. Statistical Matrix Ranking Cold Cap Subsidence with Subsidence Technique

	Without Graphite Collar				With Graphite Collar			
	With Insulation		Without Insulation		With Insulation		Without Insulation	
Electrode Spacing	Rating	No. of Tests	Rating	No. of Tests	Rating	No. of Tests	Rating	No. of Tests
0.6	--	--	2	1	10	1	10	1
1.2	--	--	3	2	8.5	2	6.7	6
4.5	4	1	1	1	--	--	--	--

between 50 cm and 80 cm without completely melting, equivalent to a rating of 7. These results were repeated during the subsequent LSVT by employing graphite collars and surface insulation. This cold cap subsidence technique is now the reference method for carrying out vitrification operations.

Depth Monitoring

During the engineering- and pilot-scale development phase, growth of the vitrification zone was monitored by thermocouples placed in the soil at designated positions. These in-ground thermocouples are not considered feasible for monitoring vitrification depth at a radioactive waste site. Therefore, a depth monitoring concept was incorporated and tested in subsequent pilot- and large-scale tests. (Figure 33 shows the design of the optical fiber depth sensor.)

A depth monitoring system is used in conjunction with the ISV process to monitor the depth of the molten soil at specific times during the ISV operation. The depth monitor consists of a signal processor and transmitter package mounted below one or more of the electrodes as shown in Figure 34. For operation, a series of fiber optic sensors runs from the signal processor to different levels on the electrode(s). As the ISV process melts downward, the sensors transmit a self-generated light to the signal processor (as shown in Figure 34) to indicate that the molten soil has reached that depth. The depth data is then passed on to the transmitter, which sends the data on to the receiver located at the ground surface. The receiver then passes the depth data to a second processor that decodes the data and displays it for the ISV operations personnel. Two depth transmitters, a receiver, and a microprocessor were

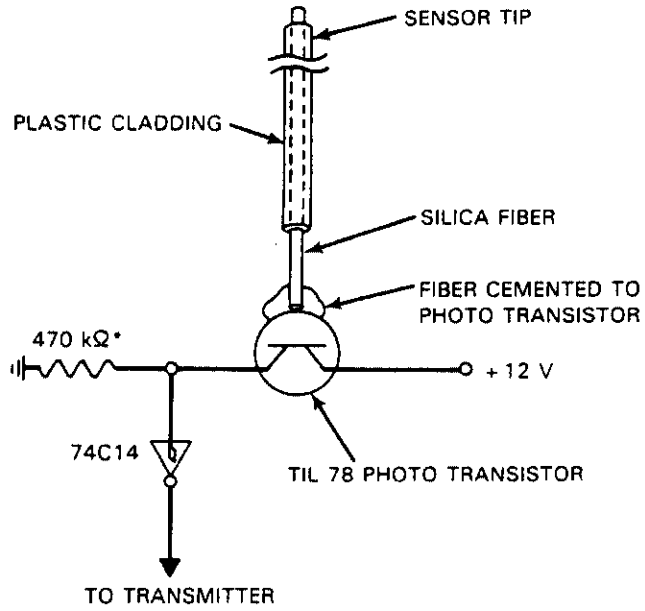

FIGURE 33. Design of Optical Fiber Depth Sensor

tested during PSCT-5 and the LSVT. Two laboratory soil-heating experiments were also conducted to aid in the understanding of the performance of candidate fiber optics under actual ISV conditions. The results of the soil-heating experiments are discussed in the following section.

Fiber-Optic Soil-Heating Experiments

Three candidate optic fibers (sensors) were compared during the experiments as shown in Table 14. The laboratory tests showed that as the soil temperature increases above 900°C, the purple optic fiber produces a phototransistor current output that exceeds 75 μA. This compares with the maximum of 6 μA for the blue optic fiber and less than 0.1 μA for the orange optic fiber. Figure 35 provides a comparison of photo transistor current output versus temperature.

The orange optic fiber did not exceed an output of 0.1 μA. During PSCT-5, the depth sensor electronics could not be adjusted below 0.5 μA sensitivity to avoid false "on" readings, especially as the transmitter package warms up. The

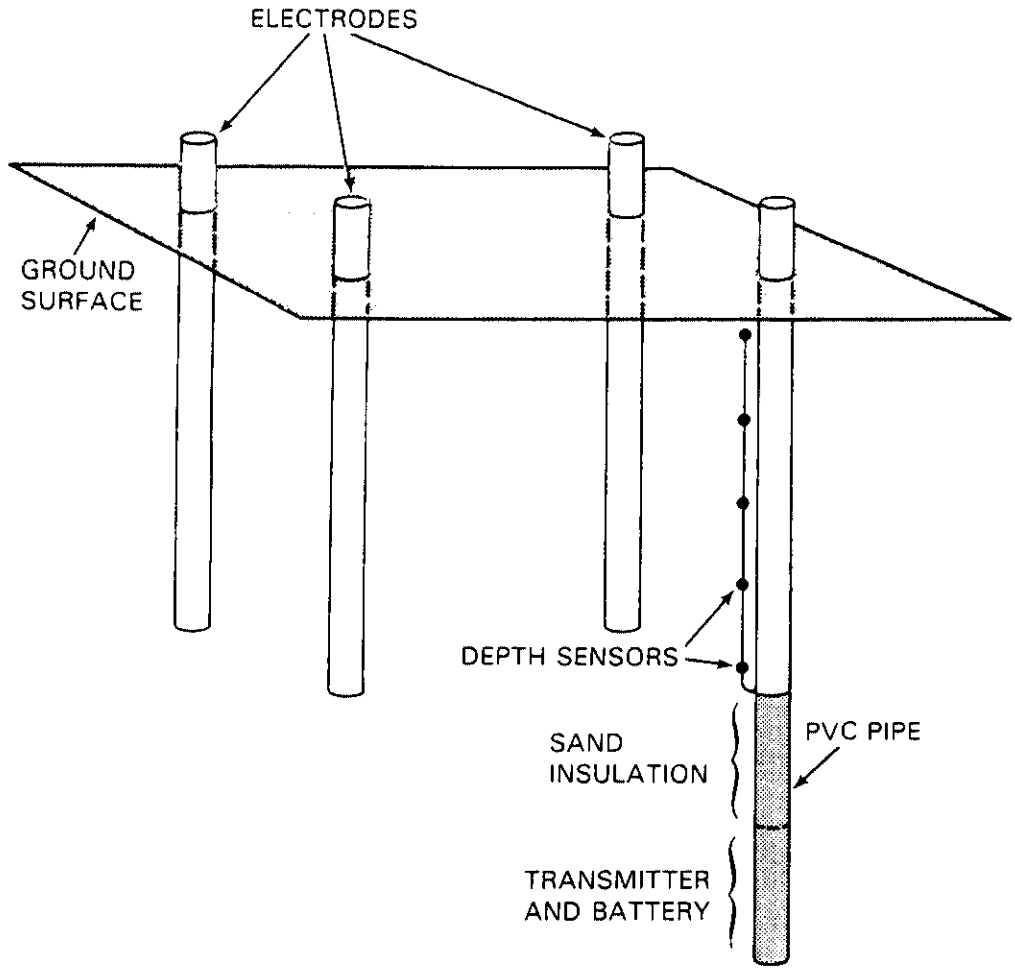

FIGURE 34. Depth Transmitter System Configuration for Monitoring Melt Depth

low output of the orange optic fiber in conjunction with the high sensitivity setting prevents this type of sensor from being selected as an ISV depth sensor. The purple optic fiber is by far the optimum choice. The silica and fluorine cladding on the purple optic fiber is the key to its superior high-temperature light conductivity.

The conclusions established by the laboratory tests are confirmed by the pilot- and large-scale tests. Prior to obtaining the information gathered from the laboratory tests, the orange sensors were used on PSCT-5. Because of their poor current output at the high temperatures of the soil, depth indications were never received. Conversely, pilot- and large-scale tests with blue and

TABLE 14. Fiber Optics Evaluated During Laboratory Soil-Heating Experiments

Manufacturer:	Maxlight MSC 200 Series	Ensign-Bickford Optics Company HCS Simplex Plenum	Raychem VSC-1B-10-17
Color of Sheath	Blue	Orange	Purple
Construction:			
Core	Silica	Silica	Silica
Cladding	RTV Silicone	Polymer(a)	Silica + F_2
Buffer	--	Tefzel	Silicone
First Jacket	Tefzel	--	Tefzel
Strength Member	Kevlar	Kevlar	Kevlar
Second Jacket	Hytrel	Copolymer	Tefzel

(a) Proprietary.

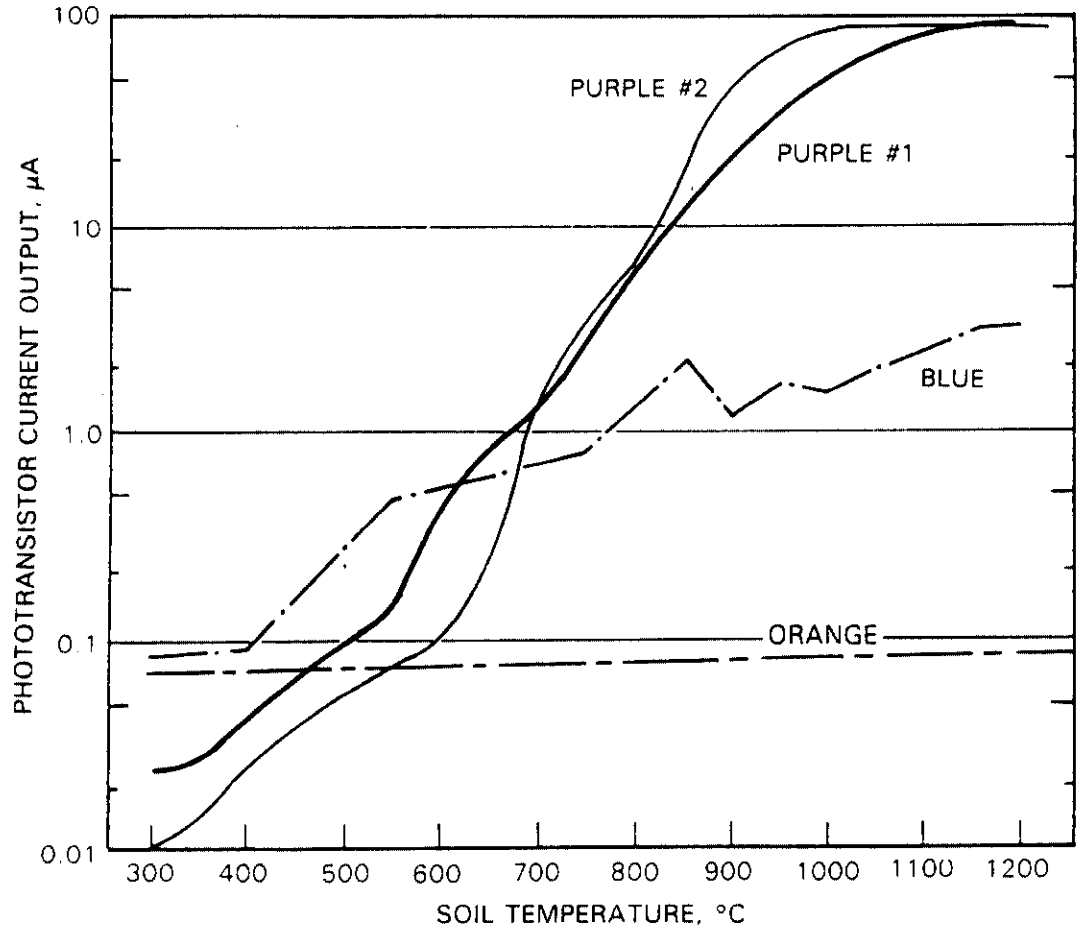

FIGURE 35. Phototransistor Current Output as a Function of Temperature During Test 2

purple sensors produced quantifiable results, giving an accurate indication of depth. Figure 36 is a plot of depth versus time obtained from the depth sensor for the LSVT.

Based on the results of the fiber optic soil-heating tests and the pilot- and large-scale ISV operating experience, the following recommendations are made for future use:

- The erroneous transmitter data produced during PSCT-5 are due to two factors: 1) low light transmission efficiency of the orange optic fiber complicated by thermal destruction of the polymeric cladding at 450 to 550°C prevented the sensors from transmitting enough light to the transmitters, and 2) the high sensitivity setting of the sensor electronics (0.5 μA) resulted in some false "on" readings. Consequently, sensitivity settings should be increased, and the orange optic fiber should not be used.
- The purple optic fiber with the silica core and silica and fluorine cladding is clearly superior as a depth monitor sensor material to the polymer-clad fiber optics tested and should be used for future ISV operations.
- The sensor electronics should be adjusted to indicate "on" at a phototransistor current output of between 5 and 50 μA. Below 5 μA, the soil temperature is too cool (less than 750°C) and the probability of false "on" readings increases. Above 50 μA, the probability of sensors turning off after being activated increases. The optimum setting is between 25 and 40 μA, which would indicate a soil temperature of 850 to 905°C.

Other Monitoring Concepts

Other depth monitoring concepts evaluated prior to the selection of the depth transmitter system were infrared sensing, ultrasonics, power/design parameters, acoustics, and ground penetrating radar (GPR). The results of the evaluation of these concepts are summarized briefly here.

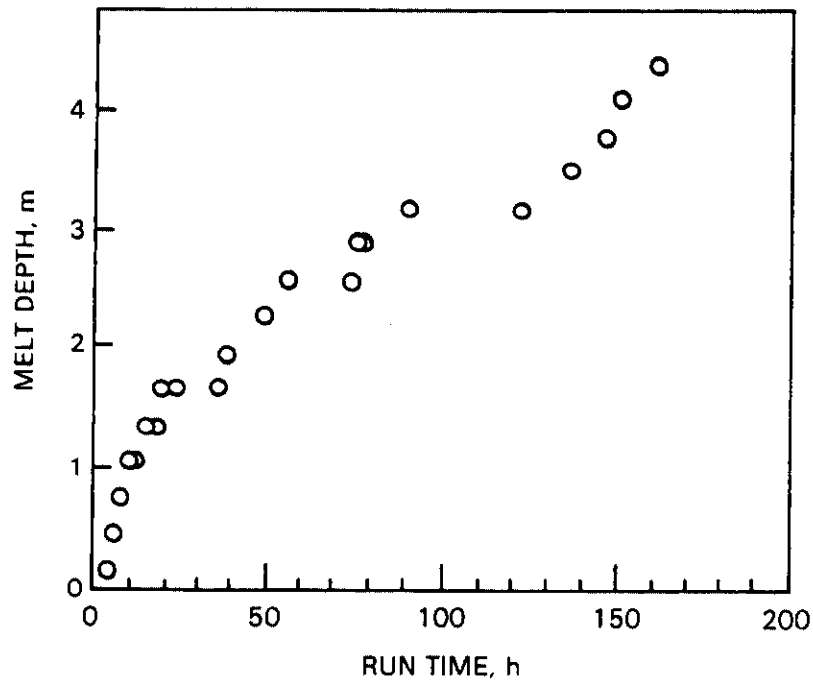

FIGURE 36. Melt Depth versus Run Time Determined by the Depth Monitor During the LSVT

- The infrared technique has little or no value for monitoring vitrification growth. Infrared sensing is strictly a surface-mapping technique and as such, cannot directly measure vitrification depth.
- The ultrasonic method involves transmitting ultrasonic pulses through a wave-guide coupled to the molten glass and measuring the travel time of the reflected pulse to determine melt depth. To do this, the wave-guide must be extended through the porous cold cap and rock layer into the molten glass during processing because these upper regions are too attenuative for transmission. The wave-guide is not capable of withstanding the high temperature (1800°C) of the molten glass. Moreover, the glass attenuation is too high for practical use of the ultrasonic technique.
- Power input and system design parameters combined with mathematical modeling are not a direct method of measurement. Substantial data on the soil and waste properties would be required before this method would be reliable for depth predictions.

- Data obtained by the acoustic and GPR methods are complex and require computer-aided interpretation. Subsurface geologic features complicate data analysis by altering the acoustic velocity and radar images. Both techniques are also subject to interference. Acoustic methods that employ subsurface or downhole sensors provide the best results for monitoring depths. This would necessitate drilling an additional shaft in potentially contaminated soil, producing additional exposure and spreading contaminants.

Electrode Performance

Use of the cold cap subsidence technique described earlier has produced a technical challenge to maintaining electrode performance. Present electrode design calls for a 5.1-cm-dia Mo rod inserted into the contaminated soil that is to be vitrified. The upper regions of the electrodes, which are exposed to air when the molten surface subsides during processing, are encased in a 6.4-cm-ID by 15-cm-OD graphite collar. Subsidence of the cold cap exposes the graphite collar to air at high temperatures (i.e., >600°C). The life of the graphite under these conditions has not been demonstrated beyond 40 hours. The graphite collar is eventually consumed by oxidation and spalling, thereby exposing the Mo electrode to the same oxidizing conditions at these temperatures. As Stanek (1977) reports, Mo exposed to temperatures greater than 600°C in air oxidizes rapidly. Successful elimination of the rising cold cap in the LSOAT-3 and the LSVT created these conditions, causing electrodes to fail, beginning at 28 hours into the tests.

The three failures experienced during the third setting of the LSOAT were caused by oxidation, not breakage, as evidenced by visual observations (Buelt and Carter 1986b). The northwest electrode that remained intact throughout the run also showed diameter loss from oxidation at the failure point of the graphite collar. During the longer term LSVT the Mo/graphite combination electrodes failed by oxidation and breakage. Breakage was caused by stresses created by the shifting and collapse of the cold cap. Table 15 summarizes the history and results of electrode use for all of the major development tests. In previous experiments, before employing the graphite collar technique for enhancing cold cap subsidence, a protective layer of molten soil adhered to the Mo electrodes,

TABLE 15. Electrode Type and Testing Schedule

Test	Date	Electrode Material	Electrode Results
ESLT-1[a]	8/80	Mo	Success with Mo
ESLT-2	12/80	Mo	Stainless steel buss failed
ESLT-3	1/81	Mo	Successful
ESLT-4	3/81	Mo	Successful
ESLT-5	4/81	Mo	Successful
ESLT-6	6/81	Graphite	Buss connection failed
ESLT-7	7/81	Graphite	Successful
ESLT-8	9/81	Graphite	Successful
ESLT-9	10/81	Graphite	Successful
ESLT-10	12/81	Graphite	Successful
ESLT-11	1/82	Graphite	Successful
ESLT-12	2/82	Graphite	Successful
ESLT-13	2/82	Graphite	Successful
ESLT-14	3/82	Graphite	Successful
ESLT-15	5/82	Graphite	Successful
ESLT-16	12/82	Graphite	Successful
ESLT-17	5/83	Graphite	Successful
ESLT-18	6/83	Graphite	Successful
ESLT-19	9/83	Graphite	Successful
ESLT-20	12/83	Graphite	Successful
ESLT-21	2/84	Graphite	Successful
ESLT-22	7/85	Mo	Successful
ESLT-23	10/85	Mo	Successful
ESLT-24	5/86	Mo/graphite & insulation	Limited oxidation
PSFT-1[b]	10/81	Mo	Successful
PSFT-2	12/81	Graphite	Excessive oxidation
PSFT-3	3/82	Graphite	Limited oxidation
PSFT-4	6/82	Graphite	Limited oxidation
PSCT-1[c]	3/83	Graphite	Limited oxidation
PSCT-2	5/83	Graphite	Limited oxidation
PSRT-2[d]	6/83	Graphite	Limited oxidation
PSCT-3	4/84	Mo	Rising cold cap
CCT[e]	3/85	Mo	Rising cold cap
CCT-2	3/85	Mo/graphite	Successful
CCT-3	4/85	Mo/graphite & insulation	Successful
PSCT-4	6/85	Mo/graphite & insulation	Graphite failed, Mo oxidized
PSLW-1[f]	12/85	Mo/graphite & insulation	Successful
PSCT-5	1/86	Mo/graphite & insulation	Graphite failed, Mo protected
LSOAT-1[g]	12/84	Mo	Rising cold cap
LSOAT-2	1/85	Mo & insulation	Rising cold cap
LSOAT-3	7/85	Mo/graphite & insulation	Oxidation & failure
LSVT-1[h]	2/86	Mo/graphite & insulation	Oxidation, breakage & failure

(a) ESLT = Engineering-Scale Laboratory Test.
(b) PSFT = Pilot-Scale Field Test.
(c) PSCT = Pilot-Scale Cold Test.
(d) PSRT = Pilot-Scale Radioactive Test.
(e) CCT = Pilot-Scale Parametric Cold Cap Test.
(f) PSLW = Pilot-Scale Lime Waste Test.
(g) LSOAT = Large-Scale Operational Acceptance Test.
(h) LSVT = Large-Scale Verification Test.

protecting them from oxidation. Since the graphite collar prevents the natural protective glass coating from forming, a substitute coating material is needed over the Mo electrodes when graphite collars are employed.

Potential solutions to the oxidation and breakage problem have been implemented in the two most recent ISV tests using larger diameter collars and coating materials in the annulus between the graphite collar and the Mo rod. The best oxidation protection technique is the use of larger diameter (30-cm) graphite collars. Experience with this material has prevented oxidation failure of the Mo electrode during the LSVT by maintaining a sheath of graphite around the electrode in the subsidence zone; this is not achieved with 15-cm-dia collars. The larger diameter collars provide sufficient material to maintain the protective sheath in the subsidence zone. The collar sections can also be screwed together to provide support for the Mo electrodes to protect them from transverse loads during cold cap subsidence or soil sloughing events.

Use of 30-cm-dia (1-ft-dia) collar is also important because excessive current densities on 15-cm-dia (6-in.-dia) graphite collars during startup cause excessive heat generation in the glass near the electrodes. The abnormally high glass temperatures contribute to a more rapid corrosion/oxidation rate for the collars and the high electrical currents create active reactions at the graphite/glass interface, which can transmit additional stresses on the Mo electrodes.

Estimated current densities during the LSVT have been determined up to 0.45 A/cm^2 for the 15-cm-dia collars. Stanek (1977) recommends maximum current densities for graphite electrodes of 0.3 A/cm^2. The 30-cm-dia collar used for one of the electrodes during the LSVT had a maximum current density of only 0.24 A/cm^2--within the established limit. Visual observations confirmed much calmer melting behavior near this electrode, whereas the 15-cm-dia collars were generating turbulent reactions and electrical arcing. Figure 37 establishes the maximum allowable current to a combination electrode with a 30-cm-dia graphite collar as a function of depth to maintain a current density of less than 0.25 A/cm^2--the recommended limit for ISV. Excessive current density can be controlled by using larger diameter collars and by controlling current during the startup sequence. Reduced amperage during a controlled startup

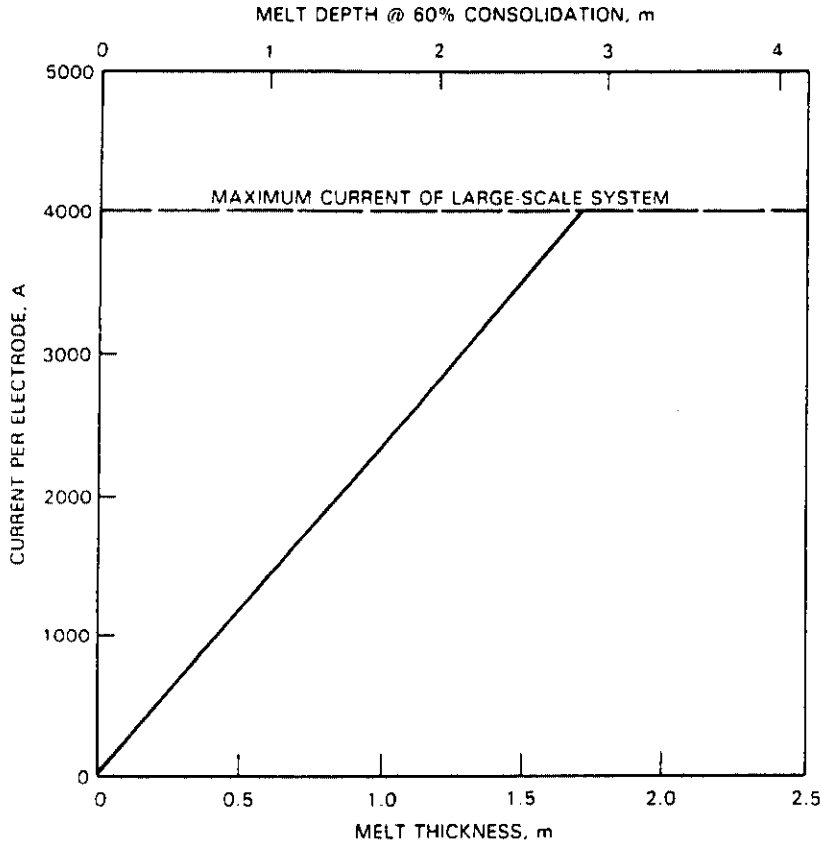

FIGURE 37. Maximum Current to Electrodes with 30-cm-dia Collars as a Function of Depth

sequence reduces the concern about excessive amperage on the graphite collars. Amperage can be maximized and the ISV process can be operated as usual once a large enough stable conductive path is established.

The most prospective coating (oxidation barrier) material used in the tests was 88% ZrB_2/12% $MoSi_2$ powder. Zirconium diboride/molybdenum disilicide was selected because of its oxidation resistance and electrical conductivity properties. The $ZrB_2/MoSi_2$ coatings were considered in three fashions: 1) as a powder that would sinter into a protective coating, 2) as a plasma-spray coating of the material on the Mo rods, and 3) as a coating painted on to protect bare Mo surfaces when lowering replacement electrodes after failure of the initial electrodes. Plasma-spray coating of the 1.8-m-long (6-ft-long) Mo rods was not achievable by commercial plasma-spray vendors due to the particle size constraints of the spraying equipment and the unavailability of large

atmosphere-controlled spray chambers. However, associated laboratory testing has been done with the $ZrB_2/MoSi_2$ and $HfB_2/MoSi_2$ coatings. The laboratory testing indicated successful use of the plasma-spray coating as an oxidation barrier for Mo.

The $ZrB_2/MoSi_2$ powder, introduced into the annulus between the graphite collar and Mo electrode, proved to be an effective oxidation barrier during PSCT-5 by forming a sintered, protective coating around the Mo rod. The sintered coating, when exposed to oxidizing conditions after the graphite had burned through, was effective in preventing any further oxidation of the Mo. This pilot-scale test also indicated that there is a time-at-temperature factor associated with the sintering process of the powder. Because of lower temperatures in the upper, startup region of the electrode, this region did not provide an effective sintering coating, which has been demonstrated to begin in the 1400 to 1600°C range. This area must rely on a plasma-spray coating of $ZrB_2/MoSi_2$ or alternative coating material(s).

The $ZrB_2/MoSi_2$ powder was also evaluated during the LSVT. In this large-scale test, all four electrodes apparently failed by oxidation and/or fracture. The exact failure mechanism is difficult to ascertain due to limitations in viewing and the inability to retrieve failed electrode samples for analysis. It is thought that the initial failures occurred because of breakage caused by forces exerted by the subsiding cold cap and/or oxidation in the initial subsidence region, where the electrodes were not exposed to high enough temperatures to fuse the $ZrB_2/MoSi_2$ protective coating. Since the exact mechanism of failure is unknown and since all four electrodes used the powder method of oxidation protection, the effectiveness of the powder could not be evaluated for large-scale use. However, based on the pilot-scale results, this technique offers extreme promise.

The $ZrB_2/MoSi_2$ paint coating on electrode replacements, on the other hand, proved to be ineffective in eliminating oxidation of electrodes. Replacement electrodes must be coated with flame spray or fused coating materials because the paint components vaporize, bubble, and form unprotected portions on the Mo electrode.

Another oxidation coating material that shows great promise is $MoSi_2$. The glass industry has shown $MoSi_2$ to be a proven oxidation-resistant material for use in sections that are prone to oxidation (Davies and Argent 1985). The coating is applied and fused in a furnace at 1400°C. This is a much simpler and less costly application technique than the atmosphere-controlled plasma-sprayed $ZrB_2/MoSi_2$ coating technique. However, to avoid diffusion of the Si into the electrode material, which results in the loss of the coating, the electrode must not be exposed to temperatures greater than 1750°C. Furnace tests of $MoSi_2$-fused coatings for 100 hours at 1600°C have shown no tendency for Si diffusion and have left the coating intact. Molten soil temperatures have been measured in the range of 1450 to 1600°C for ISV--below the maximum temperature limitation. However, since the coating is brittle, great care must be taken in handling the electrodes prior to their use to avoid generating pinholes or cracks in the coating material.

Glass frit or a glass tube when melted by the heat of the process has also been investigated as a coating material to inhibit oxidation of the Mo. The glass frit (or tube) is put in the annulus between the graphite collar and the Mo rod. However, when the glass melts, there is no way to control the effectiveness of the coating, because the glass may flow unevenly and not form a significant amount of protection. It also exhibits a higher electrical resistivity than alternative packing materials such as $ZrB_2/MoSi_2$. Limited data on the use of the glass coating require that further evaluation be performed before deciding on its usefulness as an oxidation barrier.

Another oxidation prevention method tested in the last large-scale test was the injection of N_2 into the annular region between the Mo and the graphite. This method is designed to increase the pressure inside the annulus and inhibit any O_2 diffusion and attack on the binder in the upper region of the graphite collar. This method is more complex than the coating methods and did not prove to be effective.

In previous tests, the surface area of the Mo rods has been coated with flame-sprayed stainless steel. This worked effectively in preventing oxidation in the startup region. An extension of this option would be to test a flame-sprayed stainless steel coating coupled with the $ZrB_2/MoSi_2$ powder in the

annulus between the stainless steel coated Mo rod and the graphite collar. These multi-layer barriers could provide effective oxidation prevention. However, stainless steel coatings are expected to cause contamination and hardening of the Mo at elevated temperatures resulting in embrittlement. Stainless steel coatings may still have some duplex coating benefits in the near-surface subsidence zone as a secondary oxidation barrier, but they will require further testing.

Waste Form Performance

This section discusses the analyses performed on the soil surrounding the vitrified blocks to determine if waste elements migrate. The vitrified blocks themselves were analyzed to trace the distribution of simulated waste elements. The durability of the glass product was also assessed, and the assessment results are presented in this subsection.

Migration Analysis

Most of the soil sample analyses for the pilot- and engineering-scale tests show no migration of simulated contaminant elements beyond the vitrification zone. The same result was achieved for polychlorinated biphenyls (PCBs) (Timmerman 1986). Even the partially fused soil at the molten edge approached the detection limits of these elements. Thus the high viscosity of this region apparently prevents the migration of simulated contaminants to the outside of the vitreous block. An anomalous migration of Cs and Sr to the small region directly below the center of the melt occurred during PSFT-2. No other ISV test has detected contaminant migration beyond the vitrified block.

Detection sensitivity of radionuclide migration was improved with the analysis of soil that surrounded the glass block during the radioactive field test. Soil samples surrounding the pilot-scale radioactive block were taken to determine if migration of hazardous constituents occurs beyond the vitrification zone. Five equidistant samples were taken at 6-in. intervals from the top to the bottom of the block at the northwest face directly adjacent to the block. Overall, the samples indicated no detectable migration of radionuclides outside the vitrification zone (Timmerman and Oma 1984). Activity was found in a few of the near-surface samples; these samples were probably

cross-contaminated with surface soil that contained radioactive material from off-gas releases. Most other soil measurements were low enough to indicate that no migration occurred outside the vitrification zone (excluding any sampling errors). Referencing these low activities to natural background levels puts these levels in perspective. For example, ^{137}Cs and $^{239/240}Pu$ occur naturally in western surface soil at activities of 4.5 and 0.07 pCi/g, respectively (Robertson et al. 1981). The majority of the samples are well below the natural background levels.

The contaminants were uniformly distributed throughout the vitrified soil blocks in all nonradioactive pilot-scale tests, indicating that extensive convective mixing occurred during operation. Concentration profiles show that near the edge of the vitrification zone the contaminant concentrations decrease to natural soil levels. Concentration plots also show that within the dense glass layer of the melt the contaminant concentrations reach their respective, evenly distributed amounts. In one pilot-scale test, for example, the CsO_2 concentration was 0.04 wt%, the SrO_2 concentration was 0.08 wt%, and the LaO_2 concentration was 0.05 wt% within the inner glass zone. These values correspond closely to the predicted homogeneous values of 0.04, 0.08, and 0.04 wt%, respectively. Apparently, convective mixing and an even distribution of contaminants occur within the molten core. Contaminant concentrations in the rock layer are lower due to the dilution effects of the rocks. Samples from the uppermost porous layer show the same relative distributions and concentrations of the contaminants as in the glass region of the melt; however, when employing cold cap subsidence techniques, the porous region only encompasses a small (<5 wt%) portion of the vitrified block.

While Cs selectively migrated upward in some engineering-scale tests, there was no evidence of this movement in the pilot-scale tests. Pilot-scale test results indicate that the convective mixing patterns may dominate the diffusion mechanisms through the molten soil and provide a uniform distribution of contaminants. An example of a typical distribution pattern for rare earths is provided in Figure 38 for Ce (Oma, Farnsworth, and Rusin 1982). The final concentration of Ce was 14 times less than its initial concentration. This uniform distribution of the rare earths (Ce, La, and Nd) suggests that actinides

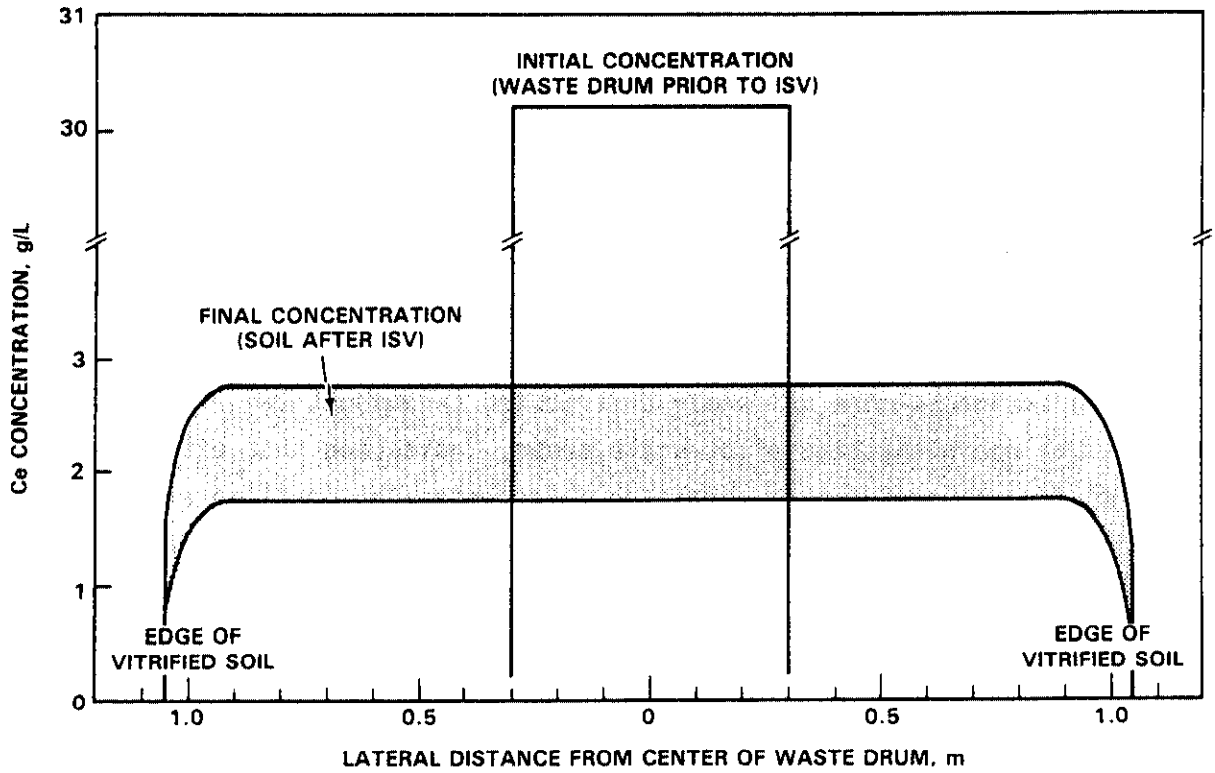

FIGURE 38. Cerium Concentration Profile Before and After Vitrification, PSFT-3

such as Pu, which the rare earth elements simulate, would not migrate either. Selective migration (mainly settling) of Pu has been a concern because of the criticality potential of Pu. This final distribution of Ce and other elements aids in dispelling this concern about selective migration effects.

These conclusions are confirmed by core section analyses of the pilot-scale radioactive block. Figures 39 and 40 provide the concentration distributions for TRUs and fission products. The distribution profiles indicate a relatively uniform distribution (within a factor of 3) for all radionuclides except Ru and for one core, Co. Plutonium and strontium data also indicate a uniform distribution. These data confirm previous indications (Oma et al. 1983) of an even distribution of Pu and allay any criticality concerns about the selective migration of Pu.

^{241}Am DISTRIBUTION

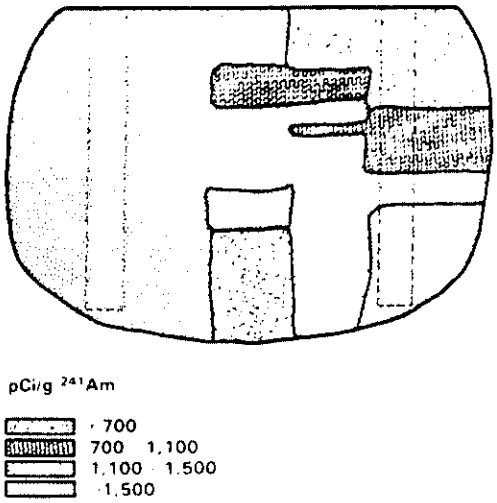

^{239}Pu DISTRIBUTION

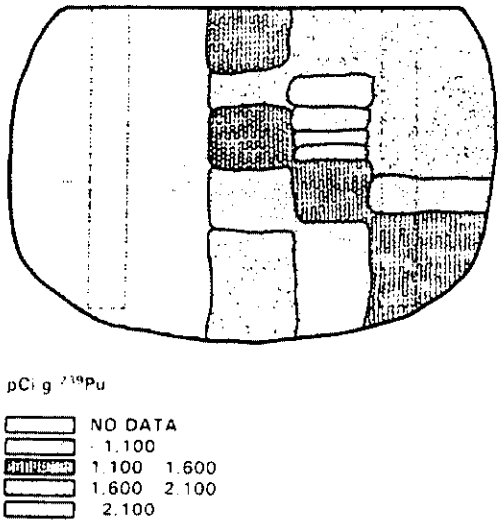

^{238}Pu DISTRIBUTION

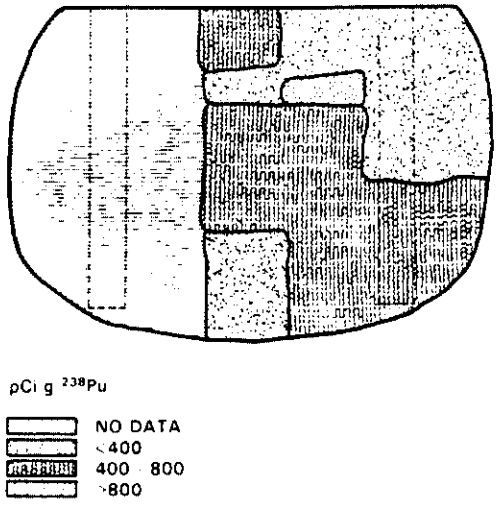

FIGURE 39. Distribution Profiles of TRU Radionuclides

^{137}Cs DISTRIBUTION

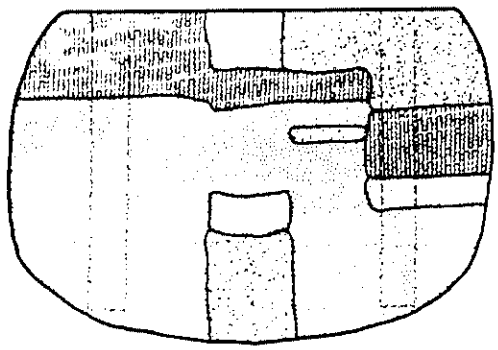

pCi g ^{137}Cs

- 2,500
- 2,500 - 3,300
- 3,300 - 4,000
- 4,000

^{106}Ru DISTRIBUTION

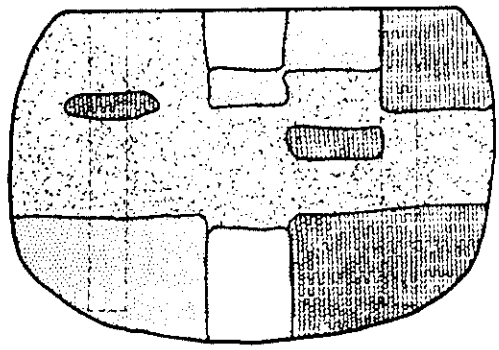

pCi/g ^{106}Ru

- <200
- 200 - 1,000
- 1,000 - 10,000
- >10,000

^{90}Sr DISTRIBUTION

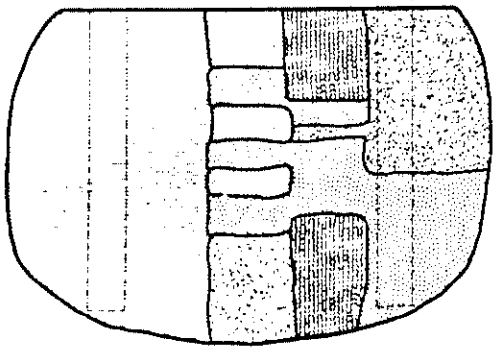

pCi g ^{90}Sr

- NO DATA
- - 100,000
- 100,000 - 170,000
- 170,000 - 250,000
- 250,000

^{60}Co DISTRIBUTION

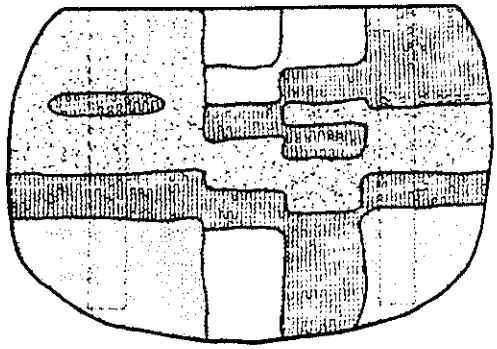

pCi g ^{60}Co

- - 250
- 250 - 500
- 500 - 1,000
- 1,000

FIGURE 40. Distribution Profiles of Fission Product Radionuclides

Product Durability

After each pilot-scale field test, the vitrified blocks were removed from the test area and sectioned for evaluation. The vitrified soil from each of the tests has remained a solid, nearly crack-free block until purposefully fractured for analysis. In general, the interior of the block is a nonporous glass similar to natural obsidian (see Figure 41).

Leaching studies of vitrified Hanford soil were conducted to determine its chemical durability. Two types of leach tests were performed on ISV field test products: a 24-h soxhlet test in 99°C deionized water and a 28-day Materials Characterization Center Test (MCC-1) (MCC 1981) in 90°C solutions of deionized water, silicate water, and brine. A comparison of the resulting corrosion rate during soxhlet leaching with published data (Platt 1973 and McElroy 1975) is provided in Figure 42, showing that the bulk leach rate of vitrified soil is significantly less than that of marble or bottle glass and is comparable to Pyrex® and granite.

Samples of the porous rock and glass layers from PSFT-1 and -2 were tested by soxhlet leaching. The second field test product also formed vitreous and crystalline phases that were leach tested. Table 16 presents the results of the soxhlet leach tests. Other materials and their respective leach losses are listed below the ISV samples for comparison. Comparable leach losses between the first two field test products and the various layers formed are also shown. The soxhlet leach test results show that the leach resistances of ISV products are better than those of other waste glasses. This is primarily due to the high silica and alumina contents and the low alkali content in the ISV glass. The soxhlet leach test results also indicate that ISV glass that contains a crystalline phase exhibits a slightly improved leach resistance. These results indicate that the crystallization of ISV glass may actually enhance waste form durability.

In the 28-day, MCC-1 leach test, glasses with and without a crystalline phase were examined. Their leach resistances are shown in Table 17. Glass

® Pyrex is a registered trademark of Dow-Corning Glassworks, Corning, New York.

FIGURE 41. Interior of a Vitrified Soil Block from a Pilot-Scale Test

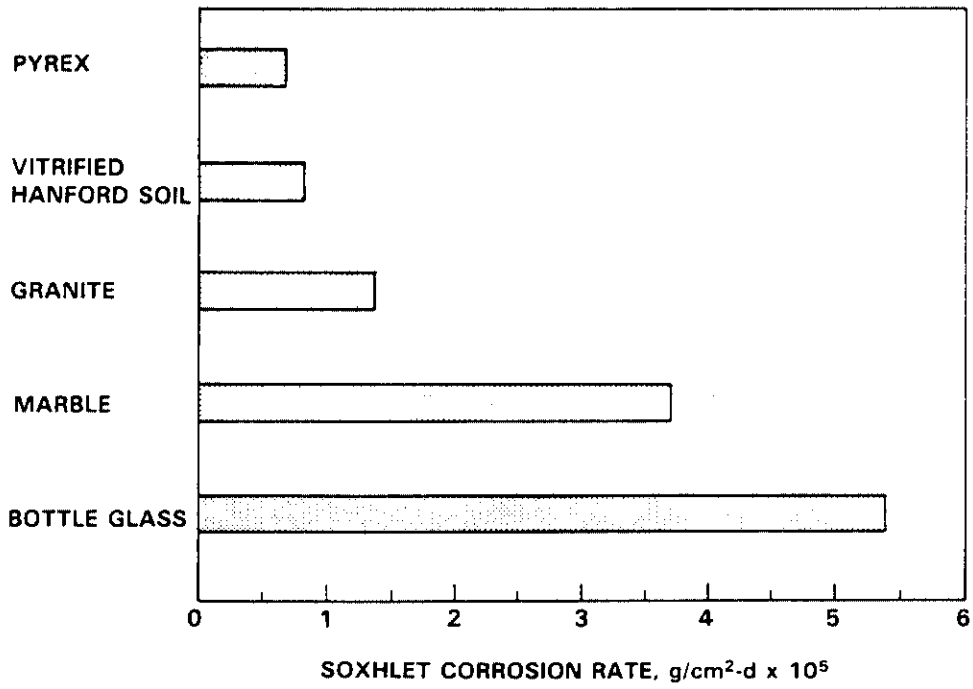

FIGURE 42. Leach Resistances of Selected Materials

TABLE 16. Soxhlet Leach Test Results for PSFT-1 and PSFT-2

PSFT-1 Samples	Wt% Loss
Surface	0.36
Porous layer	0.40
Rock layer	0.38
Glass layer	0.41
PSFT-2 Samples	
Porous layer	0.32
Rock/porous interface	0.26
Glass layer	0.26
Glass with crystalline	0.21
Comparison with Glass Samples	
Commercial waste glass (PNL 76-68)	1.6
Defense waste glass (SRL-131)	2.0 to 3.5

TABLE 17. Comparison of ISV Glass/Crystalline Leach Resistances With Commercial Waste Glass PNL 76-68

	Normalized Elemental Loss, g/m^2[a]		
Element	ISV Glass	Crystals	PNL 76-68[b]
Al	4	2	--
Ba	2	2	<0.05
Ca	4	3	0.3
Fe	0.1	0.5	<0.01
Mg	4	3	--
Na	5	3	55
Si	4	3	36
Sr	3	3	0.3
Cs	6	4	64
La	<0.01	<0.01	--
Nd	<0.02	<0.02	--

(a) MCC-1 leach test in 90°C deionized water, SA/V = 10 m^{-1} for 28 days.
(b) Strachan, Turcotte, and Barnes (1980).

contains an observable crystalline phase, which is formed by nucleation site growth and slow cooling (Timmerman and Lokken 1983), exhibits equal or better leach resistance than the single-phase glass. This is consistent with the soxhlet weight losses. The glass leach rates for the majority of elements listed are significantly less than those of the commercial HLW glass PNL 76-68. Cesium yielded the highest leach rate (although still low), while the rare earths leached less than the analytical detection limits. The leach resistance observed in the other pilot-scale tests is similar to that shown in Table 17.

Leach tests were also conducted on samples of TRU-contaminated, vitrified soil using the MCC-1 test method. A 200-g soil sample was obtained from well drilling of a TRU-contaminated soil site (Kasper 1981). The soil was vitrified at 1600°C in a crucible placed inside a resistance-heated laboratory furnace. The vitrified melt was radioactively nonsmearable and free of major cracks, thus allowing for easy cutting of the samples for the MCC-1 leach test.

Table 18 lists the MCC-1 leach test results, giving the normalized elemental releases from the vitrified soil, borosilicate glass, aluminosilicate glass, basalt-glass ceramic, and PNL 76-68 glass (Ross et al. 1982). This comparison with other waste forms allows for an evaluation of the relative benefits from ISV of soil. The overall leach rate of the vitrified soil is comparable to the PNL 76-68 glass and other TRU waste forms. However, the release of Pu is higher from the vitrified soil than from the borosilicate and aluminosilicate glasses. The similarity between Pu releases from the vitrified soil and the basalt-glass ceramic indicates that the Pu in both waste forms may be in a crystalline form that may be more readily leached. This may be due to reduced time at the 1600°C melt temperature in the crucible compared to melting times during large-scale ISV. Thus some unmelted or crystalline material might be present in the crucible melt, making Pu less leach resistant. However, the previously discussed leach resistance studies on nonradioactive vitrified soil that contained large fractions of crystalline products have indicated that the crystalline phases are not detrimental to overall leach resistance. (This is also indicated in Table 18, which gives releases for other elements.)

The level of activity in the pilot-scale radioactive block was too low to obtain absolute quantitative results from the MCC-1 leach test. Projected leach quantities are three orders of magnitude below the detection limits. To put the durability of the ISV product in perspective, concentrated hydrofluoric acid had to be used instead of concentrated hydrochloric acid to effectively remove enough Pu and Sr from the core samples to perform their respective analyses. Previous leach test results (Oma et al. 1983) have illustrated the impressive durability of the ISV waste form.

The durability of the ISV waste form can also be estimated by examining the durability of obsidian, which is a naturally occurring glass with similar physical properties and chemical composition (Ewing and Hoaker 1979). Obsidian is formed when cooling volcanic lava loses heat too quickly to permit crystallization. The weathering process of obsidian in a natural environment that is not saturated with free water involves the hydration of atmospheric water that is chemically absorbed on the surface. The water then diffuses into the

TABLE 18. MCC-1 Leach Test Results for TRU Waste Forms

Waste Form	Leach Time, d	Normalized Elemental Release, $g/m^{2(a)}$							
		Al	Ca	Fe	Na	Si	Pu	Am	pH
Vitrified TRU-contaminated soil	3	6.11×10^{-2}	2.00×10^{-1}	2.64×10^{-2}	--	1.64×10^{-1}	2.97×10^{-2}	1.41×10^{-2}	7.1
	7	7.14×10^{-2}	5.57×10^{-1}	5.40×10^{-2}	2.89×10^{-1}	5.16×10^{-1}	3.43×10^{-2}	4.63×10^{-2}	6.9
	14	7.34×10^{-1}	1.51×10^{0}	4.32×10^{-2}	7.07×10^{-1}	1.44×10^{0}	4.80×10^{-2}	1.81×10^{-2}	7.9
	28	1.05×10^{0}	2.10×10^{0}	1.63×10^{-1}	1.03×10^{0}	2.03×10^{0}	6.68×10^{-2}	3.58×10^{-2}	8.2
Borosilicate glass[b]	3	4.26×10^{-1}	1.33×10^{0}	2.46×10^{0}	2.27×10^{0}	2.33×10^{0}	6.45×10^{-3}	--	5.5
	7	3.72×10^{-1}	2.69×10^{0}	3.91×10^{-1}	2.91×10^{0}	3.32×10^{0}	7.88×10^{-3}	--	7.1
	14	8.71×10^{-1}	3.62×10^{0}	9.43×10^{-1}	4.62×10^{0}	4.27×10^{0}	6.45×10^{-3}	--	6.5
	28	3.22×10^{0}	4.49×10^{0}	5.80×10^{-2}	1.52×10^{-1}	1.21×10^{-1}	2.90×10^{-3}	--	9.5
Aluminosilicate glass[b]	3	6.93×10^{-1}	3.53×10^{0}	1.54×10^{0}	4.40×10^{0}	2.25×10^{0}	1.44×10^{-3}	--	4.7
	7	8.07×10^{-1}	3.73×10^{0}	2.21×10^{0}	5.23×10^{0}	3.51×10^{0}	2.88×10^{-3}	--	5.2
	14	7.84×10^{-1}	4.04×10^{0}	1.97×10^{0}	6.17×10^{0}	4.51×10^{0}	1.44×10^{-3}	--	6.6
	28	3.03×10^{0}	5.05×10^{0}	1.92×10^{0}	9.00×10^{0}	6.62×10^{0}	4.80×10^{-3}	1.11×10^{-2}	9.1
Basalt glass	3	9.98×10^{-1}	1.01×10^{0}	5.86×10^{-1}	2.10×10^{0}	8.27×10^{-1}	4.02×10^{-2}	--	4.0
	7	1.10×10^{0}	1.25×10^{0}	1.18×10^{-1}	1.71×10^{0}	1.29×10^{0}	4.69×10^{-2}	--	4.0
	14	1.55×10^{0}	1.67×10^{0}	1.02×10^{0}	3.05×10^{0}	1.88×10^{0}	1.67×10^{-1}	--	4.3
	28	1.60×10^{-1}	8.60×10^{0}	--	1.70×10^{0}	1.00×10^{0}	3.20×10^{-2}	5.6×10^{-2}	5.6
PNL 76-68 glass (control)	28	1.70×10^{-1}	1.05×10^{0}	6.59×10^{-1}	2.60×19^{-1}	1.81×10^{-1}	--	--	9.6

(a) Leached in deionized water at 90°C.
(b) Ross et al. (1982).

obsidian as a function of time and temperature. This type of weathering would be expected for the ISV waste form because of its chemical and physical similarity to obsidian.

The rate of hydration is expected to be limited by diffusion, with the thickness of the hydration profile increasing proportionally to the square root of the hydration time. Laursen and Lanford (1978) report that archaeological evidence shows that the hydration rate varies from 1 to 20 μm^2/1000 yr. If a fresh fracture surface is exposed for one year at a hydration rate of 10 μm^2/1000 yr, assuming a linear weathering rate, the resulting hydration layer will be 1×10^{-5}-cm thick.

A very conservative estimate that assumes that the hydrated glass formed during each one-year period has no effect on the hydration rate of adjacent fresh material would result in a hydration thickness of only 1 mm in 10,000 years. Therefore, the ISV waste form would be expected to remain virtually unweathered for a time period of much greater than 10,000 years. Thus leach testing and a long-term geologic comparison have shown that the ISV process generates a highly durable waste form.

This analysis can be correlated with the leach testing data of the ISV waste form. As described in this section, the release of various elements from ISV glass has been tested at 90°C. The release of soluble species (whose release is an indicator of the depth of hydration of the glass) increases parabolically between 14 and 28 days (the duration of the test). The rate is about 2 μm^2/yr. The activation energy for the effect of temperature on the hydration of obsidians is 20 kcal/mole (Friedman and Long 1976). Based on this, the parabolic hydration rate for the ISV glass would be 5 μm^2/1000 yr at 25°C (e.g., exposed to air) and 1 μm^2/1000 yr at 10°C (e.g., buried in soil). These values are one-tenth of the assumption used to obtain a hydration thickness of 1 mm/10,000 yr.

Obsidians have been found to be hydrating parabolically for periods as long as a million years (Friedman and Obredovich 1981). Also, the rate of hydration of a natural obsidian has been measured at 95°C and found to be about

9 $\mu m^2/yr$ (Friedman and Long 1976). Bases on this analysis, it is reasonable to assume that the ISV waste form would be effective for periods greater than one million years.

PROCESS PARAMETERS

PROCESS PARAMETERS

Parameters that may affect the performance of ISV are addressed in this section. These parameters include soil properties, site geometry, and waste type.

INFLUENCE OF SOIL PROPERTIES

Hanford soil that contains both simulated and actual radionuclides has been successfully vitrified in place. Since the properties of soils vary among the different waste sites where ISV could be applied, it is necessary to investigate potential process limitations due to soil characteristics. Soil properties that can influence the ISV process include:

- chemical composition
- thermal conductivity
- fusion temperature
- specific heat
- electrical conductivity
- viscosity
- density

Thermal conductivity is dependent on both soil composition and morphology. Fusion temperature, specific heat, electrical conductivity, and viscosity are dependent on soil composition. The bulk density of the soil depends on its morphology. The density of the vitrified material is relatively insensitive to compositional variations.

Soil property data were obtained from literature surveys and laboratory characterization tests on soil from Barnwell, South Carolina; Hanford, Washington; Idaho National Engineering Laboratory (INEL), Idaho; Los Alamos National Laboratory (LANL), New Mexico; Maxey Flats, Kentucky; the Nevada Test Site (NTS), Nevada; Oak Ridge National Laboratory (ORNL), Tennessee; Sheffield, Illinois; and West Valley Nuclear Services Co., Inc. (WVNS), New York.

A description of the effects of changes in the soil properties listed above and the effects of soil additives on the properties follow here.

Chemical Composition

The chemical compositions of soil from potential ISV sites were determined using induction-coupled plasma (ICP) spectroscopy. The averaged soil compositions from each of the locations are shown in Table 19. Individual sample analyses are presented in Table 20. All soils tested were composed primarily of SiO_2 and Al_2O_3 (70 to 98%). Higher levels of these oxides tend to increase the chemical durability of the resulting glass, but have the negative effects of increasing its viscosity and decreasing its electrical conductivity. All of the soils also contained significant amounts of Na_2O and K_2O, which act as the primary charge carriers in molten soil. A number of the soils also contained significant amounts of CaO and MgO, oxides that tend to suppress the electrical conductivities of molten silicates (Stanek 1977). The effects of NaO_2 and CaO additions to ISV soil are discussed in more detail later in this section.

Thermal Conductivity

Variations in the thermal conductivities of soil can influence the maximum temperature that can be reached by the molten zone and the rate at which heat

TABLE 19. Oxide Compositions of Soils from Selected U.S. Locations

Soil		Composition, wt%							
		Alkali		Alkaline Earth					Other Oxides[a]
Location	Type	K_2O	Na_2O	Al_2O_3	CaO	Fe_2O_3	MgO	AlO_2	
Barnwell	Fuquay	0.20	0.24	9.26	0.04	2.75	0.12	86.7	0.68
Hanford	ND[b]	1.80	3.02	13.6	6.00	9.55	2.88	60.9	1.95
INEL	ND[c]	2.52	1.35	11.4	9.97[d]	4.07	--	69.6	1.07
LANL	Carjo	2.82	2.73	12.4	0.94	2.93	0.60	76.8	0.78
	Puye	3.39	3.87	13.0	0.51	2.38	0.37	76.1	0.45
	Tuff	4.44	4.44	12.3	0.46	1.23	--	76.9	0.16
Maxey Flats	Tilsit	1.12	0.44	7.79	0.06	3.13	0.43	85.5	1.52
NTS	Beatty	3.88	3.54	13.6	2.89	2.87	1.25	71.3	0.74
ORNL	ND	2.55	0.32	17.3	0.11	11.0	0.97	66.5	1.28
Sheffield	Fayette	1.97	1.60	10.8	0.78	3.82	0.87	79.1	0.96
WVNS	Churchville	2.69	1.09	14.2	3.22	5.01	2.03	70.4	1.29

(a) Other oxides include TiO_2, P_2O_5, and ZrO_2.
(b) Not determined.
(c) From INEL Radioactive Waste Management Complex.
(d) CaO + MgO.

TABLE 20. Oxide Composition of Soils at Varying Depths

Soil			Composition, wt%									
			Alkali		Alkaline Earth					Others		
Location	Type	Depth, cm	K_2O	Na_2O	Al_2O_3	CaO	Fe_2O_3	MgO	SiO_2	P_2O_5	TiO_2	ZrO_2
Barnwell	Fuquay	0-15	0.19	0.23	2.10	0.08	0.68	0.08	96.2	--	0.42	0.03
		15-76	0.19	0.23	1.65	0.03	0.57	0.09	96.3	--	0.45	0.03
		76-107	0.24	0.25	16.3	0.02	5.04	0.16	77.1	0.14	0.71	0.03
		396-427	0.18	0.26	17.0	0.02	4.69	0.13	76.8	0.17	0.68	0.03
Hanford	ND[a]	Surface	1.57	3.14	12.5	6.81	11.5	3.40	58.0	0.47	2.06	0.03
	PSFT-1[b]	N/D	1.43	2.87	13.6	5.37	8.16	2.51	64.4	--	1.39	--
	PSFT-2[b]	N/D	1.56	2.69	13.9	6.41	9.86	3.02	60.1	0.52	1.60	--
	PSCT-1[b]	N/D	2.45	3.17	13.8	5.44	9.17	1.41	61.7	0.29	1.41	--
	LSOAT-2[b]	N/D	1.98	3.23	14.4	5.96	9.06	2.89	60.5	0.40	1.57	--
LANL	Carjo	0-5	2.68	2.54	12.2	0.98	2.67	0.62	77.5	0.13	0.60	0.04
		5-15	2.80	2.79	12.4	0.93	2.93	0.59	76.8	0.11	0.62	0.06
		15-25	2.97	2.86	12.5	0.91	3.18	0.59	76.2	--	0.65	0.13
	Puye	0-10	2.96	3.85	12.6	0.45	2.13	0.31	77.2	0.16	0.27	0.05
		10-41	3.81	3.88	13.3	0.57	2.63	0.42	75.0	--	0.36	0.05
	Tuff	N/D	4.44	4.44	12.3	0.46	1.23	--	76.9	--	0.09	0.07
Masey Flats	Tilsit	0-18	0.89	0.45	5.58	0.10	2.17	0.23	89.0	0.12	1.37	0.08
		18-61	1.10	0.47	7.85	0.07	3.66	0.40	84.9	0.10	1.33	0.07
		61-142	0.89	0.39	7.22	0.04	2.63	0.41	87.0	0.09	1.32	0.06
		142	1.61	0.44	10.5	0.03	4.07	0.69	81.2	0.20	1.29	0.06
NTS	Beatty	0-10	3.66	3.38	13.8	3.19	2.87	1.54	70.7	0.26	0.55	0.03
		10-36	4.03	3.39	13.6	3.77	3.01	1.44	69.9	0.20	0.56	0.04
		36-53	3.86	3.27	13.6	3.24	2.87	1.39	71.0	0.20	0.53	0.04
		53-122	3.98	4.10	13.2	1.37	2.73	0.61	73.5	--	0.50	0.05
ORNL	ND	Surface	2.55	0.32	17.3	0.11	11.0	0.97	66.5	0.26	0.97	0.05
Sheffield	Fayette	0-18	2.01	1.61	9.09	0.83	2.55	0.64	82.4	--	0.82	0.05
		25-102	1.99	1.49	12.0	0.62	4.44	0.99	77.3	0.20	0.78	0.06
		C Horizon	1.90	1.71	11.3	0.89	4.48	0.98	77.7	0.21	0.72	0.04
WVNS	Churchville	0-10	2.08	1.10	12.8	0.53	1.59	0.98	79.4	0.24	1.22	0.05
		10-30	2.11	1.00	12.9	0.39	5.30	1.08	75.9	0.15	1.10	0.06
		30-97	3.08	1.08	14.5	4.60	6.01	2.70	66.9	0.28	0.89	0.04
		97-157	3.13	1.14	15.3	5.50	6.03	2.69	65.0	0.28	0.90	0.06
		>157	3.05	1.11	15.7	5.10	6.14	2.72	65.0	0.25	0.92	0.03

(a) Not determined.
(b) Vitrified Hanford soil.

energy can be transferred to the unmelted soil. A low thermal conductivity soil will result in a higher molten zone temperature for a given rate of melt propagation. However, thermal conductivity variations within the molten zone will not significantly affect the temperature profile of the molten zone since convective mixing produces a relatively even temperature profile. Variations in thermal conductivity mainly affect the thermal gradient between the boundary layer of the molten soil boundary layer and the soil at ambient temperature.

Thermal conductivities of soils at ambient temperature are very low, ranging from 0.09 to 0.15 W/m°K as shown in Table 21. These low conductivities are caused by the small particles in the majority of the soils, which increase grain-to-grain contact resistance. Heat conduction by the gas phase is very low because of the extremely small effective pore size of these soils. The small pore size eliminates convective heat transfer and effectively reduces

TABLE 21. Thermal Conductivities of Soils at Ambient Temperature

Soil		Thermal Conductivity,[a] W/m°K
Location	Type	
Barnwell	Fuquay	0.151
Hanford	ND[b]	0.131
LANL	Carjo	0.109
	Puye	0.108
Maxey Flats	Tilsit	0.127
NTS	Beatty	0.117
ORNL	ND	0.104
Sheffield	Fayette	0.095
WVNS	Churchville	0.107

(a) Thermal conductivity measurements were made of disturbed soil that was compacted to simulate nondisturbed soil. Thermal conductivities of actual nondisturbed soils are expected to be 10 to 20% higher than the values reported in this table.
(b) Not determined.

conduction within pores (Parrott and Stuckes 1975). Soils that contained rocks and pebbles, such as certain samples from Hanford and NTS, had higher conductivities. This was expected because conduction through solid materials is much higher than through porous, fine-grained soil.

Both the measured and calculated values for the thermal conductivities as a function of temperature of Hanford soil are shown in Figure 43. The conductivities of Hanford soil and all other soils that were measured (NTS, Maxey Flats, and WVNS) approximately doubled when heated from 200 to 800°C. This increase was due primarily to an increase in the conductivity of the porous phase. The initial increase in conductivity of Hanford soil above 800°C is caused by a decrease in grain-to-grain contact resistance, which occurs at the onset of thermal soil fusion. Conductivity measurements could not be made at

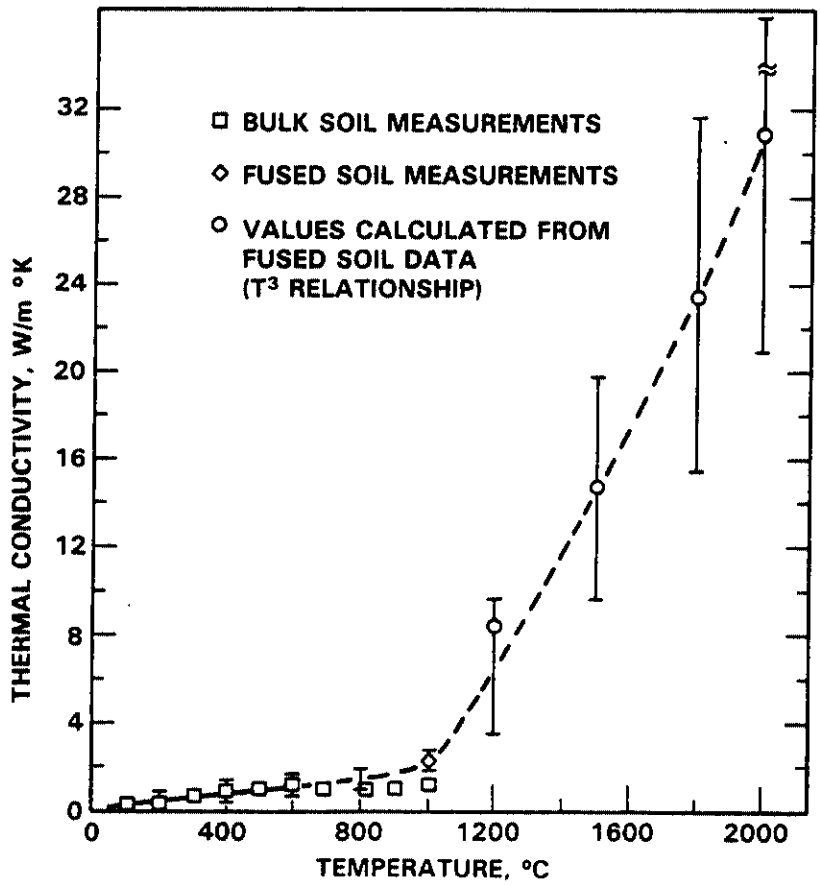

FIGURE 43. Thermal Conductivities of Hanford Soil

temperatures above 1000°C due to deformation of the samples. At these temperatures, however, increasing conductivity with increasing temperatures is caused by radiative conduction (Bates 1975). This contribution to conductivity increases proportionally to temperature cubed (T^3). The values above 1000°C were calculated using this T^3 relationship and the measured conductivity of a portion of fused Hanford soil at 1000°C. Because of the uncertainties inherent in this calculation, the error bars on the curve are fairly large. Similar behavior is expected from the remaining soil samples. The uniform temperature profile in the molten zone is attributed to the high conductivity at molten soil temperatures (>1200°C) and convective mixing. The low soil conductivity below 1000°C results in steep thermal gradients in the soil at the outer boundaries of the ISV melt zone.

Fusion Temperature

The temperatures at which soils initially fuse were determined from thermal conductivity measurements. These data were available for the Maxey Flats, Tilsit, the NTS Beatty, and the WVNS Churchville soils. The initial fusion point was assumed to be the temperature at which the conductivity began to increase at a much higher rate than it had at lower temperatures. The temperature at which the soil would completely fuse was assumed to be ~200°C higher than this initial fusion temperature. Anticipated fusion temperatures of the other soils were calculated by comparing their alkaline earth and alkali levels with those of the three previously measured soils. The fusion temperatures of the soils are listed in Table 22. Fusion temperatures for all soils tested ranged from 1100 to 1400°C, too low to impose any ISV process limitation. The glass temperatures observed during pilot-scale tests have exceeded 1700°C--well above any of the fusion points.

Specific Heat

Knowing the specific heat of a soil is important in determining the power required to melt it. A high specific heat is undesirable because it increases the energy needed to heat the soil to the point of vitrification and also slows the vitrification rate.

TABLE 22. Fusion Temperatures of Soils

Soil Location	Soil Type	Fusion Temperature, °C
Barnwell	Fuquay	1400[a]
Hanford	ND[b]	1100[a]
INEL	ND	1100[a]
LANL	Puye	1100[a]
	Carjo	1200[a]
	Tuff	1300[a]
Maxey Flats	Tilsit	1300
NTS	Beatty	1100-1200
	Tuff	1300[a]
ORNL	ND	1100[a]
Sheffield	Fayette	1100[a]
WVNS	Churchville	1100

(a) Fusion temperature estimated from soil composition.
(b) Not determined.

The specific heat values of the soils shown in Figure 44 were measured at temperatures of from 150 to 500°C using differential scanning calorimetry. Most soils had specific heat values in the range of 0.19 to 0.22 cal/g°C. The specific heat values of soil from Maxey Flats were higher, at 0.23 to 0.29 cal/g°C. These values are consistent with those found for other ceramic materials (Norton 1968). The variation in specific heat among the soils is not considered an ISV process limit. Higher specific heat materials require more power for melting; however, soil moisture content often influences power input as much or more than specific heat.

At higher temperatures (1500 to 2000°C), a specific heat value of 0.25 to 0.28 cal/g°C will be reached by most soils. The measured and anticipated specific heat values of a Hanford soil in the temperature range of 25 to 2000°C are shown in Figure 45. Since measurements could not be made at temperatures over 600°C due to equipment limitations, it was assumed that above 400°C, the

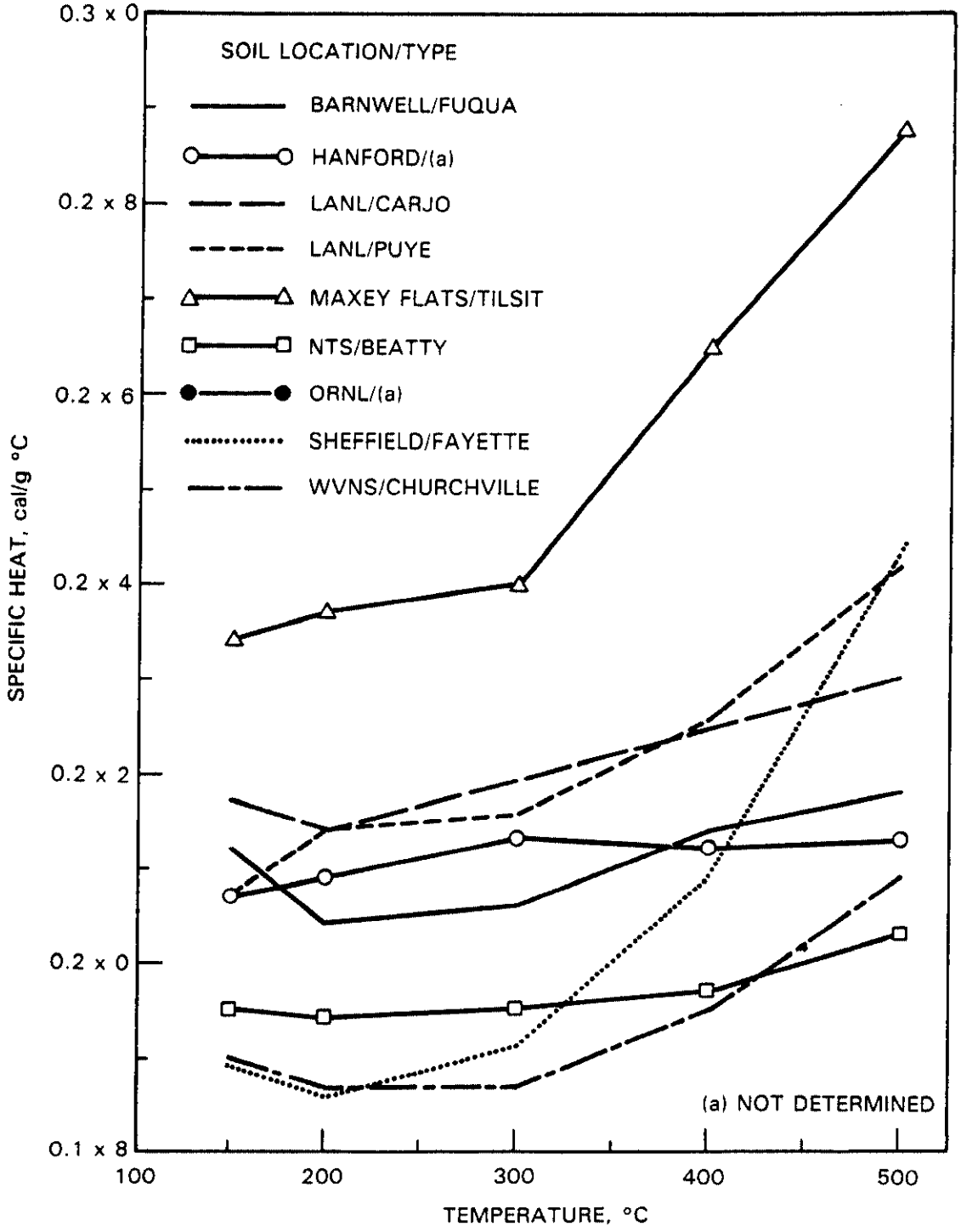

FIGURE 44. Specific Heats of Various Soil Types

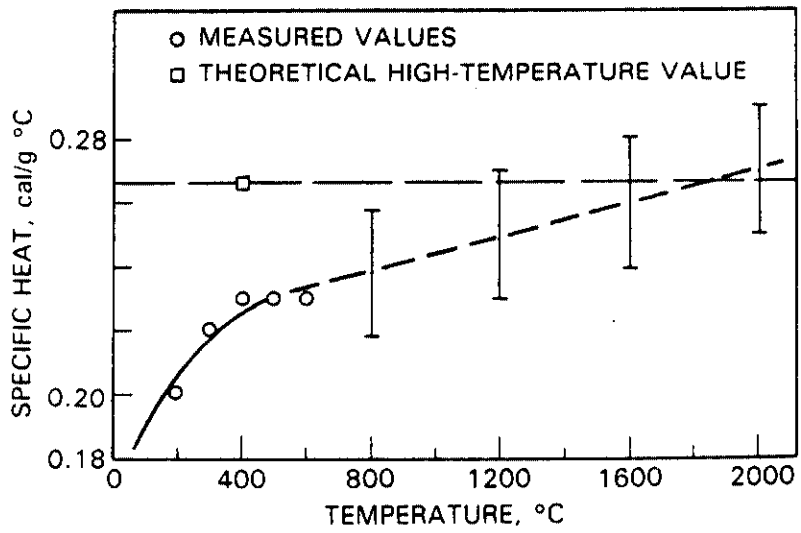

FIGURE 45. Specific Heat of Hanford Soil 28-2 at Various Temperatures

specific heat would increase linearly with temperature, and at higher temperatures should exceed 5.96 cal/g atom•°C (Kingery 1960). This is equal to 0.26 cal/g°C for Hanford soil.

Electrical Conductivity

Variations in the electrical conductivities of molten soils influence the operating voltage of an ISV system. Low-conductance soils may limit the electrode separation that is attainable if the electrical voltage required to achieve ISV startup exceeds the available supply voltage. The reference large-scale ISV system has an electrode supply voltage limit of 4160 V, a commonly supplied voltage rating, but certainly not the maximum available.

The electrode conductivities of three molten soils were measured using a two-probe method; the values obtained are shown in Figure 46. At high temperatures the Hanford and NTS tuff materials had very similar conductivities. The Maxey Flats Tilsit soil had a conductivity approximately one order of magnitude lower. This is primarily due to its lower alkali oxide ($Na_2O + K_2O$) content.

Before the capability to measure high-temperature (>1600°C) electrical conductivities existed, five soils were chosen for measurement using the two-probe method in a lower temperature system. Due to the high melting temperatures of the soils, ~10 wt% Na_2O was added to each sample to reduce the melting

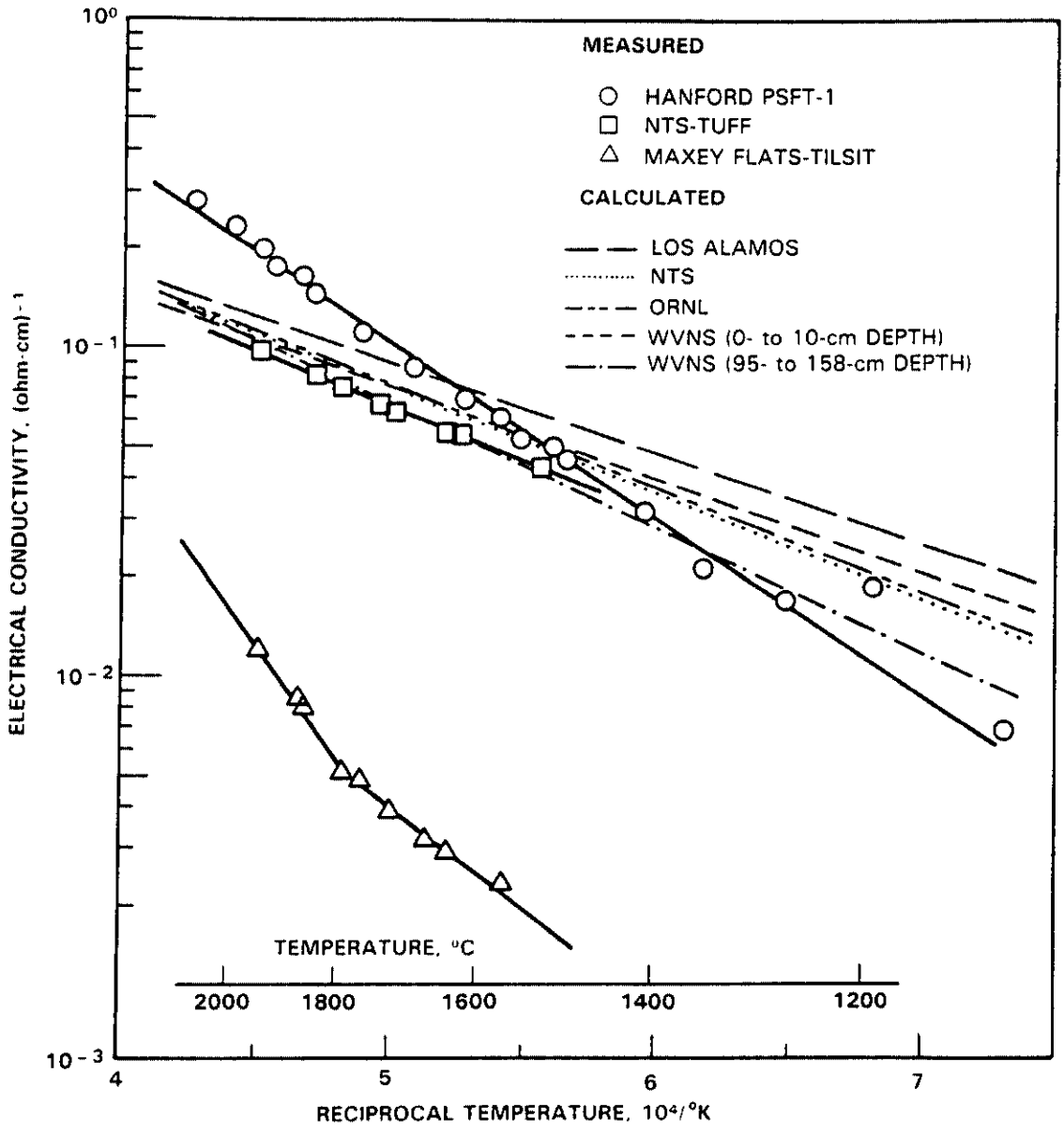

FIGURE 46. Electrical Conductivities of Molten Soils

time and temperature. The calculated conductivities, corrected for the Na_2O addition, are also shown in Figure 46. It can be seen that, with the exception of the Maxey Flats Tilsit, all of the measured and calculated electrical conductivities fall within a narrow range. The conductivities of other soils will depend, of course, on their compositions. Alkali oxides (Na_2O, K_2O, Li_2O)

increase conductivity, while the alkaline earth oxides (CaO, Mg) tend to decrease conductivity (Stanek 1977). Soil with higher amounts of refractory oxides (SiO_2, Al_2O_3) has a higher viscosity and therefore a lower electrical conductivity due to decreased conduction ion mobility. Based on comparison of soil compositions, all other soils in this study are expected to fall within the range shown in Figure 46.

The variation in electrical conductivity among the soils tested, including that of the Tilsit, does not limit the application of the ISV process. Such variation can easily be compensated for by modifying the startup technique. Voltage during startup is dependent on the graphite-frit startup mixture, not on soil conductivity. Once the graphite startup material has burned, the voltage reaches its maximum, which is dependent on the cross-sectional area and conductivity of the molten path. Beyond this point, voltage decreases as the molten zone expands. If the maximum startup voltage exceeds the supply voltage because the soil conductivity is low, the startup voltage can be lowered by increasing the width and depth of the graphite-frit path and by choosing a frit that is highly conductive. These actions will increase the cross-sectional area of the molten path and the glass conductivity in that path, thus decreasing the maximum voltage during the startup period.

Figure 47 shows the anticipated electrical conductivity of Hanford soil during the heating portion of the process. At temperatures below ~600°C the soil will not have fused at all and with the moisture evaporated, its conductivity will be very low (10^{-15} or 10^{-16} ohm^{-1}-cm^{-1}). Once the soil begins to fuse, it will start to conduct, and this conductivity will increase rapidly until the soil is completely molten. The dashed line in Figure 47 represents a possible behavior of the soil in this region. Similar behavior is expected of the other soils studied in this work. At temperatures above 1200 to 1300°C the soil should be completely melted. At these temperatures the conductivity will be the same as that of the vitrified soils whose measurements are shown in Figure 46.

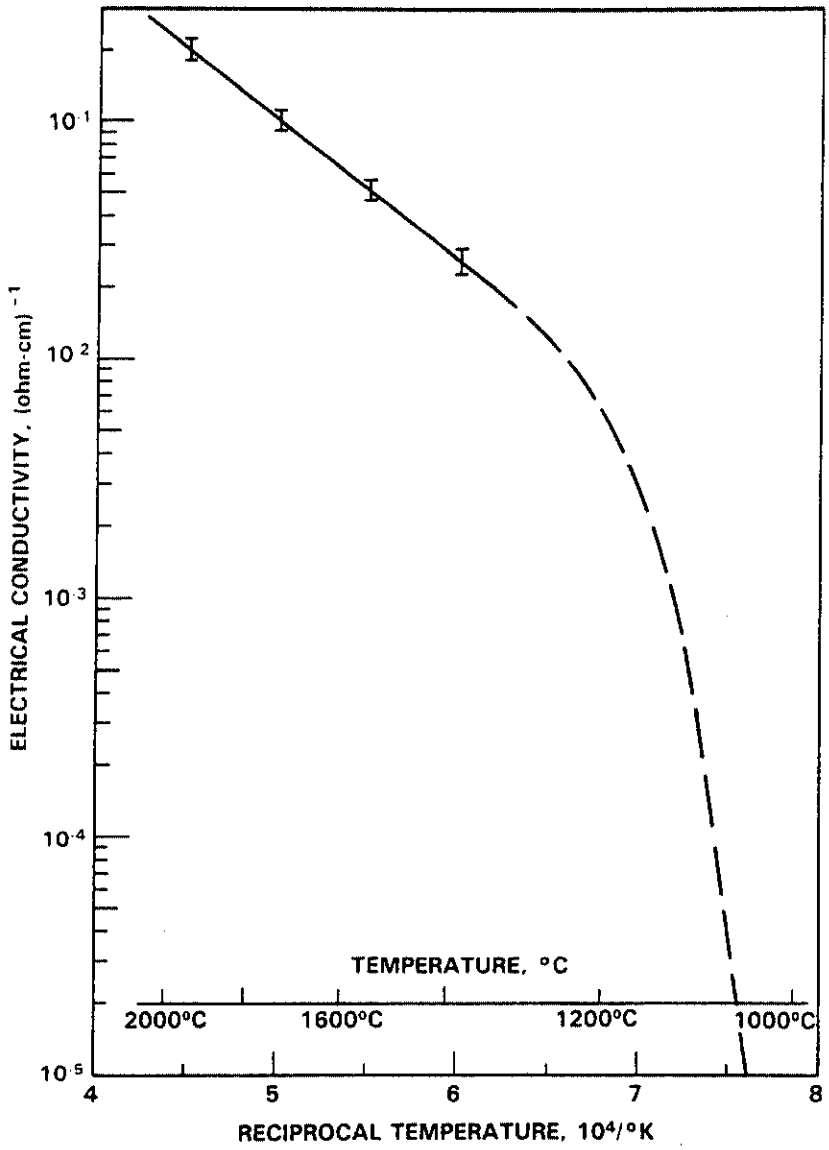

FIGURE 47. Electrical Conductivities at 40 Hz of Vitrified Hanford Soil from PSFT-4

Viscosity

A molten soil's viscosity will affect the operating temperature for a given power input rate. A more fluid medium will generally melt more quickly and will have smaller temperature gradients due to greater convective mixing in the melt.

The viscosities of four molten soils were measured using a rotating spindle technique. One sample each was obtained from Hanford PSFT-1 and -4. The other two soils were portions of Maxey Flats Tilsit and NTS tuff. Their viscosities are shown in Figure 48. The viscosities of the tuff and Tilsit are similar and about two orders of magnitude higher than those of the Hanford samples. This is due to the higher SiO_2 + Al_2O_3 and lower Na_2O + K_2O content of the tuff and Tilsit. The higher Fe_2O_3 content in the Hanford material also contributed to its lower viscosity. Based on the compositions of the other soils in this study, it is anticipated that all soils will have viscosities within the range found in Figure 48. While complete vitrification of materials such as tuff and Tilsit may require somewhat higher melt temperatures and longer melt times, melting can still be accomplished. However, soil additions should be considered to lower melt temperature when approaching temperature limitations of electrodes and their coating materials (i.e., 1750°C for $MoSi_2$-coated Mo electrodes).

Density

The decrease in soil volume due to vitrification is determined by the soil density values before and after melting. The densities of unmelted soil are most strongly affected by soil morphology and particle size, as well as the degree to which the site's soil has been disturbed. The densities of three melted soils at room temperature are shown in Table 23. Although the initial soil densities can vary significantly, the final densities of the melted materials are very similar, ranging from 2.30 to 2.43 g/cm^3.

Figure 49 shows the way in which a typical soil's density might change during processing. Hanford soil is used as an example. During heating, no density change is seen until the soil begins to fuse at ~700 to 900°C. The density then increases until the soil is completely fused at ~1400°C. A decrease in density occurs at higher temperatures due to the thermal expansion of the material. During cooling, the density increases as the molten soil contracts and then solidifies.

It is expected that all vitrified soils in this study will exhibit densities in the range of 2.2 to 2.5 g/cm^3, regardless of their initial densities.

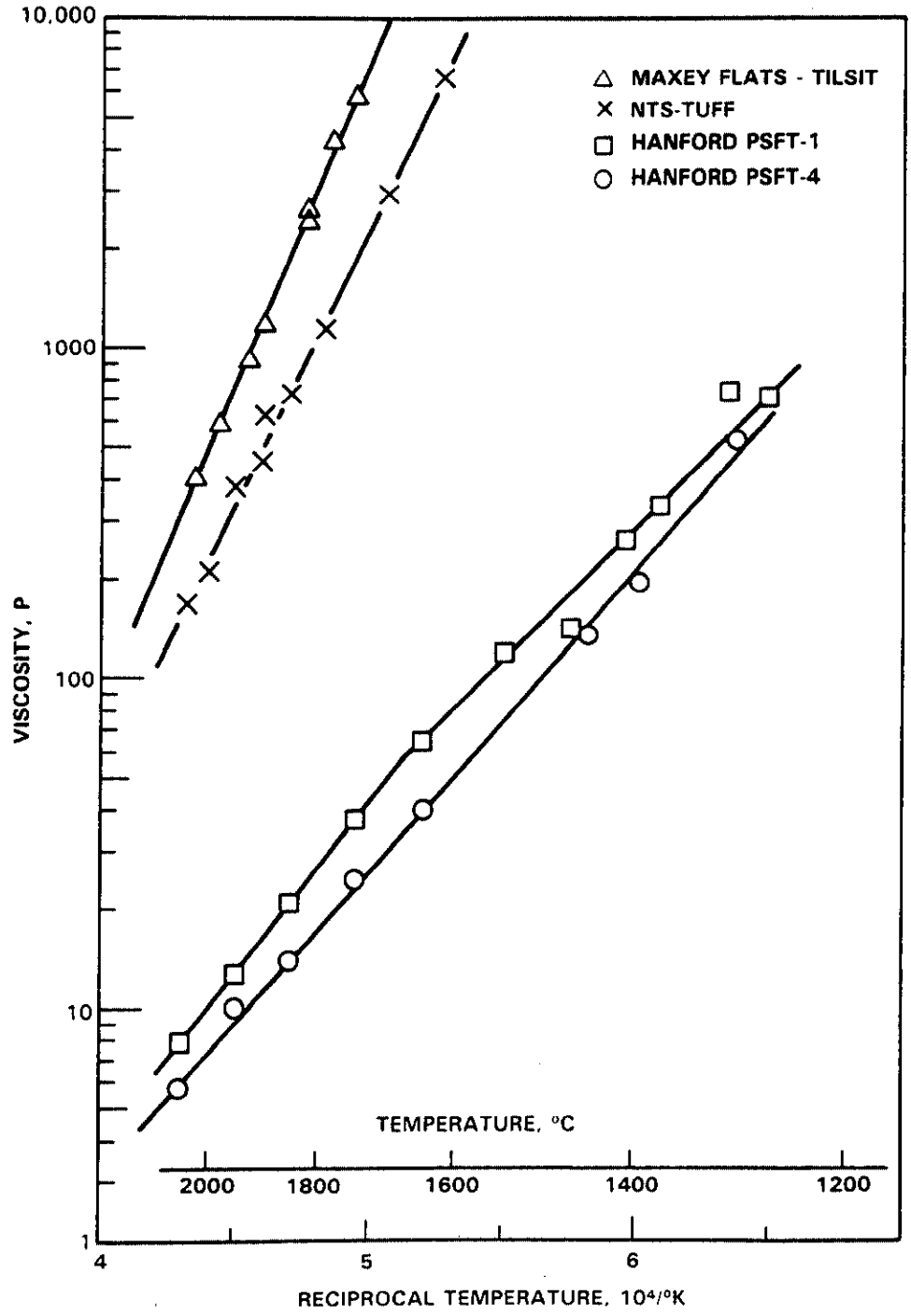

FIGURE 48. Viscosities of Molten Soils

TABLE 23. Bulk Density of Vitrified Soil

Soil		Vitrified Density, g/cm^3
Location	Type	
Hanford	ND	2.43
LANL	Tuff	2.33
Maxey Flats	Tilsit	2.30

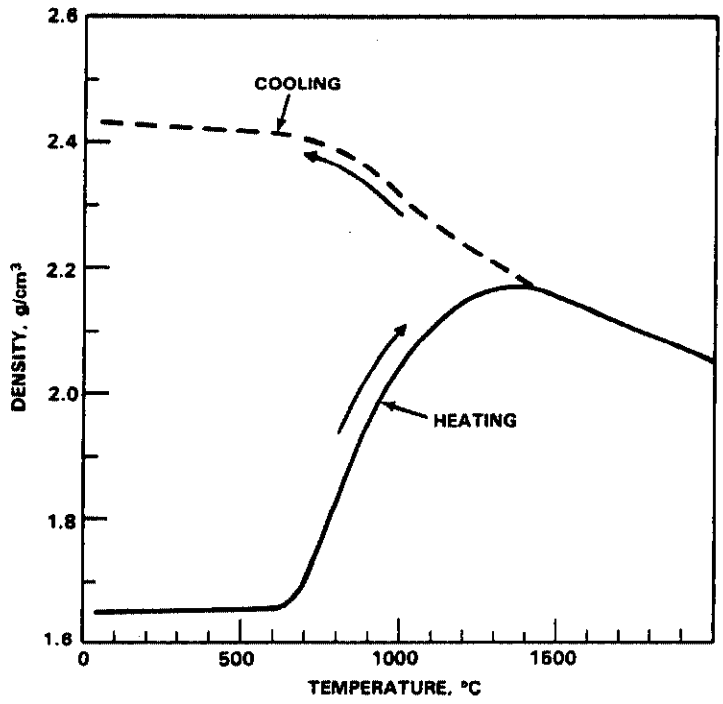

FIGURE 49. Change in Hanford Soil Density During Processing

Those sites with lower initial densities should subside more during ISV and would require more backfill material for recontouring the land after ISV.

Effects of Soil Additives

By modifying the soil composition, certain properties, including viscosity and electrical conductivity, can be adjusted to suit the ISV application. A series of experiments was conducted with vitrified Hanford soil that contained varying amounts of Na_2O and CaO as modifiers.

During the initial scoping tests, it was found that the soil crystallized rather than vitrified at Na_2O concentrations in excess of 35 to 40 wt%, even under rapid cooling conditions. The molten soil was found to be very conductive electrically at the high Na_2O concentration; on the order of 1 $(ohm\text{-}cm)^{-1}$ at low melt temperatures. Under the high Na_2O conditions, additions of CaO did not help the soil vitrify and did not act to decrease the electrical conductivity. The addition of CaO, however, did increase the melting temperature of the crystalline material.

Based on the initial findings of the extremity points, the boundaries for a three-component mixture study were defined to produce a vitrified glass product. A series of 14 different samples of Hanford soil with varying amounts of Na_2O and CaO was prepared and tested for viscosity and electrical conductivity. The compositional area of investigation was as follows: Na_2O, 3-35%; CaO, 5-20%; and base soil, 60-92%. The composition of the base soil was that of Hanford PSCT-1 soil (refer to Table 20) minus the Na_2O and CaO.

Figure 50 shows the effect of the composition of the three-phase mixture on the viscosity and electrical conductivity at a constant temperature (1325°C). Important observations from the data are listed below:

- Molten soil viscosity is mainly dependent on the concentration of the base soil. The addition of glass modifiers, such as Na_2O or CaO, cause the viscosity to decrease for a given temperature.
- Molten soil viscosity at constant temperature (1325°C) can be decreased from approximately 2000 P for the base soil composition to near 10 P by increasing the Na_2O concentration from 3% to 35%. This is over two orders of magnitude reduction in viscosity.
- The electrical conductivity is mainly dependent on the Na_2O concentration, because both CaO and base soil act to dilute the Na_2O and lower conductivity.
- Electrical conductivity at constant temperature (1325°C) can be increased from approximately 0.01 $(ohm\text{-}cm)^{-1}$ to 1.4 $(ohm\text{-}cm)^{-1}$ by

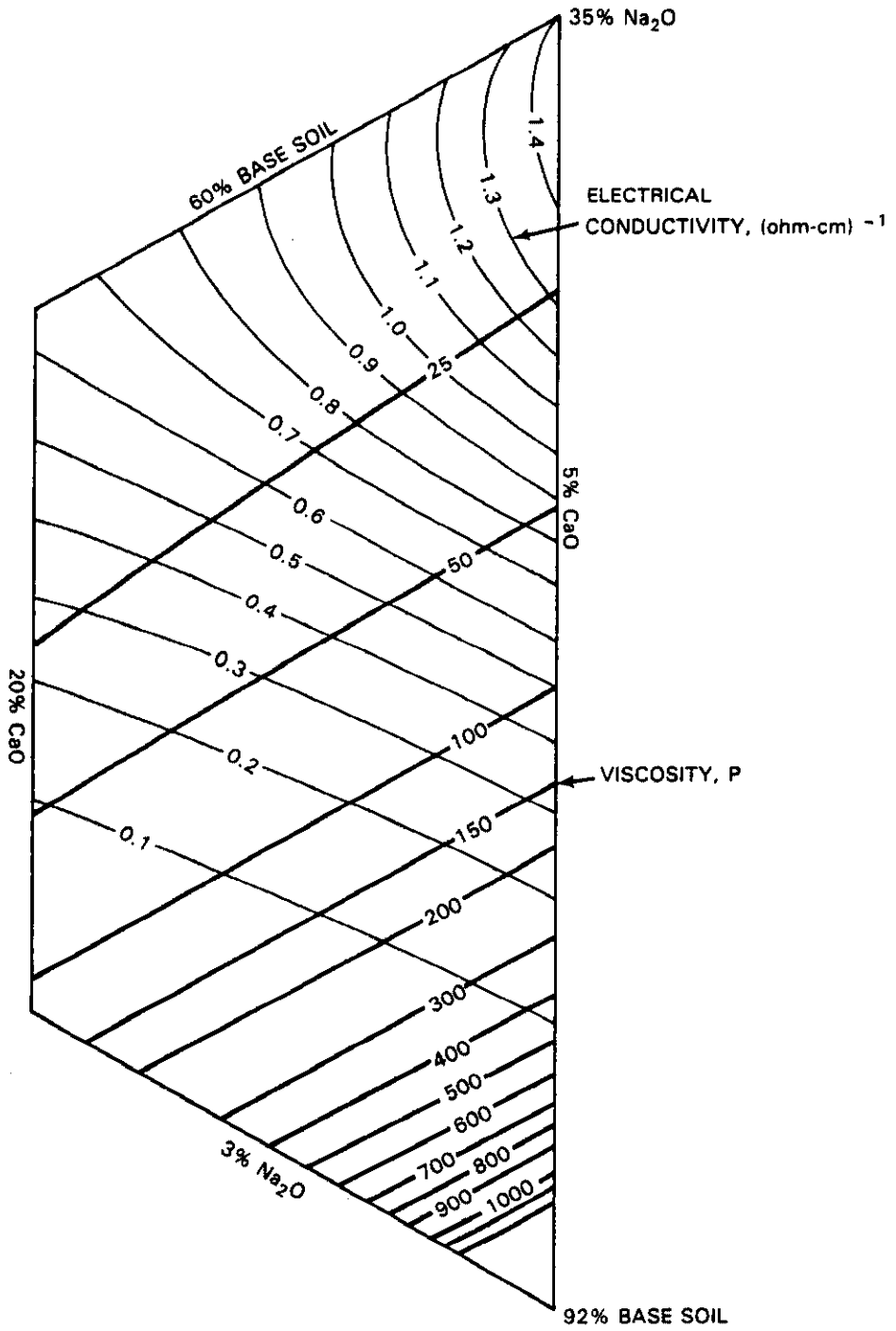

FIGURE 50. Effects of Na_2O and CaO on the Viscosity and Electrical Conductivity of Hanford Soil at Constant Temperature (1325°C)

increasing the Na_2O concentration of the base soil from 3% to 35%. This is an increase of over two orders of magnitude in the electrical conductivity.

A ternary plot showing the effects of soil concentration on temperature and electrical conductivity at a constant viscosity (100 P) is shown in Figure 51. The following conclusions were made from the data.

- The melt temperature at constant viscosity (100 P) is mainly dependent on the base soil concentration. Addition of Na_2O and CaO within the test matrix boundaries can reduce the 100-P viscosity temperature from over 1600°C to less than 1100°C.
- Electrical conductivity increases as Na_2O is added, even though the temperature is lowered to maintain a constant viscosity. The electrical conductivity increases from less than 0.1 $(ohm\text{-}cm)^{-1}$ to greater than 0.6 $(ohm\text{-}cm)^{-1}$ when the Na_2O concentration is increased from 3% to 23%.
- Adding CaO to the soil will lower the required melt temperature for a given viscosity, thereby lowering the electrical conductivity significantly.

These results suggest that the melting properties of different soils at potential ISV sites can be adjusted by additions of Na_2O, CaO, or other glass modifiers. The effects of these modifiers on electrode corrosion, cold cap formation, and off-gas releases have not been determined and may limit the upper range of quantities added. However, the reduced operating temperatures that are achievable with the modifiers should minimize any of these concerns. For Hanford soils, the practical range for the additives tested is 0 to 35% Na_2O and 0 to 20% CaO. Concentrations greater than these limits can result in excessive crystallization, even during rapid cooling.

PERFORMANCE PREDICTIONS FOR DIFFERENT SITE GEOMETRIES

Physical geometries of potential ISV waste sites range from wide, shallow zones (e.g., ponds) to narrow, deep zones (e.g., bore shafts). The zone that an ISV process can vitrify in one operation has certain width and depth limits

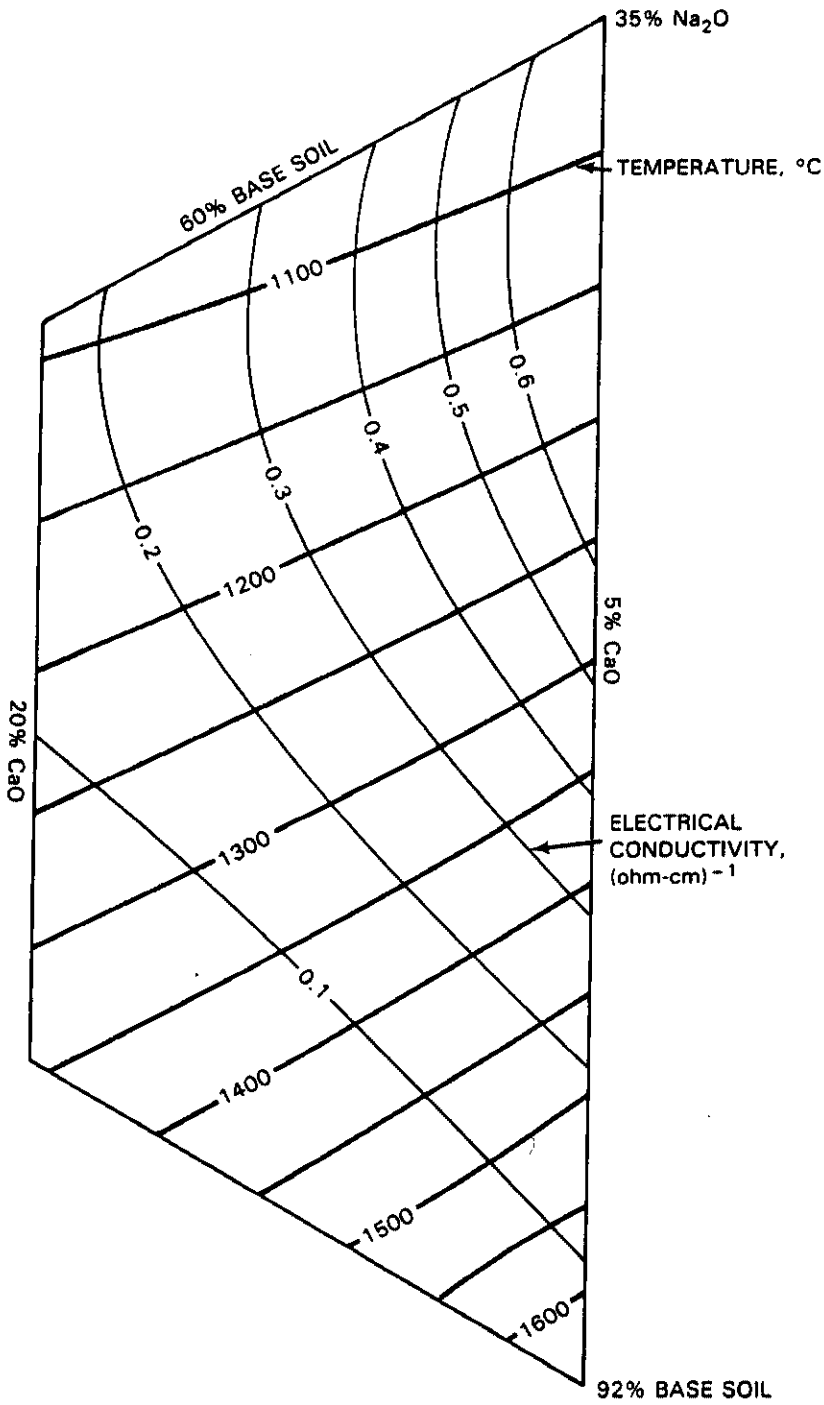

FIGURE 51. Effects of Na_2O and CaO on the Temperature and Electrical Conductivity of Hanford Soil at Constant Viscosity (100P)

imposed by the power supply rating and the specific soil properties. A mathematical model has been developed for predicting ISV process performance for different burial site geometries and for assisting with process scale-up to large commercial ISV systems. It is intended to reduce and in many cases eliminate the need for expensive and time-consuming field tests. The modeling simulation can reveal the effects that changes in soil properties, power system design, and waste site geometry will have on process performance. Information such as energy consumption, mass vitrified, operating time, melt depth, and melt width are readily available from the model.

Mathematical Model Description

The ISV mathematical model has been developed using a Hewlett Packard Series 200 computer equipped with a BASIC 3.0 or 3.1 language operating system. The model has been modified so that it will also run on an Apple 512K Macintosh computer and a Macintosh Plus computer using version 1.0 of TML Systems Pascal compiler. During operation of the program, the ISV melt zone depth grows downward in equally spaced increments. At each step, an energy balance is performed using power input, heat losses, and soil properties to determine the mass vitrified and time required for the vitrification. Power input is dependent on power transformer size, voltage tap selection, and melt zone resistance. The equations used to calculate power are

$$P = \frac{V^2}{R} \qquad \text{(constant voltage operation)}$$

and

$$P = I^2R \qquad \text{(constant current operation)}$$

The resistance is calculated between edge electrodes (R_e) and diagonal electrodes (R_d) as described by the following two equations:

$$R_e = \rho \frac{\ln\left(\frac{2 \cdot S_e}{D}\right)}{\pi D_g}$$

$$R_d = \rho \frac{\ln\left(\frac{2 \cdot S_d}{D}\right)}{\pi D_g}$$

where ρ is the average electrical resistivity of the glass, S_e is the electrode separation along the edge, and S_d is the diagonal electrode separation (Stanek 1977). The electrode diameter (D) and molten glass depth (D_g) also affect resistance. The overall melt zone resistance is then calculated by:

$$R = \frac{R_d R_e}{R_d + R_e}$$

The mathematical model calculates heat losses through the exposed upper surface and into the surrounding soil. Heat losses into the soil are calculated using a constant heat flux value applied to the molten zone side and bottom surface area in contact with soil. The surface heat losses are determined in a similar fashion using the area defined by the four corner electrodes for heat transfer. Heat flux values have been determined from pilot-scale test data. Using an average soil thermal conductivity of 0.20 W/m°K, the heat flux from molten glass to surrounding soil ranged from 2.3 to 3.2 kW/m^2. The maximum value, 3.2 kW/m^2, was conservatively selected as the heat flux term for heat losses into the surrounding soil. Based on a measured nominal surface temperature of 570°C, the heat flux through the upper surface was 32 kW/m^2. This value is consistent with actual pilot-scale and large-scale test data and was selected as the surface heat flux term for the model.

The model assumes that glass temperature is constant and thermal conduction of the electrodes has an effect. While glass temperature does change during an actual operation due to changing power density, the average temperature used by the model agrees well with actual pilot-scale data. Thermal conduction by graphite collars causes the downward growth of the molten zone to be slightly greater at the electrodes. This is not the case when only the smaller diameter Mo electrodes are extended to the bottom of the vitrified zone.

Mathematical Model Verification

The results of the model were compared with those of two pilot-scale ISV tests (PSFT-1 and PSRT). Table 24 lists the parameters used for the model.

TABLE 24. Model Parameters Used for PSFT-1 and the PSRT

Parameter	PSFT-1	PSRT
Maximum power, kW	295	400
Transformer voltage taps, V	960 & 480	1000, 560, & 422
Electrode spacing, m	1.15	1.2
Electrode diameter, cm	5.08	15.2
Surface heat flux, kW/m^2	32	32
Soil heat flux, kW/m^2	3.2	3.2
Average temperature, °C	1900	2000
Soil heat capacity, cal/g°C	0.24	0.24
Soil moisture content, %	5	5
Soil density, g/cm^3	1.6	1.6
Glass density (at temperature), g/cm^3	2.2	2.2

The model predictions agree very well with actual test data as shown in Table 25. All predicted parameters deviated <7% from the actual test parameters during PSFT-1. Figures 52 and 53 show the power input predicted by the model and that measured during PSFT-1 and PSRT, respectively. The model predictions are very close to the actual case.

TABLE 25. Actual and Predicted Test Data for PSFT-1 and the PSRT

Parameter	Actual	Predicted	% Dev.	Actual	Predicted	% Dev.
Run time, h	21.0	20.7	-1.4	23	21.8	-5.2
Melt depth, m	1.1	1.17	+6.0	1.5	1.5	0
Melt width, m	1.8	1.92	+6.3	1.8	2.17	+20
Volume vitrified, m^3	3.6	3.4	-5.9	4.9(a)	5.3	+8.2
Mass vitrified, kg	5670	5380	-5.4	8600(a)	8500	-1.2
Average power, kW	205	201	-1.5	300	300	0
Total energy, kWh	4300	4200	-2.4	6900	6500	-5.8
Energy/mass, kWh/kg	0.76	0.78	+2.6	0.80	0.76	-5.0

(a) Estimated values.

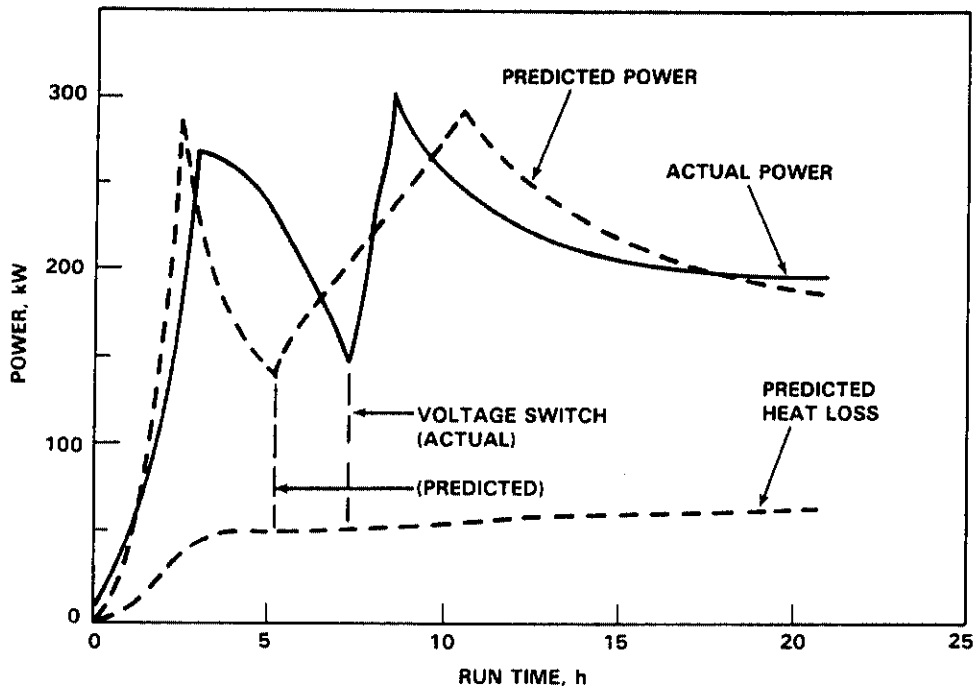

FIGURE 52. Predicted and Measured Operating Parameters for PSFT-1

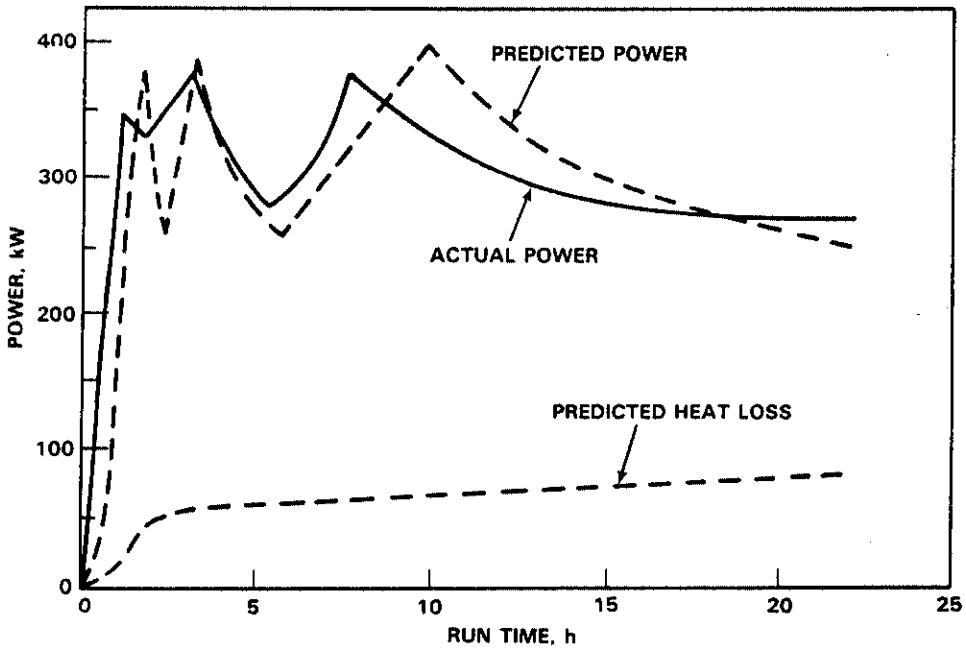

FIGURE 53. Predicted and Measured Operating Parameters for the PSRT

Large-Scale Mathematical Predictions and Verification

Since the model results agreed well with pilot-scale field test data, the model was then used to predict the performance of the 3750-kW, large-scale ISV system. The major control variables were electrode separation, soil moisture, and surface heat loss.

Because resistance between electrode pairs drops as the vitrified zone grows, the large-scale ISV system is based on a power transformer that has 16 voltage taps ranging from 4160 V and 450 A per electrode pair for startup, down to 280 V and 4000 A per electrode pair late in the run. (At this lowest voltage tap, the amperage is limited by the physical size of the transformer coils.) By selecting more voltage taps, a higher average power can be maintained during the ISV operation.

Figure 54 shows startup voltage as a function of electrode separation for engineering-, pilot-, and large-scale tests. The data point for the pilot-scale test is the average for the first three field tests. Extra graphite starter material can be added to reduce the magnitude of the startup voltage, if necessary, to achieve startups for separations larger than 6 m. Also, startup voltage can be greatly reduced by using a graduated startup technique as was done during LSVT-1. This technique involves using very low power input during startup and then gradually increasing power at a prescribed rate until full power is achieved. This may take 8 to 12 hours, but this technique significantly lowers the particulate generated during startup.

One of the objectives of the LSOAT was to determine the ability of the model to predict the run time, depth, width, and shape of the melt, energy requirements to vitrify a given volume of soil, and voltage and current relationships during large-scale processing. The accuracy of these predictions provides confidence in our ability to predict geometric limitations of the process.

Table 26 is a comparison of predicted versus measured process parameters for the three LSOAT settings and the LSVT. The range of predicted values is bounded by different assumptions related to the heat losses emanating from the surface of the vitrified zone. The low-heat-loss assumption accounts for the

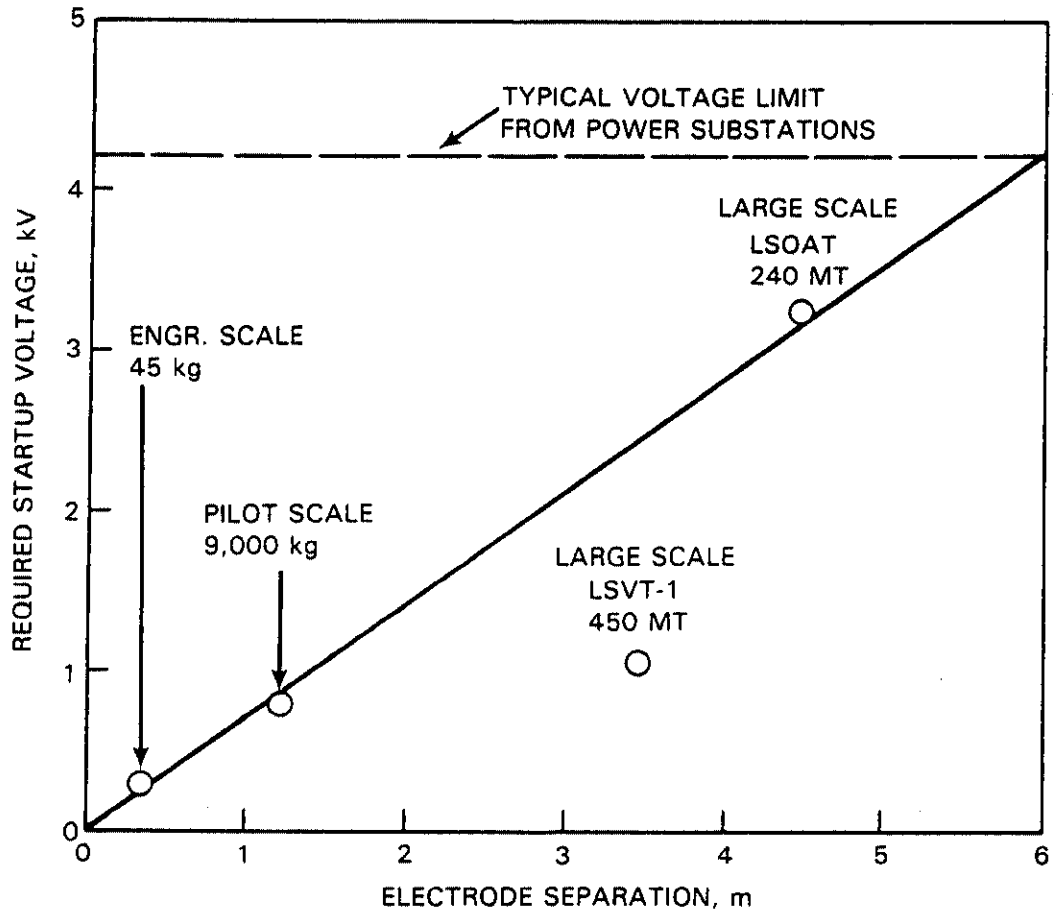

FIGURE 54. Scale-Up Correlations for Startup

presence of a cold cap over the molten soil, while the high-heat-loss model assumes the elimination of the cold cap and its associated insulation value. The different modeling assumptions only affect process efficiency, as demonstrated by run time and energy comparisons. The LSOAT-1 and -2 operated with the existence of a cold cap while LSOAT-3 and the LSVT did not. In later tests, the elimination of the cold cap was assisted by 8 cm of fiberglass insulation over the molten surface, with an insulation value equivalent to that of a cold cap. An estimate of the mass of the LSVT block, based on measurements of geometric shape obtained from core drilling, is 590,000 kg at a vitrified bulk density of 2.2 g/mL. The low- and high-heat-loss models at the energy dissipation of 435,000 kWh would predict a vitrified mass of 580,000 kg and 420,000 kg, respectively. Also, the measured surface heat losses from LSVT are

TABLE 26. A Comparison of Predicted and Measured Parameters During the Large-Scale Tests

	LSOAT					LSVT		
	Predicted Results		Actual Results			Predicted Results		
	Low Heat Loss	High Heat Loss	LSOAT-1	LSOAT-2	LSOAT-3	Low Heat Loss	High Heat Loss	Actual Results
Run Time, h - excluding downtime	62	76	62	72	71	106	147	160
Melt Depth, m	4.00	4.00	4.0	3.0	3.0	7.1	7.1	5.0
Melt Width, m	7.2	7.2	7.0	7.1 - 8.2	--	7.8	7.8	10.6
Volume, m^3	165	165	--	--	--	300	300	--
Mass, t	265	265	(265)	(187)	(265)	477	477	590
Final Voltage/ Current, V/A	735/2450	735/2450	600/2800	620/2400	620/2170	610/2900	610/2900	700/3200
Average Power, kW - excluding downtime	3370	3370	3400	2160	2900	3370	3370	3000
Energy Dissipated, MWh	210	256	210	148	210	360	490	435
Energy/Mass, kWh/kg	0.79	0.97	(0.79)	(0.79)	(0.79)	0.75	1.04	0.74

NOTE: Values in parentheses are estimated based on low heat loss model energy to mass ratio.

202 kW, whereas the low- and high-heat-loss models predict 390 and 1480 kW, respectively. Consequently, the actual process parameters more closely match the low-heat-loss model, which will be used for future geometric predictions. The measured geometric shape, however, differed slightly from the predicted results. Figures 55 and 56 depict a comparison of predicted versus achieved melt shape for the LSOAT-2 and LSVT. The large-scale system produces vitrified blocks slightly wider and shallower than predicted. The variance may be due to the fact that the large-scale tests were conducted in partially disturbed soil that may encourage outward growth. Another potential cause may be electrode failure below the melt surface, which concentrates heat in the upper molten region encouraging outward growth. The variance in measured versus predicted geometry would not affect the ability of the process to meet the attainable depth of 13 m reported by Buelt and Carter (1986b). In fact, since the results more closely match the low-heat-loss model, the practical depth limit of 25 m is more likely to be obtained.

Western Site ISV Predictions

The effect of electrode separation on melt depth and run time in Hanford soil that contains 5% moisture can be seen in Figure 57. The surface heat flux area was assumed to be nominal (low heat loss). Melt depths of 16 m or greater would be possible using electrode separations of 3 to 4 m. However, run times of greater than 500 hours would be necessary to achieve these depths.

As a conservative measure, a high-heat-loss case was considered. The surface heat flux was applied to the entire upper area of the molten glass zone, which expands during operation beyond the area defined by the four electrodes. This more closely models the case where no insulative cold cap or surface insulation is present. Figures 58 and 59 show the high-heat-loss model predictions for unsaturated soil containing 5% and 25% moisture, respectively. The melt depth at which heat losses become 80% of total power [the practical limit given by Buelt and Carter (1986b)] is illustrated by the dashed line. While the increased moisture content in unsaturated soil does not reduce the attainable melt depth, it does increase the time required to reach that depth. Increased soil moisture has the same effect on ISV as an increased soil heat capacity would since additional heat is required to convert the water at ambient

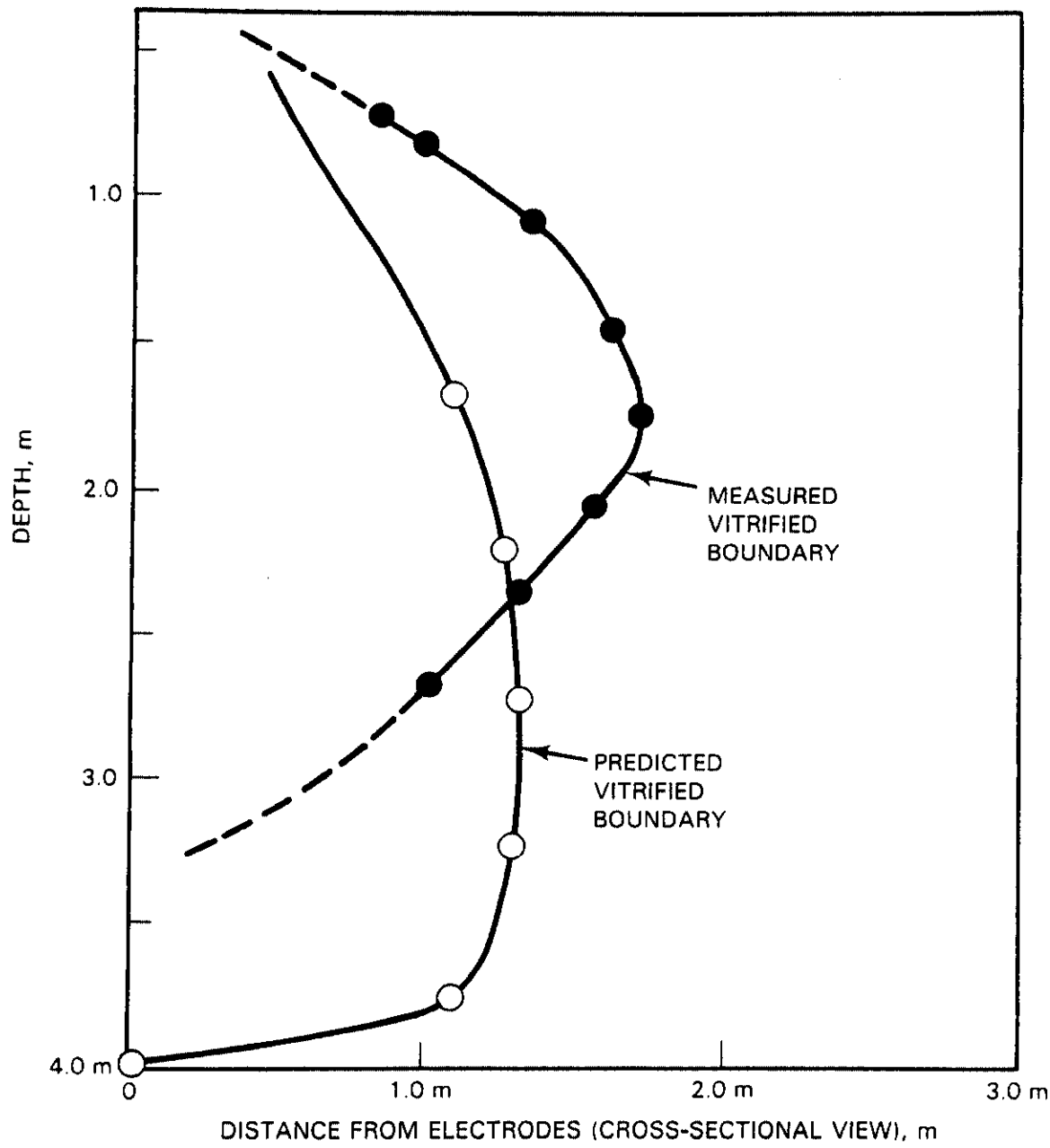

FIGURE 55. Predicted versus Achieved LSOAT Melt Shape

temperature to a superheated vapor. However, with saturated, swelling soils, this is not the case. It requires about the same amount of energy to convert a given volume of water at ambient temperature to a superheated steam as it does to heat the same volume of theoretically dense soil from ambient to 2000°C.

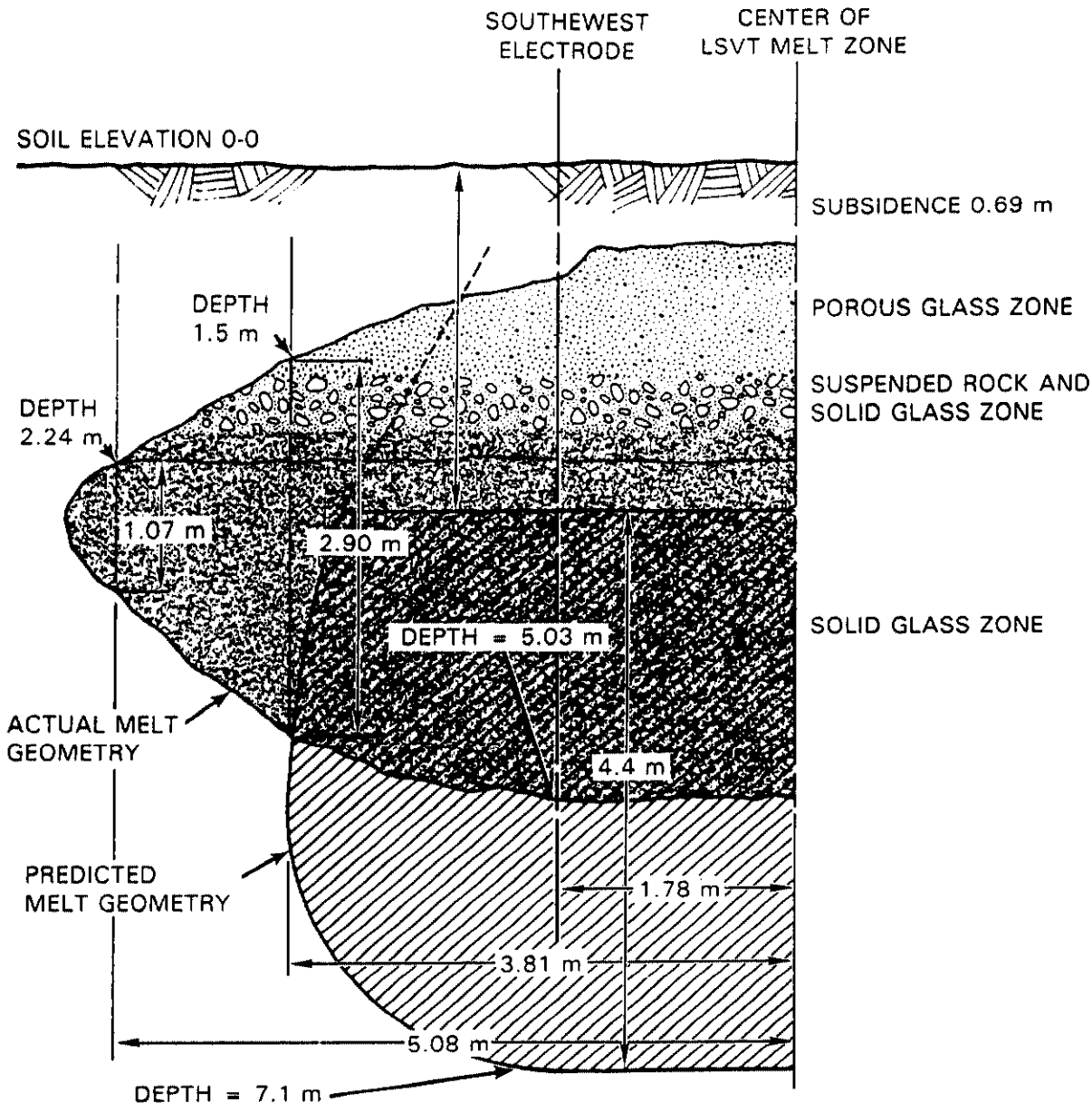

FIGURE 56. Vitrified-Mass Profile for the LSVT

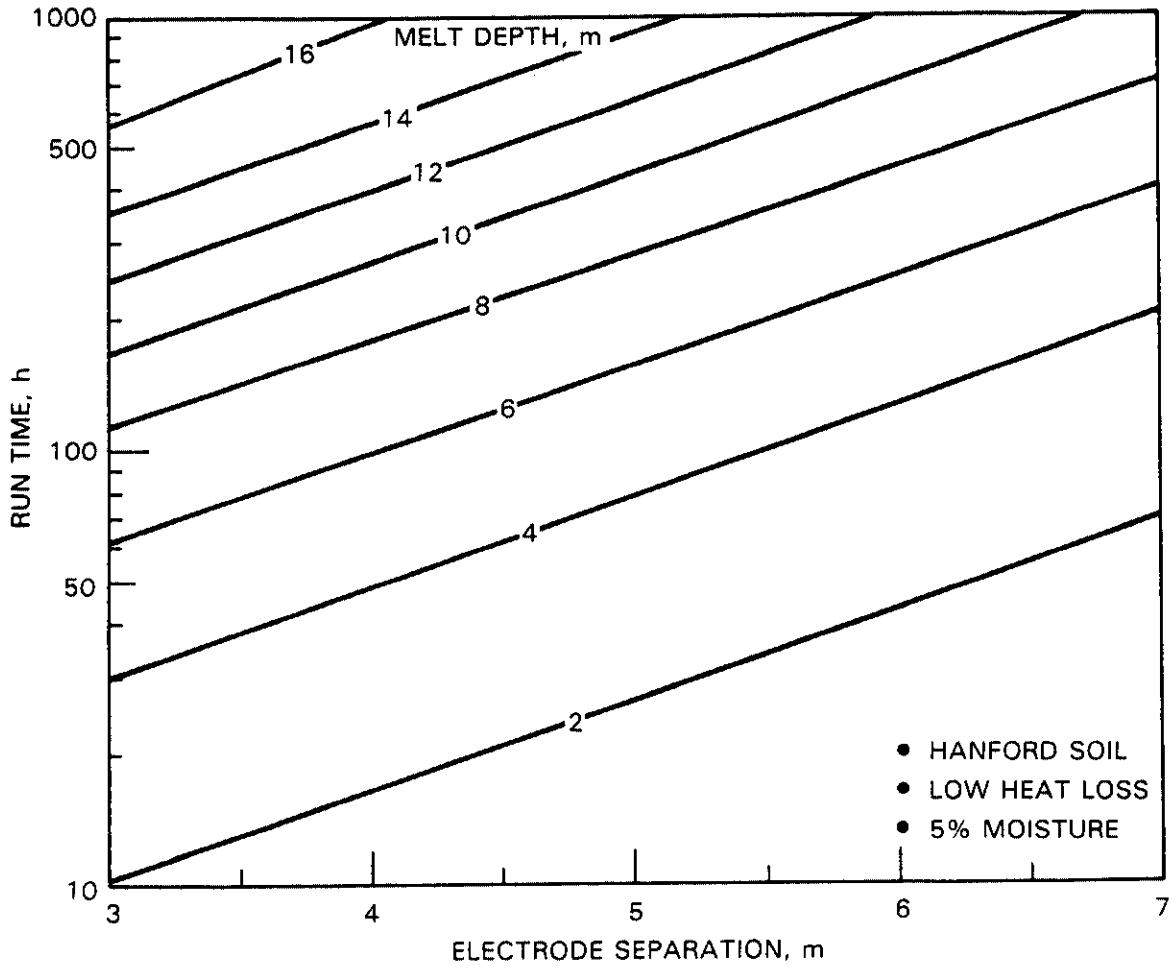

FIGURE 57. Effect of Electrode Separation on Melt Depth and Run Time for Hanford Soil with Nominal Heat Losses and 5% Moisture

Saturated sludges with 70% moisture content have been vitrified with the pilot-scale unit using no more energy than required for Hanford soil at 5% moisture (0.8 kWh/kg).

Eastern Site ISV Predictions

Although it has been shown that differences in certain soil properties at the various waste sites throughout the United States are small, differences in moisture content among sites are large. The soil moisture content above the water table at eastern sites such as ORNL or SRP averages between 20 and 25%, while at Hanford 4 to 5% is more typical.

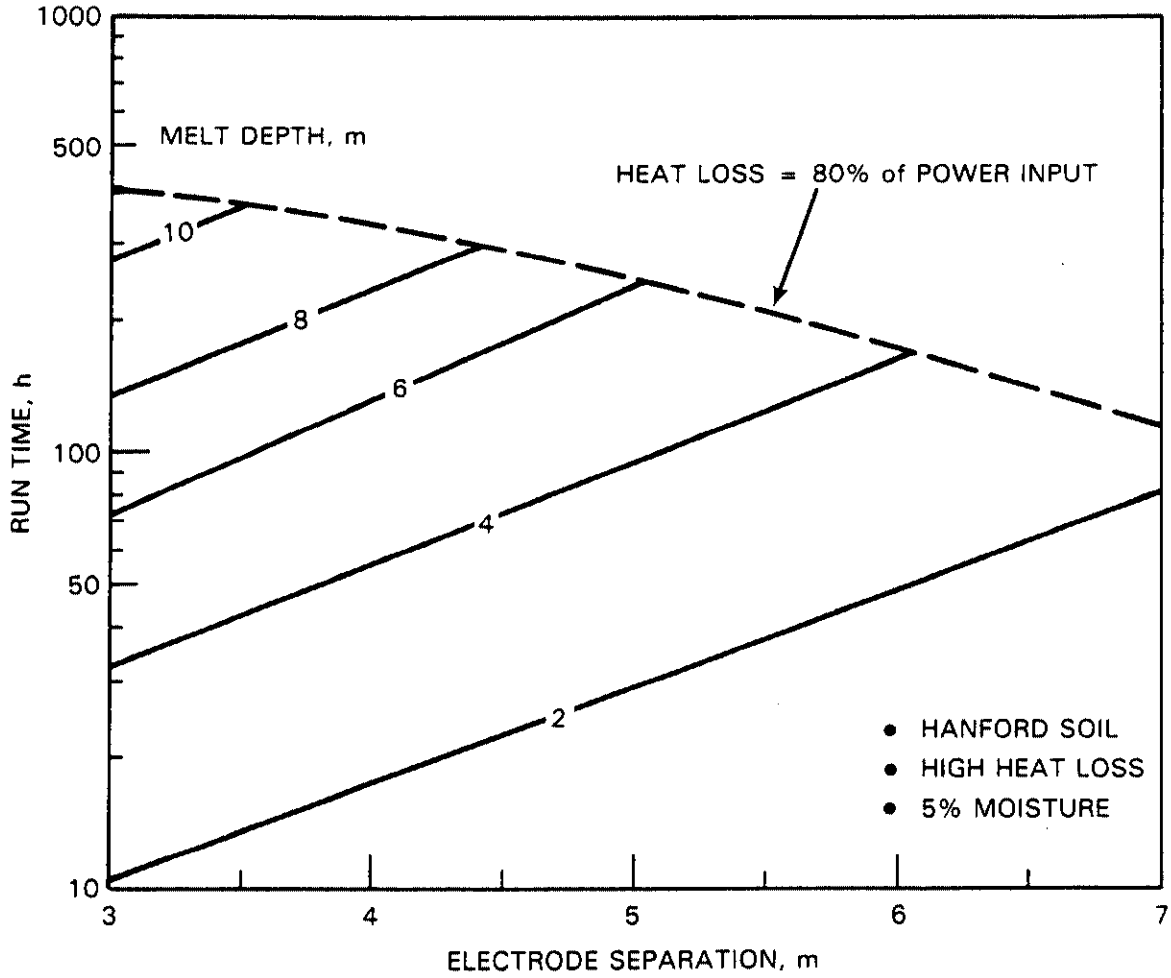

FIGURE 58. Effect of Electrode Separation on Melt Depth and Run Time for Hanford Soil with High Heat Losses and 5% Moisture

Factors that influence the level of moisture in a particular soil are water table depth, climate, and the soil's hydraulic properties. The factor that potentially has the greatest effect on ISV is the water table depth. The water table is the upper surface of the water-saturated zone when the aquifer is unconfined. The degree of saturation can range from 10 to 60%, depending on soil porosity. Additional power is required to vitrify waste below the water table since water may be recharged into the area that is being vitrified. Engineered barriers or water wells could be used to artificially lower the water table and reduce or eliminate water recharge during an ISV operation. If

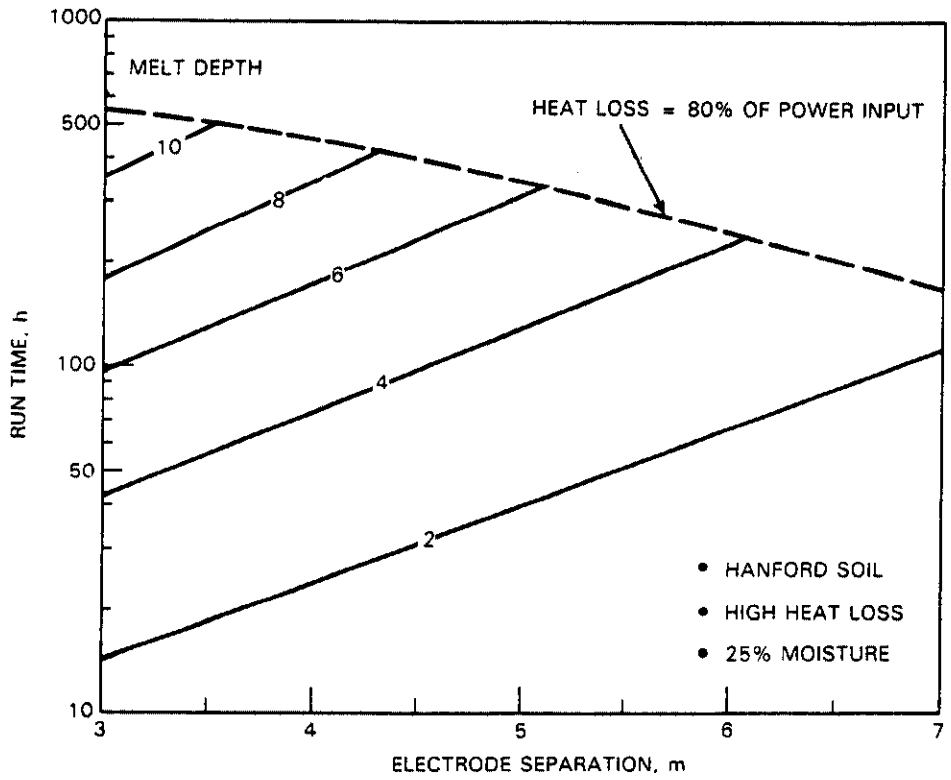

FIGURE 59. Effect of Electrode Separation on Melt Depth and Run Time for Hanford Soil with High Heat Losses and 25% Moisture

soil permeability is low enough, recharge is insignificant, and the ratio of soil to water in the saturated zone has essentially no effect on the attainable melt depth and operational time.

Climatic events, water potential, and hydraulic conductivity at saturation are responsible for the soil moisture content above the water table. The amount of precipitation controls, in part, the rate at which water is added to the soil, while soil characteristics determine the conductance of water through the waste site. The volume of bonded water in soil is also somewhat dependent on the rate of drainage.

Water can accumulate in a burial trench, even though the trench is located well above the water table. The permeability of the disturbed soil placed over the waste site is typically much higher than that of the surrounding undisturbed soil. Inclusions of solid waste in the soil, which create

irregularities and void spaces, further increases waste site permeability. Precipitation can accumulate at the bottom of the trench, becoming ponded above the actual water table, since water drains through the excavated waste area faster than through undisturbed soil. Ponded water may exist in TRU waste trench bottoms at sites like ORNL and SRP, which receive high annual rainfall. In large waste trenches above the water level with relatively impermeable soil surrounding the trench, ponded water will increase the required power input for ISV.

Limitations to ISV imposed by soil moisture are most probable at ORNL where some trenches are excavated to depths below the water table. Trenches at ORNL are typically 2.1- to 4.3-m deep, and the depth to the water table ranges from ground level to 4.6 m, depending on the location and season (Webster 1979). A burial-ground scenario under extreme conditions at ORNL was used to evaluate how moisture could limit the ISV process. The burial trench used in the scenario was excavated to a depth of 4.3 m in an area with the water table at ground level and a highly permeable, sandy layer below the 6.4-m level (see Figure 60). Water permeability for ORNL soil averages 3.0 cm/day (Luxmoore, Spalding, and Monroe 1981). Soil in the upper 6.4 m is conservatively assumed

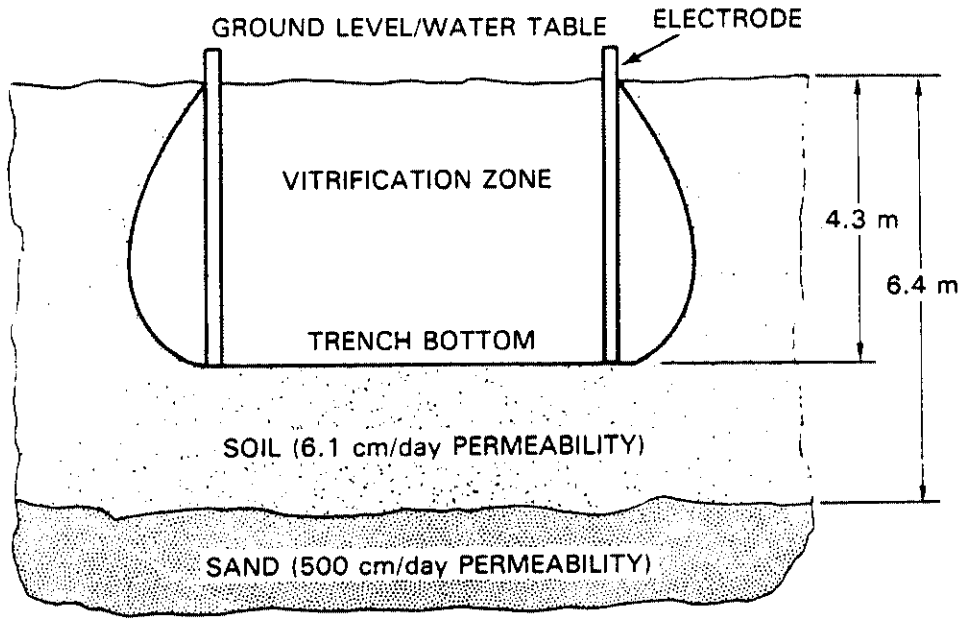

FIGURE 60. Burial-Ground Scenario for Moisture Limitations Analysis

to have a porosity of 57% and a permeability of 6.1 cm/day. The permeability of the sandy area below 6.4 m is assumed to be high, at 500 cm/day.

The mathematical model was used to determine the maximum vitrification depth attainable for ISV in the burial-ground scenario. The primary depth limitation is imposed by the aquifer depth. Based on model predictions shown in Figure 61, moisture levels will not limit the ISV process at ORNL, if the desired vitrification zone does not join with any areas of high permeability.

PERFORMANCE OF IN SITU VITRIFICATION WITH DIFFERENT WASTES

Many waste sites contain buried inclusions within the soil that may affect the ISV process. Transuranic-contaminated soil sites often include wood or concrete cribs, ceramic French drains, and tile fields. Solid-waste burial

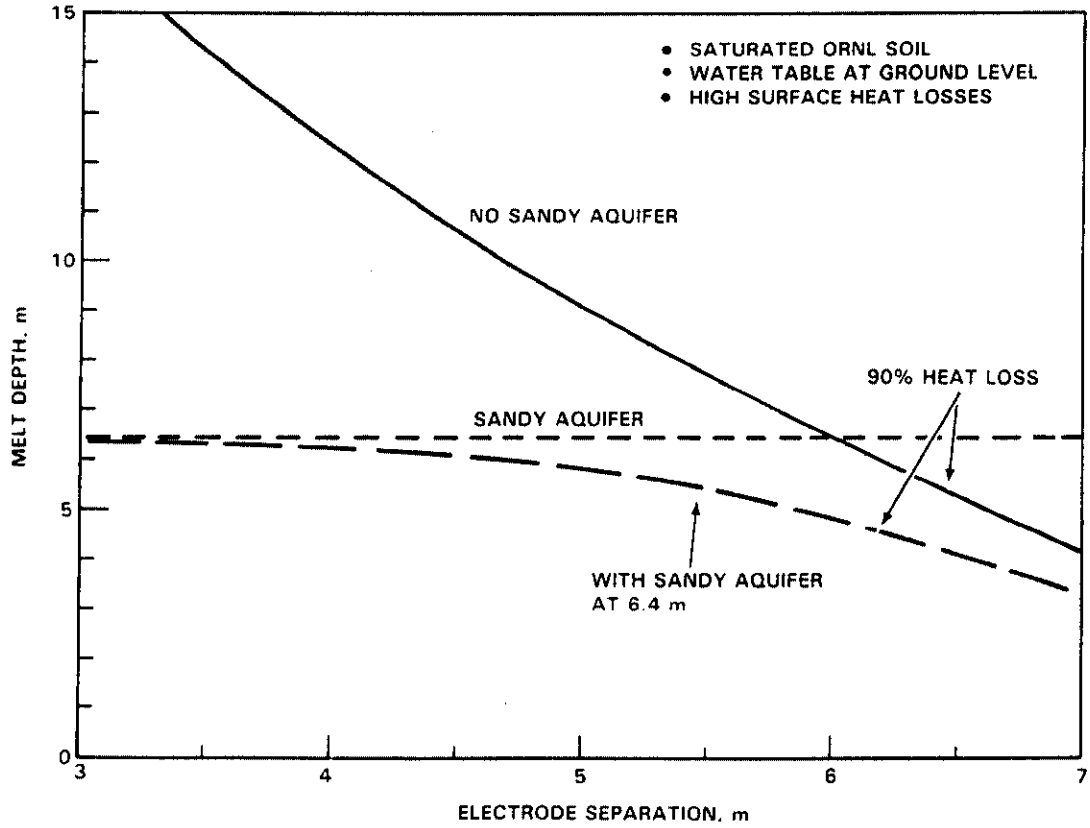

FIGURE 61. Effect of Sandy Aquifer on Melt Depth for Saturated ORNL Soil with High Heat Losses

grounds incorporate a large quantity and wider variety of wastes, such as metal drums and process components, combustibles, and concrete monoliths. The soil wastes considered here are metals, cements, ceramics, combustibles, sludges, hazardous organics, sealed containers, explosives, and elements that could cause a criticality. The predicted effects of each waste type on the ISV process are discussed in the following sections.

Metal Inclusions

Metal, which has a much higher electrical conductivity than molten soil, can decrease electrode voltage when present during ISV, and in extreme cases it can result in a short circuit. The mathematical model and a series of four engineering-scale tests were used to evaluate the effect of metals on the ISV process.

The metal inclusion model is based on a two-electrode system. Figure 62 shows the physical model, with the metal resting at the bottom of the melt in Zone 2. Zone 1 is the high-temperature glass area in which the mean temperature is ~1700°C, while Zone 2 is the cooler leading edge of the melt zone. As

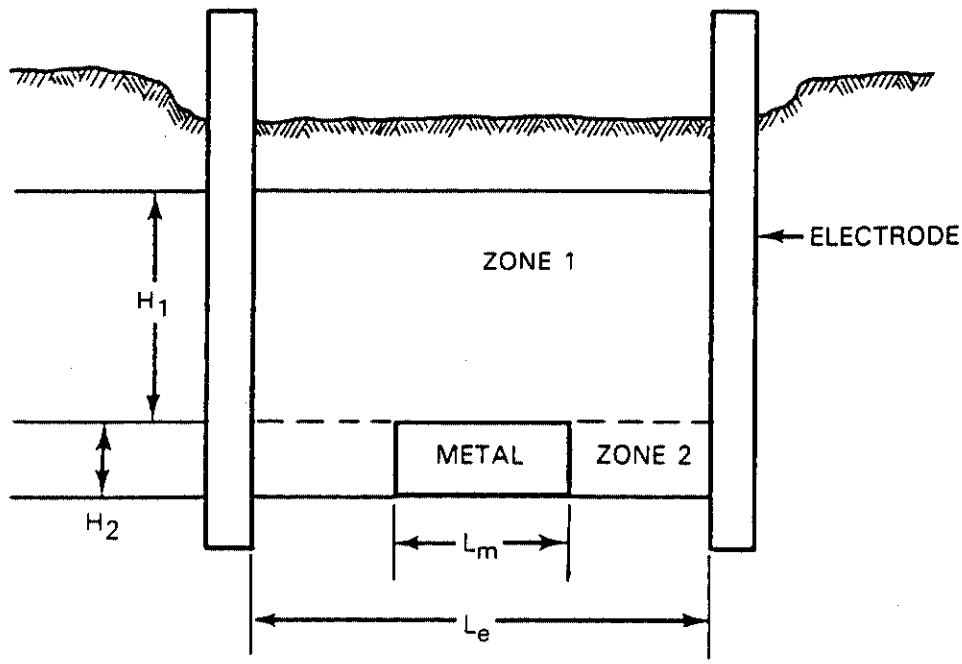

FIGURE 62. Metal Inclusion Model

the melt grows and proceeds downward through a metal object, the metal will melt and settle in the cooler Zone 2 area, resolidifying if temperatures are below the metal's melting point (1565°C for carbon steel and 1420 to 1500°C for stainless steel).

The metal inclusion model was used to evaluate the effect of varying Zone 1 depth, Zone 2 depth, metal width, and metal volume on the electrode voltage, power, and power density. The model correlates quite well with data from tests where no metal was present.

Figure 63 shows the effect of the metal width as a fraction of the electrode spacing on power and voltage for a pilot-scale electrode pair. As the fraction increases, the power and voltage decline gradually until the metal approaches the electrodes and a short circuit occurs. The power distributions as a function of L_m/L_e (length of metal divided by distance between electrodes) are shown in Figure 64. As the metal path increases between electrodes, high-temperature areas form in the melt between the metal and electrodes in

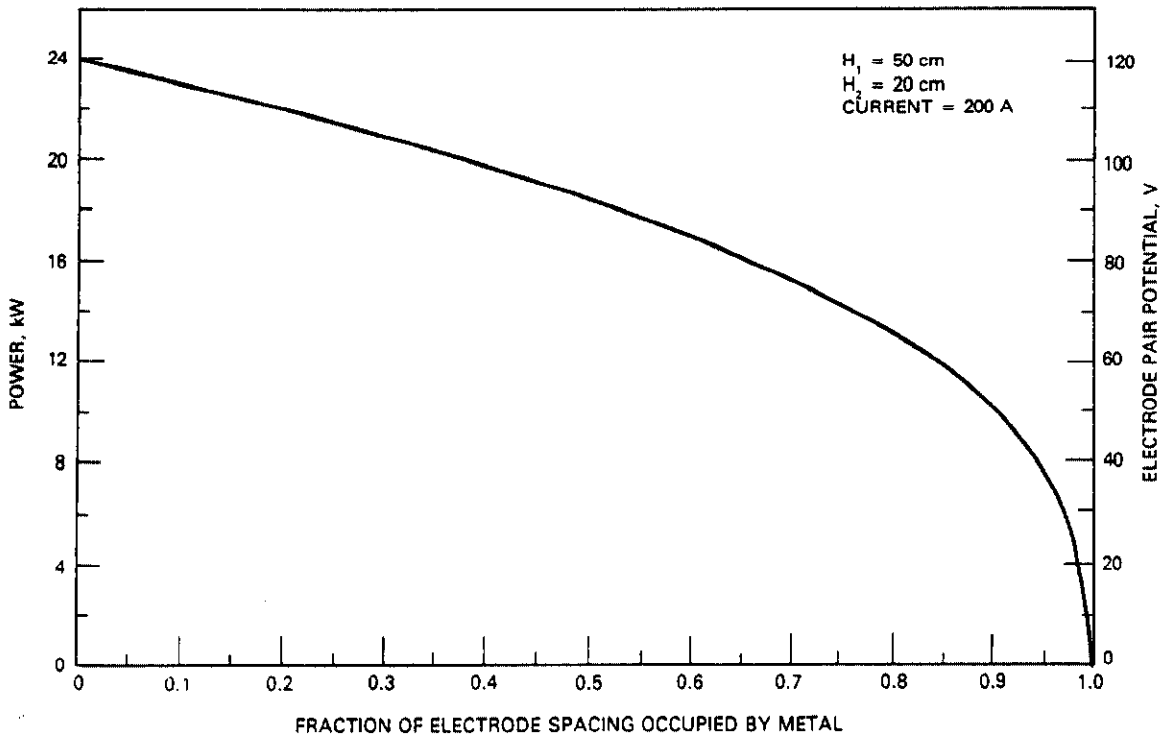

FIGURE 63. Effect of Metal Width on Power and Electrode Potential

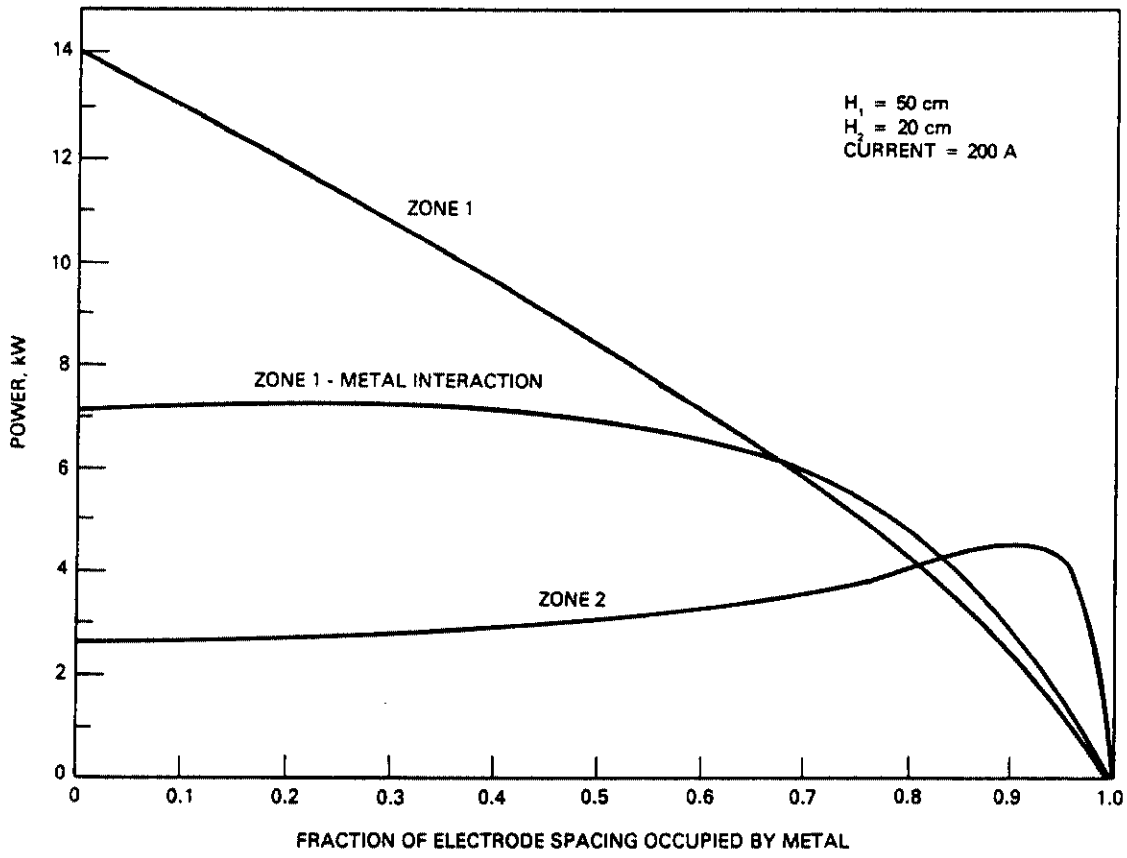

FIGURE 64. Effect of Metal Width on Power Distribution

Zone 2. A cool area is likely to form above the metal in Zone 1 if convective currents are insufficient in the molten glass. The result may be an increased cold cap.

The model also predicts that varying the mass of metal in the soil has essentially no effect on power input and electrode voltage for a given metal width. According to the model, the power and voltage decrease by <0.1% when the metallic mass is increased by a factor of 10 for a fixed L_m/L_e ratio.

Four engineering-scale laboratory tests, ESLT-10 through ESLT-13, were performed to verify the effects of metal inclusions on the ISV process. Summaries of each test are given in Table 27. The quantity of metal placed in the soil ranged from 2 to 5% of the final vitrified block weight. Each test proceeded to completion with no major difficulties. In ESLT-12, a stainless steel

TABLE 27. Summary of Results from Engineering-Scale Laboratory Tests Containing Metal Inclusions

Test Parameter	ESLT-10	ESLT-11	ESLT-12	ESLT-13
Power limit, kW	7	7	10	10
Metal mass, kg	1.5	0.9	2.4	1.2
Metal loading, wt%	3	2	5	2
Electrode spacing fraction occupied by metal, L_m/L_e	0.35	0.35	0.71	0.35
Combustible mass, kg	0	0.2	0	0
Run time, h	13	12	11	9
Total energy, kWh	78	69	68	83
Average power, kW	6	6	6	9
Mass solidified, kg	47	46	49	63
Energy/mass, kWh/kg	1.6	1.5	1.4	1.3

and a carbon steel canister, each containing metal scrap of the same composition, were placed edge to edge, occupying 71% of the distance between electrodes. To complete the test, it was necessary to increase the power to the engineering-scale unit from 7 to 10 kW. This may have been due to the heat-fin effect of the metal, which increased heat losses to the soil.

Figure 65 shows the effect of metal inclusions as predicted by the model compared to actual data from the engineering-scale ISV system. The model predicted a larger drop in voltage due to metal inclusions than was actually observed. At an L_m/L_e ratio of 0.7, engineering-scale tests showed a voltage drop of 21%. This means that the lowest voltage tap of the power transformer should be designed 21% lower than required with normal soil to maintain the same high power input level during ISV of soil with metal inclusions. The data indicate that metal may occupy up to 90% of the linear separation between electrodes.

Cement and Ceramic Inclusions

Unlike metals, the electrical conductivities of cement and ceramic waste inclusions are not high enough relative to the soil to create a short circuit. Instead, they are usually in the oxide form and are very similar to many of the

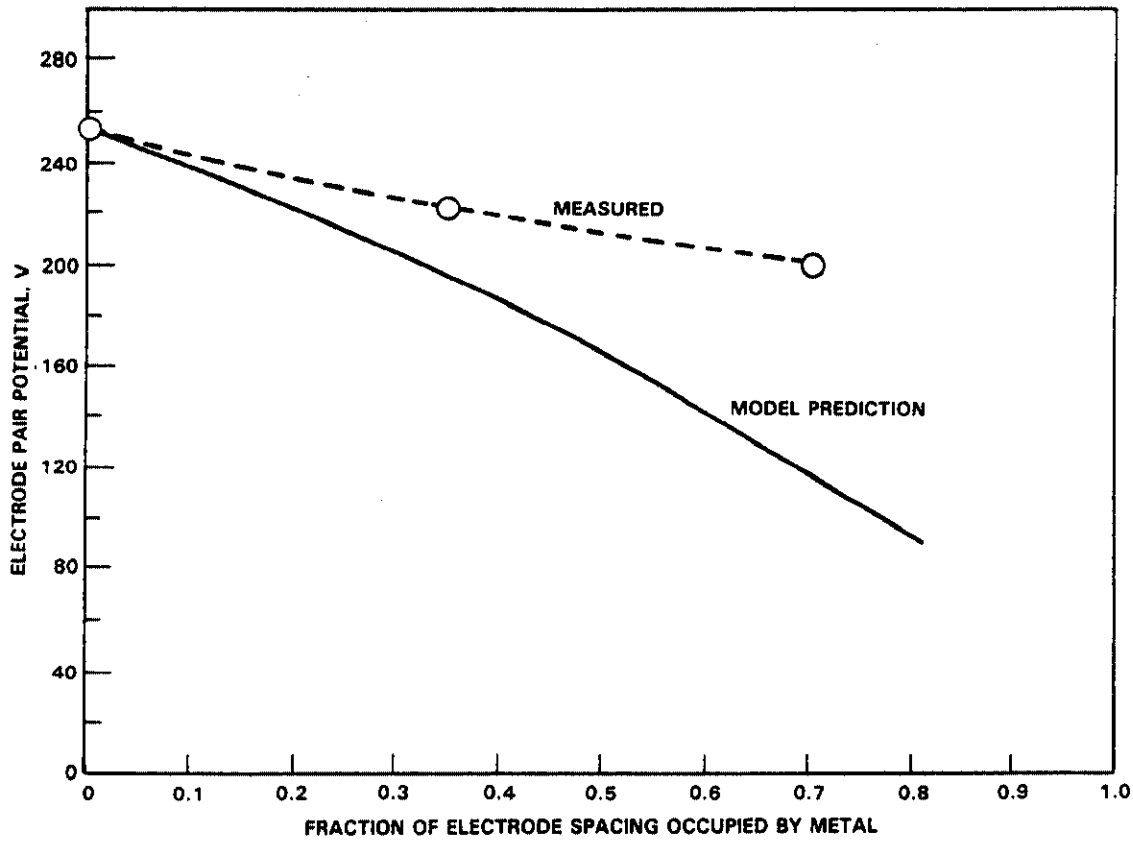

FIGURE 65. Measured and Predicted Voltage Drop Due to a Metallic Inclusion

compounds found naturally in soil. The volume of cement and ceramic waste inclusions in a waste trench is typically very small compared to combustible and metallic waste volumes. The cements and ceramics include large concrete casks used to contain industrial wastes at most TRU sites, cement paste in corrugated metal pipes at LANL, and concrete cribs and vitrified clay French drains at Hanford. Because almost all buried nonmetallic materials are some form of cement product, concrete waste inclusions are analyzed most extensively in this section, although other ceramic materials are also discussed.

Cement can be defined as an adhesive complex of nonmetallic oxides, with CaO as the primary constituent. Hardened cement contains up to 33.3 wt% (20 wt% average) water, which acts as the adhesive for the complexed oxides (Lea 1971). Concrete contains less water than pure cement (~5%) because of its high volume of sand and gravel.

The compounds in cements are formed by the interaction during the burning of CaO, SiO_2, Al_2O_3, and Fe_2O_3 compounds. Although the percentages of these compounds vary greatly among cement types (see Table 28), when combined they make up over 85% of each cement type. Portland cement is composed of over 90% CaO, Al_2O_3, and SiO_2. Of the three major oxide constituents in concrete, both CaO and Al_2O_3 lower electrical conductivity upon addition to soil, while SiO_2 does not (Stanek 1977). Concrete also has a higher specific heat than soil.

To verify the ability of the ISV process to handle cement, ESLT-14 and -15 were conducted using relatively large concrete masses in the soil. In the first test, a carbon steel can encapsulated in concrete was vitrified, while in the second test, two monoliths, one of concrete and the other of cement paste, were vitrified (see Table 29 for the test summaries). After the tests, all of the concrete had been vitrified within the blocks. Glass samples of the first concrete ISV test were analyzed and showed very uniform Ca distribution throughout the glass melt.

At ambient temperature, hardened Portland cement with >20 wt% water is much more electrically conductive than normal soil. As heat is generated in and around the concrete inclusion, it begins to expand. At temperatures above

TABLE 28. Composition of Various Cements

	Composition, wt%	
Component	Portland Cement	Other Cements[a]
CaO	64.1	38 to 65
SiO_2	22.0	5 to 27
Al_2O_3	5.5	3 to 39
Fe_2O_3	3.0	0 to 13
SO_3	2.1	0 to 4
FeO	0	0 to 4
S	0	0 to 1

(a) Includes Erz, Ferrari, Kuhl, Portland Blast Furnace, Eisen-Portland, Hochofen, Slag Supersulphated, and High Alumina cements (Lea 1971).

TABLE 29. Summary of Results from Engineering-Scale Laboratory Tests Containing Concrete Inclusions

Test Parameter	ESLT-14	ESLT-15
Power limit, kW	12	17
Cement mass, kg	4.9	6.1
Cement loading, wt%	8.8	6.5
Metal mass, kg	0.16	0.69
Metal loading, wt%	0.3	0.7
Electrode spacing fraction occupied by concrete, L_m/L_e	0.44	0.46
Total energy, kWh	63	120
Average power, kW	8	13
Mass solidified, kg	56	94
Energy/mass, kWh/kg	1.1	1.3

100°C, the expansion of the concrete paste and aggregate begins to be opposed by a contraction mechanism as water is driven off. At ~300°C, contraction due to water loss becomes greater than the thermal expansion, and the material starts shrinking, with ultimately >0.5% contraction from the original ambient dimensions (Harada et al. 1972; Zoldners 1971). This continues past 400 to 450°C, where free Ca_2OH_2 is dehydrated. The partially dehydrated cement starts expanding again at temperatures exceeding 700°C. Because the aggregate is continually expanding while the cement paste is contracting, severe cracking occurs. As a result, the concrete structure is broken up into smaller fragments that are believed to be uniformly dispersed throughout the glass by convection currents. Although the rate of complete dehydration is slow at 534°C, complete dehydration occurs quickly at temperatures above 1090°C (Petersen 1966). The ISV large-scale system, as described previously, will accommodate these water releases.

The electrical resistivity of the melted soil increases as the cement is melted and becomes uniformly dispersed. This was observed during ESLT-14, in which an 8.8% loading of concrete in the soil raised the molten zone's electrical resistivity significantly (see Figure 66). Because the ISV operating voltage depends in part on the electrical resistivity of the molten path and the

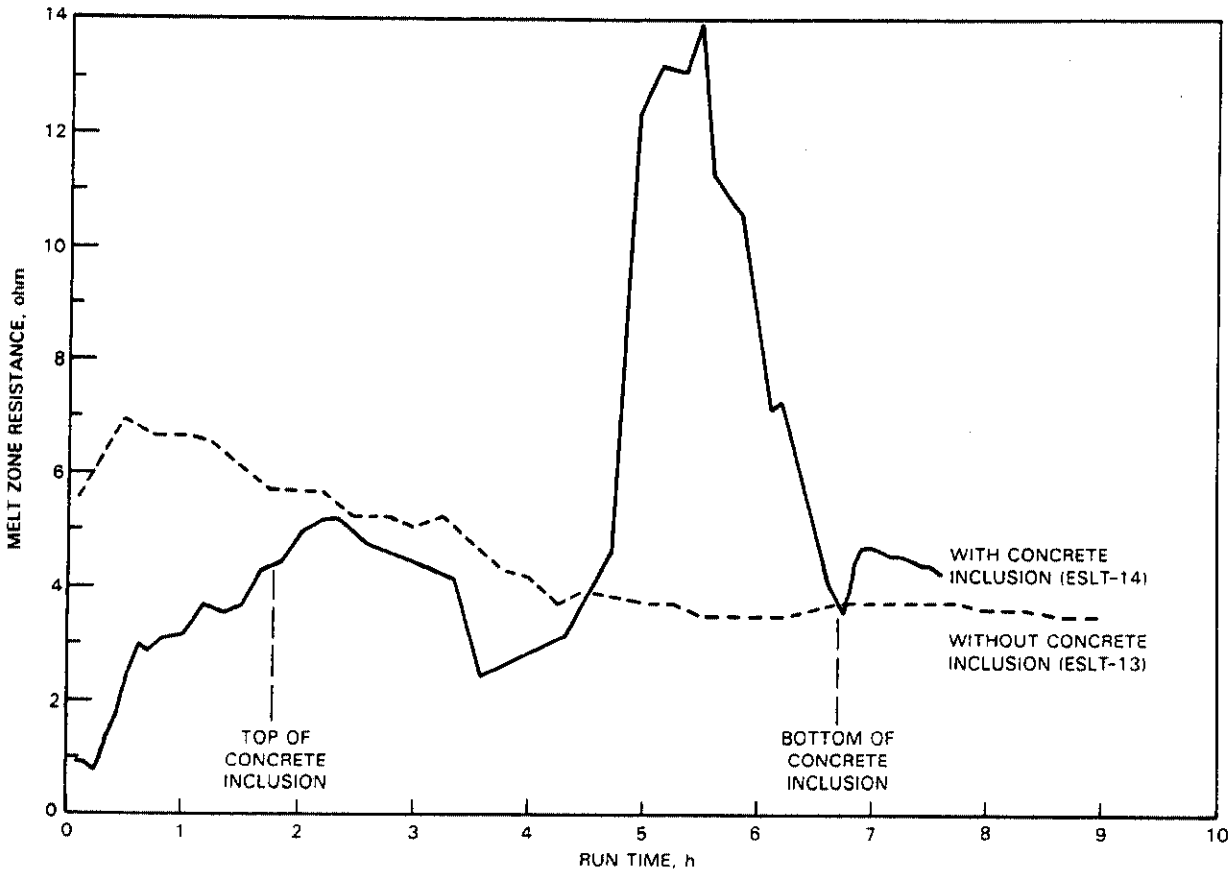

FIGURE 66. Effect of Concrete Inclusions on Melt Zone Resistance

distance between electrodes, an increase in electrical resistivity caused by concrete can be offset by a corresponding decrease in electrode spacing. A decreased electrode spacing should be required only if the cement inclusion is at or near the surface of the waste site. If the concrete is encountered after the melt zone has grown, higher voltage taps should be available on the power transformer to accommodate any increased resistivity caused by the concrete. This increased resistivity of the molten zone can be compensated for by a voltage increase to one of the previous voltage taps. The power input to the melt zone will not be reduced.

The volume of water vapor given off during concrete dehydration becomes a significant portion of the gaseous effluents that are normally treated by the ISV off-gas system. Figure 67 shows the incremental off-gas capacity required

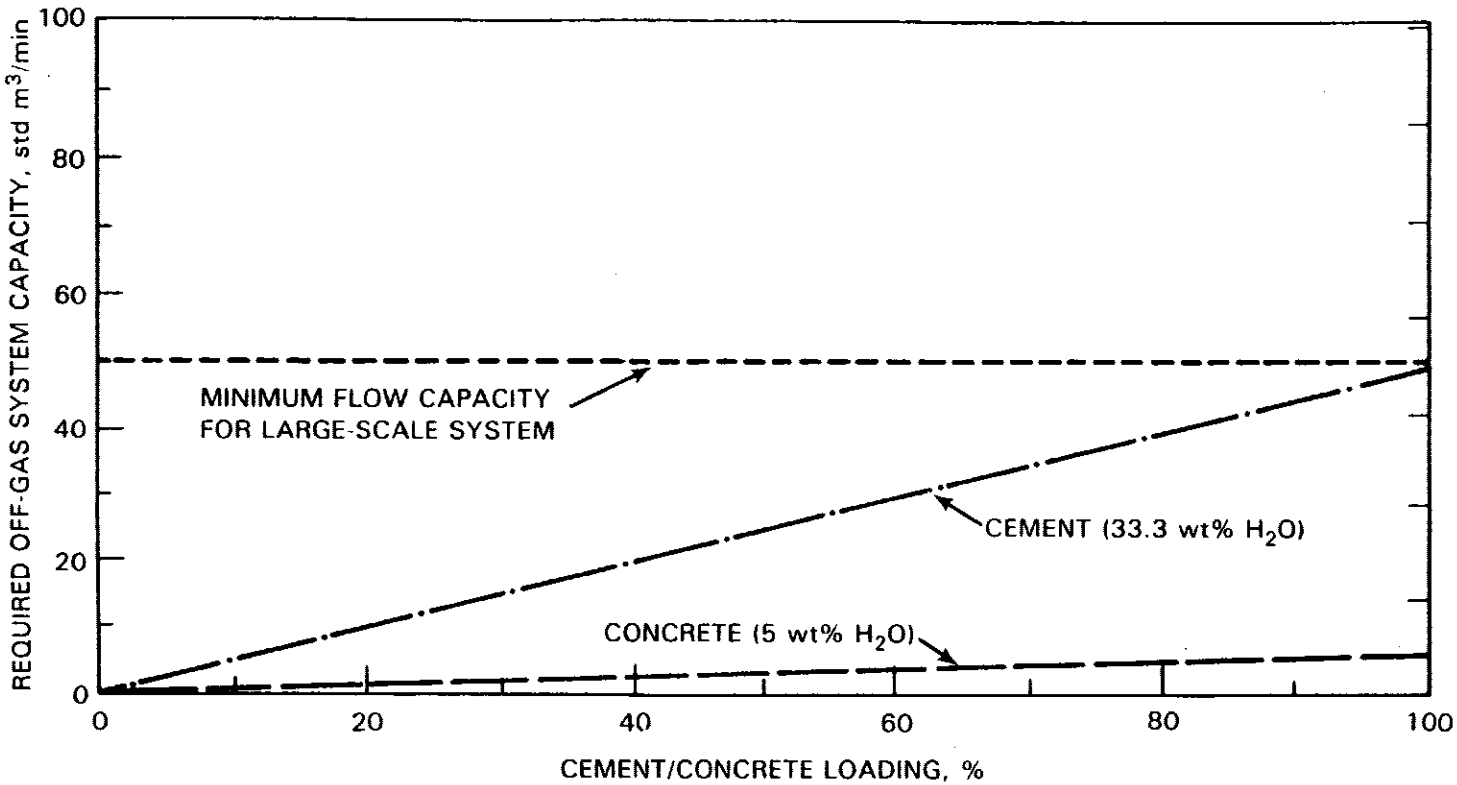

FIGURE 67. Off-Gas Capacities Required for Various Cement and Concrete Loadings

for treating water vapor from various concrete and cement loadings. The graphs assume that the specific heats and melting rates of soil, cement, and concrete are the same. At most, even a 100% loading of cement paste in a TRU site does not exceed large-scale off-gas capacities. Concrete, which is more common than cement paste, can only comprise <10% of the off gas to maintain hood vacuum.

Large concrete structures (e.g., trench caps, cribs, large industrial waste boxes) are common in TRU waste sites. Concrete is more conductive than unmelted soil; however, an electrical short circuit is not possible during ISV if the concrete occupies a large portion of the space between electrodes, because the molten soil is much more conductive than concrete.

The vitrification of ceramic materials is not expected to limit the process significantly. The high melting points and refractory nature of most ceramics may prevent them from completely melting or dissolving. To determine the degree of encapsulation in the melt, alumina and zirconia bricks were included in PSFT-3. Visual inspection of the glass after vitrification revealed a high degree of ceramic encapsulation with minimal surrounding void space.

Combustibles (Dry Active Wastes)

During ISV of a waste site, any solid combustible inclusions within the soil are pyrolyzed into combustible gases at the high temperatures of the melt. The pyrolysis gases move upward through the molten zone, expanding as they are heated. Combustion does not occur until the pyrolyzed gases contact air at the surface of the molten soil, since the molten glass is reducing in nature. With a cold cap or an insulated surface, the release of gases occurs primarily near the electrodes, because the glass is hotter and has a lower viscosity in the areas of highest current density. When a cold cap is not present, release of gases is more uniform over the molten surface. Several effects of these gas releases must be considered in establishing the design of the hood and off-gas system:

- Pyrolysis gases carry with them to the off-gas system a portion of radionuclide elements associated with the combustible waste. (Note

that only the contaminants associated with the combustibles are available for release--those already incorporated in the melt remain in the vitreous mass.)

- The protective, subsided cold cap may be broken up by active gas releases, thereby increasing heat losses and hood temperatures.
- Pyrolysis gases that are superheated in the molten zone burn in the hood plenum, thereby creating high temperatures in the hood and increasing the heat removal requirements of the off-gas system.
- The gas generation rate of buried combustibles and the air required to combust the gases determine the maximum off-gas flow rate required for that application.

The magnitude of the effects of the gas releases is directly proportional to the rate at which pyrolyzed gases are generated and released. Engineering-scale and pilot-scale tests have shown that combustible gas release is sporadic and may occur in a very short time period. During ESLT-11, 0.2 kg of simulated combustible waste was placed inside a metal canister. Active surface combustion of the pyrolyzed gases occurred over an 18-min period during the 12-h test. Thus the release period was only 2.5% of the total ISV time. Similar observations have been made during the pilot-scale tests.

For example, PSFT-3 was conducted to evaluate ISV performance with a 208-L (55-gal) metal drum containing simulated combustible waste and soil buried between electrodes. Figure 68 illustrates the simulated waste drum placement, and Table 30 gives the waste composition. When the molten soil first contacted the waste drum, rapid venting of pyrolyzed gases and carbonaceous particulate occurred for about 30 minutes. The off-gas particle loading, which was high during this period, reached 3600 mg/m^3. Slower ventings that lasted for 15 to 30 minutes each occurred at two other times later in the test. The ISV process was operated for 38 hours; however, most pyrolysis gas venting took place over a period of about 1 hour (2.6% of the total ISV time).

The large-scale off-gas system capacity of 104 std m^3/min is sufficient to contain combustion gas releases from a variety of waste configurations. Assuming an inverse exponential release rate of combustible gases over 30 minutes

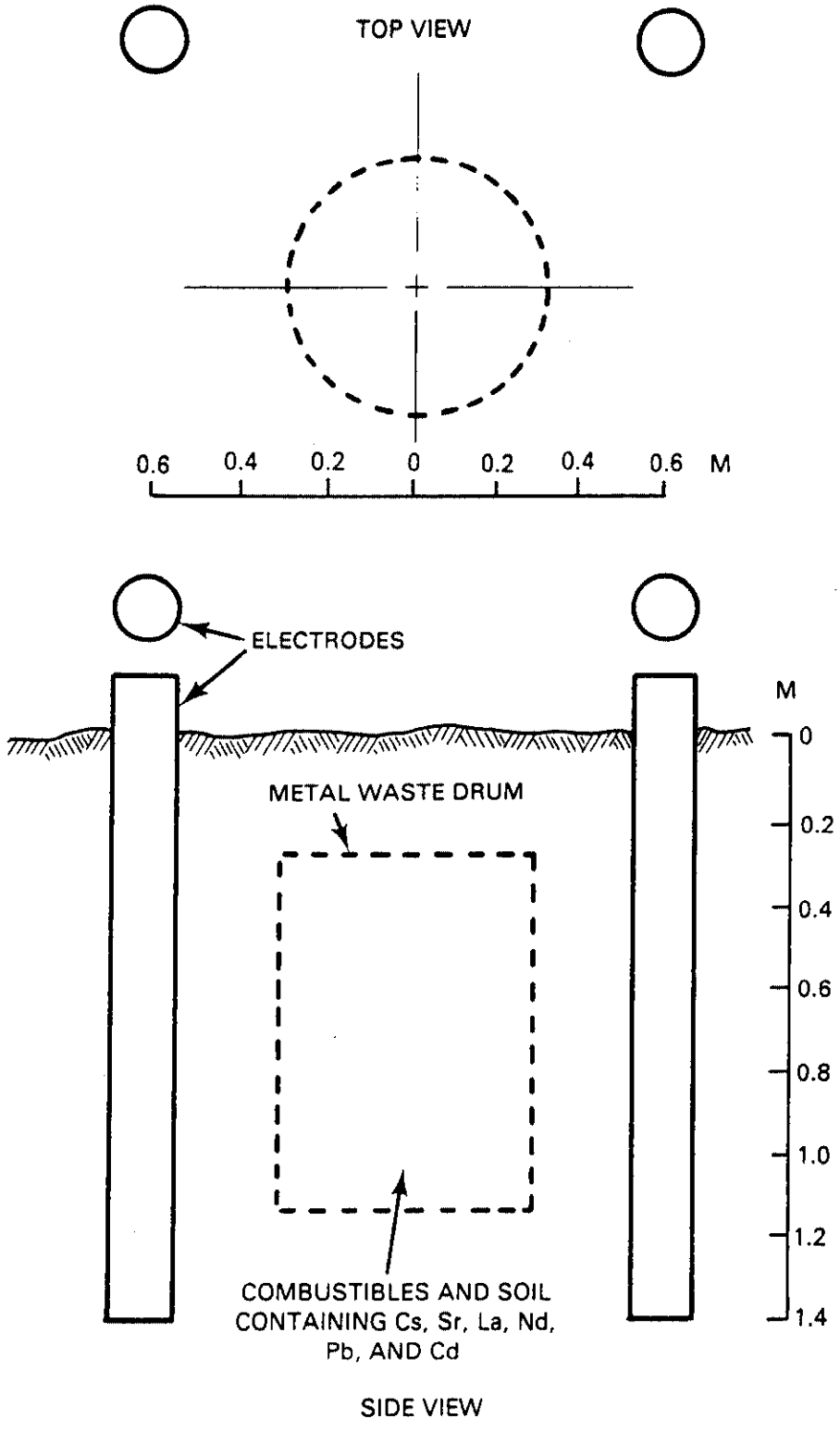

FIGURE 68. Simulated Waste Configuration for PSFT-3

TABLE 30. Waste Drum Combustibles Content During PSFT-3

Material	Weight, kg	Weight %
Paper	16.9	44.0
PVC	4.5	11.7
Polyethylene	4.5	11.7
Neopyrene	3.2	8.3
Polypropylene	2.3	6.0
Cotton	2.3	6.0
Buna rubber	1.8	4.7
Hydraulic oil	1.1	2.9
Ion exchange resin	0.91	2.4
Teflon	0.91	2.4
TOTAL	38.4	100

(based on engineering- and pilot-scale tests), the large-scale system is able to contain gas released from combustible volumes typical of that shown in Figure 69, when molten soil contacts them. Pyrolyzed gases from combustible volumes as large as 0.9 m^3 can be contained without losing hood vacuum while continually supplying 20% excess combustion air to burn the gases as they are released. Likewise, a combustible volume of >3 m^3 would be contained before

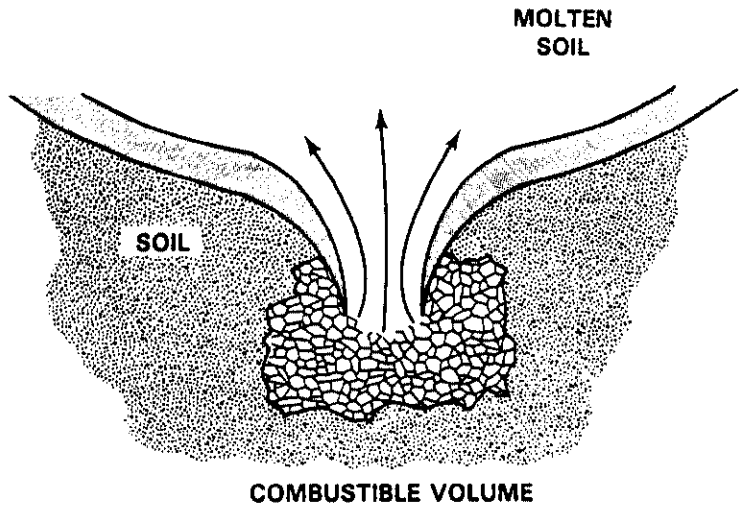

FIGURE 69. Gas Release from a Combustible Volume

hood vacuum is lost if combustion air is not supplied. The same off-gas system is capable of containing the gases generated from a void volume of 4.3 m^3; this assumes a design factor of two and the gases are released uniformly over a 5-s period as molten glass rapidly fills the void volume (see Figure 70). For homogeneous mixtures of combustibles and as little as 30 vol% soil, the large-scale off-gas system is capable of providing 20% excess combustion air and containing combustion gas from 3200 kg combustibles for every meter of depth being vitrified per setting. The predicted performance of the process under these types of conditions is also based on a design factor of two.

Wet Industrial Sludge

The process is applicable to wet industrial sludges with moisture content up to 70%. Solidification of 10,000 kg of an industrial sludge heavily laden with zirconia and lime has been successfully demonstrated by the pilot-scale ISV process (Buelt and Freim 1986). The process destroys organic constituents, fixes heavy metal and radioactive components, and drastically reduces Rn emanation from Ra sources in the sludge. As a result, the vitrified sludge can be disposed of in a smaller area in a form that is unlikely to require further treatment for environmental protection. The successful test constituted the first adaptation of the ISV process to nonsoil applications.

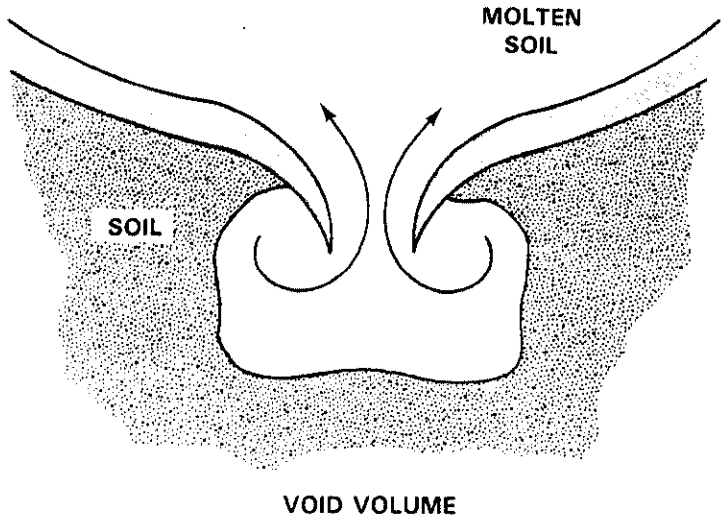

FIGURE 70. Gas Release from a Void Volume

The objective of this study was to determine the feasibility of applying ISV to a specific industrial sludge by performing tests using the bench-scale and pilot-scale equipment. The study not only verified the adaptability of the process, but provided extensive data on the characteristics of the gaseous effluents that emerge from the vitreous sludge during processing.

The basis for conducting the pilot-scale demonstration was established by the success of the bench-scale feasibility test. The bench-scale vitrification test, which was the first stage of this study, greatly reduced the mass and volume of the sludge to 30% and 15% of the original, respectively. The encouraging test results led to the decision to test the process on a more representative scale, the pilot-scale unit.

The pilot-scale ISV system was used to process 8.9 m^3 of sludge in three days. A schematic of the pilot-scale test setup is shown in Figure 71. The process successfully melted the sludge to a depth of 3.0 m, significantly reducing its volume and driving moisture and associated process effluents from the sludge.

Because of the extensive consolidation of the sludge achieved during initial startup attempts, soil and soda ash were added to the sludge surface to achieve successful process startup. The presence of the soil added to the surface of the sludge accounts for 83% of the final vitrified volume as determined by ion-coupled plasma analysis of the vitrified material. The final block volume, as determined by physical measurements, is one third of the original volume of the sludge. In other words, the process attained an effective volume-reduction factor of 3.2, even with the added soil and soda ash. Discounting the molten soil volume, the maximum achievable volume reduction of the sludge would have been 18. The pilot-scale test revealed no detrimental processing behavior as more sludge was incorporated. Therefore, we can conclude that an indefinite amount of sludge can be incorporated into the vitreous mass once startup is attained, and the higher volume-reduction value can be achieved.

The analytical data revealed low concentrations of fluorides, chlorides, and sulfur in the form of SO_x and H_2S during the pilot-scale demonstration. Measured H_2S concentrations in the off gas were only a fraction of SO_2

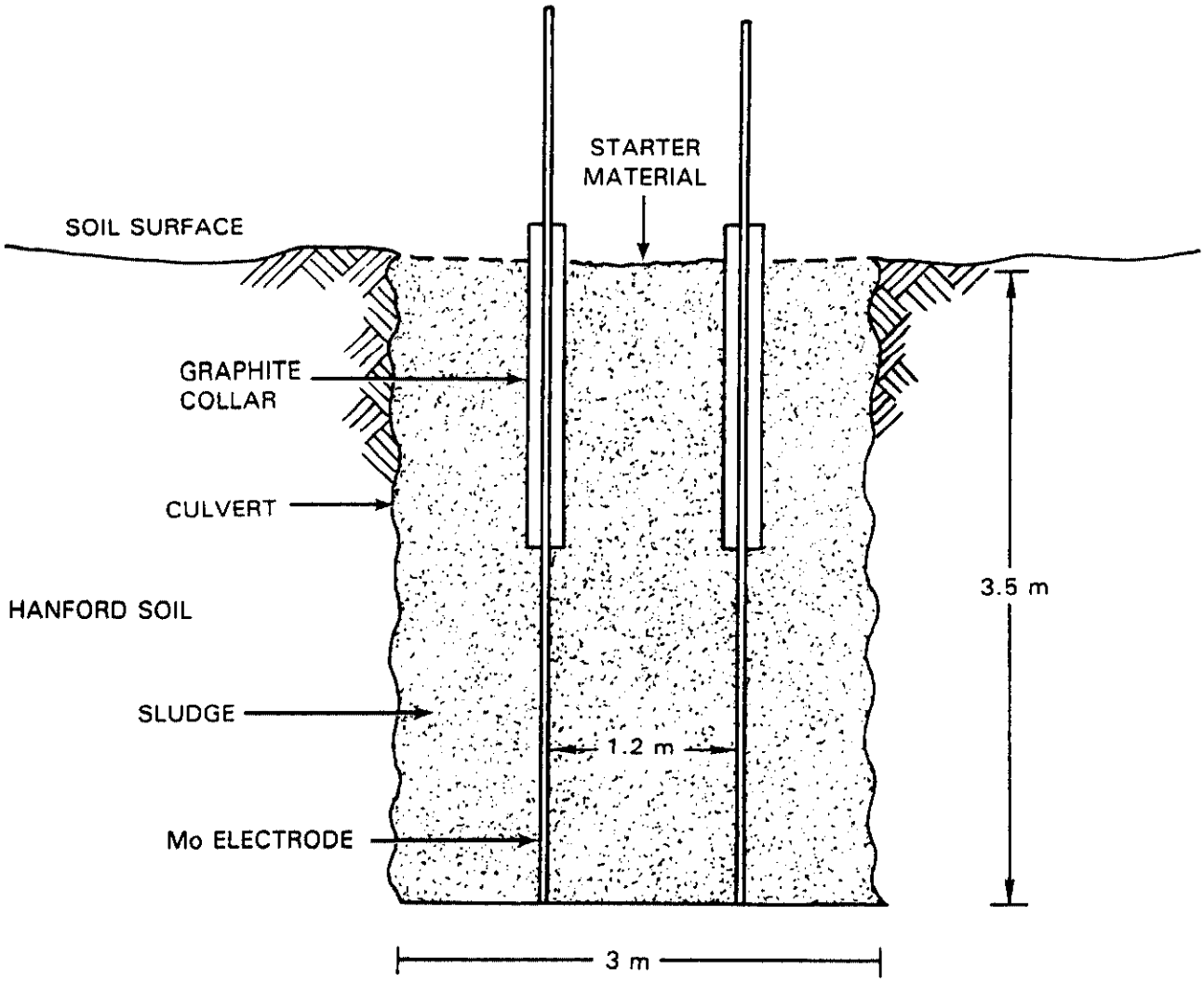

FIGURE 71. Buried Culvert with Zirconia/Lime Sludge

concentrations and were always below the threshold limit value of 10 ppm for direct worker exposure (American Conference of Governmental Industrial Hygienists 1984). The maximum SO_2 concentration in the off gas was 66 ppm, which is far below maximum permissible atmospheric emissions of 1000 ppm established by local government agencies (Washington Administrative Code). Even though the retention of fluorides and chlorides in the vitrified product was between 85 and 99% during processing, the percentage that volatilized from the melt resulted in condensate concentrations ranging from 400 to 8300 ppm. Because of dilution due to air inleakage into the hood, however, the maximum concentration

of chloride in the off gas was 15 ppm, which occurred during the initial startup phase. The concentration of chloride in the off gas decreased tenfold when soil was used to achieve startup. The additional soil increases the depth of sludge being vitrified, which improves retention of semivolatile components, as described earlier. Although fluoride was not detectable in the sampling system solutions to determine its concentration in the off gas, its concentration is expected to be similar to that of chloride. The only detectable concentration of NO_x in the off-gas effluents occurred during the initial startup phase without soil addition. Again, its concentration can be reduced as demonstrated in the pilot-scale demonstration by the use of soil during startup. The larger vitreous mass associated with the soil provides longer contact time for improved retention of F, Cl, and S and improved destruction of nitrates and organics.

Aside from the waste form characteristics described previously, the glass and crystalline material produced by the process also fixes Rn-generating isotopes in the sludge, namely ^{226}Ra, into its structure. This will reduce Ra emanation from the vitrified sludge by a factor of more than 10^3 when compared to natural sludge. Although Rn-emanation power from the sludge vitrified in this study was not determined, similar studies with uranium mill tailings with much higher Ra concentrations showed that the diffusible Rn was reduced from 9% to 0.003%.

Hazardous Organics

The ISV process has been evaluated for potential application to soils contaminated with hazardous organics, such as PCBs. An engineering-scale ISV test with PCB-contaminated soil has been successfully performed for the Electric Power Research Institute (EPRI) to determine the fate of PCBs and their byproducts when the process is applied (Timmerman 1986).

The EPRI PCB test was performed using the engineering-scale ISV system equipped with an off-gas hood to maintain the process under a slight vacuum. Loamy-clay type soil containing 500 ppm PCBs was placed in a 20-cm-dia (8-in.-dia) by 30-cm (1-ft) deep zone beginning at the 25-cm depth between the four Mo electrodes. Figure 72 shows the configuration of the engineering-scale ISV system during the EPRI PCB test. The test was performed over a 6-h period,

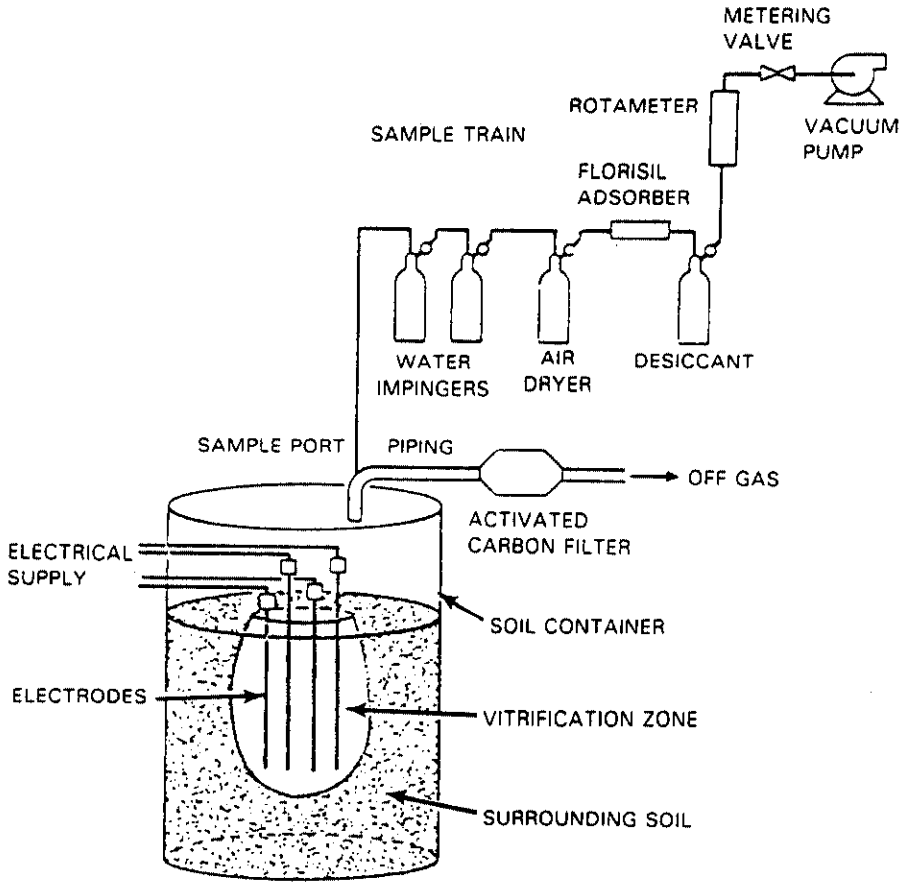

FIGURE 72. Engineering-Scale ISV System and Sample Locations for the EPRI PCB Test

achieved a depth of 81 cm (32 in.), and produced a vitrified 0.14-m^3 (5-ft^3) block that weighed 220 kg (480 lb). No operational problems were encountered during the test, and on-line grab sampling for Cl and HCl revealed less than detectable quantities (<0.33 ppm and <0.2 ppm respectively). For safety and environmental control, a dual-stage activated carbon filter was used to contain any PCBs released to the off-gas system.

Samples collected to analyze ISV processing effects on PCBs included: 1) off-gas emissions, 2) residues in off-gas lines and containment equipment, 3) migration to the soil surrounding the block, and 4) the residual level in the vitrified block. Data from off-gas release and soil container smears provided the most quantitative values on the release from the melt during and

after processing. Information collected from the florisil adsorption tubes and the smear sample extractions indicated a 4.2 mg total off-gas emission, 1.1 mg of which was deposited on container surfaces. These off-gas releases account for 0.05 wt% of the initial PCB quantity, corresponding to a greater than 99.9% thermal DRE for the ISV process. This calculation does not account for the removal efficiency of the off-gas system; therefore, a system DRE cannot be calculated from the available data. Activated carbon filters can effectively contain any of these off-gas emissions, however, to achieve an overall DRE of greater than 99.9999%.

The analysis of florisil also indicated a small amount furan (PCDF) and dioxin (PCDD) generated in total quantities of 0.4 μg and 0.1 μg, respectively. The PCDF was detected only in the tetra and penta isomers, while the PCDD was detected only in the hepta and octa isomers. However, these small quantities are less than the reported amounts typically generated by a PCB fire and do not represent a hazardous operational concern.

Sampling of the vitrified mass showed no detectable residual level of PCBs, which is to be expected considering the high processing temperatures. Also, no PCB contamination was detected in the majority of soil surrounding the vitrified block, indicating that migration outside the vitrification zone was not a significant problem. A few samples directly adjacent to the block contained measurable concentrations up to 0.7 ppm. These initial test data indicate that the vitrification rate is higher than the diffusion rate of volatilized PCBs in soil, thus overcoming migration away from the hot molten mass.

Sealed Containers

Gas may be released rapidly from a sealed container in soil that is being vitrified. Containers holding combustibles can build up pressure, and when they are breached, release that pressure, with gases escaping to the hood over a very short time period (approximately two seconds).

In some cases after the container is breached, it may reseal itself. As shown in Figure 73, the impervious, fused soil layer that borders the vitreous soil becomes sealed to the metal container. Since the melting temperature of most steels is near 1400°C and the temperature of the partially fused zone is

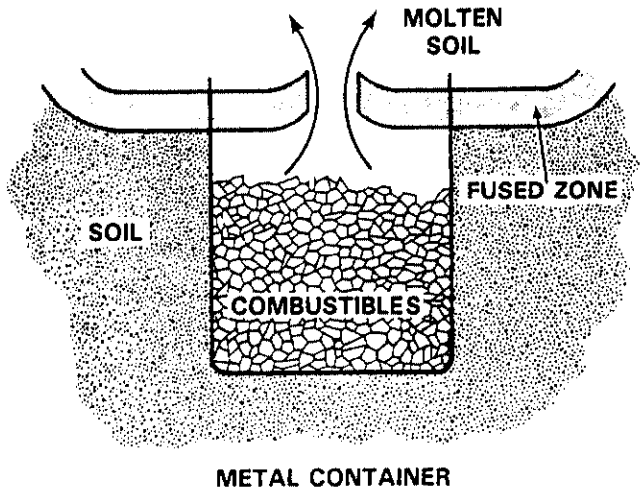

FIGURE 73. Gas Release from a Sealed Metal Container

1100°C, the metal container can protrude into the fused zone, trapping the gases inside the container. However at these temperatures, the strength of the container will be reduced substantially. When enough pressure is built up, it is postulated that the fused zone cracks, releasing gases into the hood.

Theoretical gas releases have been calculated for various geometries of sealed metal containers to determine the maximum gas release rate after the fused zone has been breached. Table 31 shows a greater release rate with a 19-L (5-gal) bucket than with a 208-L (55-gal) drum. This is because greater pressure is required to breach the fused zone over the narrower gap between the metal sides of a 19-L bucket, resulting in a higher burst pressure and a greater gas release rate.

TABLE 31. Calculated Release Rates from Sealed Metal Containers

Container	Dia, m	Burst Pressure, atm	Max. Gas Release Rate, std m^3/min
19-L (5-gal) bucket	0.27	25	64
34-L (10-gal) bucket	0.27	25	64
208-L (55-gal) drum	0.56	6	35

Actual test data indicate that during ISV pressure containers will fail at pressures far below their atmospheric burst pressure. For example, an aerosol can that was pressurized to over 300 psi before failure in air, failed at 7.6 psi during ESLT-20. When filled with 50 mL of water, the aerosol can reached a peak pressure of only 24.5 psi before failing during ESLT-21. To investigate the depressurization characteristics of a high integrity container, a 5-m-dia (2-in.-dia) by 30-cm-long (1-ft-long) Schedule 10 pipe with plates welded to the ends was vitrified during PSCT-4. The high integrity container had 17 mL of trichlorothylene as a simulated hazardous waste gas generator. The depressurization of the container was anticlimatic, occurring over about a 10-min period. Figure 74 shows the depressurization curve. The depressurization half-life during this test was higher than expected at about two minutes. The fact that actual burst pressures are much less than calculated for large-scale design adds to the conservatism and safety factor of the large-scale system when vitrifying through sealed containers.

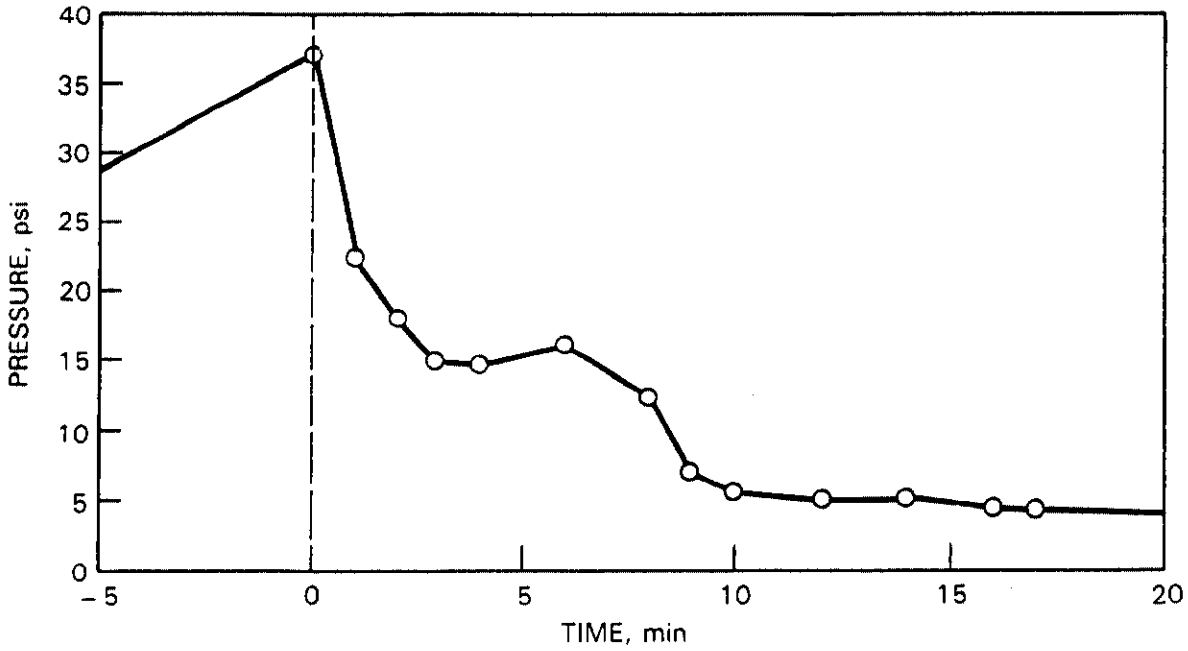

FIGURE 74. Depressurization Characteristics of a High Integrity Container During PSCT-4

Sealed containers that do not contain combustibles can also release pressurized gases when breached. During PSCT-1, a rapid (two- to five-second) release of gases exceeding hood vacuum was observed on three occasions from a 19-L (5-gal) metal bucket containing 60 kg of chemicals in nitrate form. Containers of material with a high moisture content can also release water vapor rapidly. The 220°C isotherm, which precedes the vitreous zone by ~25 cm, can vaporize vaporize water at 25 atm pressure. When the container is breached, the water vapor can create a gas release that is comparable to the releases listed in Table 31.

Note, however, that the maximum postulated gas release is well within the maximum design capacity of the large-scale off-gas system of 104 std m^3/min. Therefore, as long as the combustible or void volumes inside the sealed containers meet the criteria outlined in the previous section, the ISV process is designed to accommodate such releases. Even though sealed containers limit the applicability of the pilot-scale off-gas system, their presence does not hamper the operation of the large-scale system.

Explosives

The partial or full detonation of chemicals during ISV can result in the same undesirable effects listed previously in the section on combustibles. These effects may be more pronounced because the chemical structures of explosives, which include oxidizers, cause them to react much faster. Explosives may exist as inclusions, as homogeneous mixtures within soil, as chemicals within a waste container, or as military ordnance items. The probability of buried military-grade explosives in TRU waste sites is extremely small; chemical mixtures such as organics and nitrates are more likely.

Conditions that would nitrate organic wastes such as cotton rags by nitric acid are very unlikely at a waste site. To achieve a significant degree of nitration, a hydrophilic agent such as sulfuric acid must be present since the final degree of nitration is strongly dependent on the final water concentration equilibrium (Chedin, Tribot, and Feneant 1948; Doree 1933; Ott et al. 1947). Without such an agent, less than one-third of the hydroxide sites on cotton can become nitrated, even when concentrated 72% nitric acid is present.

The burial of military explosives would be in violation of the U.S. Army AMC Regulation Safety Manual (U.S. Army 1970), which states that collected explosives and chemical wastes must not be disposed of by being buried. The U.S. military organizations dispose of surplus explosives by burning. Nevertheless, even though it would be very poor practice to bury surplus bulk explosives with radioactive waste, the possibility exists. An analysis was performed to determine the effects of ISV on explosive inclusions and mixtures within the waste, using military-grade explosives as the worst case. Descriptions of these explosives are given in Military Explosives, U.S. Army Manual TM 9-1300-214 (U.S. Army 1967).

The hazards associated with the excavation, transportation, and incineration of dry humus soil contaminated with TNT and/or RDX have been assessed by Kirshenbaum (1982). Explosive/soil mixtures were subjected to impact, friction, electrostatic shock, and flame sensitivity tests. Contaminated soil mixtures from the Alabama Army Ammunition Plant, Umatilla Army Depot, Louisiana Army Ammunition Plant, and Savannah Army Depot were also assessed. Kirshenbaum determined that soil containing up to 25 wt% TNT and/or RDX can be excavated, transported, and incinerated safely. Soil containing >10 wt% of the explosives is thermally reactive, which indicates that such mixtures unconfined could burn when heated to 175 to 200°C. This would indicate that soil containing a homogeneous distribution of >10 wt% up to 25 wt% explosives will behave similarly to other combustible waste sites and can be vitrified safely.

Explosives can partially or fully detonate by three mechanisms: 1) self-heating when held at or above a minimum critical temperature for a period of time; 2) rapid heating of an encased or confined explosive; and 3) pressurization caused by an impact or shock wave.

The minimum critical temperature for detonation depends upon the composition, size, and concentration of an explosive. As shown in Figure 75, when the diameter of a specific explosive increases, the critical temperature decreases (Dobratz 1981). Dilution of an explosive with soil will increase the critical temperature or the size of explosive required for an explosion at a given temperature.

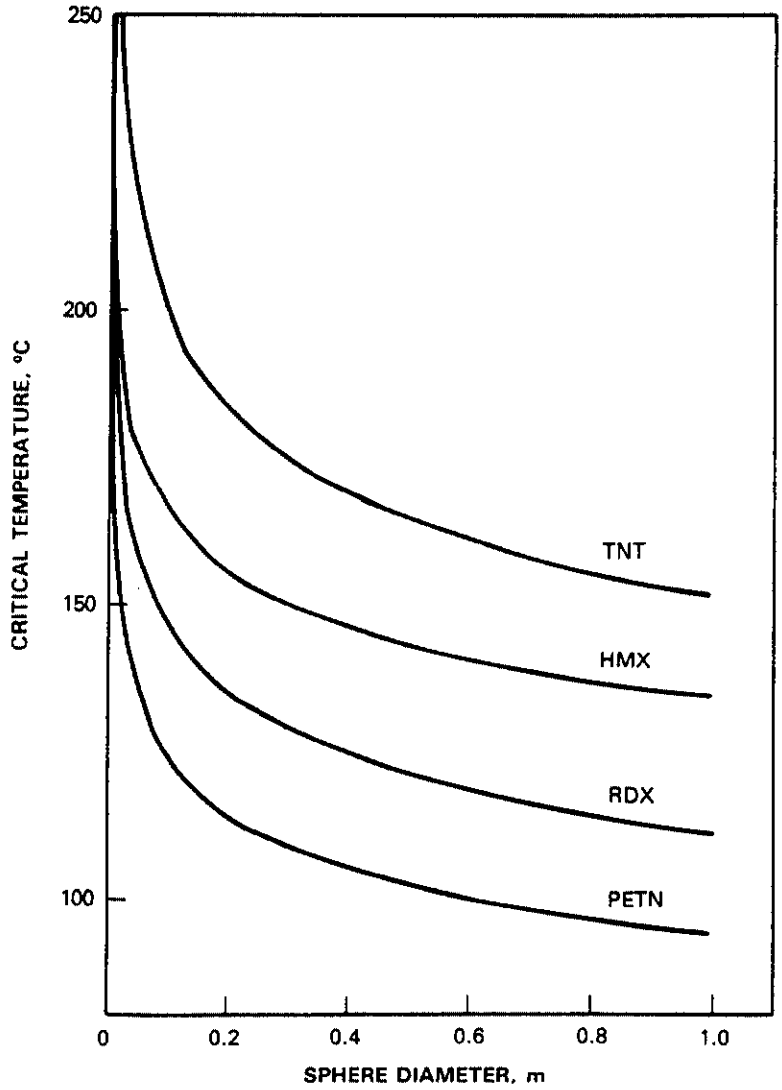

FIGURE 75. The Effect of Charge Diameters on Critical Temperatures for Some Pure Explosives (Dobratz 1981)

High explosives, which include ammonium nitrate, ammonium perchlorate, Composition A, Composition B, H-6, HMX, lead azide, lead styphnate, NC, Pentolite, PETN, picric acid, RDX, Tetryl, and TNT, will decompose completely at temperatures <400°C (Dobratz 1981). All these explosives typically melt 80 to 200°C below their decomposition temperatures. During ISV, soil below the advancing molten zone is heated to 100°C, where it remains until all moisture has evaporated (approximately two hours). Once dry, the soil heats at a rapid

rate of ~10°C/min until it fuses into the molten zone. At this heating rate, explosive inclusions that are not contained would melt, soak into the surrounding soil, and decompose rather than self-heat to a detonation. Unmelted explosives with a critical temperature of <100°C could detonate during the time that the soil moisture is evaporating. Thus the probability of a detonation within a disposal site is reduced significantly if the explosive has a critical temperature >100°C. Even a moderately stable explosive such as PETN will not have a critical temperature as low as 100°C unless the charge is greater than 0.6 m dia. The probability of such an inclusion is extremely small. Contained explosives located to the side of the ISV melt zone, however, could soak for a sufficient time above the critical temperature to cause a detonation.

Off gases produced by the decomposition or detonation of explosives such as TNT or HMX are not toxic because they are mostly N_2, NO_x, H_2O, CO_2, and CO, which can be easily treated by conventional off-gas equipment. An alkaline soil will act to absorb some of the nitric oxides. The gas volume generated by TNT and HMX ranges from 0.65 to 0.80 m^3/kg of explosive.

Intact ordnance items present a more serious detonation potential. Bombs and shells explode in a few minutes in a fuel fire, usually showing partial, if not full, detonation. Full or partial detonation of a 225-kg bomb in a shallow land burial trench would almost certainly breach the surface. For an ISV soil heating rate of 10°C/min, a high-integrity ordnance item would explode before the soil around it was fused; therefore, both soil particles and molten glass would be ejected from the trench. Ordnance items that are touching or that are within a critical distance apart will also undergo sympathetic detonation due to shock pressurization.

All possible explosives have not been evaluated, so the general safety of processing pure explosives and explosive/soil mixtures by ISV has not been fully established. Additional work is recommended to adequately address limitations to vitrifying soil that contains explosive chemical mixtures. It can be stated that without proper precautions, ISV should not be applied to sites that contain or have the potential of containing intact ordnance items.

Criticality

Transuranic radionuclides that emit neutrons may reach criticality if they are sufficiently concentrated or if the moderation properties of the waste site become suitably altered. Because ISV changes the physical and chemical nature of the waste, the potential for criticality was evaluated.

Transuranic elements capable of sustaining a nuclear chain reaction that are common to waste sites are listed in Table 32 with their estimated subcritical mass limits (ANSI 1975; ANSI 1982; Clayton 1979). Table 33 shows the radionuclide content of TRU waste that is buried at Hanford and INEL. The mass of the TRU elements that are buried at these two sites accounts for 96% of all buried TRU elements in the United States (U.S. DOE 1985). Since ^{239}Pu accounts for the greatest fraction of fissionable radionuclides at TRU waste sites, and also has one of the similar subcritical mass limits, the criticality analysis presented in this section is based on the effects of ISV on this isotope.

TABLE 32. Estimated Subcritical Mass Limits for Various TRU Nuclides

Radionuclides[b]	Subcritical Mass Limit,[a] kg (as metal)	
	Water Reflector	Steel Reflector
^{233}U	7	--
^{237}Np	30	20
^{238}Pu	4	3
^{239}Pu	5	--
^{240}Pu	20	15
^{241}Pu	6	--
^{242}Pu	60	40
^{241}Am	24	16

(a) Assumes spherical geometries and optimal moderation (ANS 1975; ANS 1982; Clayton 1979).
(b) Those found in significant quantities in TRU waste.

TABLE 33. Radionuclide Concentration of Buried TRU Waste at Hanford and INEL[a]

Isotope	Hanford %	INEL %
^{238}Pu	0.01	0.008
^{239}Pu	93.89	90.42
^{240}Pu	5.74	5.65
^{241}Pu	0.34	0.00
^{242}Pu	0.02	0.002
^{241}Am	0.00	3.90

(a) U.S. DOE 1985.

An important factor affecting the criticality potential of TRU waste trenches during ISV is the amount and degree of neutron-absorbing and neutron-reflecting material near the fissionable material. It is known that during ISV at least four changes occur that might cause changes in the neutron reflection/absorption properties of the waste site:

- Soil densifies and becomes glasslike.
- Organics and combustibles pyrolyze and are released from the melt.
- Water evaporates out of the melt area.
- Metal melts and settles to the bottom of the melt zone, leaving most of the vitrified area free of metal.

Critical limits have been calculated for Hanford soil that contains Pu (Ridgway and Carter 1972). These calculations were for soil with 30 and 40 vol% void space containing Pu and water within the void. The minimum critical mass is that mass of Pu that is required to reach a critical configuration under optimal conditions, and is greater than the subcritical mass limit discussed earlier. The minimum critical area concentration is the minimum Pu mass per unit area in an infinite slab that is required to achieve criticality, assuming a homogeneous Pu distribution within a slab of optimal thickness.

The minimum critical mass for Pu (97 wt% ^{239}Pu and 3 wt% ^{240}Pu) in soil that is fully saturated with water is given in Table 34 for three different degrees of reflection. Water-saturated soil is assumed as a worst case since the minimum critical mass is smallest when fully reflected. All of the minimum critical masses occur in the Pu concentration range of 10 to 20 kg/m^3. As a conservative measure, the minimum critical mass in Hanford soil is assumed to be 1.7 kg, the value for 40% void space and full water reflection.

The melting process during ISV actually causes the ^{239}Pu minimum critical mass to increase because water is removed. Once the moisture has evaporated, the minimum critical mass increases to that of a dry sphere of PuO_2. The subcritical limit for an oxide sphere is 10.2 kg Pu (11.5 kg as oxide). This value is for water-reflected oxide spheres at optimum conditions.

The minimum critical areal concentration for Pu in Hanford soil is about 2.9 kg/m^2 for full water reflection. The concentration at which this occurs is about 8 kg/m^3 for an infinite slab about 36-cm thick. As a conservative measure, the recommended operational limits of ISV at sites containing Pu are set at one third the critical limits. A waste site should be capable of vitrification if it has an areal Pu concentration of <1.0 kg/m^2 (33% of the 2.9 kg/m^2 critical areal concentration) with no mechanisms of lateral concentration, or if it contains a total Pu mass <0.6 kg (33% of the 1.7 kg minimum critical mass).

TABLE 34. Minimum Critical Mass of Plutonium in Water-Saturated Soil

Reflection	Minimum Critical Mass, kg Pu[(a)]	
	30 Vol% Soil Void	40 Vol% Soil Void
Unreflected	4.1	3.0
2.54 cm water	3.2	2.3
Full water reflected	2.4	1.7

(a) 97 wt% ^{239}Pu (Ridgway and Carter 1972).

When fissile and organic materials densify prior to combustible decomposition, their potential for criticality increases. Plutonium has a smaller minimum critical mass when moderated by materials with higher H densities than water. In particular, polyethylene as a moderator results in a minimum critical mass of 0.36 kg (Thompson 1977). Both polyethylene and polypropylene are commonly discarded in TRU waste as bags, gloves, bottles, etc. Normal storage of these items results in a low moderator density in waste containers and packages. Heating during ISV may cause these materials to melt and collect in a more dense form at the bottom of the waste container. The potential result is a near-optimum distribution of Pu in the organic moderator before the ISV process can decompose these materials and drive off the H. This phenomenon, although highly unlikely, could occur at temperatures under 300°C. The minimum critical areal concentration for Pu decreases to 2.4 kg/m^2 for a polyethylene reflected system. The safe ISV operating limit becomes 0.8 kg/m^2 (33% of 2.4 kg/m^2) when large quantities of hydrogenated organics like polyethylene are present in drums or other waste containers.

Mechanisms for Plutonium Concentration

Plutonium concentration mechanisms become important if the areal Pu concentration limits listed in the previous section are exceeded. Several mechanisms have been identified and evaluated:

- Various TRU radionuclides in ISV glass may become insoluble, allowing some fissionable material to settle out of the molten glass.
- Dense TRU oxide particles may settle to the melt bottom.
- Reducing conditions in the molten zone may reduce some fissionable compounds to their metallic state and subsequently cause them to settle at the melt bottom in a more concentrated form.

Although Pu may enter the waste site as a sulfate, nitrate, hydroxide, halide, or carbonate, most Pu in TRU waste is converted to an oxide during ISV heating because plutonium oxides are highly stable. Plutonium (IV) silicate is also very stable; e.g., if any PuO_2 reaction occurs during ISV, it will be to incorporate the Pu into the silicate matrix.

Reduction of Pu from the oxide to the metallic form during ISV is not thermodynamically favorable. An examination of the standard free energy of formation of various oxides as a function of temperature (see Figure 76) shows that both U and Pu are highly electropositive metals with stable oxide forms. This is usually the case with other actinide elements as well. Other major oxides in the soil (including Fe_2O_3, SiO_2, and Al_2O_3) are thermodynamically more likely to be reduced to their elemental forms than PuO_2 or UO_3.

Based on known PuO_2 solubilities in HLW glasses, solubility limits are not expected to be exceeded during ISV of any TRU waste site. High-level waste glasses, which are very similar to ISV glass, have recorded PuO_2 solubilities higher than 2% (Scheffler et al. 1977). This solubility limit is over 10 times greater than the highest Pu concentration at any TRU-contaminated soil site, with the exception of two or three reverse wells at Hanford.

The thorough convective mixing that is characteristic of ISV is expected to dilute any zones of high Pu concentration, further reducing the potential for a criticality. This was verified in actual ISV tests where simulated waste material was spiked with rare earth elements (Ce, La, and Nd), which are expected to behave similarly to Pu. An example of a typical distribution pattern is provided in Figure 76. This sampling information illustrates that Ce became uniformly distributed laterally throughout the block. This uniform distribution of the rare earths suggests that actinides such as Pu would not migrate. The distribution of Ce and other elements aids in dispelling the concerns about selective migration effects.

Concentration by settling of undissolved PuO_2 during ISV is considered unlikely for two basic reasons: 1) the ISV melt advances at a very slow rate, <10 cm/h, so that any PuO_2 in the upper part of the melt will have a long time to dissolve before it can concentrate in significant amounts with PuO_2 deeper in the waste site; and 2) PuO_2 is typically a fine powder that, even if it remained undissolved, will become thoroughly mixed within the glass by the characteristically strong convective currents.

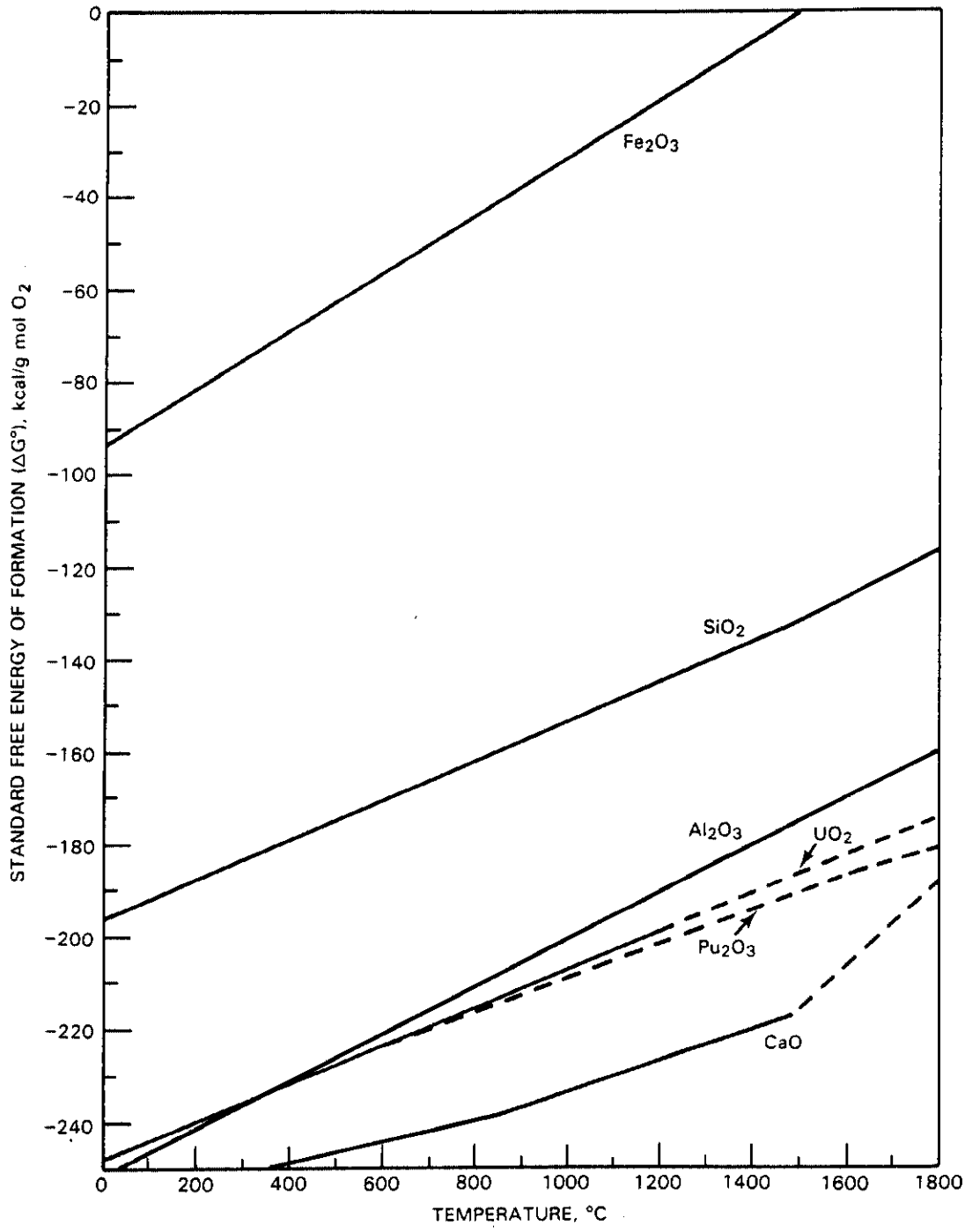

FIGURE 76. Standard Free Energy of Formation for Various Metal Oxides

ECONOMIC ANALYSIS

ECONOMIC ANALYSIS

This section presents an economic analysis of ISV based on a large-scale system at a typical site with a contaminated zone that is 90-m long x 30-m wide x 5-m deep. [A previous study (Oma et al. 1983) showed the scaling and economic efficiency of the large-scale system compared to other smaller scale systems.] The economic analysis compares the costs of vitrifying three specific wastes with various processing factors. The three wastes are TRU-contaminated soil, soil contaminated with hazardous chemicals, and wet industrial sludge. The processing factors include the effects of soil moisture contents of 5 and 25% and power and labor rates, etc.

The waste types and processing factors were combined to derive four configurations for comparison of the differences between radioactive and hazardous chemical waste operational costs and the effect of soil moisture content on processing costs. The four configurations are:

- radioactive waste in soil that has a 5% moisture content
- radioactive waste in soil that has a 25% moisture content
- hazardous chemical waste in soil that has a 5% moisture content
- hazardous chemical waste in soil that has a 25% moisture content.

Each ISV configuration has associated costs that fall into four categories: site activities, equipment requirements, operations, and consumable supplies. Each of these cost categories and its individual components (see Table 35) are described in the appropriately titled subsections. (Some of the components are not included in the cost of every configuration.)[a]

Additional subsections discuss the financing consequences of federal and commercial ownership of ISV equipment and present the cost estimates associated with implementing each of the four configurations. The costs are summarized and compared in tabular form. A wet industrial sludge test is reviewed briefly.

(a) For example, each configuration would require either power lines from the nearest source or a portable generator, but not both.

TABLE 35. Major Components of the ISV Costs

Site Activities	Equipment
Transporting equipment to and from site	Power
Clearing vegetation	Portable generator
Rough grading	Power lines
Removing overburden	Substation
Acquiring and applying backfill material	Power cables
Operations	Mechanical
Process preparations	Electrode frame and hood
Drill holes and place electrodes	Drilling machinery
Spread graphite starter material	Crane
Position frame and hood, secure electrodes	Front-end loader
Connect power cables and off-gas line	Off-Gas and monitoring
Vitrify	Off-gas treatment system
Disconnect power cables and off-gas line	Radiation and off-gas monitors/alarms
Hood fixation	**Consumable Supplies**
Remove frame and hood	Electrodes
Backfill vitrified area	Fuel
Move power cables for next setting	Electricity
Processing	
Off-gas treatment system	
Power system	
Radiation or toxic chemical monitoring	
Melt verification	
Off-gas secondary waste disposal	

SITE ACTIVITIES

Site activities include transporting equipment to and from the site, clearing vegetation, grading the ground, removing overburden, and acquiring and applying backfill material as needed (see Table 35). Soil sampling, well logging, and other activities associated with site characterization have been excluded from this analysis because of expected similarities in cost regardless of the stabilization alternative employed. Otherwise, the costs developed here represent the full cost of vitrification.

All of the configurations were analyzed on the basis that no overburden was removed. If uncontaminated overburden could be removed safely, it would always be advantageous to do so from a cost standpoint. For example, removal

of the top meter from a 2700-m^2 site would cost less than $10,000, compared to the hundreds of thousands of dollars needed for labor and power charges to vitrify the same area to a 1-m depth. In short, site activity costs will be insignificant when compared to equipment, labor, and consumable supplies, for the majority of potential ISV applications.

EQUIPMENT REQUIREMENTS

All costs associated with large-scale equipment are based on actual delivered costs escalated to 1985 dollars. Electrical equipment requirements are determined by voltage and current needs. Increased current requires increased conduction capacity, whereas increased voltage requires more insulation. At the high (4000 A) level of current required for ISV, six 750-mcm power cables that supply the secondary power through the transformer to the electrodes are required for each of the four electrodes. The primary input power is assumed to be 200 m from the nearest 13.8-kV power source. The alternative of using a portable 5-mW generator has also been investigated for remote applications and to identify an upper ceiling for power costs. The equipment costs for radioactive waste applications are identified in Table 36.

Three pieces of heavy equipment are necessary for ISV operations: a drilling or augering machine for placing the electrodes in the ground, a crane for transporting the electrode frame and hood from one setting to the next, and a front-end loader for backfilling and site preparation. Rental, rather than purchase, of this equipment was considered but dismissed because of the higher cost of renting these types of equipment (typically several hundred dollars per day) for the duration of projects that last from 9 months to 10 years. The heavy equipment costs are based on cost estimates provided by vendors. The power equipment and heavy equipment costs are itemized in Table 36.

Equipment requirements for barrier wall applications can significantly reduce the capital costs, since typically only a single-phase power controller, power cables, and an electrode support frame are necessary for most applications. These needs eliminate the most costly equipment components included in the off-gas system. Therefore, total equipment costs for barrier wall generation using ISV would be less than $500,000.

TABLE 36. Equipment Costs for a Large-Scale Radioactive Waste System

Equipment	Cost, 1985 $
Portable Generator - 4.6 smW[a]	2,300,000
Back-Up Generator - 0.75 mW	65,000
Power Line[b]	22,000
Transformer	182,000
Electrode Power Cables	18,600
Off-Gas Hood and Line	290,000
Cooling Hood and Blower	225,000
Electrode Placement Equipment	75,000
Crane	82,000
Front-End Loader	55,000
Off-Gas Equipment and Fabrication	1,735,000
Total Equipment with Line Power	3,437,000[c]
Total Equipment with Portable Power	5,628,000[c]

(a) The portable generator is only for remote service operations.
(b) Power lines are not required if a portable generator is used.
(c) Total costs include an additional 25% for design and engineering.

OPERATIONS

This section describes the manpower requirements of ISV operations. The labor-intensive nature of ISV makes the assessment of manpower requirements and wage rates a critical part of the cost analysis. The differences in cost and operational time for various soil moisture contents are examined. Process preparation and processing operations are analyzed.

Process Preparation

The time required for each setting of the electrode frame and hood is the sum of the time required to vitrify the soil to the predetermined depth plus the time required to move the off-gas equipment to the next setting. Total project time is equal to the time per setting multiplied by the number of

settings. The time per setting for the large-scale systems as a function of moisture content is shown in Table 37. The effects of moisture content on vitrification rate and operating time are evident from the vitrification time presented in Table 38. These times are calculated from the ISV model.

The number of settings depends on the dimensions of the site to be vitrified and the area vitrified per setting. This latter characteristic is a function of electrode spacing, vitrification time per setting, and acceptable allowances for overlap between vitrified blocks. Appropriate data for determining the total number of settings for the large-scale configuration are summarized in Table 37.

Personnel for process preparation (see Table 39) are required at scheduled intervals (once per setting of the off-gas containment hood). Manpower requirements were estimated for each of the process preparation activities for a large-scale system. A manpower rate was obtained for each person involved in

TABLE 37. Time Requirements for Each Setting

	Large Scale, 5-m Depth, 5% Moisture h/setting	Large Scale 5-m Depth, 25% Moisture h/setting
Vitrification	90	117
Moving equipment	16	16
Total	106	133

TABLE 38. Electrode Spacing and Vitrification Settings

Parameter	Large Scale, 5-m Depth
Electrode spacing, m	4.5
Separation between electrodes of adjacent set, m	3.0
Width vitrified per set, m	7.8
Area to be vitrified, m	90 x 30
Set matrix	4 x 12
Number of settings	48

TABLE 39. Manpower Requirements for Process Preparation

Job Classification	Manpower Rate, Man-Hours/Setting Average
Electrician	4
Laborer	34
Operator	19

ISV operations, with appropriate differentials allowed according to job class and site location. Processing personnel were classified as technicians, radiation monitors, or engineers. Process preparation personnel were classified as operators, electricians, laborers, or maintenance personnel. Manpower rates for Hanford operations reflect current costs for process preparation operations plus site work and processing operations personnel. The manpower rates cover both direct and indirect costs. Separate manpower rates were developed for process preparations and site work personnel at the generic site (Means 1981). The lower generic-site manpower rates reflect U.S. average direct-manpower costs. The manpower rates for processing operations do not vary significantly between Hanford and national averages. The rates for all of the labor categories, summarized in Table 40, were adjusted to reflect 1985 costs.

TABLE 40. Manpower Rates for In Situ Vitrification (includes indirect and overhead costs)

Job Classification	Manpower Rate, 1985 $/h	
	Hanford Site, Radioactive Waste Federal Ownership	Generic Site, Hazardous Waste Private Ownership
Electrician	45	45
Engineer	50	50
Laborer	37	37
Operator	39	39
Radiation monitoring	48	Not required
Technician	48	25
Maintenance	48	48

Processing

During the vitrification of radioactive wastes, it is estimated that two operators will be required for each shift of operation. An engineer is included on day shift as an operator (see Table 41) and to provide technical resolution of any operational problems. Maintenance and radiation monitoring personnel are included in the operations on an estimated part-time basis. The shift work and totals are provided in Table 40 and have been confirmed as reasonable through large-scale system operations.

CONSUMABLE SUPPLIES

Consumable supplies include electrodes and electrical power or fuel. The combination Mo/graphite electrodes employed for both waste types are assumed to remain in the ground and not to be reused. (Hazardous chemical waste applications may allow for reuse of the Mo core electrode, thus reducing costs even further.) The number of electrodes required for a given area is directly proportional to the number of vitrification settings. Cost data for both Mo and graphite electrodes were obtained from recent orders from manufacturing companies. Cylindrical electrode costs are proportional to the weight and length or depth of the melt. In addition to the raw material costs, there are additional costs for machining the electrode ends and joining the 1.8-m (6-ft) segments of longer electrodes with connectors. Both the material and machining costs are included in per length costs identified in the tables that follow.

TABLE 41. Labor Estimate for Processing Operations at a Radioactive Site

Job Classification	Workers Per Shift			Total Man-Hours/Day
	Day	Swing	Graveyard	
Engineer	1	0	0	1
Maintenance	0.5	0	0	0.5
Operator (Technician)	1	2	2	5
Radiation monitor[(a)]	0.25	0.25	0.25	0.75
Total				7.25

(a) Radiation monitoring personnel would not be required for a hazardous waste site.

Electrical power requirements are a significant portion of the operating cost, whether local or portable power is used. Hanford power costs roughly $0.022/kWh, while the average national industrial rate is about $0.05/kWh. The cost of power from the portable generator is between $0.04 and $0.06/kWh depending on capital recovery assumptions and based on an efficiency of 0.02 L/kWh (0.07 gal/kWh) and a fuel cost of $0.09/L ($0.32/gal). The power requirements for the low (5%) and high (25%) moisture content ISV configurations are given in Table 42. Also shown is the annual vitrification rate, which is based on an 80% operating capacity of the ISV model prediction.

In addition to the electrode and energy consumption costs, a cost must be included for disposing of the secondary liquid wastes that are collected in the off-gas system. Approximately 2000 L (530 gal) per large-scale setting must be disposed of at a cost of $0.26/L ($1.00/gal). For the site configuration being analyzed, this results in additional charges of $25,000 ($1.85/m^3).

FINANCING

Federal ownership was assumed for radioactive waste operations. Financing affects the capitalized or equipment portion of ISV costs. The cost of capital equipment must be spread out over its useful life rather than attributing purchased equipment costs to any single project or year. This spreading of the capital costs is effectively handled by multiplying capital costs by the fixed-charge rate. The fixed-charge rate is a fraction, which, when multiplied by the capital investment, represents the contribution of capital costs, income taxes, and other miscellaneous costs and taxes to a uniform annualized capital cost (Stermole 1982). The fixed-charge rate is a function of the cost of

TABLE 42. Power Requirements for Vitrification Rate as a Function of Moisture Content

Moisture Content	Energy Requirement kWh/setting	Annual Vitrification Rate, m^3/yr
5%	302,000	15,300
25%	392,000	12,200

capital, equipment life, tax rates, depreciation, and tax credit allowances. The fixed-charge rate resulting from the federal financing assumptions listed in Table 43 is 0.145.

For commercial applications to hazardous waste sites, a different fixed-charge rate can be applied to recover the capital investment. The commercial rate is allowed many of the tax incentives that are not allowed the federal government. This rate can vary depending upon the accounting methods used by individual companies and their assumptions and requirements used for inflation, debt, equity, financing, depreciation, tax credits, and income tax rate. Typical industries would derive a fixed charge rate between 15 and 25% (EPRI 1982) for a 10-yr equipment life; therefore, 20% was assumed as the fixed-charge rate for annualizing equipment costs for hazardous wastes being processed by the private sector.

The capital cost per cubic meter is calculated by dividing the annualized capital cost by the annual vitrification rate. The annual vitrification rate is 80% of the volume capacity that would be vitrified if the equipment operated 24 h/day, 365 day/yr. The 20% difference allows for regular maintenance, unplanned shutdowns, and periods when the equipment is between assigned operations.

RESULTS

The unit cost, productivity, and consumption data defined and developed in the previous sections were integrated to produce cost estimates for the various ISV configurations. These cost estimates are summarized in Table 44.

TABLE 43. Federal Financing Assumptions

Parameter	Value
Equipment life, yr	10
Cost of capital, %	7
Depreciation	N/A
Tax credit	N/A
Miscellaneous costs, %	0.25
Miscellaneous taxes, %	0

TABLE 44. Cost Summary for ISV Configurations (based on vitrifying a 90-m x 30-m x 5-m-deep site)

Configuration	Cost, 1985 $/m^3 of Soil Vitrified						
	Site	Equipment	Labor	Waste Disposal	Electrode	Power[a]	Total
Radioactive Waste							
5% moisture	2	33	74	2	94	24	227
25% moisture	2	41	90	2	94	31	259
Hazardous Waste							
5% moisture	2	20	42	2	94	24	183
25% moisture	2	25	51	2	94	31	204

(a) Power cost at 2.9 cents/kWh.

As shown in Table 46, the most costly components are the electrodes, labor, and power. The use of the combination Mo/graphite electrode has almost doubled the electrode costs reported previously (Oma, et al. 1983 and Timmerman 1986). These higher cost electrodes are required to prevent failure during processing and appear to be a necessary but costly item. Labor, power, and equipment costs increase as moisture content increases due to the additional processing time and energy required. The equipment and labor costs related to hazardous chemical wastes are less than those for radioactive wastes, because a less complex and less expensive off-gas treatment system is required for the hazardous chemical waste processing, and industrial labor rates are lower than federal labor and overhead rates. Both the off-gas treatment equipment and off-gas hood containment features and requirements are greatly reduced for hazardous chemical wastes as determined by privately sponsored studies by Battelle (Buelt and Freim 1986 and Timmerman 1986). No glove-box type containment module, extensive treatment equipment, or specialty hood design are required for hazardous chemical waste operations because of the much lower toxic level of releases from the melt.

When reviewing the difference in costs among the configurations, the variation in power and energy costs across the United States and comparison of dry western soil (5% moisture) with wetter eastern soil (25% moisture) need to be considered. Details of this information and the summary information of Table 44 are derived from the tables of ISV cost-estimate information on the four configurations:

Table 45 - Radioactive Waste, 5% Moisture
Table 46 - Radioactive Waste, 25% Moisture
Table 47 - Hazardous Chemical Waste, 5% Moisture
Table 48 - Hazardous Chemical Waste, 25% Moisture

These tables provide detailed cost breakdowns for moisture and waste-type processing differences and compare the different energy rates of 2.2 cents/kWh and between 4.1 and 5.3 cents/kWh to correspond to an equivalent cost for portable power. The highest power cost represents the equivalent obtained by using a portable 5-mW generator.

TABLE 45. In Situ Vitrification Cost Estimate (1985$) - Radioactive Waste, 5% Moisture

Cost Breakdown	Line Power $0.022/kWh	Line Power $0.042/kWh	Portable Power	Specific Basis
Site Costs				
Site Costs	25,000	25,000	25,000	Access, leveling, etc.
Site Cost/m^3	2	2	2	Original soil volume basis
Equipment Costs				
Design and Engineering	687,000	687,000	666,000	25% of equipment costs
Equipment - Total	2,750,000	2,750,000	4,963,000	
Total Equipment Cost	3,437,000	3,437,000	5,628,000	
Annualized Fixed Charge Rate	0.145	0.145	0.145	
Annualized Equipment Charges	498,000	498,000	652,000	
Annual Vitrification Rate/m^3	15,000	15,000	15,000	80% operating capacity
Site Vitrification Settings	48	48	48	
Site Volume, m^3	14,000	14,000	14,000	90- x 30- x 5-m site
Site Equipment Costs	440,000	440,000	720,000	
Equipment Cost/m^3	33	33	53	Original soil volume basis
Labor Costs				
Vitrification Crew				
Operator	613,000	613,000	613,000	2 operators/shift at $48/h
Maintenance	61,000	61,000	61,000	4 h/day at $48/h
Radiation Monitor	86,000	86,000	86,000	6 h/day at $48/h
Engineer	129,000	129,000	129,000	8 h/day at $50/h (1-shift coverage)
Heavy Equipment Crew				
Operator	36,000	36,000	36,000	19 h/setting at $39/h
Laborer	60,000	60,000	60,000	34 h/setting at $37/h
Electrician	9,000	9,000	9,000	4 h/setting at $45/h
Total Labor	994,000	994,000	994,000	
Labor Cost/m^3	74	74	74	Original soil volume basis
Consumable Costs				
Electrodes	1,267,000	1,267,000	1,267,000	4 electrodes/setting, $1,320/m of depth
Secondary Wastes	25,000	25,000	25,000	2,000 L/setting at $0.26/L
Energy Consumption/Setting, kWh	302,000	302,000	302,000	
Energy Cost	319,000	609,000	325,000	Cost for all settings
Total Consumables	1,611,000	1,901,000	1,617,000	
Consumable Cost/m^3	119	141	120	Original soil volume basis
Total Site Cost	3,069,000	3,359,000	3,355,000	
Total Cost/m^3 (5% moisture)	227	249	249	Original soil volume basis
Total Cost/ft^3 (5% moisture)	6.44	7.05	7.04	Original soil volume basis

The cost ranges plotted as a function of total cost ($/$m^3$) versus electrical rate (c/kWh) are provided in Figure 77, which provides the following:

- illustrates the range of ISV costs on a per volume basis that can be expected for processing various waste types that have varying moisture contents
- illustrates the major influence that consumables (electrodes and power) have on the ISV process by the tight grouping of all costs and the relatively small impact that equipment costs (radioactive versus hazardous chemical wastes) have on the process

TABLE 46. In Situ Vitrification Cost Estimate (1985$) - Radioactive Waste, 25% Moisture

Cost Breakdown	Line Power $0.022/kWh	Line Power $0.041/kWh	Portable Power	Specific Basis
Site Costs				
Site Costs	25,000	25,000	25,000	Access, leveling, etc.
Site Cost/m^3	2	2	2	Original soil volume basis
Equipment Costs				
Design and Engineering	687,000	687,000	666,000	25% of equipment costs
Equipment - Total	2,750,000	2,750,000	4,963,000	
Total Equipment Cost	3,437,000	3,437,000	5,628,000	
Annualized Fixed Charge Rate	0.145	0.145	0.145	
Annualized Equipment Charges	498,000	498,000	816,000	
Annual Vitrification Rate/m^3	12,000	12,000	12,000	80% operating capacity
Site Vitrification Settings	48	48	48	
Site Volume, m^3	14,000	14,000	14,000	90- x 30- x 5-m site
Site Equipment Costs	551,000	551,000	903,000	
Equipment Cost/m^3	41	41	67	Original soil volume basis
Labor Costs				
Vitrification Crew				
Operator	769,000	769,000	769,000	2 operators/shift at $48/h
Maintenance	77,000	77,000	77,000	4 h/day at $48/h
Radiation Monitor	108,000	108,000	108,000	6 h/day at $48/h
Engineer	162,000	162,000	162,000	8 h/day at $50/h (1-shift coverage)
Heavy Equipment Crew				
Operator	36,000	36,000	36,000	19 h/setting at $39/h
Laborer	60,000	60,000	60,000	34 h/setting at $37/h
Electrician	9,000	9,000	9,000	4 h/setting at $45/h
Total Labor	1,220,000	1,220,000	1,220,000	
Labor Cost/m^3	90	90	90	Original soil volume basis
Consumable Costs				
Electrodes	1,267,000	1,267,000	1,267,000	4 electrodes/setting, $1,320/m of depth
Secondary Wastes	25,000	25,000	25,000	2,000 L/setting at $0.26/L
Energy Consumption/Setting, kWh	392,000	392,000	392,000	
Energy Cost	414,000	771,000	421,000	Cost for all settings
Total Consumables	1,706,000	2,064,000	1,714,000	
Consumable Cost/m^3	126	153	127	Original soil volume basis
Total Site Cost	3,502,000	3,960,000	3,861,000	
Total Cost/m^3 (25% moisture)	259	286	286	Original soil volume basis
Total Cost/ft^3 (25% moisture)	7.35	8.10	8.10	Original soil volume basis

- distinguishes the effect (~15% increase) that a 20% moisture increase has on costs.

A major cost differential is also illustrated by comparing the ISV costs for radioactive and hazardous chemical wastes with the ISV costs for a wet industrial sludge that contains 70% moisture (Buelt and Freim 1986). This differential is created by the high volume reduction attained by ISV and reduced density of the sludge (1.1 kg/L versus 1.6 kg/L for soils). This results in reduced operating and electrode costs. Sludge density is closer to that of water because of the hydroscopic incorporation of its water content

TABLE 47. In Situ Vitrification Cost Estimate (1985$) - Hazardous Chemical Waste, 5% Moisture

Cost Breakdown	Line Power $0.022/kWh	Line Power $0.053/kWh	Portable Power	Specific Basis
Site Costs				
Site Costs	25,000	25,000	25,000	Access, leveling, etc.
Site Cost/m^3	2	2	2	Original soil volume basis
Equipment Costs				
Design and Engineering	304,000	304,000	279,000	25% of equipment costs
Equipment - Total	1,215,000	1,215,000	3,802,000	
Total Equipment Cost	1,519,000	1,519,000	4,081,000	
Annualized Fixed Charge Rate	0.200	0.200	0.200	
Annualized Equipment Charges	304,000	304,000	816,000	
Annual Vitrification Rate/m^3	15,300	15,300	15,300	80% operating capacity
Site Vitrification Settings	48	48	48	
Site Volume, m^3	14,000	14,000	14,000	90- x 30- x 5-m site
Site Equipment Costs	268,000	268,000	720,000	
Equipment Cost/m^3	20	20	20	Original soil volume basis
Labor Costs				
Vitrification Crew				
Operator	322,000	322,000	322,000	2 operators/shift at $25/h
Maintenance	15,000	15,000	15,000	1 h/day at $48/h
Engineer	129,000	129,000	129,000	8 h/day at $50/h (1-shift coverage)
Heavy Equipment Crew				
Operator	36,000	36,000	36,000	19 h/setting at $39/h
Laborer	60,000	60,000	60,000	34 h/setting at $37/h
Electrician	9,000	9,000	9,000	4 h/setting at $45/h
Total Labor	571,000	571,000	571,000	
Labor Cost/m^3	42	42	42	Original soil volume basis
Consumable Costs				
Electrodes	1,267,000	1,267,000	1,267,000	4 electrodes/setting, $1,320/m of depth
Secondary Wastes	25,000	25,000	25,000	2,000 L/setting at $0.26/L
Energy Consumption/Setting, kWh	302,000	302,000	302,000	
Energy Cost	319,000	768,000	325,000	Cost for all settings
Total Consumables	1,611,000	2,060,000	1,617,000	
Consumable Cost/m^3	119	153	120	Original soil volume basis
Total Site Cost	2,475,000	2,924,000	2,933,000	
Total Cost/m^3 (5% moisture)	183	217	217	Original soil volume basis
Total Cost/ft^3 (5% moisture)	5.19	6.13	6.15	Original soil volume basis

into the volume of the sludge. The water in most sludges causes a swelling action and becomes part of the to-be-vitrified volume, while increased moisture contents in typical sandy soils simply fill the interstitial voids between the particles. Since the energy required to vitrify soil is the same as that to drive off the water (theoretically 0.8 kWh/kg), the added water in the sludge significantly reduces the mass to be vitrified per unit volume, thus contributing to a lower-cost-per-original-volume basis for wet sludge. Volume

TABLE 48. In Situ Vitrification Cost Estimate (1985$) - Hazardous Chemical Waste, 25% Moisture

Cost Breakdown	Line Power $0.022/kWh	Line Power $0.053/kWh	Portable Power	Specific Basis
Site Costs				
Site Costs	25,000	25,000	25,000	Access, leveling, etc.
Site Cost/m^3	2	2	2	Original soil volume basis
Equipment Costs				
Design and Engineering	304,000	304,000	278,000	25% of equipment costs
Equipment - Total	1,215,000	1,215,000	3,802,000	
Total Equipment Cost	1,519,000	1,519,000	4,081,000	
Annualized Fixed Charge Rate	0.200	0.200	0.200	
Annualized Equipment Charges	304,000	304,000	816,000	
Annual Vitrification Rate/m^3	12,000	12,000	12,000	80% operating capacity
Site Vitrification Settings	48	48	48	
Site Volume, m^3	14,000	14,000	14,000	90- x 30- x 5-m site
Site Equipment Costs	336,000	336,000	903,000	
Equipment Cost/m^3	25	25	67	Original soil volume basis
Labor Costs				
Vitrification Crew				
Operator	404,000	404,000	404,000	2 operators/shift at $25/h
Maintenance	19,000	19,000	19,000	1 h/day at $48/h
Engineer	162,000	162,000	162,000	8 h/day at $50/h (1-shift coverage)
Heavy Equipment Crew				
Operator	36,000	36,000	36,000	19 h/setting at $39/h
Laborer	60,000	60,000	60,000	34 h/setting at $37/h
Electrician	9,000	9,000	9,000	4 h/setting at $45/h
Total Labor	689,000	689,000	689,000	
Labor Cost/m^3	51	51	51	Original soil volume basis
Consumable Costs				
Electrodes	1,267,000	1,267,000	1,267,000	4 electrodes/setting, $1,320/m of depth
Secondary Wastes	25,000	25,000	25,000	2,000 L/setting at $0.26/L
Energy Consumption/Setting, kWh	392,000	392,000	392,000	
Energy Cost	414,000	997,000	421,000	Cost for all settings
Total Consumables	1,706,000	2,289,000	1,714,000	
Consumable Cost/m^3	126	170	127	Original soil volume basis
Total Site Cost	2,756,000	3,340,000	3,331,000	
Total Cost/m^3 (25% moisture)	204	247	247	Original soil volume basis
Total Cost/ft^3 (25% moisture)	5.78	7.01	6.99	Original soil volume basis

reduction allows for additional sludge to be deposited in the same setting without disturbing the electrodes. This allows them to be reused three times per setting, thus significantly reducing electrode costs.

In summary, the ISV processing economic analysis indicates the following:

- Costs range from $70 to $290/$m^3$ (1985 $) depending on waste type and moisture content.
- Electrode, labor, and power costs constitute the major cost components (in descending order).

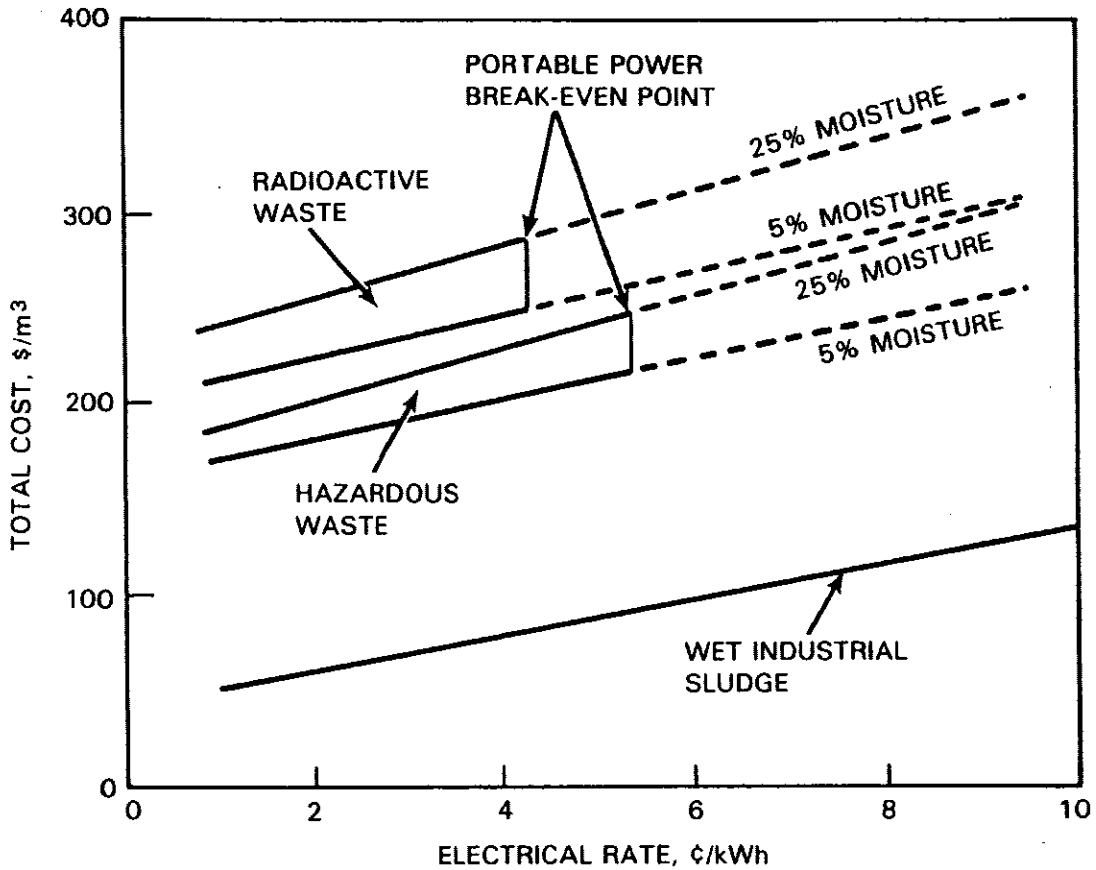

FIGURE 77. Cost of In Situ Vitrification as Functions of Electrical Rates and Soil Moisture

- Major revisions in equipment features have minor effects on total costs.
- Volume-incorporated water in sludges that have high moisture contents can significantly reduce per original volume costs.

ANALYSIS OF OCCUPATIONAL AND PUBLIC SAFETY

ANALYSIS OF OCCUPATIONAL AND PUBLIC SAFETY

The general procedure for performing a safety analysis of a proposed operation is to first develop a "source term," i.e. the quantity of material available for release to the human environment during normal conditions or accidents; to secondly develop "exposure scenarios," which are the ways that people would possibly be exposed to the sources; and finally to prepare dose estimates, which can then be related to standards to give a quantitative estimate of the safety of the operation. This chapter presents the results of a safety analysis of the application of ISV to a selected representative TRU waste site, including estimates of potential radiation dose to workers and the general public. The reference site (source term) is described, followed by an analysis of the planned operations and the site in its final state (Oma et al. 1983).

SELECTION AND DESCRIPTION OF THE REFERENCE SITE

The reference TRU-contaminated soil site described by Kasper et al. (1979) and Price et al. (1979) was chosen for the ISV occupational and public safety analysis because it is highly characterized as a result of well drilling, monitoring, and analytical programs. [A description of typical tile fields and cribs is given by Oma, Farnsworth, and Rusin (1982).] Gibson (1982) has developed an empirical relationship based on conditions at the reference site to estimate Pu migration through the soil.

The reference site was built in 1949. Details of the tile field construction are shown in Figure 78. The surface dimensions of the tile field are about 60 x 110 m. The side walls of the 5.8-m-deep excavation were sloped inward, resulting in floor dimensions of about 30-m wide by 80-m long. An evaluation of a contaminated zone that is 5- to 7.5-m wide by 90-m long was made and represents an accurate estimation of the area that requires vitrification at this particular site. These dimensions are used to calculate the number of settings required for both pilot- and large-scale systems.

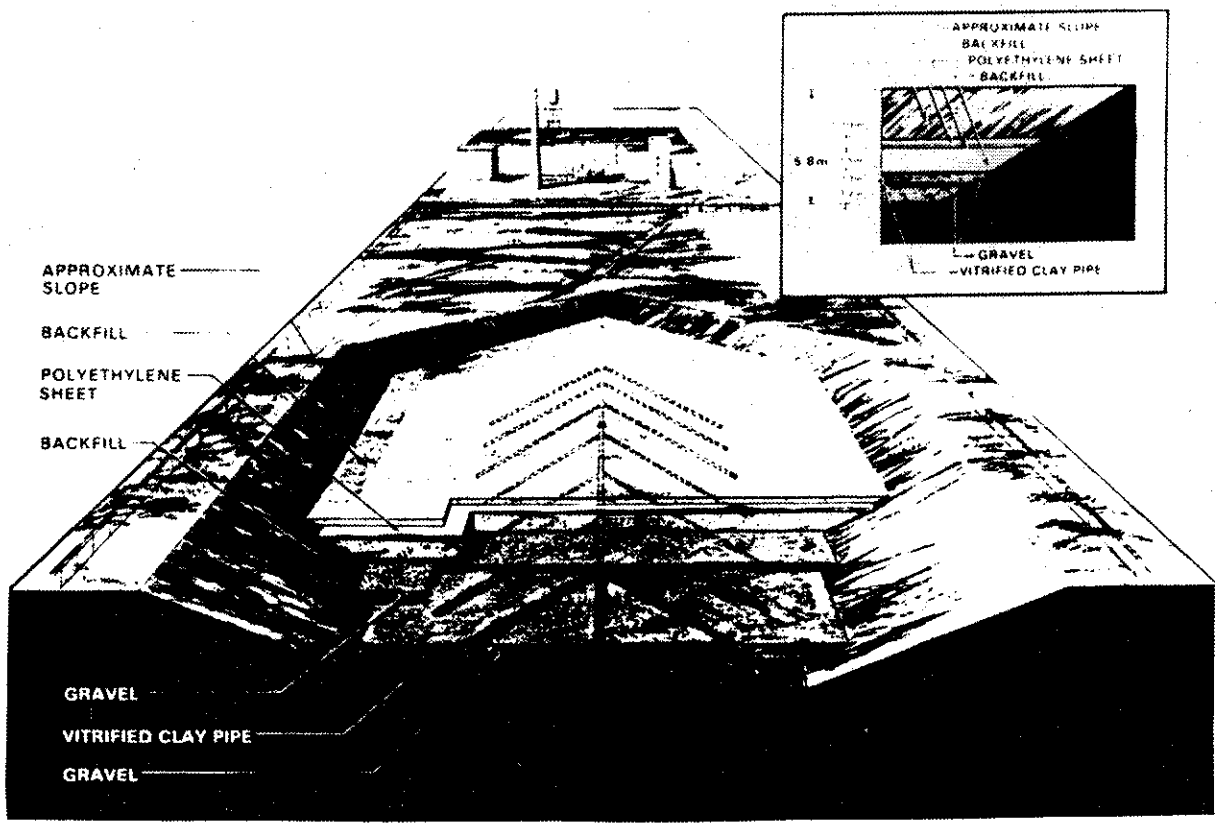

FIGURE 78. Construction of the Reference Site (Price et al. 1979)

The tile field distribution system for the liquid waste is composed of 20-cm-dia fired clay pipe laid out in a herringbone pattern with a 79-m-long trunk line and 7 pairs of 21-m lateral sections. The clay distribution system lies on top of about 1 m of gravel and is in turn covered by almost 2 m of gravel. This layer of gravel is covered with 3250 m^2 of 0.05-cm-thick polyethylene sheeting to act as an impermeable barrier.

From 1949 to 1959 the tile field received overflow wastes from three adjacent cribs (see Figure 79). By 1959 the cribs were deactivated and the reference site was removed from service until 1964, when it was reopened to receive aqueous and organic waste from a Pu reclamation facility. The waste was released to the tile field in batches. Calculations suggest that the volume of liquid disposed at any one time was normally not sufficient to

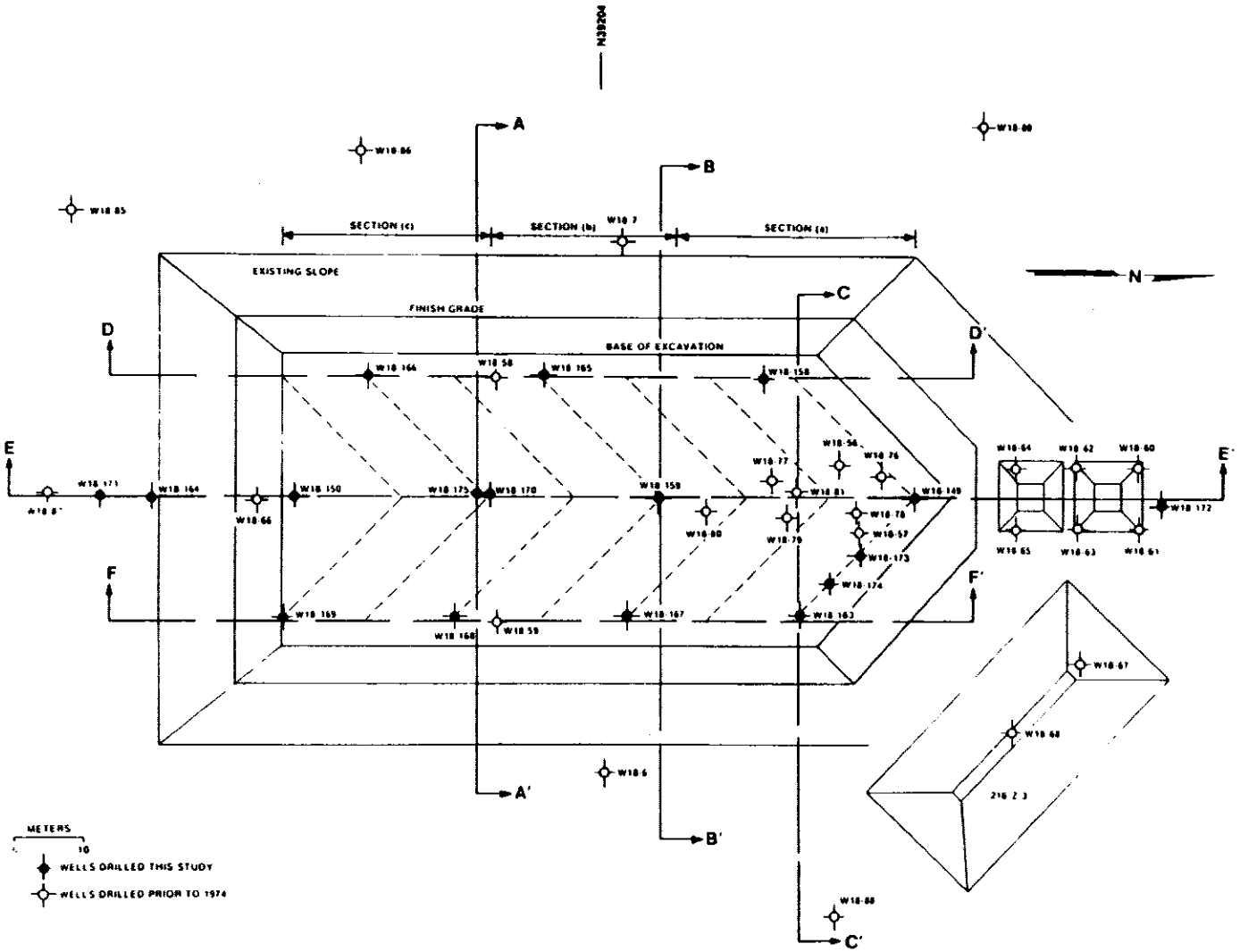

FIGURE 79. Plot Plan for the Reference Site and Three Adjacent Cribs (Price et al. 1979)

distribute through the entire pipe system (Crawley 1969). As a result, the waste entered the sediments within a few meters of where it entered the distribution system.

To make effective use of the tile field, it was divided into three sections (see Figure 79). Waste was discharged to the head of the A section from 1964 to 1966. In 1966 the A section was bypassed. A 5-cm, stainless steel pipe was placed within the clay pipe (see Figure 78) to change the point of discharge to the head of the B section. In 1967 the B section was bypassed using additional stainless steel pipe (for a total of 53 m), and then waste was discharged to the head of the C section. In 1969 the tile field was retired from service.

Radionuclide Waste Form and Inventory

From 1949 to 1959 the reference site received wastes originating from analytical and developmental laboratories and process operations. The waste consisted primarily of a dilute, basic, aqueous solution that contained Pu. About 50 g of Pu in 1 x 10^6 L of aqueous waste reached the tile field during this 10-yr period (Price et al. 1979). During the second period of activity (1964 to 1969), the tile field received waste originating from the Pu reclamation facility. The bulk of the waste was a concentrated aqueous solution of nitrates with an average pH of 1.0. The volume of waste received has been estimated at about 5.2 x 10^6 L aqueous waste containing about 57 kg of Pu. The inventory of waste discharged to the individual sections of the tile field is shown in Table 49.

Well drilling, monitoring, and analytical programming were conducted to determine the distribution of Pu beneath the complex (Kasper et al. 1979; Price et al. 1979). The data generated from this effort were used to construct activity profiles for individual wells. Based on gravimetric data and the activity profile (Price et al. 1979), cross sections beneath the tile field revealed the geology and the distribution of the TRU elements. Figure 80 shows a north-south cross section and Figures 81, 82, and 83 show east-west cross sections of the combined Pu and Am activity beneath the tile field complex.

TABLE 49. Estimate of Waste Volume, Plutonium, and Americium Discharged to the Reference Site (Kasper et al. 1979)

Section	Volume, L	Pu, kg	Am, kg
A	1.9×10^6	30.0	--
B	1.9×10^6	16.6	--
C	1.4×10^6	10.8	--
Total	5.2×10^6	57.4	1(a)

(a) Based on the estimated efficiency of the Am recovery process.

Price et al. (1979) concluded that the highest concentrations of Pu and Am (3.8×10^4 nCi/g and 2.6×10^3 nCi/g of sediment, respectively) occur within the first 3 m of sediment beneath the central distribution pipe. The maximum vertical extent of TRU activity was found about 30 m below the bottom of the tile field (which is still 25 m above the regional water table). The data are reported in Price et al. (1979) for the test well (299-W18-149) that contains the highest concentration of Pu and Am as a function of depth.

The fission products present in the tile field are ^{60}Co, ^{90}Sr, ^{106}Ru, and ^{137}Cs. The activities of each of these materials are <0.3 Ci.

Chemical Waste Form

Organic wastes consisting mainly of CCl_4 and tributylphosphate (TBP) were discharged to the tile field in an aqueous solution with an average pH of 1.0 during the 5-yr period from 1964 to 1969 (Owens 1981). Additional nonradioactive effluent species and their molarities were 0.15 M HNO_3, 0.2 M $AlF(NO_3)_2$, 0.3 M $Mg(NO_3)_2$, 0.2 M $Ca(NO_3)_2$, and 0.95 M $NaNO_3$.

POTENTIAL SHORT-TERM (OPERATIONAL) RADIATION EXPOSURES

During vitrification of the reference site, the proposed ISV activities would place workers in proximity to radiation fields. Minor atmospheric releases of radionuclides would expose members of the general public to very

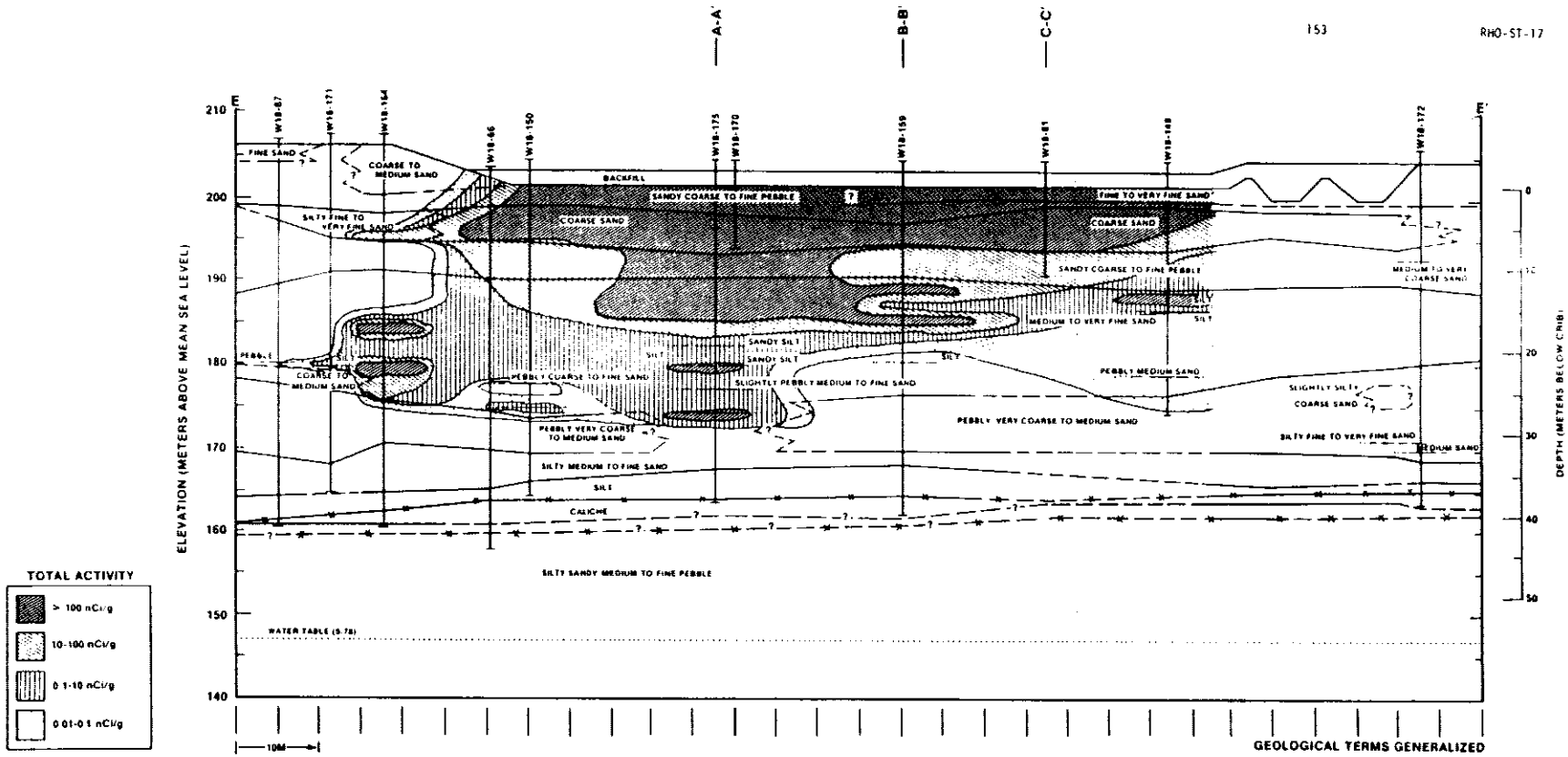

FIGURE 80. Distribution of Total TRU Activity, North-South Cross Section E-E' of the Reference Site (See Figure 64) (Price et al. 1979)

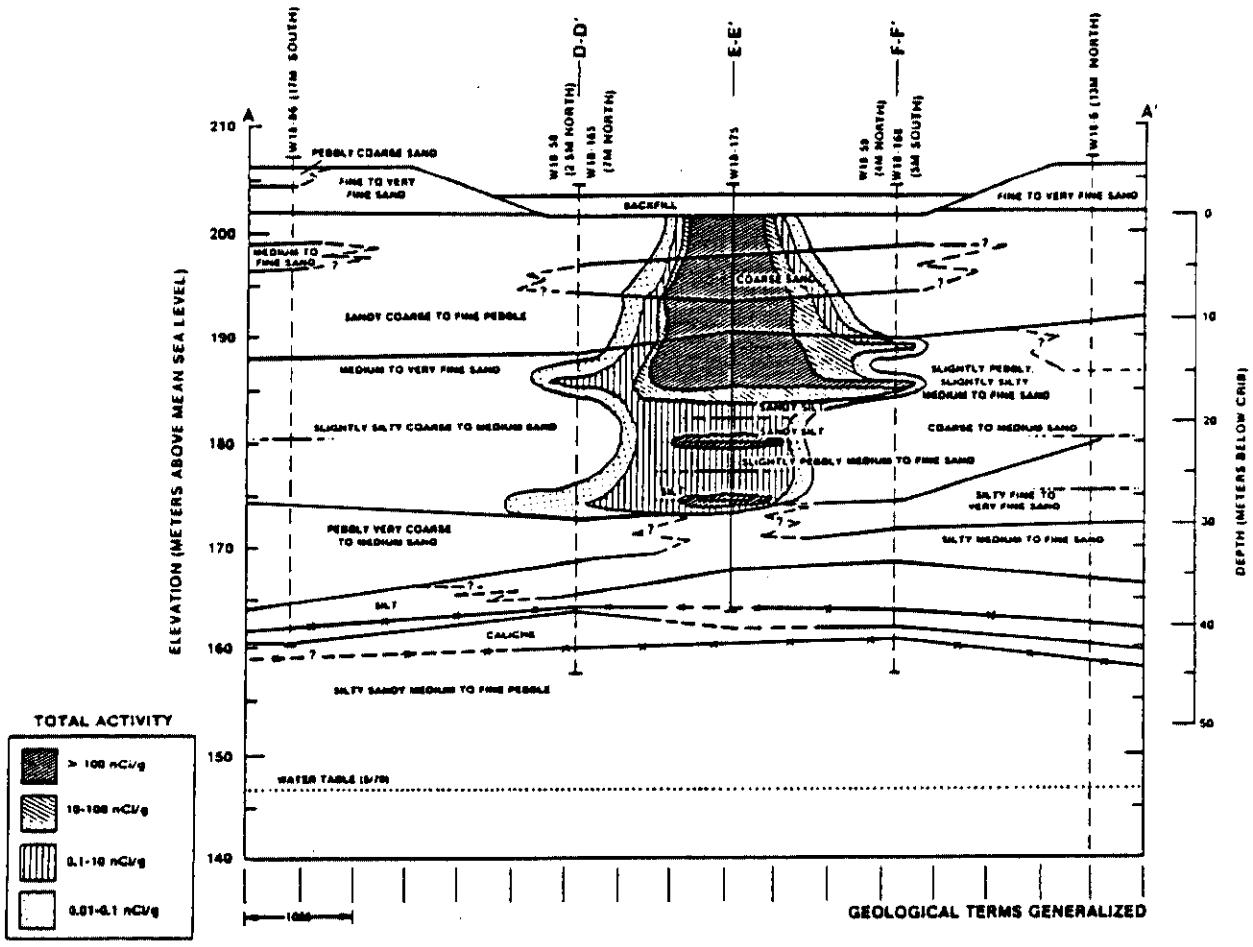

FIGURE 81. Distribution of Total TRU Activity, East-West Cross Section Through Points A-A' (see Figure 80) (Price et al. 1979)

low levels of radiation. Accidents or unplanned events could further expose both workers and the public. These cases are developed and examined in the following sections.

Normal Operations

The source terms used for the calculation of the occupational and public exposures are based on 1) measurement of the gaseous evolution of elements during vitrification, 2) capabilities of the off-gas system as presently designed, and 3) estimates of the radionuclide inventory in the waste site.

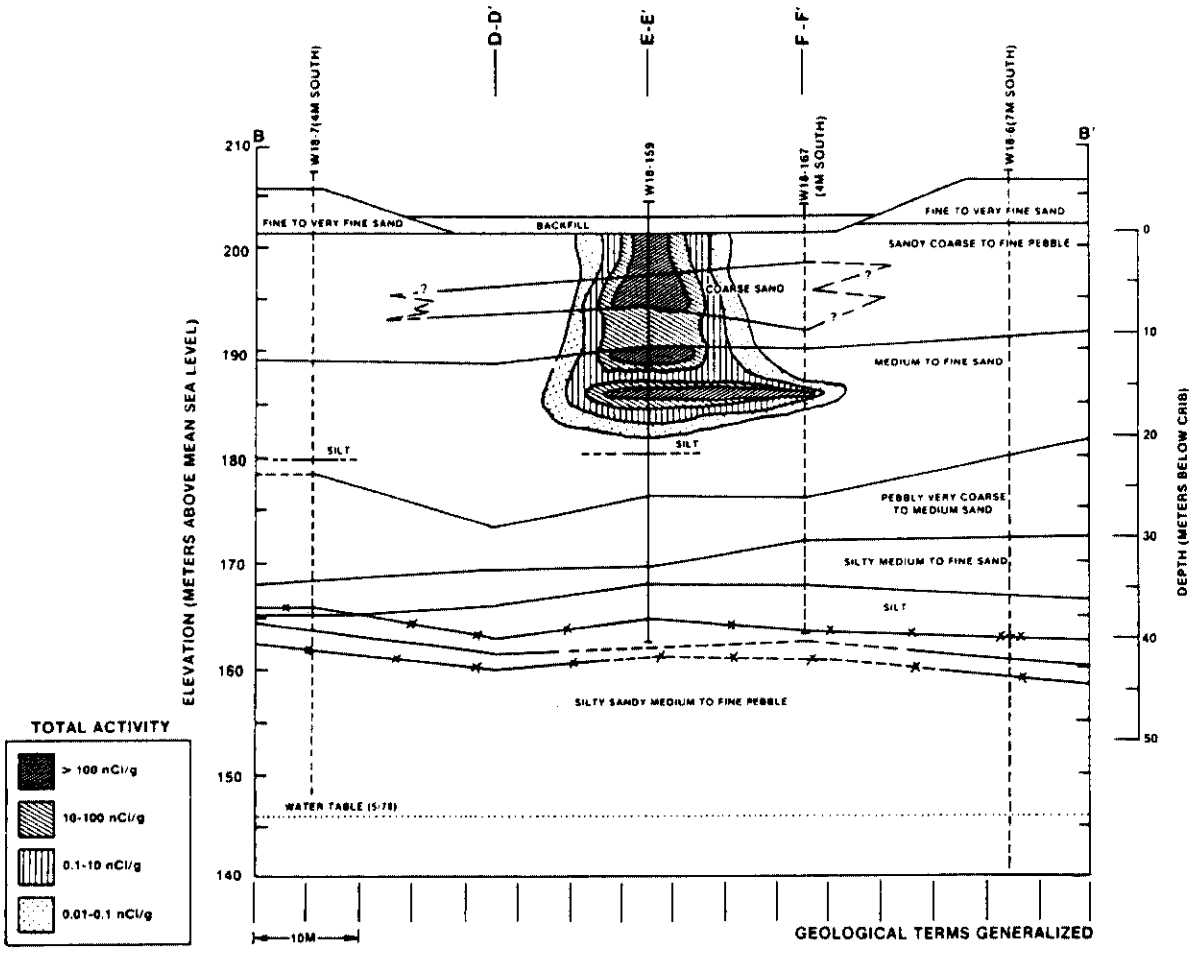

FIGURE 82. Distribution of Total TRU Activity, East-West Cross Section Through Points B-B' (see Figure 80) (Price et al. 1979)

Release rates from the soil during vitrification were estimated from previous ISV field tests (Oma, Farnsworth, and Rusin 1982). Rate constants were developed for three possible operating conditions: operation with a cold cap, operation without a cold cap, and operation with rapid venting. Release rate fractions for elements in the site are listed in Table 50. Operation with a cold cap of solidified soil was assumed to occur during 75% of the runs. Routine operation without a cold cap was assumed for the remaining 25%. Rate constants for venting pertain only to sites containing combustibles and were used only as a basis for release in some of the accident scenarios. Total fractions of material released in a single run were based on a 120-h run time.

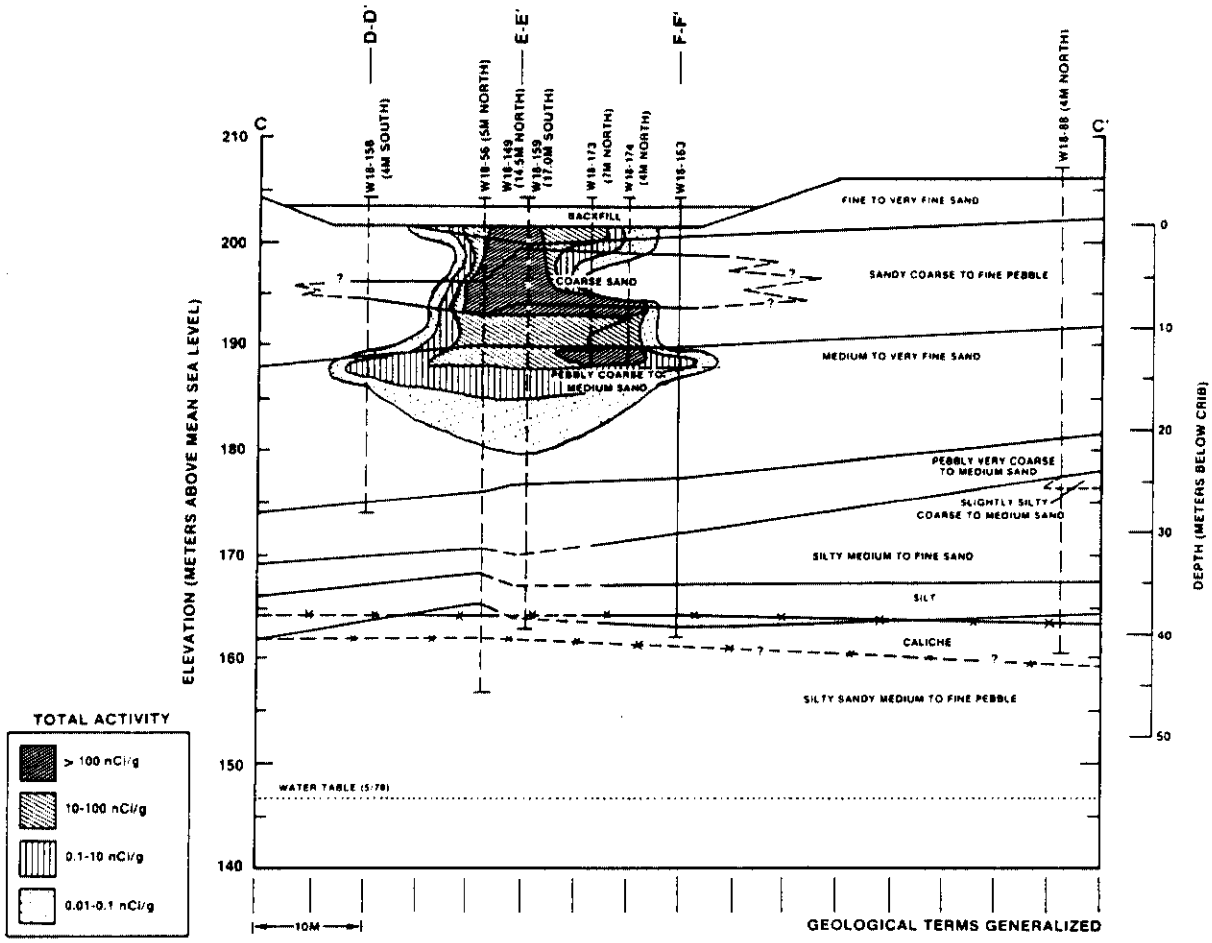

FIGURE 83. Distribution of Total TRU Activity, East-West Cross Section Through Points C-C' (see Figure 80) (Price et al. 1979)

The collection efficiency of each component of the off-gas system was estimated from previous tests and from manufacturers' data. Conservatively estimated DFs for each component are listed in Table 51 for the elements present in the waste site.

The reference site waste inventory as reported by Owens (1981) (with slight modifications) provided the basis for the radionuclide source term. Table 52 lists the isotope inventory for the entire waste site and for the region vitrified during each run. For purposes of analysis, the waste inventory was assumed to be concentrated along the waste distribution pipe, in a volume approximately 90 m x 5 m x 4 m (see Figure 84). A highly radioactive

TABLE 50. Elemental Fractions Released During Vitrification of the Tile Field

Element	With Cold Cap, %/h	Without Cold Cap, %/h	Gas Venting, %[a]
Co	$<5 \times 10^{-3}$[b]	5×10^{-3}	0.58 avg; 1.2 max[c]
Cs	$<5 \times 10^{-3}$[b]	5×10^{-3}	1.6 avg; 3.5 max[c]
Sr	0	5×10^{-4}	0.1 avg; 0.12 max[b]
TRU	0	5×10^{-3}	0.38 avg; 1.0 max[c]
Ru	0	0	

(a) Percent of element associated with combustibles only.
(b) Release fractions of 5×10^{-3} were used for the exposure analysis.
(c) Maximum gas venting rate was used for certain accidental release scenarios.

TABLE 51. Hood-to-Stack Decontamination Factors for the Off-Gas Treatment System

Component	Cs or Sr	TRU or Co
Quench tower	10	10
Tandem nozzle scrubber	10	10
Separator	1	1
Tube and shell condenser	1	1
Separator	1	1
Heater	1	1
HEPA filter	10^2	10^3

zone (10 times the activity of the remaining contaminated areas) was located at each of the main distribution points. The concentrations of radionuclides in each of these "hotter" zones are given in Table 52, as are the integrated 120-h release fractions for operation with and without a cold cap. Also given in this table are the total quantities released per run (over a hot spot). The setting was assumed to have a cold cap during 75% of the run and no cold cap for the remaining 25%. The fraction released during venting was not used for normal operation calculations.

TABLE 52. Inventories and Release Fractions for 120-h Runs at the Reference Site

Radionuclide	Reference Site, Inventory, Ci	Inventory Per Set, Ci[a]	Fraction Released: With Cold Cap	Fraction Released: Without Cold Cap	Quantity Released from Soil During Set, Ci[a,b]
^{238}Pu	1.8×10^{1}	4.3×10^{0}	0	6.0×10^{-3}	6.5×10^{-3}
^{239}Pu	8.5×10^{2}	2.0×10^{2}	0	6.0×10^{-3}	3.0×10^{-1}
^{240}Pu	2.1×10^{2}	5.0×10^{1}	0	6.0×10^{-3}	7.5×10^{-2}
^{241}Pu	2.5×10^{3}	6.0×10^{2}	0	6.0×10^{-3}	9.0×10^{-1}
^{242}Pu	7.0×10^{-2}	1.7×10^{-2}	0	6.0×10^{-3}	2.6×10^{-5}
^{241}Am	3.4×10^{3}	8.1×10^{2}	0	6.0×10^{-3}	1.2×10^{0}
^{90}Sr	7.7×10^{-1}	1.8×10^{-1}	0	6.0×10^{-4}	2.7×10^{-4}
^{106}Ru	8.9×10^{-3}	2.1×10^{-3}	0	0	0
^{137}Cs	1.4×10^{-1}	3.3×10^{-2}	6.0×10^{-3}	6.0×10^{-3}	2.0×10^{-4}
^{60}Co	3.0×10^{-2}	7.1×10^{-3}	6.0×10^{-3}	6.0×10^{-3}	4.3×10^{-5}
^{233}U	3.6×10^{-2}	8.6×10^{-3}	0	6.0×10^{-3}	1.3×10^{-5}
^{234}U	3.7×10^{-2}	8.8×10^{-3}	0	6.0×10^{-3}	1.3×10^{-5}
^{235}U	1.1×10^{-3}	2.6×10^{-4}	0	6.0×10^{-3}	3.9×10^{-7}
^{238}U	2.7×10^{-2}	6.4×10^{-3}	0	6.0×10^{-3}	9.6×10^{-6}

(a) Inventory is for one of three "hot spots"; other runs contain 1/10 this activity.
(b) Assumes runs had cold cap 75% of time, no cold cap 25% of time.

Occupational Exposure During Routine Operations

Occupational doses for routine operations were estimated for activities that occurred during vitrification runs and during the changeover period between runs.

Activities during the run for which doses were calculated include 1) observing the melt, 2) working in the van that contains the off-gas system, and 3) other activities that cause a worker to be in the vicinity of the site. Activities during the changeover period include 1) placing the electrodes, 2) placing the hood, and 3) draining and flushing the off-gas system scrub solution tanks. Worker locations and task durations developed for each

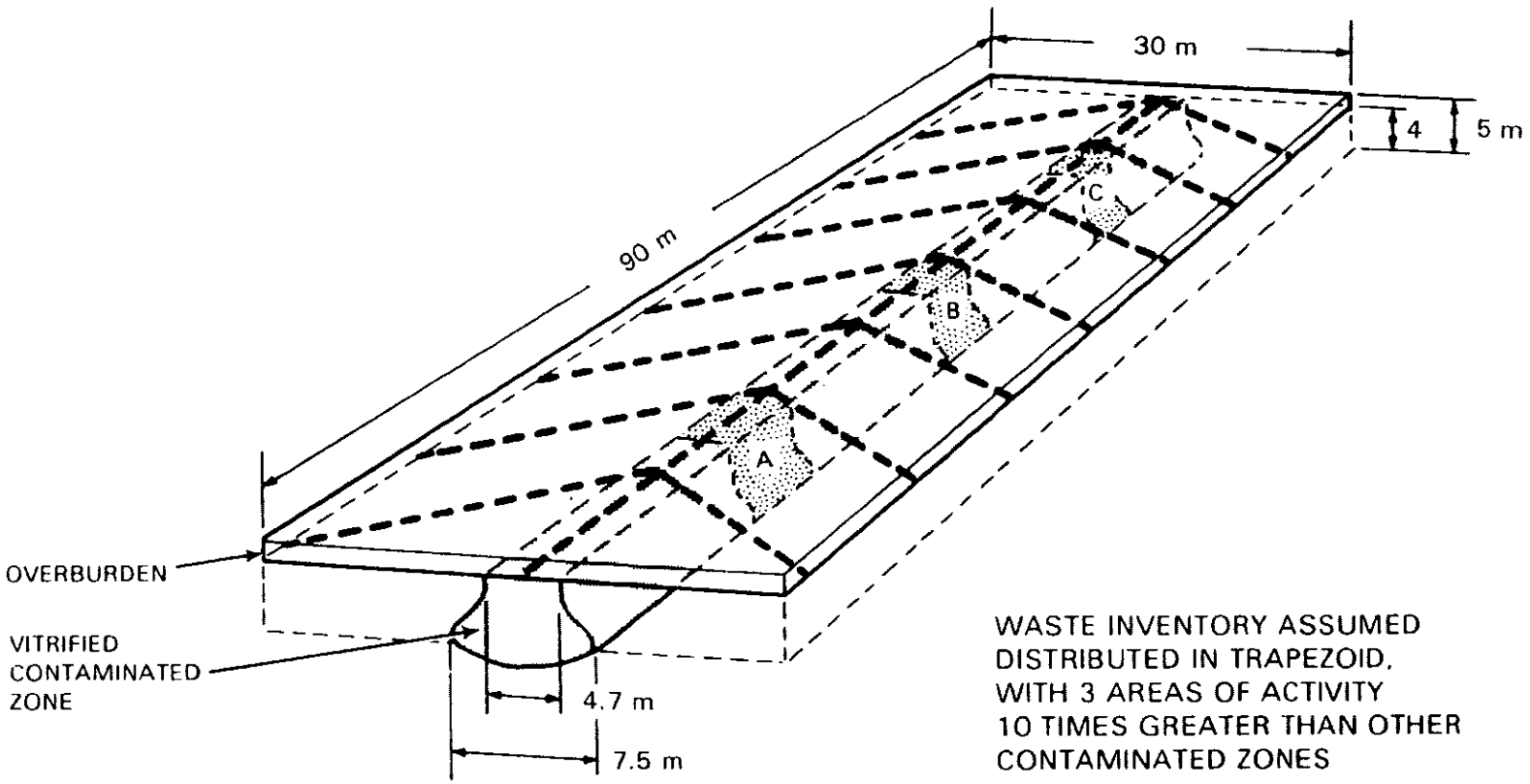

FIGURE 84. Waste Distribution in a 90- x 4- x 4-m Site

activity are listed in Table 53. For this analysis, placing the electrodes includes drilling the holes for the electrodes, inserting the electrodes, and spreading the graphite/frit between the electrodes. Placing the hood includes moving the hood from one location to the next, and hooking up and checking the electrical and off-gas systems. Draining the scrub tanks takes 48 man-hours and includes preparing and flushing each tank three times. An additional activity, removing overburden, was not required for the reference site but has been included in this analysis of the vitrification process.

The ISOSHLD model (Engel, Greenborg, and Hendrickson 1966) was used to calculate the doses from routine occupational activities. The calculations further assumed that 1) the site would be covered by a 1-m layer of uncontaminated overburden and 2) the entire site inventory would be contained within the zone to be vitrified, i.e., the top 4 m of waste. All of the routine doses estimated are contributed primarily from ^{60}Co and ^{137}Cs.

The greatest occupational doses for the entire site result from electrode emplacement because of the workers' assumed proximity to contaminated materials

TABLE 53. Occupational Doses for Reference Site Vitrification (120-h run, 15 settings)

Activity	Number of Personnel	Man-Hours per Run	Total Man-Hours	Total Occupational Whole Body Dose, man-rem
Overburden removal	1	--	100	2×10^{-10}
Electrode emplacement	4	60	900	9×10^{-2}
Hood placement	4	16	240	1×10^{-8}
Observation of melt	1	24	360	2×10^{-3}
Work in off-gas van	1	30	450	5×10^{-4}
Draining of collection tanks	1	48	720	7×10^{-4}
Work in site vicinity	1	120	1800	1×10^{-8}
Background radiation[a]	1	120	1800	1×10^{-2}

(a) Background exposure rate in uncontaminated area assumed to be 7 μR/h.

brought to the surface during hole-drilling for the electrodes. The maximum collective dose is 9×10^{-2} man-rem, while the maximum individual dose is 1×10^{-2} rem (see Table 53). This dose is significantly less than the DOE guidelines of 5 rem/yr or 3 rem/quarter whole body exposure to an individual worker [DOE Order 5480.1A, (U.S. DOE 1981a)], even with conservative assumptions. For comparison, the natural background exposure rate in the area of the reference site is about 7 μR/h, so the highest routine occupational dose received by a worker from ISV-related activities is less than or equal to the exposure from natural background.

The low dose associated with 100 hours of overburden removal, 2×10^{-10} man-rem, indicates that this activity will not measurably contribute to the overall dose of ISV.

Public Exposure During Routine Operations

The quantities of radionuclides released to the off-gas system from the vitrification of the reference site are shown in Table 50. The off-gas DFs given in Table 51 indicate that the release fraction will be $\sim 1 \times 10^{-5}$ of the amount vented from the soil to the off-gas system. This airborne release of radioactivity is the dominant exposure pathway to the public from vitrification of the site.

Standard models and methods for the reference site were used to calculate doses to members of the public from these releases (Napier 1982). These models include contributions to dose from submersion in contaminated air, inhalation of gases and particulates, and ingestion of food crops upon which the airborne matter may be deposited.

One-year dose and fifty-year dose commitments for the critical organ[(a)] of a maximum exposed individual living on the reference site boundary and to the general public living within 80 km of the site are given in Table 54. The largest site-specific doses to the body from airborne releases are to bone: a 50-yr dose commitment of 1×10^{-5} rem to the maximum exposed individual, and

(a) The critical organ is the organ that receives the highest dose.

TABLE 54. Critical Organ Dose Commitments to the Public from Routine ISV Operations

Dose	Maximum-Exposed Individual, rem	Population, man-rem
1st yr	3×10^{-8}	9×10^{-3}
50 yr	1×10^{-5}	5×10^{-1}

5×10^{-1} man-rem to the entire population. The major contributors to dose are the nuclides ^{239}Pu, ^{240}Pu, and ^{241}Am.

The DOE regulations on exposure to the general public, DOE Order 5480.1A, Chapter 11 (U.S. DOE 1981a), limit the dose to the maximum-exposed individual to <0.5 rem/yr, and 0.170 rem/yr based on the average dose to a suitable sample of the exposed population. The doses calculated for ISV operation at the reference site are insignificant in comparison with these standards, thus providing an indication of the overall safety of the ISV operation.

Postulated Abnormal Operations

This section presents the estimated radiological effects of potential credible accidents (or abnormal operating conditions) during ISV. The accidents considered are believed to represent the worst impacts possible during ISV. The accident scenarios are based on present designs and planned operating conditions. They are not predictions that any of these accidents will happen.

The approach used to develop the accident analysis and subsequent dose evaluation was to 1) identify the various steps of the ISV operation, 2) determine release mechanisms that could breach the radionuclide containment systems and release radionuclides to the biosphere for each step, 3) estimate the maximum fraction of radionuclides that might be released, and 4) calculate doses resulting from the estimated releases.

The accident scenarios are briefly described, followed by a discussion of the occupational and public doses resulting from the accidental releases.

Description of Accidental Release Scenarios

The consequences of accidents possible during the vitrification of an area are dependent on the quantities of radionuclides involved. To put an upper bound on the possible releases, all accidents described are assumed to occur during or after 120 hours of operation at the most highly contaminated zones in the reference site. This condition represents the largest contaminated soil volume that would be available for any single event and the maximum source for the various accidents.

Four accident scenarios have been identified as having the potential to occur at the reference site. These are 1) an uncontrolled venting from a subsurface structure, 2) a break in the off-gas containment pipe, 3) a liquid leak in the off-gas control van, and 4) a gaseous leak in the off-gas van. Two additional scenarios are also considered. These include 5) the possibility of accidental excavation of the waste while removing overburden, and 6) criticality of fissionable materials. These later two accidents are only addressed qualitatively to give perspective to potential hazards of the ISV process.

1. Uncontrolled venting from a subsurface structure. The run is proceeding normally when localized venting of gas from the surface of the waste site outside the hood is noticed. The phenomenon, which is investigated by a radiation monitor, is short-lived, and the run continues unabated. It is later determined that the venting was due to limited volatilization and pressurization of waste liquid remaining in a 6-m-long section of the stainless steel distribution pipe. Doses for this scenario were estimated using the waste concentration listed in Table 52. The source term is listed in Table 55.

2. Break in line between hood and off-gas system. The run is proceeding normally, with no cold cap. The effluent line between hood and off-gas system breaks, releasing the gaseous effluents directly to the atmosphere. Power to the electrodes is cut off immediately. As a cold cap forms over the melt area, the effluents released to the atmosphere decrease exponentially with a half-hour half-time. Gaseous effluents are released to the atmosphere for a four-hour period

TABLE 55. Radionuclides Released from Postulated Accidents, Ci

Radionuclide	Uncontrolled Venting	Break in Off-Gas Line[a]	Collection Tank Leak[b]	Release to Van[b]	Excess Overburden Removal[a]
^{238}Pu	1.7×10^{-7}	2.6×10^{-2}	5.9×10^{-3}	1×10^{-9}	1.8×10^{-4}
^{239}Pu	8.1×10^{-6}	1.2×10^{0}	2.7×10^{-1}	5×10^{-8}	9.0×10^{-3}
^{240}Pu	2.0×10^{-6}	3.0×10^{-1}	5.8×10^{-2}	1×10^{-8}	2.2×10^{-3}
^{241}Pu	2.4×10^{-3}	3.6×10^{0}	8.1×10^{-1}	2×10^{-7}	2.6×10^{-8}
^{242}Pu	6.6×10^{-10}	1.0×10^{-4}	2.3×10^{-5}	4×10^{-12}	7.5×10^{-7}
^{241}Am	3.2×10^{-5}	4.9×10^{-2}	1.1×10^{0}	2×10^{-7}	3.5×10^{-2}
^{90}Sr	7.3×10^{-9}	1.1×10^{-4}	2.4×10^{-4}	5×10^{-11}	8.0×10^{-6}
^{106}Ru	8.4×10^{-11}	0	0	0	9.0×10^{-8}
^{137}Cs	1.3×10^{-9}	2.0×10^{-4}	1.8×10^{-4}	3×10^{-11}	1.5×10^{-6}
^{60}Co	2.8×10^{-10}	4.3×10^{-5}	3.9×10^{-5}	2×10^{-12}	3.1×10^{-7}
^{233}U	3.4×10^{-10}	5.2×10^{-5}	1.2×10^{-5}	2×10^{-12}	3.7×10^{-7}
^{234}U	3.5×10^{-10}	5.3×10^{-5}	1.2×10^{-5}	2×10^{-12}	3.8×10^{-7}
^{235}U	1.0×10^{-11}	1.6×10^{-6}	3.5×10^{-7}	7×10^{-14}	1.2×10^{-8}
^{238}U	2.5×10^{-10}	3.8×10^{-5}	8.6×10^{-6}	2×10^{-12}	2.8×10^{-7}

(a) Occupational source term is a fraction of this value.
(b) No offsite releases above routine operating levels.

before a sufficient cold cap is formed to prevent further discharge. The doses for this scenario were estimated assuming the release rates determined for the absence of a cold cap, listed in Table 50. The quantities of radionuclides released are reported in Table 55.

3. Collection tank leak. The run is progressing in a normal manner with only 20 hours remaining until the run is to be completed. A leak develops in the bottom of one quencher-scrubber collection tank, which allows the entire contents of the tank to spill into the pan that lines the floor of the hood. The decision is made to complete the run without one of the scrubbers. Ten half-hour sampling periods are spent in the off-gas van, resulting in an additional dose to the worker. No radionuclides are released to the atmosphere, so this accident does not affect the public. The total quantities of radionuclides spilled to the hood are listed in Table 55.

4. Gaseous effluent release to the off-gas vans. The run is progressing in a normal manner when a leak develops in the off-gas system after the off gas clears the blower and is inside the van. Because the off gas is very humid and could damage the equipment, the run is terminated at this point. Therefore, the workers spend only one half-hour sampling period in the contaminated atmosphere. This accident would not increase the exposure of the offsite population above that received from normal operations. The source term is listed in Table 55.

5. Excess overburden removal. The reference site has only ~1.5 m of overburden, making its removal unnecessary. However, other sites may be more deeply buried. Vitrification of deep layers of overburden may not be practical or economically justifiable. Therefore, the overburden may be removed using conventional earth-moving techniques.

As the overburden is removed using large earth-moving equipment, it is checked by radiation monitors. It is assumed that, due to inaccurate survey or operator error, a section of contaminated soil is uncovered. The error is discovered immediately by the monitor,

and the area is covered with clean soil. The area that was uncovered is assumed to be the width of the contaminated zone, about 6 m x 2 m. The amount of contaminated dust suspended from clearing and covering this area is 2 kg, released over a period of 10 minutes. The soil is assumed to have the radionuclide concentration of the "hot zones." The radionuclide release is listed in Table 55.

6. Criticality. Detailed calculations have shown that a minimum critical areal concentration of Pu metal in wet soils at the reference site is 2.9 kg/m^2, with full water reflection (Oma, Farnsworth, and Rusin 1982). According to the same study, this value increases to 14.5 kg/m^2 for dry soil with Pu in the oxide form. A safety factor of 0.33 is applied, suggesting that any site with <1.0 kg/m^2 for wet soil (or about 5 kg/m^2 for dry soil with PuO_2) would be acceptable for ISV without danger of inducing a criticality.

The peak soil concentration of ^{239}Pu in the reference site is 4×10^4 nCi/g ^{239}Pu and ^{240}Pu in a limited area around the distributor pipe (Kennedy et al. 1982). This level of contamination reaches a depth of 1 m below the pipe. Using an activity fraction of 80% ^{239}Pu, this would be about 5×10^{-4} g ^{239}Pu/g soil. Thus, the areal concentration would be 0.9 kg/m^2 ^{239}Pu. This is below the acceptable areal concentration for wet soil, and well below the critical concentration. No mechanisms during the ISV process can be postulated, which result in lateral concentration of the Pu (Oma, Farnsworth, and Rusin 1982); therefore, a criticality incident is not considered possible for this site. Because the reference site contains a greater contamination level than other typical contaminated soil sites, criticality is not of great concern for these types of sites. However, if ISV application is to be used for other site types, such as caissons or retrievably stored TRU wastes, a more detailed criticality investigation may be in order.

Doses Resulting from Postulated Releases

The accident with the most severe consequences is a break in the off-gas line before the off gases are treated. First-year lung doses to a worker

standing downwind of the vented gases could be as high as 10 rem. First-year doses to members of the general public out of the immediate vicinity would be much lower, on the order of 0.03 rem to the lung of a maximum exposed individual 8 km away. The cumulative first-year dose to the entire population 80 km around the site would be 100 man-rem, much less than that attributed to background dose. Doses to workers from releases during vitrification are given in Table 56. Doses to the public from these same activities are listed in Table 57.

The radiological consequences of uncontrolled venting of a fraction of the waste inventory are lower than those for a break in the off-gas line. The first-year lung dose to the maximum exposed worker would be 2 rem, as shown in Table 55. First-year lung doses to members of the general public remain low, 5×10^{-5} rem for the maximum exposed individual and 0.2 man-rem to the surrounding population (see Table 56).

The only other accident with potential for offsite release of radionuclides is the accidental penetration of the waste while removing overburden (although overburden removal is not necessary for the reference site). The monitors and equipment operators could receive as much as 5 rem, if neither one was wearing respirators at the time, while the offsite individual would probably receive 0.01 rem.

The other accidents studied have no atmospheric release of radionuclides. The nuclides are contained in the glove boxes in the off-gas system trailer. Doses to workers in the van are 0.5 rem for the liquid leak and 0.04 rem for the gaseous leak, as reported in Table 55.

POTENTIAL LONG-TERM RADIATION EXPOSURES

Following ISV of a waste site, the radionuclides that were initially present remain locked inside a large, obsidian-like monolith. A key question in determining the suitability of a site for ISV is the relative benefit gained by vitrifying the site. The measure of benefit is the reduction of potential radiation dose from the waste site to individuals in the future.

TABLE 56. Occupational Doses from Postulated Accidental Releases (120-h run, 15 settings, concentrated inventory)

Accident	Number of Personnel	Length of Exposure	1st Year Dose Commitment to Each Worker, rem		
			Total Body	Bone	Lung
Uncontrolled venting	1	1 min	1×10^{-3}	2×10^{-2}	2×10^{0}
Off-gas line break	1	5 min	6×10^{-3}	1×10^{-1}	1×10^{1}
Collection tank leak[a]	1	5 h	5×10^{-1}	---	---
Gaseous release to van	1	30 min	2×10^{-5}	3×10^{-4}	4×10^{-2}
Excess overburden removal	2	10 min	3×10^{-3}	4×10^{-2}	5×10^{0}

(a) External radiation exposure only.

TABLE 57. Public Dose Commitments from Postulated Accidental Releases

Accident	Maximum-Exposed Individual, rem		Population, man-rem	
	1st Year[a]	50 Year[b]	1st Year[a]	50 Year[b]
Uncontrolled venting	5×10^{-5}	5×10^{-4}	2×10^{-1}	2×10^{0}
Off-gas line break	3×10^{-2}	3×10^{-1}	1×10^{2}	1×10^{3}
Excessive overburden removal	1×10^{-2}	9×10^{-2}	3×10^{1}	3×10^{2}

(a) Lung dose.
(b) Bone dose.

The potential routes through which people may be exposed to radionuclides or radiation are called exposure pathways. The general pathways can be thought of as external exposure, inhalation, and ingestion. External exposure results from direct radiation from air, water, soil, and contaminated structures. Inhalation doses can result from breathing aerosols released from facilities or

resuspended materials. Pathways of ingestion are water, fish, waterfowl, other game, food crops, animal products, or direct consumption of small amounts of material transferred from contaminated surfaces to the hands. The potential dose to an individual that might result from residual contamination at a site (the Allowable Residual Contamination Level, or ARCL; Napier 1982) is calculated in a radiation exposure scenario analysis by summing the exposures through all of the selected pathways.

The key to ARCL is an analysis of the maximum annual radiation dose to an individual. This dose is calculated by summing the doses from appropriate exposure pathways. The pathways are chosen depending on the ways an individual could be exposed for the release mode considered. The collection of appropriate pathways is called an exposure scenario. The ability to choose the exposure scenario is what gives the method the flexibility to handle many types of sites, inventories, and locations.

Preliminary investigations have been performed to determine the location of the individual most likely to be affected by contaminated sites. In a previous study of conditions at the reference site, individuals were postulated to live downwind and downstream at distances of 10 km, 1 km, and onsite (Napier 1982). For all times and for all exposure scenarios, radiation dose rates to the individuals living out of the immediate vicinity of the contaminated areas were found to be orders of magnitude smaller than those received by the onsite individual. Thus, the onsite exposure scenarios have been determined to be the most critical. For unrestricted use, the general types of potential exposure scenarios for maximum-exposed individuals are as follows:

- Transient
- Permanent resident
  - well drilling, excavation
  - contact with soil, inhalation of resuspended material
  - drinking of well water
  - backyard garden

- Inadvertent intruder
- Intentional intruder
  - resource recovery
  - use of recovered resource.

The potential for radiation doses to individuals has been examined for each of these general scenarios. The most restrictive are examined in detail in this report. For contaminated soil areas, the permanent resident is the individual most likely to receive radiation doses, although the intruder has the possibility of receiving the highest doses.

For the purposes of this analysis, dose estimates have been calculated for individuals exposed at times 1,000 and 10,000 years in the future. Dose estimates are provided for the reference site with the most highly contaminated zone vitrified and the remainder covered with a barrier.

For the exposure scenario discussed above, several pathways exist that provide a route for radionuclide transport from the waste to the biosphere. These may be generalized as groundwater transport, biotic transport (as in crops or animal products), atmospheric transport, and direct contact.

The pathways of interest to the resident individual for ISV waste forms are direct irradiation, inhalation of resuspended material, and ingestion of contaminated crops and animal products (illustrated in Figure 85). The relative importance of each of these pathways is a function of the length of exposure, as defined by the exposure scenario.

The site does not pose any hazard for transients, either as it now exists or with any barriers or vitrification applied. The dose rate at the ground surface at any time in the future will be essentially at background levels. This is shown in Table 58. The presence of the overburden on the site acts as shielding to any penetrating radiation and eliminates any possibility of inhalation of contaminated surface materials.

It is possible that a future inhabitant of the site might grow a home vegetable garden directly on top of the waste site. An effective barrier to crop penetration of the wastes, such as a rock/soil cap or vitrification, could

lower the dose potential to around 10 mrem/yr, if it did not preclude the pathway entirely. These results are also shown in Table 58.

The scenarios where selective ISV plays an important role at the reference site are those that involve physical intrusion into the actual waste zone such as well-drilling through the waste zone or digging basements, irrigation ditches, sewer lines, or highways.

A drilling scenario is the worst case for a vitrified waste form. The action of a drill bit on the hard waste causes it to fragment into very small particles that can be inhaled. However, the particles are more dense and less soluble than unvitrified soil, so their resuspension is slightly less than for soil, and the translocation of inhaled particles from lung to bone (the critical organ) is greatly reduced. The quantity of radioactive material that may be brought to the surface from drilling through a hot spot is also reduced through vitrification, since the hot spot soil is diluted by a large volume of cleaner material when the site is vitrified. Thus, even though drilling tends to maximize the exposure potential for the glassified waste, the potential doses are expected to be less than for drilling through the unvitrified soil beneath the surface of a site.

The presence of the intruder in the waste zone, as might occur from digging through the site for a basement or ditch, potentially results in an extremely high dose for nonvitrified material. The forces involved in digging result in high resuspension of the nonagglomerated soils, and therefore could result in high inhalation doses. The glass monolith of the vitrified site, however, will break into large chunks upon impact, and the fraction available for resuspension and inhalation will be very small (much less than background). This can be seen in Table 59. The dose to an intruder from the vitrified soil is actually of the same order of magnitude as that dose he might receive if he never intruded at all and only grew crops on the vitrified site (see Table 58). The process of vitrification reduces the potential dose to future intruders from that for unvitrified material.

The vitrified soil block resembles black, shiny obsidian. If a future intruder reclaimed a large piece and used it in his home (for example, to build

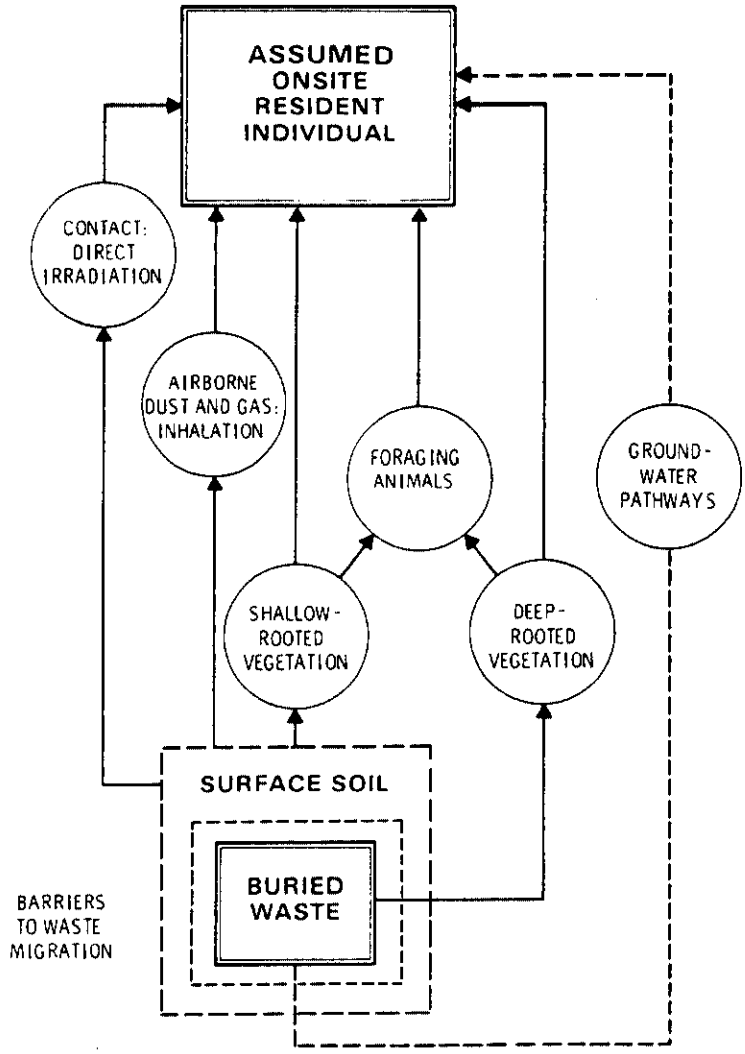

FIGURE 85. Important Exposure Pathways for the Reference Site (Napier 1982)

TABLE 58. Public Dose Estimates for Long-Term Routine Scenarios

	Year 1,000	Year 10,000
Direct Irradiation	Maximum Annual Total Body Dose	
Vitrified site	~0.0	~0.0
Ingestion	Maximum Annual Bone Dose, rem	
Vitrified site	0.01	0.01

a fireplace or coffee table), he could be exposed to direct penetrating radiation. For the radionuclide mixture in the reference site, this could result in an additional dose rate of about twice the natural background (0.1 rem) in 1,000 years, falling to an added dose rate equal to that of background in 10,000 years. These values are given in Table 59.

POTENTIAL CHEMICAL HAZARDS

The reference site has received unknown quantities of potentially hazardous organic chemicals (Owens 1981) such as CCl_4, TBP, and DBBP (dibutylbutylphosphonate). Carbon tetrachloride is a highly toxic substance and suspected carcinogen (IARC 1971). Much of its toxicity may be the result of metabolic transformations, which include conversion to chloroform, hexachloroethane, and phosgene (Cook, Daughton, and Alexander 1978; Kubic and Anders 1980). It appears that CCl_4 is relatively stable in soils and groundwater with no evidence of microbial decomposition.

The alkyl-phosphates such as TBP are apparently prone to chemical hydrolysis and therefore should be degraded in soils. However, a recent survey of Canadian drinking water supplies (Williams and Lebel 1981) shows that TBP is present in rivers, lakes, wells, and brooks. While assessments have assured rapid hydrolysis and biodegradation of alkyl-phosphates such as TBP in aquatic environments, these substances have been found in aquatic organisms.

The alkyl-phosphonates have been studied more intensively, yet firm data are still lacking. Alkyl-phosphonates such as DBBP are believed to be persistent in the environment because of the resistance of the C-P bond to chemical hydrolysis, thermal decomposition, photolysis, and biological drainage. This, coupled with the fact that alkyl-phosphonates are now being found in surface waters, suggests that they may be persistent in the environment.

Soils at the reference site probably do not support a large enough microbial population for a long enough period during the year to significantly reduce TBP, DBBP, and CCl_4, so any losses would most likely be minor, resulting from volatilization and dissolution in soil water.

TABLE 59. Public Dose Commitments for Long-Term Intrusion, rem

	Year 1,000		Year 10,000	
	1st Year[a]	50 Year[b]	1st Year[a]	50 Year[b]
Drilling				
Vitrified site	6	15	3	8
Excavation				
Vitrified site	0.006	0.02	0.003	0.008
Vitrified Curio[c]	0.2	10	0.1	5

(a) Lung dose.
(b) Bone dose.
(c) Total body dose.

Carbon tetrachloride, TBP, and DBBP present health hazards in their own right, and form other toxic substances when heated to decomposition. Several papers document the formation of perchloroethane and perchlorobenzene from thermal pyrolysis (Tsuge, Leary and Isenhour 1974; Keiter et al. 1978), and several papers describe the formation of substantial quantities of perchloroethylene from pyrolysis of CCl_4 in the presence of catalytic materials (including metal oxides) (Kuznetsov and Pekhov 1967, Dynsenov et al. 1974). Gaseous chlorine can also be expected (Jarvis 1970), as well as oxides of chlorine and phosgene. Carbon tetrachloride, tetrachloroethylene, and perchlorobenzene are on the U.S. EPA's list of 129 priority pollutants (Keith and Teilliard 1979) from industrial and wastewater discharges. However, in ISV pilot-scale tests, pyrolyzed organics ignited upon release from the melt zone and actively burned within the off-gas containment hood. An engineering-scale test with PCB-contaminated soils showed nondectable formation of secondary hazardous compounds and an overall DRE of PCBs of greater than 99.9999%. Therefore, the organics present at a particular site are not expected to pose a serious health hazard during the ISV process.

ASSESSMENT OF WASTE SITE APPLICATIONS

ASSESSMENT OF WASTE SITE APPLICATIONS

This section presents the philosophical and technical considerations for the application of ISV to the stabilization of radioactive, mixed, and hazardous chemical wastes. Prior to exploring various application scenarios, the operational capabilities and limitations of the large-scale system are reviewed.

OPERATIONAL CAPABILITIES AND LIMITATIONS OF THE LARGE-SCALE SYSTEM

The capabilities of the large-scale system to treat various soil characteristics and inclusions can be divided into two categories: 1) capabilities of the power supply system and 2) capabilities of the off-gas system to maintain a negative pressure during transient events. The capabilities of the electrical system in terms of electrode width, depth, and shape have been discussed previously.

The two factors that can influence the ability of the power supply system are the presence of groundwater and buried metals. As discussed in the Process Parameter Section, soils that have low permeabilities do not exhibit a significant effect on the ISV process, even in the water table, because the rate of recharge is not significant in terms of the processing rate. The melt proceeds at a rate of about 8 to 15 cm/h. Thus, soils with permeabilities in the range of 10^{-5} to 10^{-9} cm/s are considered vitrifiable even in the presence of the groundwater table. Soils with permeabilities in the range of 10^{-5} to 10^{-4} cm/s are considered marginal, and soils with permeabilities higher than 10^{-4} cm/s are difficult to vitrify in the water table unless additional steps are taken.

There are two common alternatives available for applying the ISV process to soils that have a high permeability and in the groundwater table. These are drawing the local water table down by pumping and installing underground barriers. A schematic of the type of conical depression that can be created by pumping is shown in Figure 86. This technique can be either effective or of limited value, depending on local groundwater gradients and the extent of groundwater contamination from the prior intrusion into the waste site. Sites near a river, where the local water table fluctuates due to seasonal variations

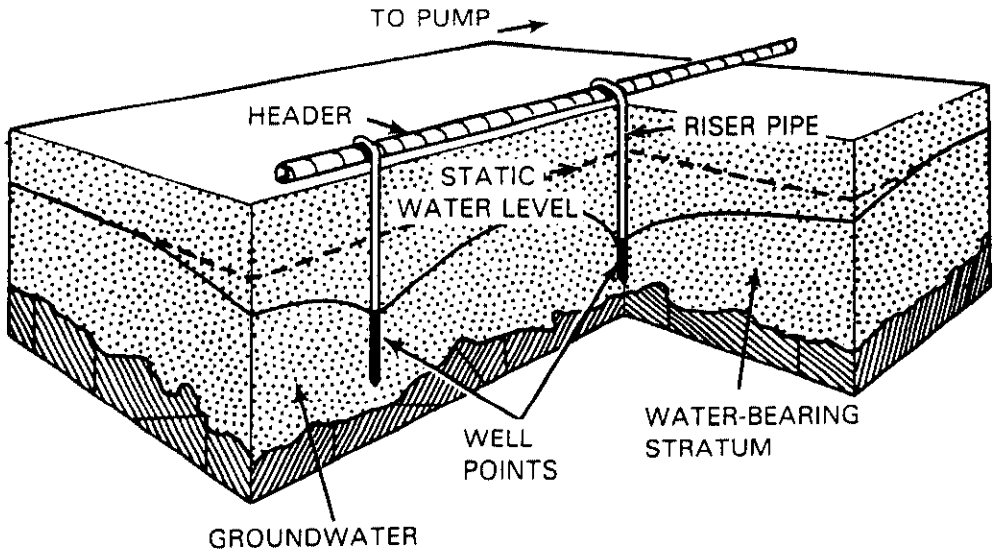

FIGURE 86. Conical Depression Created by Pumping

in the river level and where groundwater flow reversals have occurred should be carefully investigated prior to attempting a pumping operation.

The installation of barriers can divert groundwater flow from a site or limit the rate of groundwater intrusion to the site as shown in Figure 87.

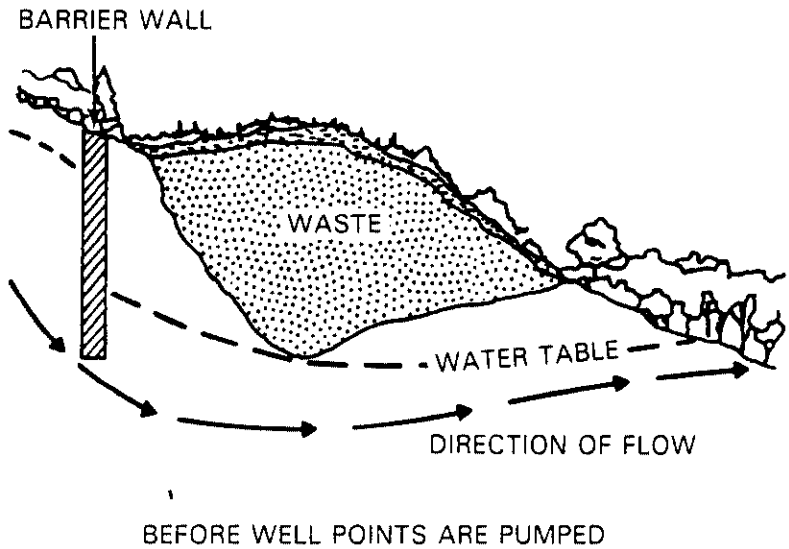

FIGURE 87. Barrier Wall to Divert Groundwater

This technique limits the rate by cutting off the direct flow into the processing site. Common barrier installation techniques range from the installation of slurry walls to the placement of sheet piling. In some cases the barrier may be formed by vitrification operations using local pumping to depress the water table during the initial processing and using the vitrified material produced during these operations as a barrier. There are several other scenarios where the two techniques may be used together.

A cursory review may produce the conclusion that these extra efforts for onsite treatment may be unwarranted. However, with the federal and state regulatory agencies moving strongly toward onsite treatment and with costs for disposal at a certified landfill rapidly increasing, these extra efforts to attain onsite treatment should not be dismissed without careful analysis.

The presence of buried metals can result in a conduction that would lead to electrical shorting between the electrodes, however, the processing margins are quite generous. Buried metals that occupy up to 90% of the linear distance between the electrodes can be accommodated without suppressing the voltage between the electrodes. Also, once melted, the impact of the metal is less significant. Miscellaneous buried metal, such as drums, should have little or no effect on the ability to process a candidate site. Metal limits by volume are currently 5 wt% of the melt. How much these limits can be increased is not known at this time. This is a large fraction when considering drums of waste. In fact, drum arrays that are placed to take advantage of the melt configuration may become a method of disposing of hazardous and/or classified wastes contained in drums (see Figure 88). Here the metal content of 273 drums in a setting is 1.5% of the melt weight, leaving a considerable capacity for miscellaneous metal contained in the drums.

The capacity of the off-gas system to maintain a negative pressure during processing, thus preventing the spread of contamination or fugitive emissions, is a function of the gas generation rate within the processing area. Gas generation resulting from the decomposition of humus and other natural chemicals in the soil are considered insignificant. Gas generating situations are generically shown in Figure 89. These represent the intrusions of the molten glass into void spaces, which result in the release of the entrapped air, penetration

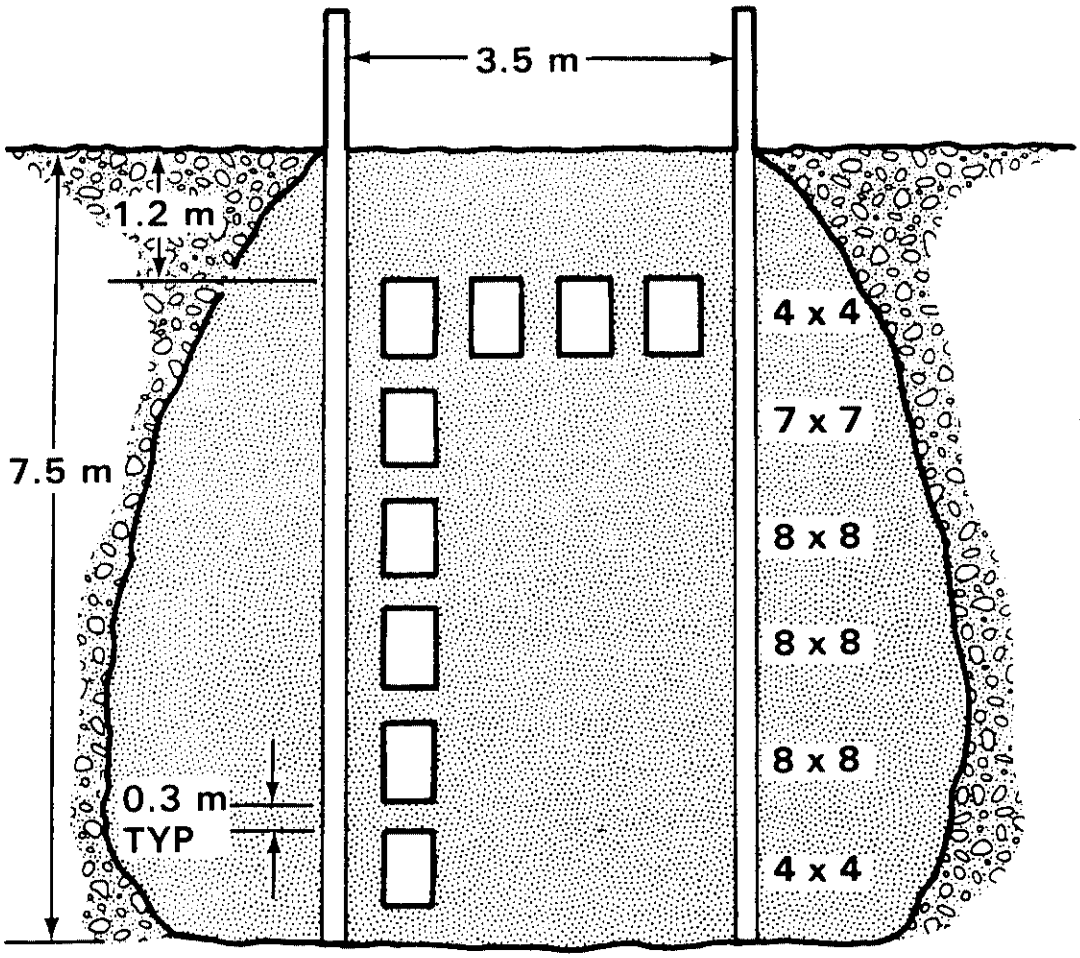

FIGURE 88. Application of In Situ Vitrification with Metal Drums (metal weight - 1.5% of melt mass; acceptable conditions: 90% linear distance and 5 wt%)

of a drum that contains combustible materials, and intrusion into soil inclusions that contain combustible materials, either solids or liquids. Schematically Figure 90 shows the capacity of the off-gas system to contain the gas resulting from the processing event. These capacities are representative of what might be encountered in a solid waste burial ground. The release of the gas is a transient event with a duration of about one minute. Therefore, once the transient event has passed, the system still has the capacity to handle another transient event. These are time order limits, not cumulative capacities.

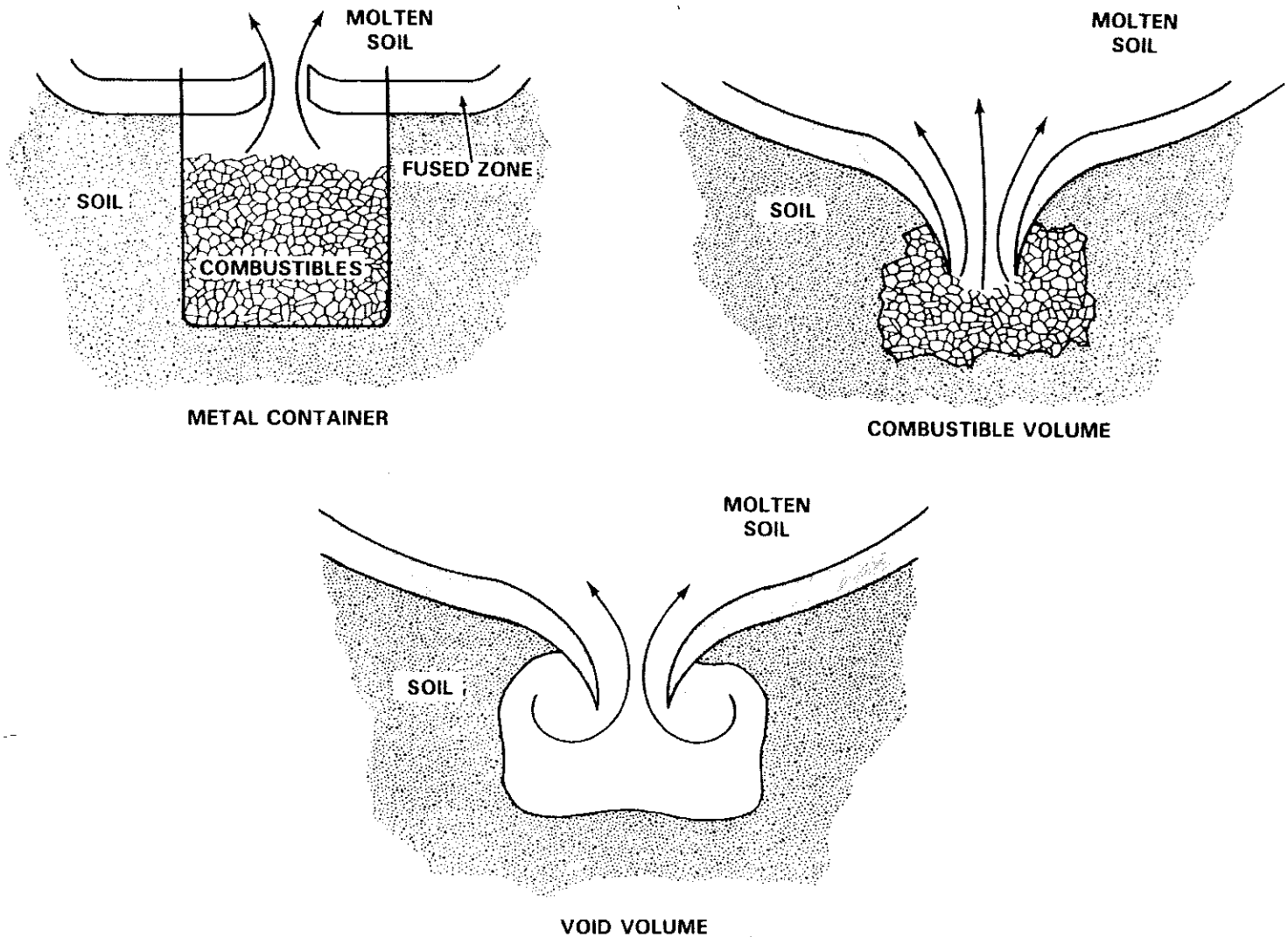

FIGURE 89. Generic Gas Generating Configurations

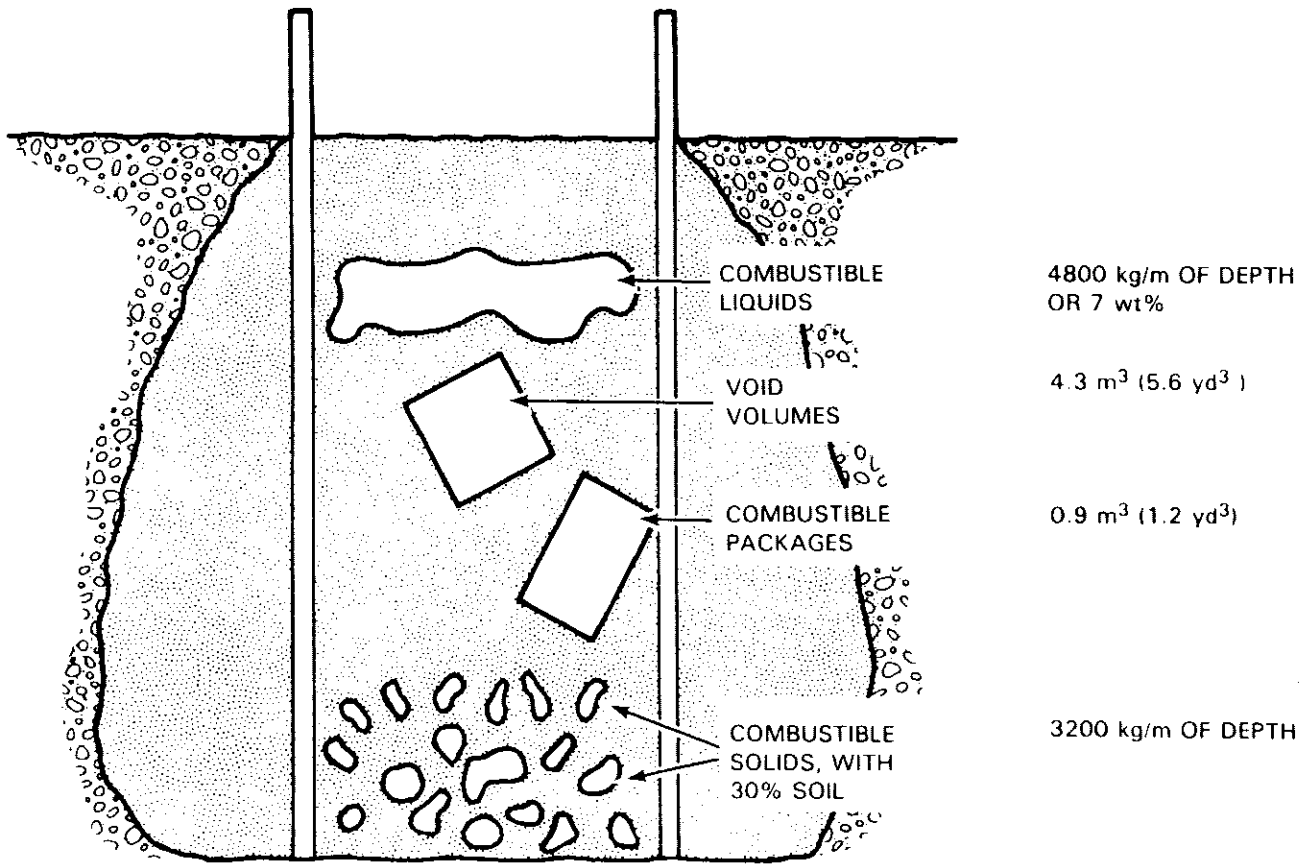

FIGURE 90. Combustible Limits for ISV Processing

The ISV process can be applied to a wide variety of waste treatment needs and, in some cases, the process can be used to produce structural materials. To facilitate the review of potential applications, the ensuing discussion is divided into four main topics: 1) radioactive wastes, 2) mixed hazardous wastes, (those that contain both radioactive and chemical hazardous materials), 3) chemically hazardous wastes, and 4) other applications such as structural barriers, footings, foundations, etc. The discussion explores potential application scenarios and presents the processing limits as they are understood based on existing data. Additional data that either define new limits or extend the potential range of applications are pointed out.

RADIOACTIVE WASTES

The focus of the ISV development program has been to develop the ISV process as an alternative technology to provide enhanced isolation and in-place stabilization of previously disposed TRU wastes. This is a portion of the program that the DOE is conducting to evaluate options for the long-term disposal of TRU wastes (DOE 1983). This effort is consistent with DOE Order 5820.2 (DOE 1984), which allows field organizations to establish new or alternative TRU waste management practices based on appropriate, documented safety, health protection, and economic analyses. The ISV process is a candidate waste management tool to provide an environmentally sound and cost-effective alternative to exhumation, treatment, and subsequent geologic disposal of previously disposed TRU waste. A discussion of the options for using the ISV process in conjunction with engineered barriers is presented by Oma et al. (1983), so only the highlights of that material are presented here.

The principal conclusion of the study (Oma et al. 1983), was that the most effective application of the technology appeared to be the selective use of ISV in conjunction with engineered barriers. Selective use should be based on performance assessment considerations and a detailed evaluation of the future hazard to mankind. For example, it does not appear to be appropriate to use a process that produces a waste form that is geologically significant on a radioactive material that has a half-life of only a few years. For very short-lived radioactive materials, simpler approaches such as maintaining administrative

control would probably be sufficient. In general, performance assessments will only show a benefit for ISV applications where the threat is toxic and persistent.

Many pre-1970 wastes were disposed of directly to the soil column in either liquid or solid form. Often, wastes currently defined as TRU wastes, were co-disposed with wastes that are currently defined as LLW. (NOTE: Remember that the term "transuranic wastes" did not exist before 1970.) The current large-scale system is designed for application to radioactive contaminated soil sites. Selective application of the large-scale system to contaminated soil sites is illustrated in Figure 91 (a tile field application). In this application, the >100 nCi/g isopleth is located immediately adjacent to the central distribution pipe, and levels rapidly drop off with distance. Subsequent installation of an engineered barrier to protect the other contaminated areas is shown in Figure 92.

Partial subsidence to eliminate large voids in contaminated soil sites may be achieved with vibratory techniques, such as those developed by Phillips et al. (1985). In candidate applications such as caissons it may be possible to pretreat the area by filling the void volumes with sand or gravel. Development and demonstration of injection techniques is needed prior to undertaking an application such as a caisson. The conceptualization of an application configuration for vitrifying a caisson is shown in Figure 93.

Further research into the mechanisms that might suppress the volatilization of radioactive materials is recommended. Elution of radioactive materials that are co-disposed near the surface with combustibles could increase release to the off-gas treatment system. An example of this is shown in the Performance Analysis Section (Figure 30) where the Cs concentration in the scrub solution increased by a step function whenever gas generating events occurred. Volatile radioactive materials could be transported up through the melt with pyrolytic gases that are generated when the molten glass contacts either solid or liquid combustibles. This transport of radioactive materials such as Cs could result in levels of activity in the off-gas treatment system that would impact contact maintenance operations. Materials could be added that would result in increased scrubbing of the pyrolytic gases, thus, increasing the

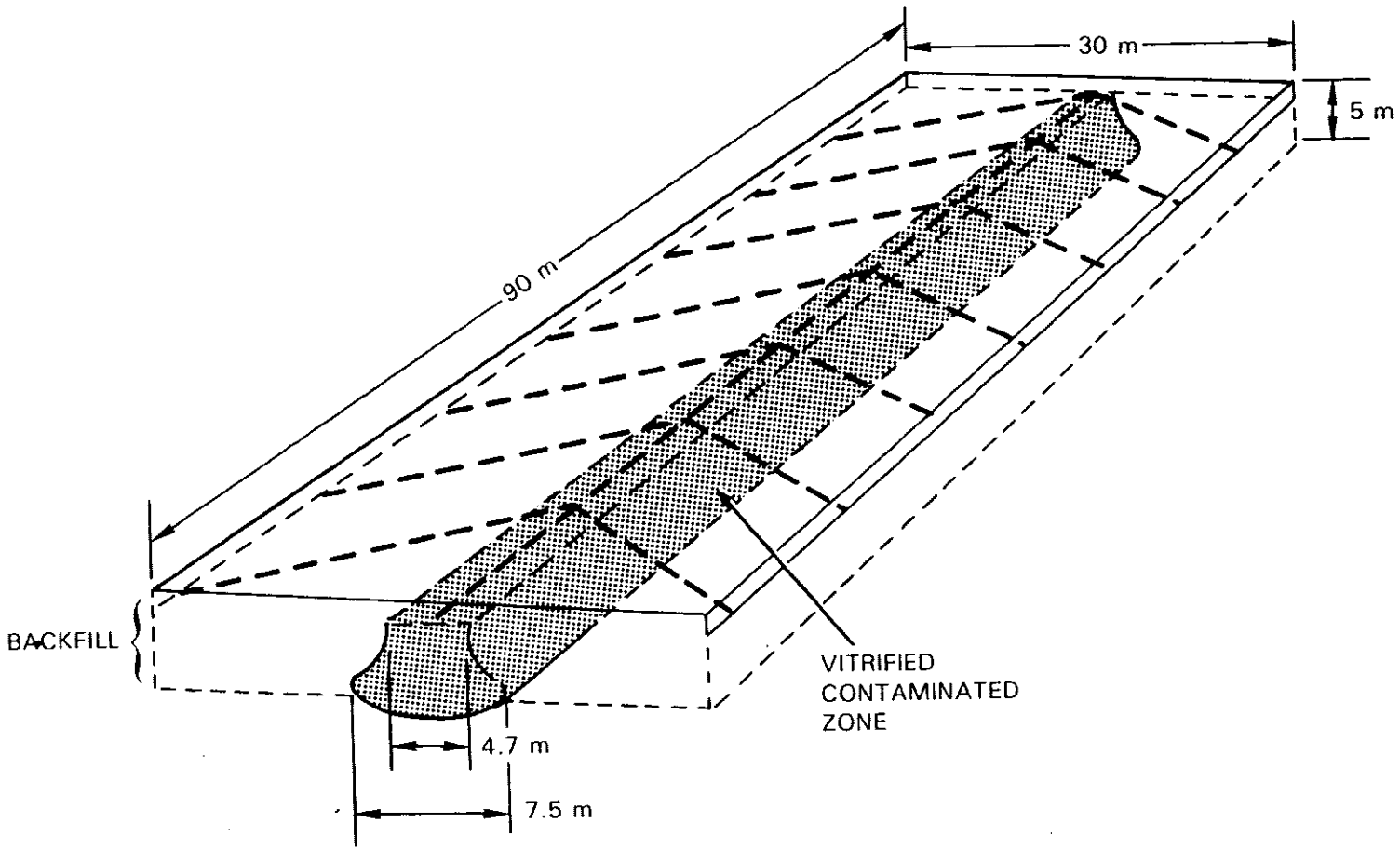

FIGURE 91. Selective Vitrification of a Tile Field and Crib

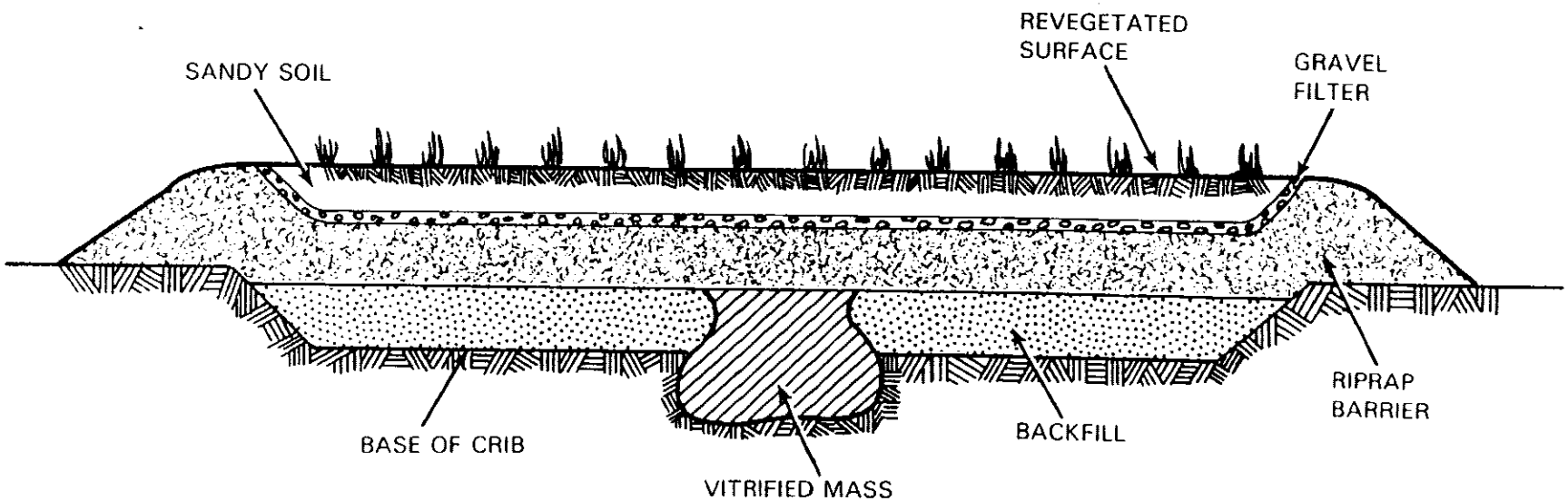

FIGURE 92. Cross-Sectional View of Vitrified Zone and Engineered Barrier

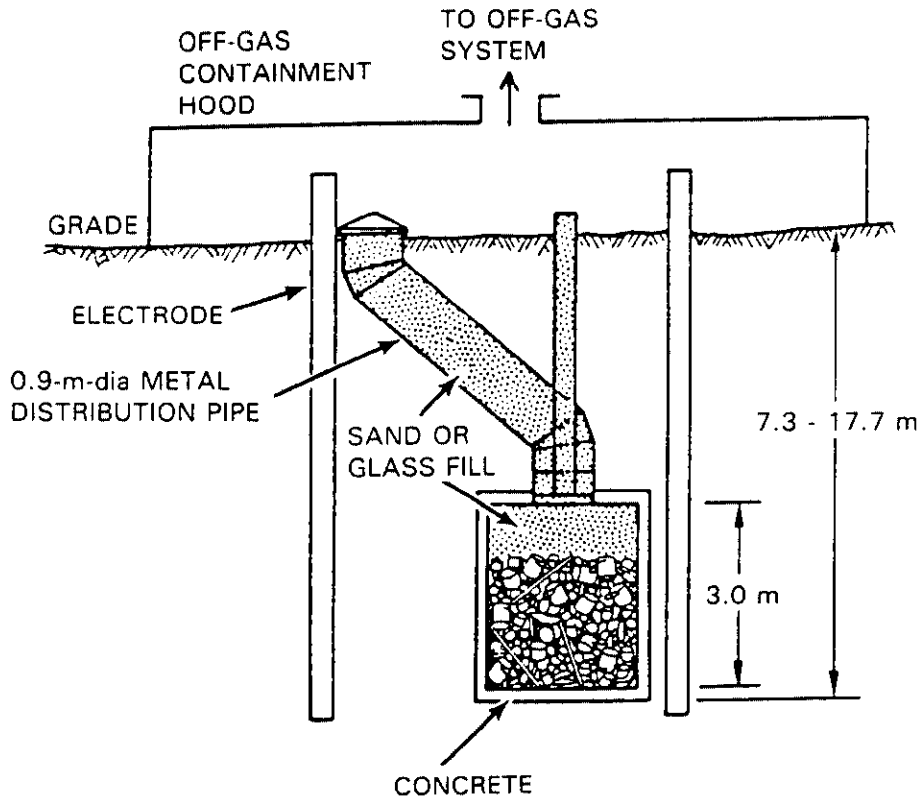

FIGURE 93. Vitrification of a Typical Hanford Caisson

retention. Analyses of data show that increased depth is an effective retention device; therefore, adding clean overburden to the surface will improve retention. However, feasibility tests to determine the actual retention factors for specific applications are recommended. A recent study for ORNL showed that Cs retention factors as high as 10^4 can be achieved.

MIXED HAZARDOUS WASTE

In situ vitrification is particularly well suited to in-place disposal of mixed hazardous waste. The radioactive and toxic heavy metals are encapsulated or incorporated into the glass, and the organics in containers are destroyed. Certain inorganic compounds such as nitrates are also destroyed by the reducing conditions of the melt, as explained in the Performance Analysis Section. This is particularly fortuitous because nitrates are very common in mixed hazardous waste. Sulfates are partially decomposed and the remainder can easily be

removed by the off-gas treatment system. Up to 98% of fluorides are retained in the molten soil for source terms of several hundred parts per million. The fluorides that are not dissolved in the glass can be scrubbed out by the off-gas treatment system using a caustic scrub solution.

There are four general areas where the ISV process might be applied to mixed hazardous waste: 1) contaminated soil sites, 2) tanks that contain a hazardous heel in the form of either a sludge or salt cake, 3) classified or mixed waste that is already in containers or amenable to being placed in containers, and 4) process sludges and tailings piles that contain radioactive materials. The application of the ISV process to mixed hazardous waste soil sites is similar to its application to general soil sites that was discussed in the beginning of this section with the same processing limits for metal and combustibles.

The use of ISV to immobilize and/or destroy the toxic heel in tanks has been tested in the engineering-scale unit with simulated fission products and chemical salts. The results of the feasibility study showed that the release of fission products was within acceptable limits for the off-gas system and that a vitreous mass was formed. The original tests were performed on the basis of adding glass formers during processing to achieve a vitreous waste form. The data could be extended to a scenario that would dispose of the residual heel and the tank, and immobilize the contaminated soil in the immediate vicinity of the tank. By adding soil and/or rock backfill, the tank could be filled with glass-forming materials prior to processing. This could eliminate the concerns about tank dome and/or wall collapse that were identified during the original testing. Techniques for filling to the peak of the tank dome have been developed (Anderson, McKenney, and Adams 1985). Electrodes would be inserted into the tank through existing openings as shown in Figure 94. The vitreous area would grow downward and outward encompassing the tank, its contents, and a portion of the surrounding soil. Estimates of the maximum size of tank that can be processed by this technique indicate that tanks in the range of 100,000 to 300,000 gal could be permanently disposed of by this technique. By appropriately placing the electrodes, larger tanks may

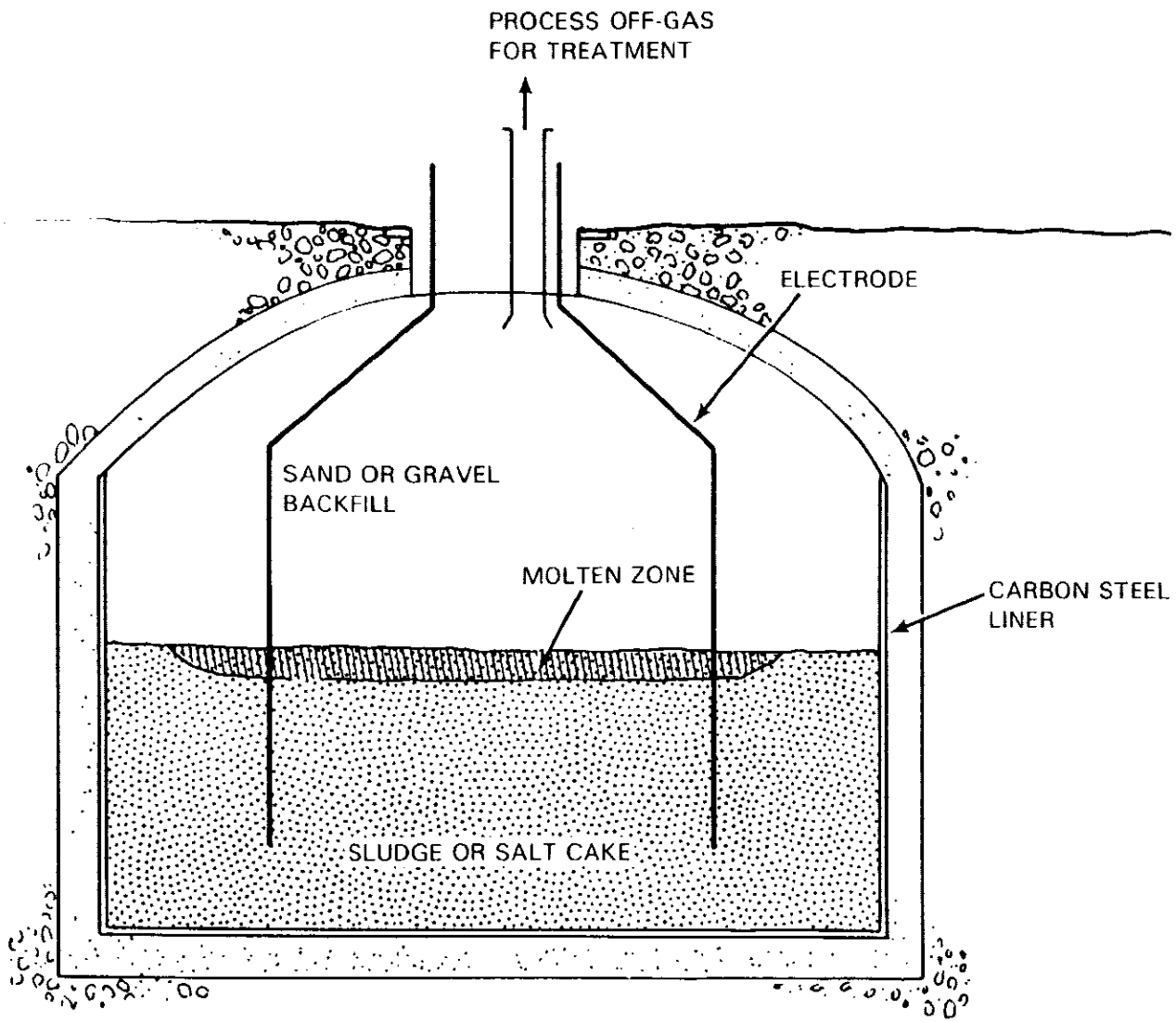

FIGURE 94. Cross Section of a Tank Undergoing Vitrification

be processable by multiple settings. The metal content of the tank structure would not impose a processing limit, provided the electrodes are positioned properly.

Classified waste can contain hazardous and/or radioactive material. In general, the classified waste will be classified either by configuration, composition, or both. A process like ISV will destroy the classification by melting and changing the configuration and/or changing the composition. Classified waste that is mixed with hazardous waste is especially troublesome because it cannot be sent to an uncontrolled hazardous landfill nor can it be placed in a radioactive burial ground. Classified waste in containers or classified waste that can be placed in containers is amenable to declassification and destruction by the ISV process. Containers can be placed in the ground in an array similar to the array of drums shown in Figure 88. Electrodes can be placed during the filling operation, and the soil backfill will provide sufficient glass formers to produce a vitreous mass after processing. Wooden and/or cardboard containers may also be used. The main requirement is to provide sufficient backfill over the containers so that the process is not impeded by the flow of glass into the top row of containers. Also, 0.3 m of backfill between each row of buried containers is recommended.

Process sludges and tailing piles that contain natural radioactive materials and hazardous chemicals can be processed by the ISV process. Applications that involve natural radioactive elements that result in relatively high Rn fluxes at the surface are considered potential candidates for remediation by ISV. Tests with zirconia/lime sludges showed that the material was not only vitrifiable, but that the Rn emanation level was reduced by a factor of greater than 10^3 after processing (Buelt and Freim 1986). This is a practical solution where the Rn emanation levels are high. However, for large piles, barriers over the pile have also been shown to be quite effective. Each potential application must be examined on its own merit for its ability to conform to environmental regulations and for its cost-effectiveness.

In general, the mobility of metals, inorganics, and organics in containers will not be a factor when considering processing scenarios. The area of uncertainty is the mobility of the low-boiling-point, uncontained organics. To

understand this concern, it is necessary to examine the thermal profile in the vicinity of the vitreous mass. Figure 95 shows the isotherms around an ISV melt during processing. The 100°C isotherm is about 20 to 30 cm away from the molten material. The 400°C isotherm is only 5 to 8 cm away from the molten

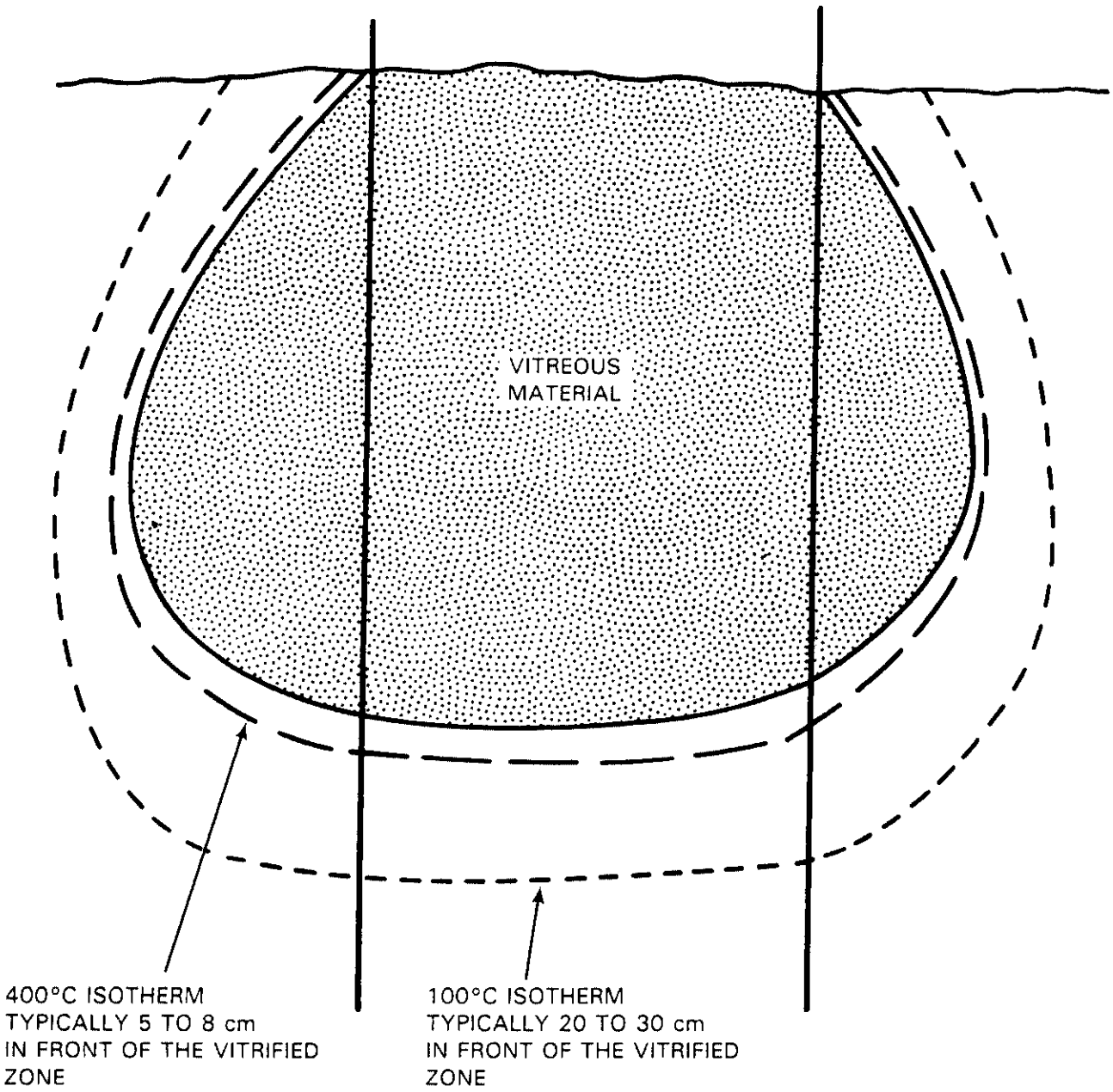

FIGURE 95. Isotherms Around an ISV Melt During Processing

zone. However, most organics of concern are volatile in or near the 100°C to 200°C isotherms, hence, the cause for concern. How organics will behave in this temperature regime is not well understood. There is a variety of competing forces and these forces are greatly influenced by the properties of the soil, which further complicates the assessment. Organics will volatilize and tend to migrate away from the heated area. Their movement is retarded by the sorptive properties of the soil for the contaminant(s) of interest, in both the liquid and gas phase. Capillary action in the liquid phase tends to draw the organic back into the heated area. The literature lacks appropriate technical data from which to make a theoretical estimate. It is even likely that once volatilized, the vapor will move up the isotherm to the surface where the materials will be combusted. The only way that a degree of certainty can be established is by obtaining empirical data from site-specific experiments. An experimental apparatus for measuring the mobility of organics is shown in Figure 96. By maintaining a negative pressure on the sample cups and by sampling with chromatographic techniques, the distribution of organics in the vicinity of the molten zone can be determined. It is strongly recommended that samples for the actual site be tested to ensure that the correct soil characteristics are evaluated.

HAZARDOUS CHEMICAL WASTES

Much of the material presented in the sections on radioactive and mixed hazardous waste is applicable to hazardous chemical wastes with three important differences: 1) the hazardous chemical waste is more amenable to supplementary handling operations without having to employ a confinement structure such as a greenhouse, 2) once treated by the ISV process, the waste may be reclassified as nonhazardous (delisted), requiring no further administrative control of the processing area, and 3) onsite treatment avoids the extended liability associated with shipping hazardous waste to a landfill.

In situ vitrification is applicable to two general areas of hazardous waste treatment: 1) contaminated soil sites [either Comprehensive

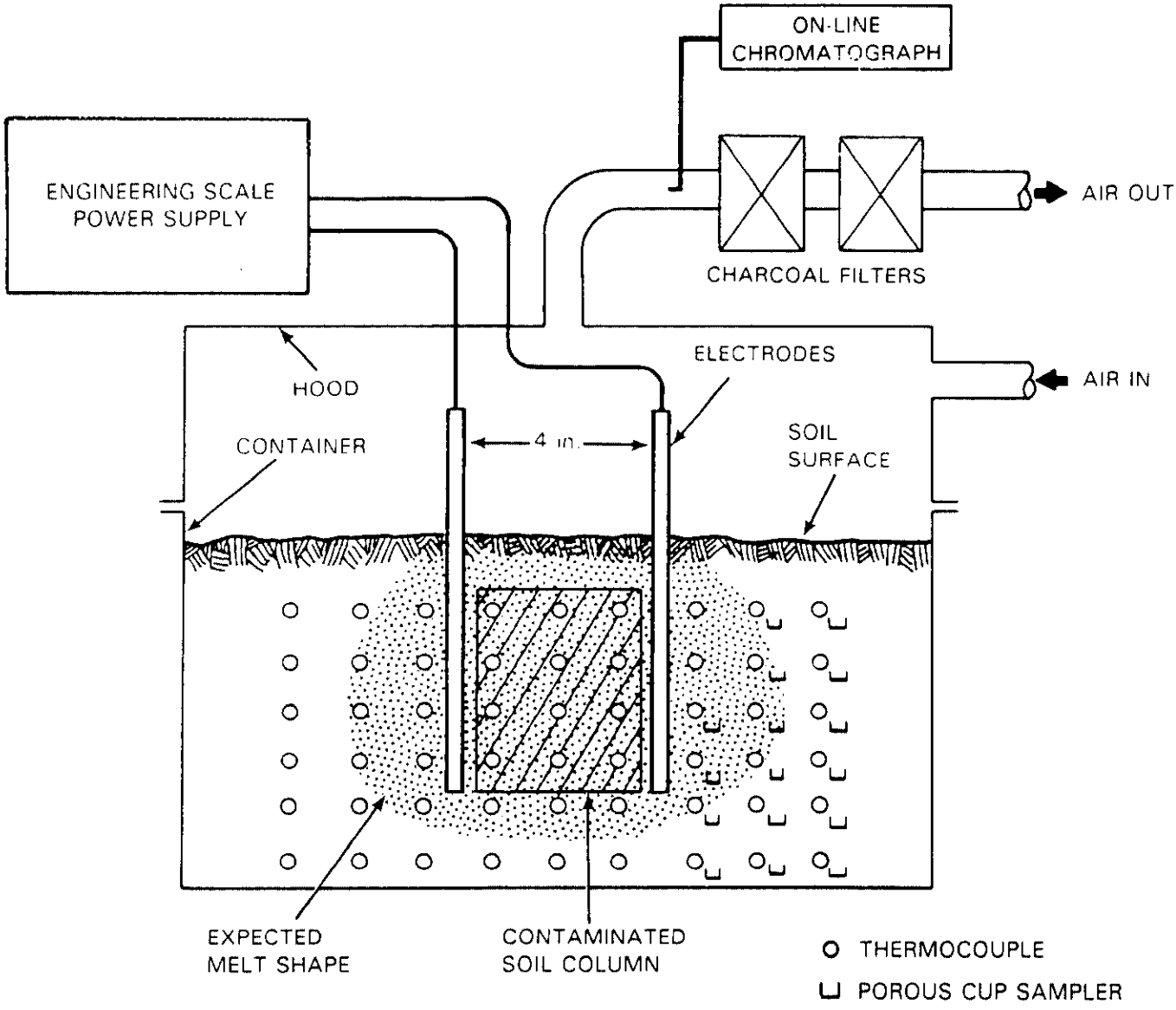

FIGURE 96. Experimental Apparatus for Determining ISV Effectiveness on Organically Contaminated Soils

Environmental Response Compensation Liability Act (CERCLA) sites or Resource Conservation and Recovery Act (RCRA) surface impoundments], and 2) process sludges and tailings piles.

The principal difference between handling soil sites that are contaminated with hazardous chemicals and handling those that are contaminated with mixed

hazardous or radioactive is the ability to use conventional earth-moving techniques to stage or move soils to a centralized treatment area. Where the contamination is 3 m or more deep, this consolidation is not a major consideration. In these cases, the ISV process is employed using one machine (as previously described with the three trailers and the hood) and moving the machine from electrode placement to electrode placement. For this conventional type of application of ISV, the only post-treatment action required is the acquisition and placement of clean backfill. This type of scenario applies to a relatively large area, usually an acre or more where the site is vitrified to depth. For large areas (several acres) it may be desirable to employ more than one machine to complete processing at a faster rate. An alternative would be to employ two power supplies and a single off-gas treatment system, thus doubling the processing rate with only one basic machine, plus nominal extra equipment. The advantages of this type approach are twofold: 1) the off-gas treatment system usually comprises 80% of the capital costs where the electrical power supply comprises about 20% of the capital costs and 2) greatly reduced labor costs. It should be quite possible for a crew of two to operate two power systems and a single off-gas treatment system, thereby effectively cutting operational labor costs in half.

However, where the soil is contaminated to depths of only 0.6 to 1.5 m it is much more economical to stage the contaminated soil to a treatment area or a trench. At such shallow depths, the time for processing will equal the time required to move to the next processing position, and the economics of the operation will be significantly affected. Where there are large volumes of soil, it may be prudent to consider operation with two power systems, with the trailers between the two processing trenches.

Valuable land that is contaminated can be reclaimed by processing, thereby converting a corporate liability to a capital asset. Old transformer and capacitor storage and repair areas that are now in the business district, but contaminated with PCBs, are an example of this concept. The ISV process has been shown to be effective on PCB-contaminated soils, achieving a system DRE of 99.9999% (Timmerman 1986). Further, there will be some limitations associated with equipment access, however, these can usually be dealt with by a

combination of equipment design and staging operations. Also, simplifications in the equipment can be achieved if the task is large enough to support single mission equipment. This would require that the client have several such sites or combine the investment with companies that have similar needs. This rationale is not limited to PCBs; other potential candidate industries are plating companies or manufacturers that employ plating as part of their manufacturing process.

For surface impoundments, it is often desirable to consolidate the waste to one area for treatment. The moisture removal and chemical destruction that occurs during processing often leads to volume reductions of 5 or more. With the zirconia/lime sludge, the volume reduction obtained was 3.2, but with alternate application configurations, volume reductions greater than 10 could be attained. This volume reduction combined with chemical destruction often will simplify the requirements for the off-gas treatment system to where a single venturi-ejector scrubber is all that may be required if any off-gas treatment system is required. The consolidation also makes previously contaminated land available for other uses. Land reuse can be an important consideration depending on the plant location, and this consideration should be figured into the overall economic assessment when selecting a treatment process.

Shipping to a hazardous waste landfill is becoming more expensive and the "gate charges" are approaching $\$260/m^3$ for simple wastes. For wastes that require special treatment or handling the cost is even greater. However, from a corporate viewpoint, the real cost may be even greater when the strict, joint and several liability for future environmental impairment is considered. The extended liability and the associated publicity should be of great concern to the larger waste generators. These same considerations apply to onsite disposal facilities, process sludges, and tailings piles. The corporate priorities in descending order of importance, should be waste minimization or avoidance, recycle, and onsite treatment.

In some cases where volume reduction attained by the thermal treatment is high, as with some hazardous waste sludges, it may be more prudent to consolidate the materials into a single setting by conveying sludge or contaminated soil to the electrodes. This is especially true when the contamination depth

is shallow (i.e., less than 5 m). In these cases, feeding sludges to the electrodes would eliminate the amount of downtime necessary to move process equipment from setting to setting. Feeding sludges to the electrodes would also consolidate all the sludge at a disposal site into a much smaller area, leaving the remainder of the disposal site available for future operations. One feeding technique may be repetitive batch operations to consolidate large quantities of material into one electrode setting. Another vitrification technique, continuous feeding, is analogous to the feeding techniques employed by glass-production furnaces and high-level nuclear waste electric melters. However, the ISV process eliminates the capital necessary for the melter and its support equipment and the costly glass-pouring operation.

In the repetitive batch feeding approach, sludge or contaminated soil could be piled 9- or 10-m high in a culvert as shown in Figure 97. In the cases where volume reduction is extreme, (i.e. >5), 1 m of soil may be necessary on the surface to achieve startup. Vitrification would be initiated at the surface and would consolidate all the sludge within the confines of the electrodes leaving a vitreous mass at the bottom. More sludge would then be added to the top of the culvert, soil would be added to the surface, if necessary, and the melting process would be reenacted. This procedure would be continued until the vitrified material is brought to the desired grade level. The process would then continue in an adjacent culvert while the vitrified sludge in the original culvert cooled. Since the vitrified sludge would never come in contact with the culvert, the culvert could be reused, limiting the number of culverts for the entire operation to two. This type of operation can result in tremendous cost savings in electrode materials and equipment movement operations.

Continuous feeding is done routinely in the glass and high-level nuclear waste industries. With continuous feeding, waste materials are fed directly onto the molten surface. The sludge may be fed onto the molten surface by a conveyor belt through the off-gas hood as shown in Figure 98. Then, an off-gas blower can draw air through the sludge inlet opening to prevent the direct release of process effluents. The material is accumulated on the molten surface to form a batch blanket or cold cap. Semivolatile constituents, such as

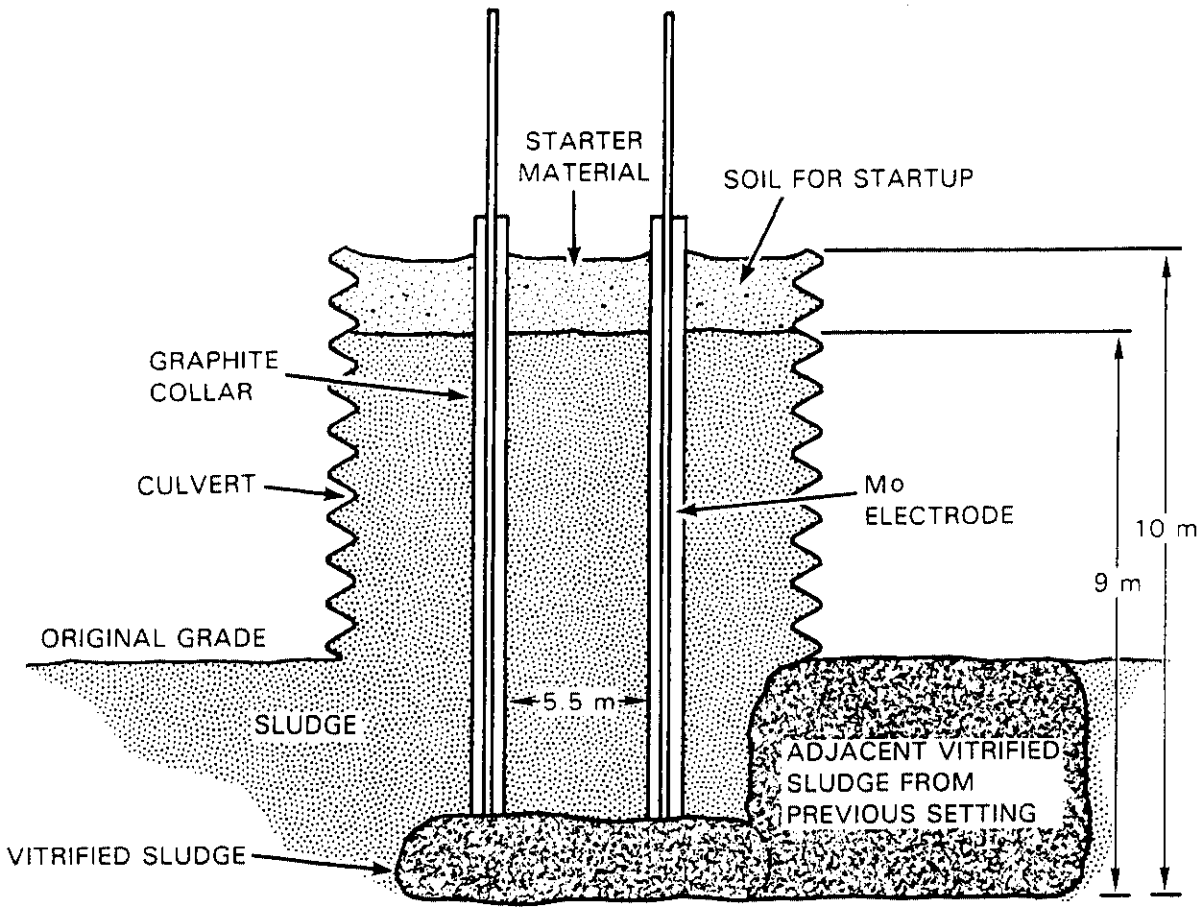

FIGURE 97. Repetitive Batch Operation

fluorides, heavy metals, and heavy organics that tend to migrate out of the molten zone or lower regions of the batch blanket, are condensed in the upper, cooler regions of the batch blanket and recycled back to the vitreous zone (Tooley 1974). The continuous feeding technique also holds tremendous potential for reducing operational costs when consolidating sludges or contaminated soils into a smaller area. However, when movement and handling of contaminated soils are impractical or hazardous, such as with TRU-contaminated soils movement of the process equipment to individual settings is required.

Other Applications

Structural testing has shown that the ISV product is very strong. The data are shown in Table 60.

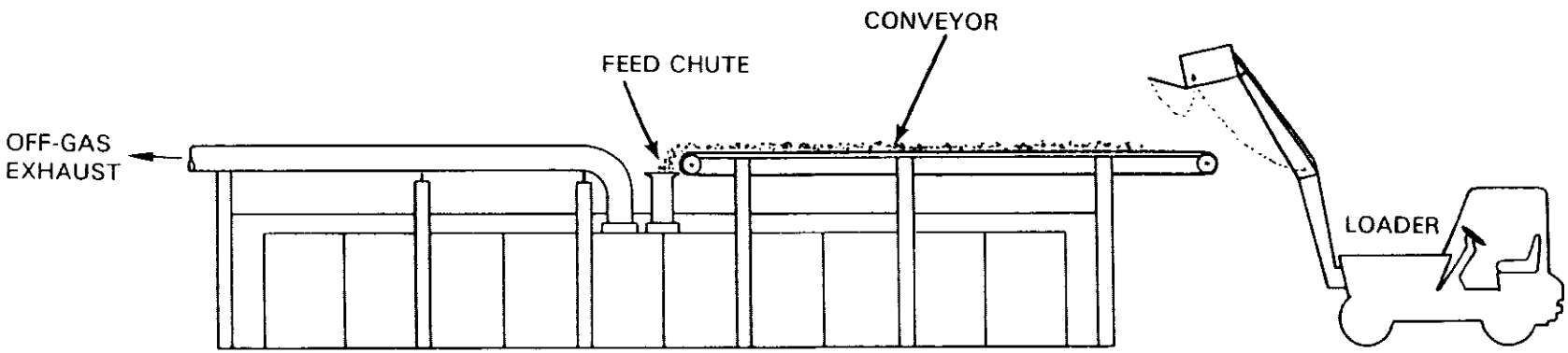

FIGURE 98. Off-Gas Hood and Sludge Conveyor

TABLE 60. Comparison of the Strength of Concrete and Vitrified Soil

	Concrete	Vitrified Soil
Compressive Strength (psi)	3,000 to 8,000	35,000 to 45,000
Splitting Tensile Strength (psi)	400 to 600	4,000 to 8,000

The structural properties of the ISV product are about one order of magnitude higher than those of unreinforced concrete. This has lead to the conceptualization of a variety of applications that supplement waste disposal operations and some applications that are completely independent of waste management operations.

An alternate waste management technique would be to use ISV to produce a barrier around a hazardous waste site where groundwater intrusion is a concern. This concept is shown in Figure 99. In this concept the molten material is fused to an underlying impermeable layer to achieve a water seal. It is recognized that there are many other types of barrier systems, including slurry walls, injected grout curtains, and poured-in-place walls. However, there are many chemicals that leach out of hazardous waste sites and interfere with the setting of cementitious products, thus leading to the formation of windows or

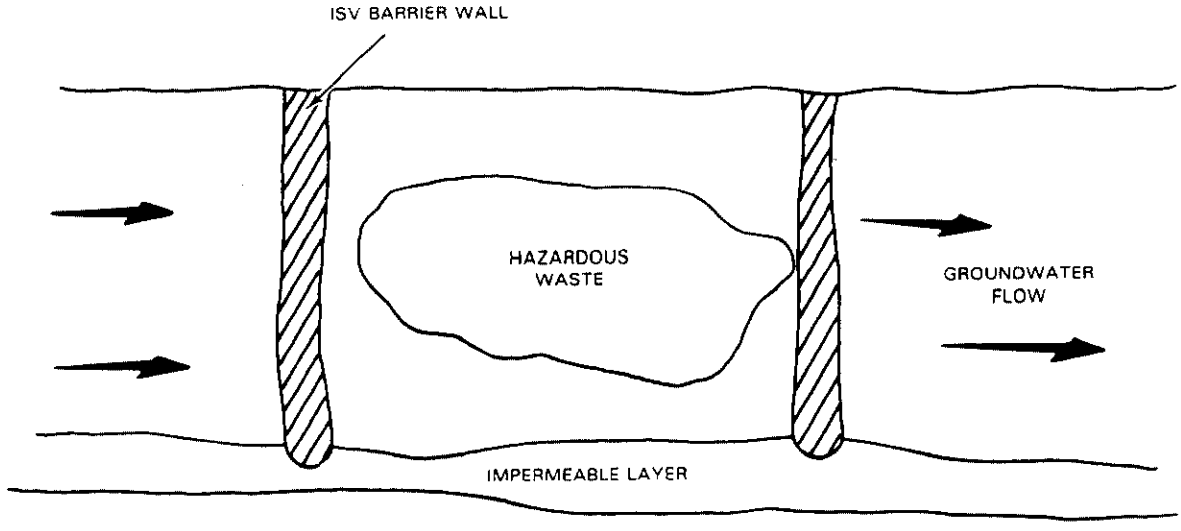

FIGURE 99. In Situ Vitrification Barrier Concept

holes in the walls. When these chemicals are present at a site, a glass wall may be a cost-effective way to halt the migration of chemicals away from the site.

The early engineering-scale tests employed two electrode systems, thus testing the basic concept of generating underground ISV barriers. The remaining development activity is to tailor the thickness of the wall so that the resultant barrier is reasonably cost competitive. Logical approaches for achieving the tailoring would be to inject flux materials into the area to be processed, lowering the melting temperature of the soil. Another possible technique would be to place the electrodes at angles that retard the spread of the melt width as the molten zone grows deeper. Some consideration has been given to a movable electrode system, much like a ripping bar, but to be successful, this must be combined with the flux additions. Even if ISV barriers are not considered a permanent solution, they may be a very cost-effective interim solution where significant intrusion has occurred and plans for final remediation have not been completed. The barrier would be very strong and there should be no problems with driving heavy equipment over the site. Prudent engineering would indicate that the installation of a clay cap in the subsidence zone associated with the barrier would help to ensure that there was no damage from the movement of heavy equipment. This is a common technique used to protect slurry walls and no new technology is required. Subsequent installation of a clay cap over the site would help to prevent water intrusion from precipitation of burial sites, thus eliminating the potential for creating a "bath tub" effect that could fully saturate the confined wastes.

As a derivative of the barrier concept, the ISV process could be used to generate footings and structural foundations as shown in Figure 100. While this application will not find much application in the contiguous 48 states because of the relative availability and low cost of concrete, to remote areas this may prove to be a cost-effective application. For example, in the days of the Alaskan pipeline, concrete was $\$780/m^3$ delivered to the site. Placement costs were in addition to that cost. Also, concrete for footings for school buildings in the Aleutian Islands is currently in the range of $\$780/m^3$. Considering that the structural applications would not require an off-gas

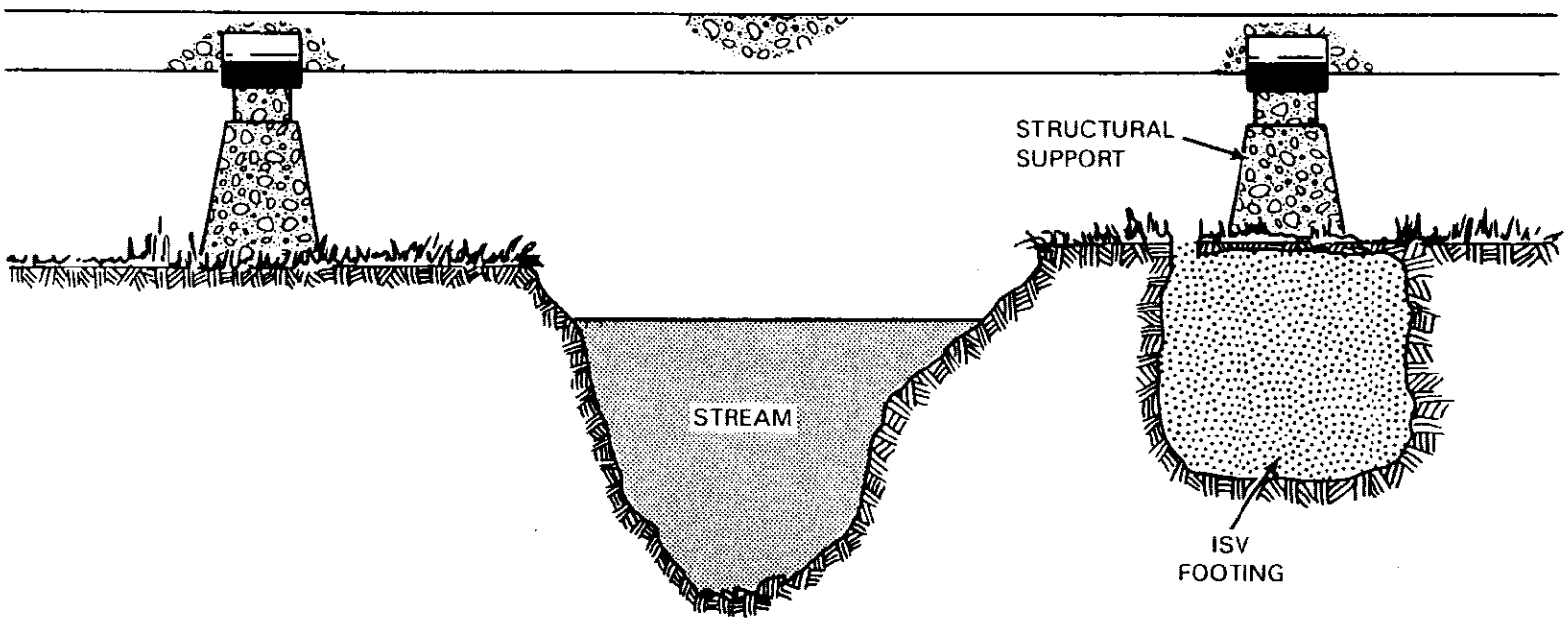

FIGURE 100. Generation of Soil Stabilization/Footing and Foundation

treatment system, the costs for generating footings in place would be on the order of \$190 to \$260/m^3. Further, without an off-gas treatment system, only one trailer would be required to transport the processing equipment, thus simplifying the transportation and site access requirements. Another application would be the onsite generation at Prudoe Bay of rip-rap for ice armorment systems for drill islands in the Beauford Sea. Blocks could be generated as slabs employing the two electrode system or as blocks with the four-electrode system. The former is recommended because quarrying the block may induce stress risers that weaken the remaining structure. There are a variety of alternate scenarios, but the key to consideration of the process is a remote site where cement is over \$260/m^3 delivered.

The process may also be used for sealing shafts to prevent the intrusion of water in the distant future. Such an application could be used in the selective placement of seals in a repository shaft. The concept is illustrated in Figure 101. Backfill would be placed along with the electrodes in the shaft, and the melting process would not only melt the backfill, but the liner, the grout behind the liner, and the disturbed rock zone. This may reduce the crack density to more nearly that of the host rock. The length of the seal would be controlled by adding additional backfill during processing and by withdrawing the electrodes. Seals up to 30-m long appear to be quite feasible. The economic incentive for such an application is that the liner does not have to be removed and the disturbed rock zone may be annealed, thus limiting the pathways for water intrusion. Removal of a shaft is a complicated and expensive operation with considerable risk associated with subsequent operations. If the idea of placing hazardous waste in old lead mines gains acceptance, then ISV could be used to seal the mine shaft. The number of seals required would depend on the location of aquifers with respect to the shaft. Seals above and below aquifers would seem to be prudent as a general rule. The concept was tested on a proof-of-principle basis during one of the LSOATs. A 0.3-m x 0.3-m x 2.4-m basalt monolith was buried adjacent to the area to be vitrified and steel and grout were affixed to the top of the basalt to simulate a liner. The block was exposed after the processing and cored to obtain samples of the interface material. Samples taken from five different locations show excellent fusion between the basalt and the vitreous material. Considerable testing

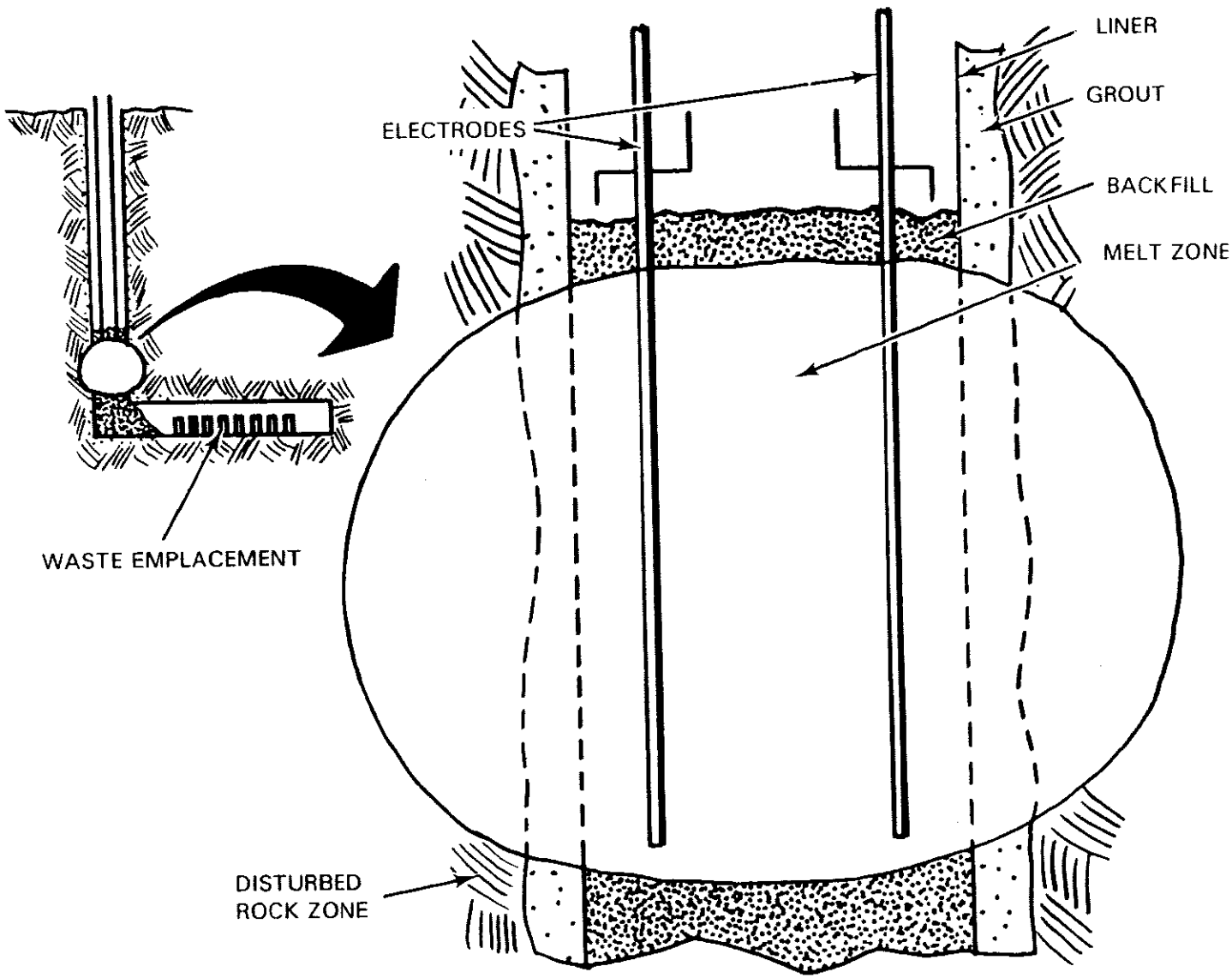

FIGURE 101. Shaft Sealing with In Situ Vitrification

would be required to validate this technique for use in an actual repository. Tests in an exploratory shaft would probably be required to determine the performance with in situ rock stresses.

REFERENCES

REFERENCES

American Conference of Governmental Industrial Hygienists. 1984. Threshold Limit Values for Chemical Substance and Physical Agents in the Workroom Environment. Cincinnati, Ohio.

American National Standards Institute. 1975. "Nuclear Criticality Safety in Operations with Fissionable Materials Outside Reactors." ANS-8.1, ANSI N16. 1-1975, American Nuclear Society.

American National Standards Institute. 1982. "Nuclear Criticality Control of Special Actinide Elements." ANS-8.15, American Nuclear Society.

Anderson, B. N., D. E. McKenney, and M. R. Adams. 1985. "Single-Shell Tank Technology Demonstration," Waste Isolation in the U.S. Technical Programs and Public Education. Paper presented at Symposium on Waste Management, March 24-28, 1985, Tucson, Arizona.

Bates, J. L. 1975. Properties of Molten Coal Slags Relating to Open-Cycle MHD. Final report to the National Science Foundation. BNWL-B-466, Pacific Northwest Laboratory, Richland, Washington.

Brouns, R. A., J. L. Buelt, and W. F. Bonner. 1983. "In Situ Vitrification of Soil." U.S. Patent 4,376,598, March 1983.

Buelt, J. L., et al. 1979. A Review of Continuous Ceramic-Lined Melters and Associated Experience at PNL. Presented at The International Symposium on Ceramics on Nuclear Waste Management in Cincinnati, Ohio, April 1979.

Buelt, J. L., V. F. FitzPatrick, and C. L. Timmerman. 1985. "Waste Management-Electrical Technique for In-Place Stabilization of Contaminated Soils." Chemical Engineering Process, March 1985, pp. 43-48.

Buelt, J. L., and J. G. Carter. 1986a. In Situ Vitrification Large-Scale Operational Acceptance Test Analysis. PNL-5828, Pacific Northwest Laboratory, Richland, Washington.

Buelt, J. L., and J. G. Carter. 1986b. Description and Capabilities of the Large-Scale In Situ Vitrification Process. PNL-5738, Pacific Northwest Laboratory, Richland, Washington.

Buelt, J. L., and S. T. Freim. 1986. Demonstration of In Situ Vitrification for Volume Reduction of Zirconia/Lime Sludges. Prepared for Teledyne Wah Chang, Albany, Oregon, under Contract 2311205327. Pacific Northwest Laboratories, Richland, Washington.

Chedin, J., A. Tribot, and S. Feneant. 1948. "The Particulate State of Concentrated Nitric Acid and the Nitrating Ability of Cellulose." Comptes Rendus 226:2068-70.

Clayton, E. D. 1979. Anomalies of Nuclear Criticality. PNL-SA-4868, Rev. 5, Pacific Northwest Laboratory, Richland, Washington.

Cook, A. M., C. B. Daughton and M. Alexander. 1978. "Phosphate Utilization by Bacteria." Journal of Bacteriology 133(1):85-90.

Crawley, D. T. 1969. Plutonium-Americium Soil Penetration at 234-5 Building Crib Sites. ARH-1278, Atlantic Richfield Hanford Company, Richland, Washington.

Davies, P. R. H., and R. D. Argent. 1985. "Use of Molybdenum by the Glass Industry in the Glass Melting Process." In Proceedings for Symposium on Physical Metallurgy and Technology of Molybdenum and its Alloys. 1985, Ann Arbor, Michigan.

Del Toro, V. 1972. Principles of Electrical Engineering. Second edition. Prentice-Hall, Inc., Englewood Cliffs.

Dobratz, B. M. 1981. LLNL Explosives Handbook. UCRL-52997, Lawrence Livermore National Laboratory, Berkeley, California.

Doree, C. 1933. The Methods of Cellulose Chemistry. Van Nostrand, New York.

Dynsenov, M. I., G. I. Nikishin, Zh. B. Dandybaev, M. Zh. Zhanshin, and T. G. Sarbaev. 1974. "Preparation of Perchloroethylene by Carbon Tetrachloride Pyrolysis." Dokl. Resp. Nauchno-Tekh. Konf, Neptekhim, 3rd Vol. 1:119-126. Chem. Abst. 83(21)178187.

Electric Power Research Institute. 1982. Technical Assessment Guide. EPRI-2410-SR, Prepared by EPRI Planning and Evaluation Division, May 1982, Electric Power Research Institute, Palo Alto, California.

Engel, R. L., J. Greenborg, and M. M. Hendrickson. 1966. ISOSHLD--A Computer Code for General Purpose Isotope Shielding Analysis. BNWL-236, Pacific Northwest Laboratory, Richland, Washington.

Ewing, R. C., and R. F. Hoaker. 1979. Naturally Occurring Glasses: Analogues for Radioactive Waste Forms. PNL-2776, Pacific Northwest Laboratory, Richland, Washington.

Flanders Filters. 1984. "Nuclear Grade HEPA Filters," Bulletin No. 812A. Washington, North Carolina.

Friedman, I., and W. Long. 1976. "Hydration Rate of Obsidian." Science 191, 347.

Friedman, I., and J. Obradovich. 1981. "Obsidian Dating of Volcanic Events." Quarternary Research, 16:37.

Gibson, M. W. 1982. Estimated Radioactive Waste Inventories and Contaminated Soil Volumes at Hanford. RHO-SD-RE-TI-017, Rockwell Hanford Operations, Richland, Washington.

Harada, T., et al. 1972. "Strength, Elasticity and Thermal Properties of Concrete Subjected to Elevated Temperatures." In Concrete for Nuclear Reactors, Vol. 1, pp. 377-406. Publication SP-34. American Concrete Institute, Detroit, Michigan.

International Agency for Research on Cancer. 1971. "The Evaluation of Carcinogenic Risk to Man." Monograph 1:53-60.

Isaacson, R. E., and D. J. Brown. 1978. Environmental Assessment Related to Hanford Radioactive Waste Burial. RHO-SA-36, Rockwell Hanford Operations, Richland, Washington.

Jarvis, A. 1970. "Combustion Reactions of a Pyrotechnic White Smoke Composition." Combust. Flame 14(3):313-320.

Kasper, R. B., S. M. Price, M. K. Addition, R. M. Smith, G. V. Last, and G. L. Wagernar. 1979. Transuranic Distribution Beneath a Retired Underground Disposal Facility, Hanford Site. RHO-SA-131, Rockwell Hanford Operations, Richland, Washington.

Kasper, R. B. 1981. Field Study of Plutonium Transport in the Vadose Zone. RHO-SA-224, Rockwell Hanford Operations, Richland, Washington.

Keiter, R., T. Ahnger, A. Marucie, and T. Baldwin. 1978. "The Preparation of Anhydrous Chromium (III) Chloride and the Pyrolysis of Carbon Tetrachloride." Journal of Chemical Education 55:52.

Keith, L. H., and W. A. Teilliard. 1979. "Priority Pollutants I--A Perspective View." Environmental Science and Technology 13(4):416-423.

Kennedy, W. E., Jr., R. L. Aaberg, B. A. Napier, and J. K. Soldat. 1982. Transuranic Advanced Disposal Systems: Preliminary ^{239}Pu Waste Disposal Criteria for Hanford. PNL-4254, Pacific Northwest Laboratory, Richland, Washington.

Kingery, W. D. 1960. Introduction to Ceramics. John Wiley and Sons, New York.

Kirshenbaum, M. S. 1982. Reactivity of Explosives/Sediment Mixtures. ARLCD-TR-82007, U.S. Army Armament and Development Command, Large Caliber Weapon Systems Laboratory, Dover, New Jersey.

Kubic, R. L., and M. W. Anders. 1980. "Metabolism of Carbon Tetrachloride to Phosgene." Life Sciences 26:2151-2155.

Kuznetosov, A. F., and G. F. Pekhov. 1967. "Tetrachloroethylene." Izobret., Prom. Obraztsy, Tovarnye znaki 44(18):32. USSR Patent SU201386.

Laursen, T., and W. A. Lanford. 1978. "Hydration of Obsidian." Nature 276(9):153-156.

Lazar, I. 1977. "Making the Choice Among Dry, Liquid, and Gas Transformers." Specifying Engineer 37:130-131.

Lea, F. M. 1971. The Chemistry of Cement and Concrete. 3rd ed. Chemical Publishing Co., Inc., New York.

Luxmoore, R. J., B. P. Spalding, and I. M. Monroe. 1981. "Areal Variation and Chemical Modification of Weathered Shale Infiltration Characteristics." Soil Sci. Soc. Am. J. 45:687-691.

Materials Characterization Center. 1981. Nuclear Waste Materials Handbook--Waste Form Test Methods. DOE/TIC-11400, Department of Energy, Washington, D.C.

McElroy, J. L. 1975. Quarterly Progress Report -- Research and Development Activities, Waste Fixation Program, April through June 1975. BNWL-1932, Pacific Northwest Laboratory, Richland, Washington.

Means, R. S. 1981. 1981 Labor Rates for the Construction Industry. Robert Snow Means Co., Inc., Kingston, Massachusetts.

Mori, V., and K. Ohtake. 1977. "Decomposition Rate of Nitric Oxide on Alumina Surface in the Temperature Range 920-1220K." Combustion Science and Technology 16:11-20.

Murphy, E. S., and G. M. Holter. 1980. Technology, Safety, and Costs of Decommissioning a Reference Low-Level Waste Burial Ground. NUREG/CR-0570, Vol. I, Prepared for the U.S. Nuclear Regulatory Commission by Pacific Northwest Laboratory, Richland, Washington.

Napier, B. A. 1982. A Method for Determining "Allowable Residual Contamination Levels" of Radionuclide Mixtures in Soil. PNL-3852, Pacific Northwest Laboratory, Richland, Washington.

Norton, F. H. 1968. Refractories. McGraw-Hill Book Co., New York.

Oma, K. H., R. K. Farnsworth, and J. M. Rusin. 1982. In Situ Vitrification: Application Analysis for Stabilization of Transuranic Waste. PNL-4442, Pacific Northwest Laboratory, Richland, Washington.

Oma, K. H., D. R. Brown, J. L. Buelt, V. F. FitzPatrick, K. A. Hawley, G. B. Mellinger, B. A. Napier, D. J. Silviera, S. L. Stein, and C. L. Timmerman. 1983. In Situ Vitrification of Transuranic Wastes: Systems Evaluation and Applications Assessment. PNL-4800, Pacific Northwest Laboratory, Richland, Washington.

Oma, K. H., R. K. Farnsworth, and C. L. Timmerman. 1984. "Characterization and Treatment of Gaseous Effluents From In Situ Vitrification." In Radioactive Waste Management and the Nuclear Fuel Cycle, pp. 319-341. Hardwood Academic Publishers gmbh.

Oma, K. H. and C. L. Timmerman. 1984. "Off-Gas Treatment and Characterization for a Radioactive In Situ Vitrification Test." In: Proceedings of the 18th Nuclear Airborne Waste Management and Air Cleaning Conference, Technical Information Center, Oak Ridge, Tennessee.

Ott, E., et al. 1947. Volume V of High Polymers Cellulose and Cellulose Derivatives. Interscience, New York.

Owens, K. W. 1981. Existing Data on the 216-Z Liquid Waste Sites. RHO-LD-114, Rockwell Hanford Operations, Richland, Washington.

Parrott, J. E., and A. D. Stuckes. 1975. Thermal Conductivity of Solids. Pion Ltd., London, United Kingdom.

Petersen, P. H. 1966. "Hardened Concrete--Resistance to High Temperature." In Concrete and Concrete-Making Materials. STP169-A, American Society for Testing and Materials, Baltimore, Maryland.

Phillips, S. W., J. A. Winterhalder, D. L. Berrard, and T. W. Gilbert. 1985. "Liquid Disposal Site Void Fill and Isolation: Systems Descriptions." Paper presented at the Seventh Annual DOE LLWMP Participants; Information Meeting, September 10-13, 1985, Las Vegas, Nevada.

Platt, A. M. 1973. Quarterly Progress Report -- Research and Development Activities, Waste Fixation Program, December 1972 Through March 1973. BNWL-1741, Pacific Northwest Laboratory, Richland, Washington.

Platt, S. 1958. "The Saturable Reactor. Magnetic Amplifiers: Theory and Application, Chapter 4. Prentice-Hall, Englecliffs, New Jersey.

Price, S. M., R. B. Kasper, M. K. Addition, R. M. Smith, and G. V. Last. 1979. Distribution of Plutonium and Americium Beneath the 216-Z Crib: A Status Report. RHO-ST-17, Rockwell Hanford Operations, Richland, Washington.

Ridgway, K. R., and R. D. Carter. 1972. Criticality Prevention Parameters of Plutonium in Soils. ARH-2622, Atlantic Richfield Hanford Company, Richland, Washington.

Robertson, D. E., C. W. Thomas, R. W. Perkins, and V. W. Thomas. 1981. Transuranium and Other Long-Lined Radionuclides in the Terrestrial Environs of Nuclear Power Plants. EPRI-EA-2045. Prepared by Battelle, Pacific Northwest Laboratories for the Electric Power Reserach Institute, Palo Alto, California.

Ross, W. A., et al. 1982. Comparative Leach Testing of Alternative TRU Waste Forms. PNL-SA-9903, Pacific Northwest Laboratory, Richland, Washington.

Scheffler, K., et al. 1977. Long Term Leaching of Silicate Systems: Testing Procedure, Actinide Behavior and Mechanism (German). KFK 2456, Gesellschaft fur Rernforschung. Mbh, Karlsruhe, West Germany.

Stanek, J. 1977. Electric Melting of Glass. Elsevier Scientific Publishing Company, Amsterdam, The Netherlands.

Stermole, F. J. 1982. Economic Evaluation and Investment Decision Methods. 4th ed. Investment Evaluations Corporation, Golden, Colorado.

Strachan, D. M., R. P. Turcotte, and B. O. Barnes. 1980. MCC-1: A Standard Leach Test for Nuclear Waste Forms. PNL-SA-8783, Pacific Northwest Laboratory, Richland, Washington.

Thompson, J. K. 1977. "Technical Note--Minimum Critical Mass of Plutonium-Polyethylene System Found to be Significantly Lower than Plutonium-Water System." Nuclear Technology 33:235-236.

Timmerman, C. L., and R. O. Lokken. 1983. Characterization of Vitrified Soil Produced by In Situ Vitrification. Presented at the Second International Symposium of Ceramics in Nuclear Waste Management, April 24-27, 1983, Chicago, Illinois. PNL-SA-10759, Pacific Northwest Laboratory, Richland, Washington.

Timmerman, C. L., R. A. Brouns, J. L. Buelt, and K. H. Oma. 1983. "In Situ Vitrification: Pilot-Scale Development." Nuclear and Chemical Waste Management, p. 4:267.

Timmerman, C. L. and K. H. Oma. 1984. An In Situ Vitrification Pilot-Scale Radioactive Test. PNL-5240, Pacific Northwest Laboratory, Richland, Washington.

Timmerman, C. L. 1986. "In Situ Vitrification of PCB-Contaminated Soils." In Proceedings: 1985 EPRI PCB Seminar, ed. R. Y. Komai, V. Niemeyer, and G. Addis, pp. 10-1 to 10-4. Electric Power Research Institute, Palo Alto, California.

Tooley, F. V. 1974. "Electric Melting of Glass." The Handbook of Glass Manufacture, pp. 387-400, Books for Industry, Inc., New York.

Tsuge, S., J. J. Leary and T. L. Isenhour. 1974. "CCl_4--Reactions at High Temperatures." Journal of Chemical Education 51:256-267.

U.S. Department of the Army. 1967. Military Explosives. Department of the Army Technical Manual TM 9-1300-214 C2, Washington, D.C.

U.S. Department of the Army. 1970. AMC Regulation Safety Manual. AMCR-385-100, Army Material Command, Alexandria, Virginia.

U.S. Department of Energy. 1981a. Environmental Protection, Safety, and Health Protection Programs for DOE Operations. Order 5480.1A, Washington, D.C.

U.S. Department of Energy. 1981b. Environmental Protection, Safety, and Health Protection Information Reporting Requirements. Order 5484.1, Washington, D.C.

U.S. Department of Energy. 1982. Long-Range Master Plan for Defense Transuranic Waste Management. DOE-TRU-8201, Washington, D.C.

U.S. Department of Energy. 1983. Long-Range Master Plan for Defense Transuranic Waste Management. DOE-TRU-8201, Washington, D.C.

U.S. Department of Energy. 1984. Radioactive Waste Management. Order 5820.2, Washington, D.C.

U.S. Department of Energy. 1985. Spent Fuel and Radioactive Waste Inventories, Projections, and Characteristics. DOE/RW-0006, Rev. 1, Washington, D.C.

U.S. Nuclear Regulatory Commission. 1984. Code of Federal Regulations. Title 10 Energy; Part 71, Standards for Protection Against Radiation. Revision January 1, 1983. U.S. NRC, Washington, D.C.

Wallace, R. W., et al. 1980. Topical Report on Release Scenario Analysis of Long-Term Management of High-Level Defense Waste at the Hanford Site. PNL-3363, Pacific Northwest Laboratory, Richland, Washington.

Webster, D. A. 1979. "Land Burial of Solid Radioactive Waste at Oak Ridge National Laboratory, Tennessee: A Case History." In Management of Low-Level Radioactive Wastes, ed. M. W. Carter et al., pp. 731-746. Pergamon Press, New York.

Williams, D. T., and G. L. Lebel. 1981. A National Survey of Tri(haloalkyl)-Trialkyl-, and Triarylphosphates in Canadian Drinking Water. Bull. Environm. Contam. and Toxicol. 27:450-457.

Zeldovich, J. 1946. Acta Physicoehim. 21:477. U.R.S.S.

Zoldners, N. G. 1971. "Thermal Properties of Concrete Under Sustained Elevated Temperatures." In Temperature and Concrete, Publication SP-25, pp. 1-32. American Concrete Institute, Detroit, Michigan.

GLOSSARY OF CHEMICAL SYMBOLS

Al	Aluminum
Al_2O_3	Aluminum oxide
$AlF(NO_3)_2$	Alumino-fluoro nitrate
Am	Americium
CCl_4	Carbon tetrachloride
CO	Carbon monoxide
CO_2	Carbon dioxide
Ca	Cadmium
$Ca(NO_3)_2$	Calcium nitrate
$Ca_2(OH)_2$	Calcium hydroxide
CaO	Calcium oxide
Ce	Cerium
Cl	Chlorine
Cm	Curium
Co	Cobalt
CoO	Cobalt oxide
Cs	Cesium
Cs_2O	Cesium oxide
$CsNO_3$	Cesium nitrate
F	Fluorine
F_2	Fluorine
Fe	Iron
Fe_2O_3	Ferric oxide
FeS	Ferrous sulfide
H	Monatomic hydrogen
H_2	Hydrogen
H_2O	Water
H_2S	Hydrogen sulfide
HNO_3	Nitric acid
HfB_2	Hafnium diboride
K	Potassium
K_2O	Potassium oxide

La	Lanthanum
Li_2O	Lithium oxide
Mg	Magnesium
$Mg(NO_3)_2$	Magnesium nitrate
MgO	Magnesium oxide
Mo	Molybdenum
$MoSi_2$	Molybdenum disilicide
N	Monatomic nitrogen
N_2	Nitrogen
NO	Nitrogen oxide
NO_3	Nitrogen trioxide
NO_x	Nitrogen oxides
Na	Sodium
Na_2O	Sodium oxide
Na_2SO_4	Sodium sulfate
$NaNO_3$	Sodium nitrate
Nd	Neodymium
Np	Neptunium
O	Monatomic oxygen
O_2	Oxygen
P_2O_5	Phosphorus pentoxide
Pb	Lead
Pu_2O_3	Plutonium trioxide
PuO_2	Plutonium dioxide
$PuSiO_3$	Plutonium silicate
Ru	Ruthenium
SO_2	Sulfur dioxide
SO_3	Sulfur trioxide
SO_x	Sulfur oxides
Sb	Antimony
Si	Silicon
SiC	Silicon carbide
SiO_2	Silicon dioxide
Sr	Strontium

$Sr(NO_3)_2$	Strontium nitrate
SrO	Strontium oxide
Ta	Tantalum
Te	Tellurium
TiC	Titanium carbide
TiO_2	Titanium dioxide
U	Uranium
UO_2	Uranium dioxide
UO_3	Uranyl oxide
Zn	Zinc
ZrB_2	Zirconium diboride
ZrO_2	Zirconium oxide

DISTRIBUTION

No. of Copies

OFFSITE

30 DOE Technical Information Center

G. H. Daly, DP-124
DOE Office of the Assistant Secretary for Defense Programs
A-213A/6TN
Washington, DC 20545

S. P. Mathur, DP-123
DOE Office of the Assistant Secretary for Defense Programs
A-227/GTN
Washington, DC 20545

D. J. McGoff, NE-42
DOE Office of the Assistant Secretary for Nuclear Energy
E-455/GTN
Washington, DC 20545

J. E. Lytle, DP-12
DOE Office of the Assistant Secretary for Defense Programs
A-241/GTN
Washington, DC 20545

J. J. Jicha, DP-132
DOE Office of the Deputy Assistant Secretary for Nuclear Materials
A-202/GTN
Washington, DC 20545

J. E. Baublitz, NE-20
DOE Office of Remedial Action and Waste Technology
D-429/GTN
Washington, DC 20545

No. of Copies

J. A. Coleman, NE-24
DOE Office of the Assistant Secretary for Nuclear Energy
E-435/GTN
Washington, DC 20545

W. R. Voigt, NE-20
DOE Office of the Assistant Secretary for Nuclear Energy
E-435/GTN
Washington, DC 20545

W. J. Dircks
Office of the Executive Director of Operations
Mail Station 6209
Nuclear Regulatory Commission
Washington, DC 20555

D. Egan
Environmental Protection Agency
Office of Radiation Programs
401 M Street, S.W.
Washington, DC 20460

M. McFadden
DOE Albuquerque Operations Office
P. O. Box 5400
Albuquerque, NM 87185

J. McGough
DOE Albuquerque Operations Office
P.O. Box 5400
Albuquerque, NM 87185

W. H. Hannum
DOE West Valley Operations Office
P.O. Box 191
West Valley, NY 14171

No. of
Copies

J. E. Solecki
DOE Idaho Operations Office
550 Second Street
Idaho Falls, ID 83401

M. J. Barainca/S. Henchberger
DOE Idaho Operations Office
550 Second Street
Idaho Falls, ID 83401

L. Lanni
DOE San Francisco Operations
1333 Broadway
San Francisco, CA 94612

D. R. Brown
DOE Oak Ridge Operations Office
P.O. Box E
Oak Ridge, TN 37830

S. A. Mann
DOE Chicago Operations Office
9800 South Cass Avenue
Argonne, IL 60439

M. G. O'Rear
DOE Savannah River Operations Office
P.O. Box A
Aiken, SC 29801

D. L. Vieth
DOE Nevada Operations Office
P.O. Box 14100
Las Vegas, NV 89114

C. S. Abrams/J. H. Kittel
Argonne National Laboratory
9700 South Cass Avenue
Argonne, IL 60439

W. A. Cargeiner/S. H. Basham
Battelle Memorial Institute
Project Management Division
505 King Avenue
Columbus, OH 43201

No. of
Copies

J. F. Kircher
Battelle Memorial Institute
Project Management Division
505 King Avenue
Columbus, OH 43201

B. Rawles
Battelle Memorial Institute
Project Management Division
505 King Avenue
Columbus, OH 43201

L. D. Ramspott
Lawrence Livermore National Laboratory
University of California
P.O. Box 808
Livermore, CA 94550

D. T. Oakley, MS 671
Los Alamos Scientific Laboratory
P.O. Box 1663
Los Alamos, NM 87544

T. H. Row
Oak Ridge National Laboratory
P.O. Box X
Oak Ridge, TN 37830

F. Homan
Oak Ridge National Laboratory
P.O. Box Y
Oak Ridge, TN 37830

L. Mezga
Oak Ridge National Laboratory
P.O. Box Y
Oak Ridge, TN 37830

D. Eyman
Oak Ridge National Laboratory
P.O. Box Y
Oak Ridge, TN 37830

No. of
Copies

B. Spalding
Oak Ridge National Laboratory
P.O. Box Y
Oak Ridge, TN 37830

D. R. Anderson
Sandia Laboratories
P.O. Box 5800
Albuquerque, NM 87185

Technical Library
Sandia Laboratories
P.O. Box 5800
Albuquerque, NM 87185

B. R. Wheeler
Westinghouse Idaho Nuclear
Co., Inc.
P.O. Box 4000
Idaho Falls, ID 83401

M. D. Boersma
E. I. du Pont de Nemours
Company
Savannah River Laboratory
Aiken, SC 29801

E. A. Jennrich
EG&G Idaho
P.O. Box 1625
Idaho Falls, ID 83415

K. V. Gilbert/P. G. Hagen
Rockwell International
Rocky Flats Plant
P.O. Box 464
Golden, CO 80401

R. A. Shaw
Electric Power Research
Institute
3412 Hillview Avenue
P.O. Box 10412
Palo Alto, CA 94304

No. of
Copies

J. M. Pope
West Valley Nuclear Services
Company
P.O. Box 191
West Valley, NY 14171

J. W. Bartlett
The Analytic Sciences
Corporation
6 Jacob Way
Reading, MA 01867

W. A. Freeby/J. L. Jardine
Bechtel National, Inc.
P.O. Box 3965
San Francisco, CA 94119

Librarian
Westinghouse Electric
Corporation
Technical Library
P.O. Box 40039
Albuquerque, NM 87196

R. G. Post
College of Engineering
University of Arizona
Tucson, AZ 85721

K. McKinley
Joint Integration Office
Rockwell
Box 3150
Albuquerque, NM 87190

S. Evert
Joint Integration Office
Rockwell
Box 3150
Albuquerque, NM 87190

No. of Copies

ONSITE

5 DOE Richland Operations Office

E. A. Bracken
J. L. Rhoades
M. W. Shupe
J. D. White
N. T. Karagianes

14 Rockwell Hanford Operations

B. N. Anderson
L. Fitch
D. Fukamoto
K. A. Gasper
R. N. Gurley
N. W. Kirch
H. E. McGuire
D. E. McKinney
R. D. Prosser
J. H. Roecker
T. B. Venziano
D. D. Wodrich
R. J. Wojtasak
File Copy

UNC Nuclear Industries

T. E. Dabrowski/W. J. Kyriazis

No. of Copies

61 Pacific Northwest Laboratory

W. Ballard
W. F. Bonner
R. A. Brouns
D. R. Brown
J. L. Buelt (20)
H. C. Burkholder
J. G. Carter
D. B. Cearlock/W. R. Wiley
T. D. Chikalla
T. Claudson
S. K. Ennor
V. F. FitzPatrick (5)
J. E. Hansen
M. S. Hanson
L. T. Kaley
Y. B. Katayama
S. S. Koegler
J. M. Latkovich
R. C. Liikala
J. L. McElroy
T. McLaughlin
J. E. Minor
S. J. Mitchell
I. C. Nelson/P. Bramson
K. H. Oma
R. E. Nightingale
D. J. Silviera
S. L. Stein
J. Straalsund
C. L. Timmerman
C. R. Wentz
Technical Report Files (5)
Publishing Coordination (2)